

UNIVERSIDAD DE LA FRONTERA
FACULTAD DE INGENIERIA, CIENCIAS Y ADMINISTRACION
INSTITUTO DE AGROINDUSTRIA



“USE OF PETROLEUM COKE FLY ASHES AS POTENTIAL FILLING
MATERIAL IN PERMEABLE REACTIVE BARRIERS TO DECONTAMINATE
ACID WASTEWATERS WITH HIGH HEAVY METAL CONTENT”

TESIS PARA OPTAR AL GRADO ACADEMICO
DE DOCTOR EN CIENCIAS DE RECURSOS
NATURALES

AIXA GONZALEZ RUIZ
TEMUCO-CHILE
2011

USE OF PETROLEUM COKE FLY ASHES AS POTENTIAL FILLING
MATERIAL IN PERMEABLE REACTIVE BARRIERS TO
DECONTAMINATE ACID WASTEWATERS WITH HIGH HEAVY METAL
CONTENT

*Esta tesis es presentada bajo la supervisión del director de
tesis Dr. Rodrigo J. Navia Diez, del Departamento de
Ingeniería Química para su aprobación por la comisión.*

AIXA GONZALEZ RUIZ

DIRECTOR DEL PROGRAMA
DE POSTGRADO EN
CIENCIAS DE RECURSOS
NATURALES

Dr. RODRIGO NAVIA

Dr. CHRISTIAN BORNHARDT

Dr. ALFREDO GORDON

DIRECTOR DE POSTGRADO
UNIVERSIDAD DE LA FRONTERA

Dr. PATRICIO REYES

Acknowledgements

A los proyectos FONDECYT 1060309 y 7070022 del Dr. Rodrigo J. Navia Diez por el apoyo financiero en este estudio.

Al proyecto de Cooperación Científica Internacional 2007-136 CONICYT/CSIC, 2007CL0014 CSIC/CONICYT por financiar una estadía en el departamento de Geociencias en el Instituto de Diagnóstico Ambiental y Estudios de Agua (IDAEA-CSIC), Barcelona, España.

Sinceras gracias a la profesora María de la Luz Mora, por darme la oportunidad de entrar al programa y de apoyarme.

A CONICYT por financiar una estadía de investigación en el Instituto de Ciencias de la Terra “Jaume Almera” (IJA-CSIC), Barcelona, España.

Quiero agradecer a la Dra. Natalia Moreno, del IDAEA/CSIC por su apoyo incondicional como investigadora y amiga. También gracias a Carlos y Carla, por hacerme sentir parte de la familia (Barcelona, Conques y Figuerola d’ Orcau) en los momentos solitarios.

También, quiero agradecer al Dr. Xavier Querol, Carles Ayora y Joseph Elvira por su apoyo y colaboración en la realización de esta tesis

Gracias a mis tres amores, por estar a mi lado, de hacerme siempre reír y de enseñarme la luz en los momentos difíciles. Sin ustedes nada hubiera sido posible.

Gracias a mi familia cubana por los votos de confianza y que a pesar de la incomunicación siempre me han hecho sentir acompañada fuera de Cuba. A mis amigos cubanos que no importan donde estén, se sentirían contentos por el logro de este pequeño paso.

Liebe Familie, zuweit und gleichzeitig zunah. Ich bedanke mich für Alles. Die Zeit, die ich in Deutschland vollgebracht habe, war am schönste. Mutti und Vati, vielen Dank für das Geschenk, eine Heimat zu fühlen und spüren.

No quiero dejar de agradecer a todos los viejos amigos, que no importa cuan lejos estaban, me apoyaron. A Rubén, Nicolás, Anita, Gustavo, Cecilia, Fran, la comunidad científica y otros que no me vienen a la memoria, por aguantar mis chistes cubanos y comida cubana, mi risa y las largas conversaciones.

Resumen

La presencia de metales pesados en el medioambiente representa un problema global debido a la persistencia, bioacumulación y toxicidad hacia los organismos vivos. La contaminación por metales pesados en aguas residuales ácidas ha generado graves daños tanto a ecosistemas acuáticos como a terrestres por diferentes medios. De acuerdo a la Organización para la Cooperación y el Desarrollo Económico, hasta el año 2005 existían 256 tranques de relave en Chile (39% del total de tranques de relave) en un estado deficiente de operación. Además se han encontrado un alto contenido de metales pesados en ríos chilenos del Norte, sugiriendo como causa de la contaminación las actividades mineras. Entre los procesos de tratamiento para minimizar los impactos negativos provenientes de los metales pesados y las aguas ácidas se emplea normalmente la precipitación por medio de materiales alcalinos. Sin embargo, al ser materiales que se extraen de la naturaleza (calcita, cal y cal hidratada) son más costosos en la mayoría de los casos que los materiales secundarios. Uno de los materiales secundarios más estudiados son las cenizas volantes, las cuales dependiendo del proceso de combustión del cual provienen pudieran presentar un alto contenido de calcio. En Chile, la reciente aprobación para la operación de diferentes centrales termoeléctricas que emplean la combustión de coque de petróleo hace necesario el estudio de las cenizas volantes provenientes de este proceso.

El trabajo en sí se enfoca en la reutilización de cenizas volantes de la combustión en lecho fluidizado de coque de petróleo como potencial material reactivo en barreras permeables reactivas.

Para ello se trazaron como principales objetivos la caracterización mineralógica, física y química de las cenizas volantes de la combustión en lecho fluidizado de coke de petróleo y de los materiales aglomerados (sorbentes) resultantes de la mezcla entre licor negro o lignimerina y la ceniza; la evaluación de la lixiviación de todos los materiales, la neutralización de aguas ácidas y la capacidad de remoción de metales pesados tanto en ensayos batch como en columnas.

Los resultados de la caracterización revelaron un alto contenido de calcio para todos los materiales, así como también de los elementos trazas Ni y V, los cuales pueden limitar las aplicaciones potenciales de las cenizas y de los aglomerados. El tratamiento de aglomeración de la ceniza de coke de petróleo con licor negro y con lignimerina (obtenida de aguas residuales de la industria de celulosa Kraft) incrementó el área superficial específica, conductividad hidráulica y el tamaño de partícula, manteniéndose una composición química similar a la de la ceniza original. Además prácticamente todos los materiales resultaron ser no peligrosos.

El test de lixiviación en columnas sirvió de herramienta para la selección del material aglomerado más apropiado (sorbente), en cuanto a la liberación de elementos como Ni, V, As y Zn para períodos de tiempo más largo, siendo seleccionado el sorbente 3.

La remoción de metales pesados en ensayos batch y en lecho fijo indica que las cenizas volantes de la combustión en lecho fluidizado de coke de petróleo y el sorbente 3 son capaces de remover Cu^{2+} y Pb^{2+} de aguas ácidas principalmente por precipitación. De acuerdo a los resultados de la extracción secuencial, estos precipitados quedaron retenidos en la fases menos disponibles de los materiales estudiados (carbonatos y residual). De acuerdo a estos resultados, las cenizas volantes de la combustión en lecho fluidizado de coke de petróleo pudieran ser consideradas como material reactivo con posible aplicación en procesos de remoción de metales pesados y en la neutralización de aguas residuales ácidas; donde no se requiera un flujo continuo.

El sorbente 3 aparece como la mejor opción para ser utilizado como potencial material reactivo en las barreras reactivas permeables en la remoción de Pb^{2+} (28.3 mg/g) y Cu^{2+} (8.1 mg/g) de aguas ácidas.

Finalmente, a pesar de no detectar valores elevados de Ni y V durante la remoción en columnas del Cu^{2+} y del Pb^{2+} , se recomienda prestar una atención cuidadosa a la lixiviación de Ni y V, ya que ambos pudieran incrementar el riesgo de peligrosidad tanto de la ceniza como de los sorbentes.

Palabras claves: Cenizas volantes, metales pesados, precipitación, sorbente, aguas residuales, neutralización.

Abstract

The presence of heavy metals in the environment represents a global problem due to its persistence, bioaccumulation and toxicity to living organisms. Heavy metals pollution coupled with acid wastewaters have been damaging worldwide terrestrial and aquatic ecosystems by different pathways. According to the Organization for Economic Cooperation and Development, there were 256 Chilean tailing ponds (39% of total tailing ponds) in deficient conditions in 2005. In addition, high heavy metals content in some Chilean rivers in the northern regions has been detected, being a possible reason for contamination the mining activities.

The most common treatment process to minimize the potential negative impacts of heavy metals in acid wastewaters is chemical precipitation. Nevertheless, the extraction and use of raw alkaline materials (lime, limestone and hydrated lime) is not cheap in almost cases compared to secondary raw materials. One of the most studied secondary raw materials is fly ashes, which depending of the combustion process could have high calcium content. In Chile, several projects have been recently approved concerning petroleum coke combustion in power plants, leading to higher fly ashes generation.

This work is focused on the reuse of raw petroleum coke fly ashes from circulated fluidized bed combustion and a sorbent from the blending between these fly ashes and black liquor or lignimerin as potential reactive material in permeable reactive barriers. Our main goals deal with the mineralogical, physical and chemical characterization of raw petroleum coke fly ashes from circulated fluidized bed combustion and the resulting developed materials (blending of fly ashes with black liquor or lignimerin), their evaluation of environmental performance (through leaching

tests and chemical sequential extractions), and their neutralization of acid wastewaters and heavy metals removal capacity in batch and column tests.

Results of characterization revealed high calcium content in all studied materials, as well as trace elements Ni and V, which could represent a limitation in potential application of the studied materials. Besides of an increase of specific surface area and grain size of resulting developed materials (or sorbents) from circulated fluidized bed combustion, all materials indicated a similar chemical composition. Regarding to environmental characterization, leaching test allowed concluding that almost materials in this work are non-hazardous materials.

Furthermore, leaching column test results were used as selecting criteria for the suitable sorbent in relation to the leaching of environmental concerning elements such as Ni, V, As and Zn in long term, selecting as suitable developed materials sorbent 3.

Heavy metals removal in batch and column tests indicated that raw and treated petroleum coke fly ashes from circulated fluidized bed combustion are able to remove Cu^{2+} and Pb^{2+} mainly due to precipitation process, at high liquid to solid ratios and moderate acid pH values. Moreover, chemical sequential extraction results indicated that precipitation products were retained onto the spent material surface, being the precipitation products associated to the less available phases. According to these results, petroleum coke fly ashes from circulated fluidized bed combustion could be considered a potential reactive material in heavy metals removal process and to neutralize acid wastewaters.

Sorbent 3 seems to be the best option for reuse as potential reactive material in permeable reactive barriers for the removal of Pb^{2+} (28.3 mg/g) and Cu^{2+} (8.1 mg/g) from acid wastewaters.

Finally, despite no detect high values of Ni and V during Cu^{2+} and Pb^{2+} removal column tests. It is recommended to pay carefully attention to Ni and V leaching during heavy metals removal and

neutralization applications. Both trace elements could increase the hazardous risk of the raw petroleum coke fly ashes and sorbent 3.

Keywords: *fly ashes, heavy metals, precipitation, petroleum coke fly ash, sorbent, wastewater, neutralization*

General index

Chapter 1:	<i>Introduction</i>	<i>(1)</i>
1.1	<i>Heavy metals contamination issues and current solutions</i>	<i>(1)</i>
1.2	<i>Hypothesis</i>	<i>(9)</i>
1.3	<i>General objective</i>	<i>(9)</i>
1.4	<i>Specific objectives</i>	<i>(9)</i>
Chapter 2:	<i>Literature review</i>	<i>(10)</i>
2.1	<i>Combustion by-products: Fly ashes</i>	<i>(11)</i>
2.1.1	<i>Coal fly ashes</i>	<i>(11)</i>
2.1.2	<i>Petroleum coke fly ashes</i>	<i>(13)</i>
2.2	<i>Current applications</i>	<i>(16)</i>
2.3	<i>Novel applications</i>	<i>(17)</i>
2.3.1	<i>Acid mine drainage remediation</i>	<i>(18)</i>
2.3.2	<i>Filling material in permeable reactive barriers</i>	<i>(20)</i>
2.4	<i>Evaluation of a potential reactive material</i>	<i>(23)</i>
2.4.1	<i>Batch removal tests</i>	<i>(23)</i>
2.4.2	<i>Column removal tests</i>	<i>(25)</i>
2.4.3	<i>Environmental performance</i>	<i>(27)</i>
Chapter 3:	<i>Materials & methods</i>	<i>(29)</i>
3.1	<i>Materials</i>	<i>(30)</i>
3.2	<i>Characterization analyses</i>	<i>(31)</i>
3.3	<i>Leaching tests</i>	<i>(33)</i>

3.3.1	<i>Batch leaching test</i>	(33)
3.3.2	<i>Column leaching test</i>	(34)
3.4	<i>Sequential extraction</i>	(34)
3.5	<i>Batch tests</i>	(36)
3.5.1	<i>Neutralization trials using CFBC-PCFA</i>	(36)
3.5.2	<i>Cu²⁺, Pb²⁺ and Cr(VI) removal kinetic</i>	(36)
3.5.3	<i>Cu²⁺, Pb²⁺ and Cr(VI) sorption isotherms</i>	(36)
3.6	<i>Column tests</i>	(37)
3.6.1	<i>Neutralization trials using CFBC-PCFA and NCS3</i>	(37)
3.6.2	<i>Cu²⁺ and Pb²⁺ removal kinetic in fixed bed column tests</i>	(37)
3.7	<i>Geochemical modelling</i>	(38)

Chapter 4:	<i>Results & discussion</i>	(39)
-------------------	--	-------------

4.1	<i>Mineralogical, chemical and physical characterization of the studied materials</i>	(40)
4.2	<i>Leaching tests</i>	(53)
4.2.1	<i>Batch leaching test</i>	(53)
4.2.2	<i>Column leaching test</i>	(55)
4.3	<i>Applications in batch tests using CFBC-PCFA</i>	(60)
4.3.1	<i>Neutralization trials using CFBC-PCFA</i>	(60)
4.3.2	<i>Cu²⁺, Pb²⁺ and Cr(VI) removal kinetics</i>	(63)
4.3.2.1	<i>Cu²⁺ removal kinetics</i>	(63)
4.3.2.2	<i>Pb²⁺ removal kinetics</i>	(65)

4.3.2.3	<i>Cr(VI) removal kinetics</i>	(66)
4.3.3	<i>Kinetic parameters</i>	(69)
4.3.4	<i>Sequential extraction from original and residual CFBC-PCFA after removal kinetics</i>	(70)
4.3.5	<i>Heavy metals sorption isotherms</i>	(72)
4.4	<i>Applications in column tests</i>	(74)
4.4.1	<i>Neutralization fixed bed column tests by CFBC-PCFA</i>	(74)
4.4.2	<i>Neutralization tests using NCS3</i>	(77)
4.4.3	<i>Cu²⁺ and Pb²⁺ removal in fixed bed column tests using NCS3</i>	(80)
4.4.3.1	<i>Prediction of breakthrough curves</i>	(83)
4.4.3.2	<i>Sorption mechanism</i>	(85)
4.4.4	<i>Sequential extraction from raw and residual NCS3 and NCS3 after heavy metals removal column tests</i>	(87)
Chapter 5:	<i>General conclusions</i>	(91)
	<i>References</i>	(95)
	<i>Appendixes</i>	(112)
	<i>Papers</i>	(130)

Figure captions

Chapter 1:	Introduction	(1)
Figure 1.1:	Input of heavy metals into the environment	(3)
Chapter 2:	Literature review	(10)
Figure 2.1:	Fly ash image captured through scanning electron microscopy (SEM)	(13)
Figure 2.2:	Sulfation patterns of CaO particles	(15)
Figure 2.3:	Some PRB system; a) continuous barrier and b) passive collector with batch reactor cells.	(21)
Figure 2.4:	General representation of a typical s-shape breakthrough curve	(25)
Chapter 3:	Materials and Methods	(29)
Figure 3.1:	Cascade impactor equipment	(33)
Figure 3.2:	Performance of the column leaching test	(34)
Figure 3.3:	Chemical sequential extraction procedure	(35)
Chapter 4:	Results & Discussion	(39)
Figure 4.1:	Photos of circulated fluidized bed combustion petroleum coke fly ashes (a) and resulting non-conventional sorbents (b)	(40)
Figure 4.2:	X-Ray diffraction (XRD) patterns from circulated fluidized bed combustion petroleum coke fly ashes (CFBC-PCFA) sampled in 2006, 2007 and 2008.	(42)
Figure 4.3:	XRD pattern from non-conventional sorbent (NCS) samples	(44)
Figure 4.4:	Ternary diagram of different fly ashes	(46)

- Figure 4.5:** Scanning electron microscopy (SEM) coupled with energy-dispersive X-ray spectroscopy (EDX) of CFBC-PCFA samples with the presence of (a) unburned carbon (UC), (b) crystals of vanadium associated to calcium and (c) CFBC-PCFA fraction around 17 μm with the presence of aluminum-silicates (spherical particles). (49)
- Figure 4.6:** SEM-EDX of NCS. All samples have the same magnification (50)
- Figure 4.7:** Particle size distribution of CFBC-PCFA. Values expressed as μm (51)
- Figure 4.8:** pH (a) and EC (b) time development in column leaching test of CFBC-PCFA, NCS1, NCS2 and NCS3. (56)
- Figure 4.9:** Main major and trace elements detected during column leaching test of CFBC-PCFA, NCS2 and NCS3. (58)
- Figure 4.10:** pH (a), alkalinity (b), Electric conductivity (c), Ca (d), S (e) and V concentrations (f) during neutralization batch test with increasing CFBC-PCFA dose from 0.2 to 3 g/L at pH 2, 4 and 6 at 25°C. (61)
- Figure 4.11:** Cu^{2+} removal kinetics test at 25°C and 0.1M KCl using CFBC-PCFA doses of 0.2, 0.6 and 1 g/L. (62)
- Figure 4.12:** SEM-EDX and XRD of CFBC-PCFA from Cu^{2+} removal kinetics test, (a) at 8 min and (b) at 20 h. Po: posnjakite, $\text{Cu}_4\text{SO}_4(\text{OH})_6\text{H}_2\text{O}$; A: anhydrite and C: calcite (64)
- Figure 4.13:** Pb^{2+} removal kinetics test at 25°C and 0.1M KCl using CFBC- (65)

	PCFA doses of 0.2, 0.6 and 1 g/L	
Figure 4.14:	SEM-EDX of CFBC-PCFA from Pb ²⁺ removal kinetics test	(66)
Figure 4.15:	Cr(VI) removal kinetics test at 25°C and 0.1M KCl using CFBC-PCFA doses of 0.2, 0.6 and 1 g/L	(67)
Figure 4.16:	Evidence about color change during Cr(VI) removal.	(68)
Figure 4.17:	SEM-EDX of CFBC-PCFA from Cr(VI) removal kinetics test	(68)
Figure 4.18:	Release of different elements during chemical sequential extraction of CFBC-PCFA (a), and after (b) Cu ²⁺ , (c) Pb ²⁺ and (d) Cr(VI) removal kinetics tests, respectively.	(71)
Figure 4.19:	pH development in fixed-bed column neutralization tests using CFBC-PCFA at pH 2. BV: bed volume	(75)
Figure 4.20:	XRD pattern of residual CFBC-PCFA from fixed-bed column neutralization test at pH 2. C: calcite; A: anhydrite and G: gypsum (CaSO ₄ ·2H ₂ O)	(76)
Figure 4.21:	pH development in fixed-bed column neutralization tests using NCS3 at pH 2 (a) and 4 (b)	(77)
Figure 4.22:	Main major and trace elements detected from fixed-bed column neutralization tests using NCS3 at bed height of 3 cm (h ₃), at pH 2 (a) and 4 (b), and at bed height of 6 cm (h ₆) at pH 2 (c) and 4 (d).	(79)
Figure 4.23:	Cu ²⁺ (a) and Pb ²⁺ (b) removal test in fixed-bed columns at pH 4 and at bed height of 6 cm (a) and 3 cm (b).	(81)
Figure 4.24:	SEM-EDX of residual NCS3 from Cu ²⁺ (a) and Pb ²⁺ (b) removal	(87)

column tests at maximum saturation capacity, pH 4 and bed height of 6 cm.

Figure 4.25: Chemical sequential extraction of NCS3. (88)

Figure 4.26: Release of different elements during SEP of residual NCS3 residual from Cu^{2+} at pH 2 (a) and pH 4 (b), Pb^{2+} at pH 2 (c) and pH 4 (d) removal column tests. (90)

Appendix I: (112)

Figure A.1.1: SEM-EDX analyses of CFBC-PCFA fractions with the same magnification, except fraction $>65\mu\text{m}$. (114)

Figure A.1.2: XRD of different size of CFBC-PCFA $<65\mu\text{m}$ and $>65\mu\text{m}$ samples. P: portlandite; C: calcite; A: anhydrite (115)

Appendix II: (116)

Figure A.2.1: XRD spectra from CFBC-PCFA dose of 1.4 (a) and 2.6 g/L (b) at pH 2. A: anhydrite; C: calcite and Q: quartz: (116)

Appendix III (117)

Figure A.3.1 Electrophoretic mobility measurement of CFBC-PCFA at 0.1 M KCl (117)

Appendix IV: (118)

Figure A.4.1: Speciation diagram for Cu (100 mg/L of Cu^{2+} at 25°C) (118)

Figure A.4.2 Speciation diagram for Pb (100 mg/L of Pb^{2+} at 25°C) (118)

Figure A.4.3 Speciation diagram for Cr(V) (100 mg/L of Cr(VI) at 25°C) (118)

Appendix V (119)

Figure A.5.1: Speciation diagram for Cu^{2+} (100 mg/L of Cu^{2+} at 25°C, including solution initial conditions) (119)

Figure A.5.2 Speciation diagram for Pb^{2+} (100 mg/L of Pb^{2+} at 25°C, including solution initial conditions) (119)

Figure A.5.3 Speciation diagram for Cr(VI) (100 mg/L of Cr(VI) at 25°C, including solution initial conditions) (119)

Appendix VI: (120)

Figure A.6.1 Chemical sequential extraction procedure (120)

Appendix VII: (121)

Figure A.7.1: Cu^{2+} (a), Pb^{2+} (b) and Cr(VI) (c) removal isotherms at 25°C and 0.1 M KCl. (121)

Appendix VIII: (122)

Figure A.8.1: Main major and trace elements detected in neutralization test by CFBC-PCFA at pH 2 for h_3 (a) and h_6 (b). (122)

Appendix IX: (123)

Figure A.9.1: SEM-EDX of NCS3 after neutralization fixed bed column test at pH 2 and bed height of 6 cm. (123)

Appendix X: (124)

Figure A.10.1: Cu^{2+} and Pb^{2+} removal at pH 2 and at bed height of 6 cm. (124)

Figure A.10.2: Cu^{2+} (a) and Pb^{2+} (b) removal at flow rate of 1.5 and 5 mL/min. (125)

Appendix XI (126)

Figure A.11.1: Bohart-Adams model fitting for Cu^{2+} (left) and Pb^{2+} (right) (126)

column removal tests using NCS3

Figure A.11.2: Thomas model fitting for Cu^{2+} (left) and Pb^{2+} (right) column (127)

removal tests using NCS3

Figure A.11.3: Yoon-Nelson model fitting for Cu^{2+} (left) and Pb^{2+} (right) column (128)

removal tests using NCS3

Appendix XII (129)

Figure A.12.1 Effluent pH during Cu^{2+} and Pb^{2+} removal column tests, pH 4 and (129)

bed height of 6 cm

Table captions

Chapter 1:	Introduction	(1)
Table 1.1:	Concentration of heavy metals in rivers of the world	(5)
Table 1.2:	Cost for conventional reactive materials in heavy metals removal	(6)
Table 1.3:	Cost of different non-conventional sorbents (NCS)	(6)
Chapter 2:		(10)
Table 2.1:	Chemical composition of fly ashes from different sources.	(12)
Table 2.2:	Mineralogical compounds of fly ashes from different sources	(12)
Table 2.3:	Composition of some alkaline materials and fly ashes (w/w %)	(19)
Table 2.4:	Different reactive materials used in permeable reactive barriers	(22)
Chapter 4:		(39)
Table 4.1:	Major oxides detected in circulated fluidized bed combustion petroleum coke fly ashes samples (CFBC-PCFA) and in non-conventional sorbents (NCS)	(45)
Table 4.2:	Minor and trace elements in CFBC-PCFA and NCS samples	(48)
Table 4.3:	Particle size distribution of the developed NCS	(52)
Table 4.4:	Leaching batch test values of European Norm EN 12457-2 (mg/kg). Limit values from Council Decision 2003/33/EC	(54)
Table 4.5:	Kinetic parameters from removal kinetics batch test at 25°C using a CFBC-PCFA dose of 0.2 g/L.	(69)
Table 4.6:	Heavy metals sorption isotherm parameters at 25°C using CFBC-PCFA dose of 0.2 g/L	(73)

Table 4.7: Sorption column parameters of Cu^{2+} and Pb^{2+} in a NCS3 fixed-bed column tests (83)

Table 4.8: Parameters from the linearized models for Cu^{2+} and Pb^{2+} removal. (84)

Appendix I: (112)

Table A.1.1: Chemical characterization and particle size distribution of CFBC-PCFA $65\mu\text{m}$. (113)

Nomenclature

AMD:	Acid mine drainage
GDP:	Gross domestic product
PRB:	Permeable reactive barrier
NCS:	Non-conventional sorbent
FA:	Fly ash
KCMW:	Kraft cellulose mill wastewater
PCFA:	Petroleum coke fly ash
LOI:	Loss on ignition
MSW:	Municipal solid waste
CFA:	Coal fly ash
UC:	Unburned carbon
CFBC:	Circulated fluidized bed combustion
PFBC:	Pressurized fluidized bed combustion
IGCC:	Integrated gasification combined cycle
CFBC-PCFA:	Circulated fluidized bed combustion petroleum coke fly ash
XRD	X-ray diffraction
q_e:	Sorption capacity at equilibrium (mg/g)
q_t:	Sorption capacity at any time (mg/g)
t:	Time (min or h)
k_f:	Pseudo-first-order rate constant (min^{-1})
k_s:	Pseudo-second-order rate constant (g/mg min)

K_L:	Equilibrium constant (L/mg)
C_e:	Concentration of heavy metal at equilibrium in solution (mg/L)
b:	Maximal sorption capacity (mg/g)
K_F:	Empirical constant related to maximum sorption capacity
n:	Empirical constant as indicator of sorption intensity
C/C_o:	Ratio of effluent contaminant concentration (C) to inlet contaminant concentration (C_o)
V_{eff}:	Effluent volume (mL)
h:	Bed height (cm)
q_{total}:	Total removed contaminant quantity (mg)
G:	Flow rate (mL/min)
m:	Sorbent mass (g)
K_{AB}:	Bohart-Adams rate constant (L/mg min)
K_{Th}:	Thomas rate constant (mL/g min)
K_{Y-N}:	Yoon-Nelson rate constant (min^{-1})
v:	Linear flow velocity (cm/min)
τ:	Time required for 50% sorbate breakthrough (min)
N_o:	Volumetric sorption capacity (mg/L)
<i>USA EPA-TLCP</i>:	Toxicity characteristic leaching procedure by United States Environmental Protection Agency.
<i>EN 12457-2</i>	Characterisation of waste - Leaching - Compliance test for leaching of granular waste materials and sludges - Part 2: One stage batch test at a

liquid to solid ratio of 10 l/kg for materials with particle size below 4 mm
(without or with size reduction)

<i>BL:</i>	Black liquor
<i>BET</i>	Brunauer, Emmett and Teller
<i>SEM-EDX:</i>	Scanning electron microscopy- energy-dispersive X-ray spectroscopy
<i>DS° 148:</i>	Decreto Supremo 148
<i>k:</i>	Hydraulic conductivity (m/s)
<i>SI:</i>	Saturation index
<i>BV:</i>	Bed volume
<i>m_{total}:</i>	Total contaminant quantity passed through the NCS3 fixed bed (mg)
<i>M_e²⁺:</i>	Heavy metal cation
<i>SEP:</i>	Sequential extraction procedure

CHAPTER 1:
INTRODUCTION

1 Introduction

1.1 Heavy metals contamination issues and current solutions

Heavy metals are known as elements that occur in natural and perturbed environments in small amounts and that, when present in sufficient bio-available concentrations are toxic to living organisms [1]. Their anthropogenic sources are diverse, ranging from agriculture (fertilizers, animal manures, and pesticides), metallurgy (mining, smelting, and metal finishing), energy production (leaded gasoline, battery manufacture, power plants) and microelectronics to waste scrap disposal [1][2].

Heavy metals are highly dispersed in a wide variety of economic concerning minerals. They are released during minerals extraction and a subsequent environment exposition. Therefore, mining activities are considered their primary anthropogenic source (Figure 1.1).

Mining wastes resulting from mineral extraction (waste rocks, acid mine drainage: AMD), beneficiation (tailings and acid wastewater) and further processing of metal and industrial mineral ores (smelting and electrolytic refining processes), potentially impact the lithosphere and hydrosphere and in a lower degree the atmosphere [3].

Once heavy metals, which are persistent, pass into the environment, they can not be biodegraded and thus follow a number of different pathways [4]. Heavy metals can be adsorbed onto the soil or sediments, runoff into the rivers or lakes or leached into the groundwater. In what extent, heavy metals pollution coupled with acid effluents have been damaging the environment, it is difficult to evaluate [5].

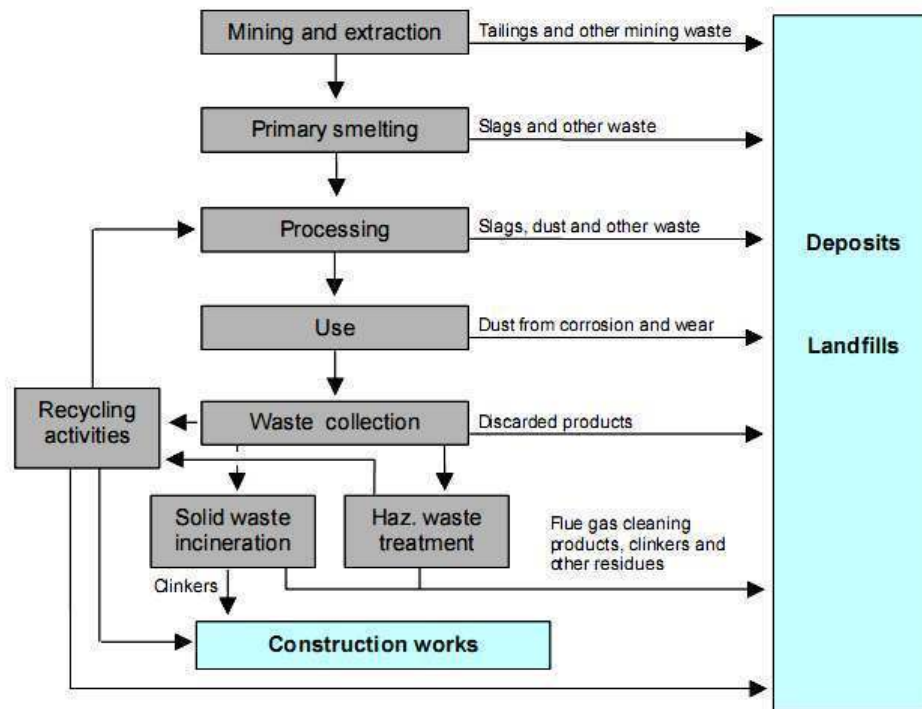


Figure 1.1: Input of heavy metals into the environment [3]

Nevertheless, it is estimated that mine effluents have affected about 19300 km of streams and rivers, 72000 ha of lakes and reservoirs by different pathways like as explained by [6]:

- Chemical: increasing acidity, soluble heavy metals concentration and others
- Physical: increasing sedimentation process and turbidity and decreasing in light penetration
- Biological: changing vital processes such as growing and reproduction of organisms due to trace elements toxicity
- Ecological: habitat modification, bioaccumulation within food chain, elimination of sensitive species.

Based on *Gray* statements [6], mine effluents should be considered a multi-factor pollutant, which must be carefully controlled worldwide. The Chilean mining sector represents about 24%

of national Gross Domestic Product (GDP) [7]. The mining sector in Chile is made up of the mining of metals, non-metals and fuels. The most important sub-sector corresponds to the mining of metals, being copper the most important metal within this sub-sector, followed by gold, molybdenum, iron and silver. The second most important sub-sector corresponds to the mining of non-metals, being iodine, saltpeter, lithium carbonate and table salt the most important within this sub-sector [8]. Taking into account data from Chilean Central Bank it can be observed that Chile is the first copper producer worldwide and just copper profit alone is about the 90% of mining sector GDP [7].

Chilean mining sector experienced in the last decade an explosive expansion [9], producing significant environmental effects, including air emissions from smelting processes, dust from mineral extraction, water contamination due to tailings or acid mine drainage, soil contamination from wastewater containing heavy metals, solid waste (sources of chemical species, such as As, Cu, Cr, Hg, SO_4^{2-} , Cd, Mo and Pb) and landscape interventions.

There is neither systematic monitoring nor specific studies of the impact of the mining activities on water quality. In Chile there is increasing interest in determining which polluting compounds are responsible for decreased water quality. Current studies of Chilean rivers have revealed an increase in the concentrations of heavy metals during the last two decades. Several authors suggested that mining discharges into important Chilean rivers (e.g., Elqui, Limarí, Choapa, and Maipo), can be important to account for high concentrations of Cu, Zn, Cd, Fe, Mn, and Pb [9][10][11][12]. According to Table 1.1, the magnitude of water pollution in Elqui River leads us to state that urgent policies are required for controlling and reducing the levels of heavy metals in Chilean rivers. Furthermore, according to the OECD, in 2005 there were 256 tailings ponds in

Chile, from which 39% are in deficient conditions [13], causing that copper, molybdates, sulfates, arsenic and high concentration of H^+ reach soil and groundwater [14].

Table 1.1: Concentration data of heavy metals in rivers of the world. Information extracted from [12]

River/Country	As	Cu	Cr	Cd	Mo	Pb	Reference
mg/L							
Mississippi/USA	3.0	2.0	0.5	0.1	-	0.2	[15]
Rhine/Germany	13.0	34.0	33.0	5.5	-	57.0	[15]
Seine/France	0.4–1.3	0.5–3.5	-	<2.4	<2.2	<1.0	[16]
Tinto/Spain	3.0–7.5	37.1–72.4	-	1.3–6.8	-	3.5–7.4	[17]
Nakkavagu/India	<116.5	-	4.6–46.8	-	-	0.2–13.8	[18]
Thames/England	2.9	4.3	0.4	-	3.2	0.4	[19]
Huanghe/China	2.7	3.3	0.3	1.2	-	4.5	[20]
Elqui/Chile	1705.0	6082.0	26.0	28.0	70.0	147.0	[12]

Therefore, it is necessary to prevent or minimize the potential negative impacts of acid wastewaters. Nowadays, among the main techniques to reduce heavy metals concentration and neutralize acid pH values from wastewaters can be mentioned chemical precipitation, ion exchange, membrane filtration, electrolytic separation, adsorption and other processes [21][22]. These techniques are involved in process such as aeration and alkaline materials addition, anoxic limestone drains, bioreactors and permeable reactive barriers (PRB) [5]. However, these technologies may present some limitations such as regarding high operational costs (e.g. activated carbon cost) and difficulties to meet strict regulatory requirements (precipitation) (Table 1.2). In some cases, the contact between sorbent and heavy metals during the removal process

produces sludge with high metallic hydroxides content, which is expensive to treat and dispose [23].

Table 1.2: Cost for conventional sorbents in heavy metal removal processes

Sorbents	Cost (US\$/kg)	Reference
activated Carbon	1.0-3.0	[24]
zeolites	0.03-0.12	[25]
NaOH	0.43	[26]
CaO	0.13	[26]
Limestone	0.024	[26]
Hydrated lime (Ca(OH) ₂)	0.08-0.1	[27]
Ionex resin (Ion exchange resins)	50-70	[28]

Due to the above mentioned disadvantages, the number of investigations focused on finding novel cost-effective alternative sorbents is growing [24][29]. Generally, alternative sorbents or reactive materials can be assumed as low cost or non-conventional sorbents (NCS), as it requires little processing, is abundant in nature or is a by-product or waste material (Table 1.3).

Table 1.3: Cost of different non-conventional sorbents

Sorbents	Cost (US\$/kg)	Reference
Chitosan	2.0-4.0	[30]
Activated slag	0.04	[31]
Peanut hulls	2.0	[32]
Coconut shell charcoal	0.25	[33]
Indian fly ash + coal (1:1)	0.03	[34]
South African fly ash	0.003	[35]

Fly ashes are considered one of the cheapest sorbents and because of their alkaline nature; it is possible to replace conventional alkaline materials by fly ashes (Table 1.3). According to *Potgieter-Vermaak et al.* [35], FA could be up to 10 times cheaper than limestone (Table 1.2), with comparable heavy metal removal effectiveness.

Numerous agricultural wastes and industrial by-products have been also studied for a potential use as inexpensive sorbents or reactive materials for heavy metals removal, such as hazelnut shell, lignin, rice husk, fly ashes and slags [29]. A wide spectrum of wastes and by-products with suitable high carbon content for NCS development has been also reported in the literature: Wastewater from Kraft pulp process and black liquor [36][37], polyethylene terephthalate [38], fly ashes [39], treated sewage sludge [40], sugar beet pulp [41], sawdust [42], tea waste [43] and biomass granules [44]. Under heating treatment, these materials give place to a carbon precursor, being the resulting NCS utilized as nutrient source and low release fertilizer or alternative activated carbon with posterior application in wastewater purification and heavy metals removal processes [45].

Two common residues in Chile are fly ash (FA) and Kraft mill cellulose wastewater (KMCW). Their relevance is related to the severe impact they have on the environment and the amounts generated. KMCW are characterized by a high organic material content [46], whereas FA is mainly composed of inorganic material [39]. The Chilean environmental protection commission (CONAMA) has approved several projects concerning petroleum coke combustion in power plants implying an increasing interest for petroleum coke fly ash (PCFA). Because of the high calcium content of PCFA, it can be considered a secondary raw material with possible use for neutralization and heavy metals removal in acid wastewaters. However, PCFA like other FA has a low particle size distribution implying a low hydraulic conductivity coupled with low heavy

metals removal efficiencies, particularly in the case of continuous column removal processes. This problem can be avoided with agglomeration techniques [38], such as blending with KMCW and a subsequent heating treatment. One advantage of the pellets resulting from this process could be a decrease in toxic trace elements leaching, which would broaden the potential application field of PCFA. Therefore, it is necessary to characterize Chilean PCFA and resulting agglomerates and evaluate possible use for neutralization and heavy metals removal in acid wastewaters.

Hypothesis

Taking into account the above mentioned issues, it can be stated that fly ashes from petroleum coke combustion are able to decontaminate acid wastewaters with high content of heavy metals by means of a permeable reactive barrier process.

1.3 Objectives

1.3.1 General objective

To evaluate the use of fly ashes from petroleum coke combustion for the decontamination of acid wastewaters with high heavy metals content.

1.3.2 Specific objectives

- i. To determine kinetic parameters for heavy metals removal from synthetic acid wastewater in batch and columns test using petroleum coke fly ashes.
- ii. To evaluate the pH effect in the neutralization capacity of petroleum coke fly ashes as permeable reactive material in batch and columns test.
- iii. To determine heavy metals removal capacity from synthetic acid wastewater using petroleum coke fly ashes in batch and columns test.
- iv. To evaluate heavy metals (Cr, Cu, Pb) chemical speciation in exhausted petroleum coke fly ashes by means of chemical sequential extraction and biogeochemical models in batch and columns test.

CHAPTER 2:
LITERATURE REVIEW

2.1 Combustion by-products: Fly ashes

The generation of combustion by-products is a global problem with severe implications for human health, environment and industry. On the one hand, high storage, transport and disposal costs must be faced by plant operators and waste management companies and, on the other hand, leaching of elements with environmental concern through the soil to the groundwater may impact negatively the terrestrial and aquatic ecosystems [47]. Nowadays industry is very interested in the reuse of such by-products as fly ashes (FA) whenever the reuse allows saving costs and to maintain the product quality as well as process stability at the same time. Many investigations are aimed to find new applications for these by-products as raw materials, simultaneously avoiding possible potential risks for the environment and human health, when they are disposed.

FA are mainly produced from combustion processes, as well as smelting, gasification and incineration processes of solid residues [49]. Understanding physical and chemical as well as mineralogical properties of FA is important because these properties influence the possibilities of FA reuse [50]. According to several reports, depending on original fuel and process, FA may present differences in their chemical reactivity, which depends on the chemical (Table 2.1) and mineralogical composition (Table 2.2) and their physical parameters.

2.1.1 Coal fly ashes

The generation of FA from coal combustion (CFA) is around 500 Mt per year worldwide [51][52]. Handling CFA is considered to be a very complex issue due to their variable composition and fine particle size. Chemically, CFA mainly consist of silica (SiO_2), alumina (Al_2O_3), calcium oxide (CaO), iron oxide (Fe_2O_3), magnesium oxide (MgO), sodium oxide

(Na₂O) and potassium oxide (K₂O), unburned carbon (UC) and sulphate (SO₄²⁻) (see Table 2.1) [49][53].

Table 2.1: Chemical composition of FA from different sources. Mean values in %w/w.

Fly ash source	SiO ₂	Al ₂ O ₃	Fe ₂ O ₃	CaO	MgO	LOI	Reference
MSW Incineration*	13.6	0.9	3.8	45.4	3.2	nd	[54]
Coal Combustion	50	27	8	5	2	4	[55]
Coal Gasification	57	19	3.8	6.4	0.8	4	[56]
Steel Smelting	8.3	6.4	49.9	24.3	8.2	2.3	[57]

LOI (%): Loss on ignition; MSW: Municipal solid waste. nd: not-detected

Table 2.2: Mineralogical compounds of FA from different sources

Fly ash source	Main Minerals	Reference
MSW Incineration	Calcite, Quartz, Zincite, Halite, Silvite	[58]
Coal Combustion	Glass, Mullite, Hematite, Magnetite, Anhydrite, Quartz	[55]
Coal Gasification	Galena, Sphalerita, Wurtzite, Pyrrhotite, Nickeline	[56]
Steel Smelting	Magnetite, Zincite, Quartz, Magnesium Aluminium Silicate	[59]

MSW: Municipal solid waste

It has been reported that CFA may contain some elements of environmental concern, such as As, Ba, Cr, Cd, Pb, Se and Hg, which can limit the potential applications of CFA [60]. The study of *Jegadeesan et al.*, based on chemical sequential extraction, concluded that the highest mobility of heavy metals in CFA was observed at pH < 4 and pH > 9 in leaching tests, depending on the distribution (affinity) of these elements [61].

Most of the CFA show a similar morphology (Figure 2.1). They consist of irregularly shaped, oval and spherical particles, such as plerospheres (larger particles filled with smaller ones) and cenospheres (hollow particles).

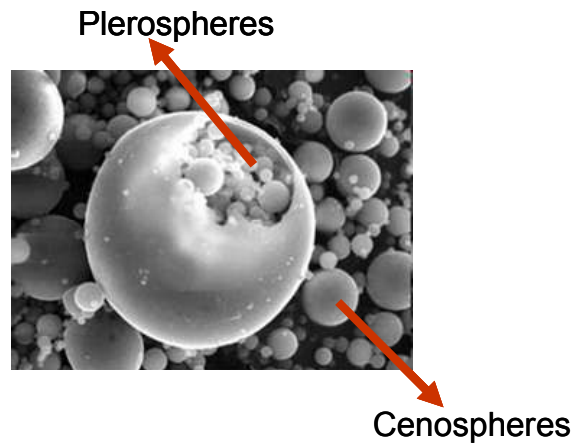


Figure 2.1: Fly ash image captured through scanning electron microscopy (SEM). Extracted from geoinfo.nmt.edu/

Other common characteristic of CFA is the particle size distribution, which normally ranges between 0.5 and 400 μm , with an average size between 12 and 80 μm . In addition the specific surface area ranges between 1.3 and 12.4 m^2/g [55]. Low grain sizes together with the presence of pozzolanic compounds in CFA could lead to a low hydraulic conductivity, which guides to think that CFA could potentially be used as a compacted mineral layer in landfills.

2.1.2 Petroleum coke fly ashes

Petroleum coke, a by-product of the petroleum refining process, is considered as an attractive primary or supplementary fuel for power generation [62], mainly because of its low price and availability [63] and due to its properties such as low volatility and high heating value [64]. Additionally, the increasing use of petroleum coke may provoke a decrease in the expected coal

mining activities [65] and an increase in the generation rate of fly ashes from the combustion of petroleum coke (PCFA).

At present, there are three main technologies that allow an efficient combustion of petroleum coke: circulating fluidized bed combustion (CFBC), pressurized fluidized bed combustion (PFBC) and integrated gasification combined cycle (IGCC). One of the most used technologies in the world is CFBC, which has gained widespread acceptance in the last years and has provided important experience in petroleum coke burning performance [66]. In CFBC technology calcium compounds such as calcite (CaCO_3) are used to remove the high sulphur dioxide (SO_2) content of petroleum coke combustion off-gases. These reactions are summarized by *Anthony & Granatstein* [67]:



During petroleum coke combustion through CFBC process, are generated mainly three particles types: (1) carbonaceous material or unburned carbon, (2) ash derived from non-combustible material and inorganic constituents from petroleum coke, and (3) particles derived from interaction between SO_2 and a sorbent (calcite or dolomite). However, according to *Anthony & Granatstein* [67], the generated ash is almost entirely constituted by particles of type “3”, as petroleum coke typically has less than 1% ash.

Regarding Equation 1 and 2, limestone particles are first calcined giving CaO as product, following a sulfation process, resulting in particles mainly constituted by calcium sulphate (Type

“3”). As seen in Figure 2.2, the generated CaO particles can undergo different sulfation patterns coupled with hydration, being the possible resulting compounds CaO, CaSO₄ and Ca(OH)₂.

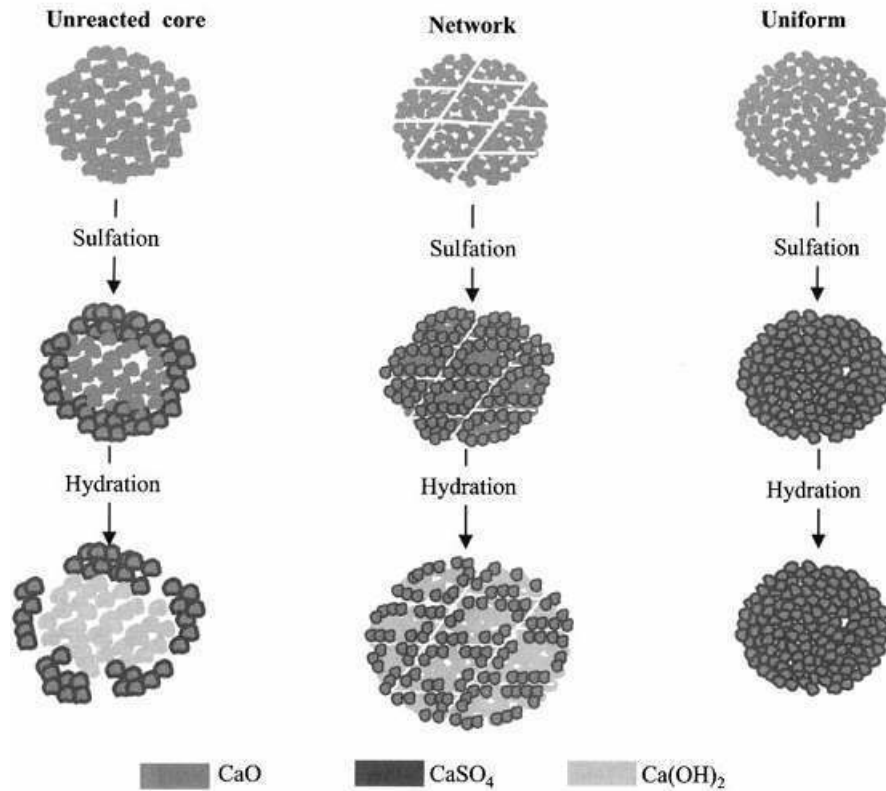
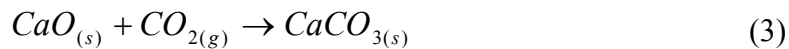


Figure 2.2: Sulfation patterns of CaO particles. Extracted from [68]

In addition, remaining unreacted CaO from calcinations process may also suffer a re-carbonation process as seen in Equation 3.



PCFA from CFBC have been characterized by *Anthony et al.* [69]. High contents of trace elements such as Mo (20 mg/kg), Sr (472 mg/kg), Ni (743 mg/kg) and V (4940 mg/kg) in CFBC-PCFA have been detected. It has been shown that V occurs mainly in large particles without any

specifically morphology and associated mostly with Ca [70]. Using routine X-ray diffraction (XRD) analysis it is difficult to determine the form of occurrence of vanadium phases in CFBC-PCFA due to the presence of major and minor mineral phases such as anhydrite, lime and calcite. However, *Jia et al.* [70] by means of wet extraction and high resolution XRD analysis deduced the occurrence of a mineral phase described as $(\text{Mg, Ca, Na, K, Fe}) \text{V}_2\text{O}_7 \cdot x\text{H}_2\text{O}$.

Research focused on the leachability of trace elements in fly ashes from coal/petroleum coke combustion has been already carried out [71][72]. These works identified changes in the quality of co-fired fly ashes from coal and petroleum coke and demonstrated that the incorporation of petroleum coke contributes to an increment in elements of environmental concern such as Ni, V, Mo and As compared to coal combustion fly ash (CFA). In fact V, Mo and As were identified as the most potentially harmful species in coal/petroleum coke combustion fly ashes. Considering the mobility of such trace elements *Henke* reported that Ni and V were found in very low concentrations in the leachate of coal/petroleum coke combustion fly ashes, with values of 7.2 mg Ni/L and 16.8 mg V/L [75]. Notwithstanding, research about the leachability of 100% CFBC-PCFA has not been performed, up to date and it will be performed in this study (See *Section 4.2*). Chemical and mineralogical composition of petroleum coke fly ashes from circulated fluidized bed combustion (CFBC-PCFA) and their possible applications have been investigated in few studies. However, it is important to characterize them and investigate the potential applications, due to the increasing production of petroleum coke as fuel.

2.2 Current applications

According to data from 2007, fly ash use in Europe is about 48% [73], whereas the cement (20%) and concrete (14%) industries are the principal application areas. Other high amounts are used in

geotechnical applications (such as grouting, asphalt filler, sub-grade stabilization, pavement base course, general engineering fill, structural fill, soil amendment and infill), representing a 11.5%, whereas for concrete blocks manufacturing account a 2.5%.

The American Coal Ash Association (ACAA) states that fly ash use in USA was about 44% in 2007 [74]. A percentage of 55% of the reused fly ashes were delivered to cement and concrete industry, whereas the contribution of reused CFA in geotechnical application was about 26%.

In relation to CFBC-PCFA, despite the occurrence of Ni, V, Sr and unburned carbon, some investigations focused on the reuse of coal/petroleum coke fly ashes or 100% CFBC-PCFA. They stated that fly ashes from coal/petroleum coke combustion could be used as concrete [76] and cement admixture [77], depending on the coal/petroleum coke fly ash ratio used. In 100% petroleum coke combustion, some authors have reported that CFBC-PCFA may be useful as sulphur-source, improving alfalfa growth and nutrient availability in soil [78]. In addition, *Thenoux et al.* [79] observed that the addition of CFBC-PCFA ameliorates and modifies mechanical properties and water susceptibility of different types of soils. *Conn et al.* [80] stated that due to the high content of calcium sulphate, CFBC-PCFA can replace gypsum in the cement industry.

2.3 Novel applications

The above mentioned applications may demand smaller quantities of fly ashes compared to the increase in their generation. Therefore, other applications and markets are necessary to be established. Current research has been focused on: fly ashes zeolitization [81]-[85], valuable elements extraction [56][86][89], low cost adsorbents development [24][30][90], geological

barriers [91]-[94], filling material in permeable reactive barriers [95]-[97] and acid mine drainage and mining residues neutralization [98]-[100].

In spite of high calcium content, the possibility of employing CFBC-PCFA for the neutralization and heavy metals removal in acid wastewaters, replacing alkaline raw material has not been reviewed.

2.3.1 Acid mine drainage remediation

Acid mine drainage (AMD) is generated by the oxidative dissolution of pyrite and other metallic sulphides, resulting from their long term exposure to oxygen and water [101]. This oxidation leads to an extremely acidic drainage, enriched with high concentrations of sulphate, iron, aluminum, manganese and other metals [102]. Among the high number of techniques to remediate or prevent AMD, the most widespread process used is the addition of neutralizing agents [103]. Nevertheless, it implies a high economical and environmental cost, because of the use of natural resources as raw materials [104]. Lignite combustion and fluidized bed combustion fly ashes could substitute alkaline materials like hydrated limestone and dolomite, because of their similar chemical composition (Table 2.3).

Table 2.3: Composition of some alkaline materials and FA (w/w %)

Compound	Limestone	Dolomite	Lignite Fly Ash	CFBC-PCFA
SiO ₂	0.5	3.3	31.2	0.7
Al ₂ O ₃	0.3	0.9	13.0	0.1
Fe ₂ O ₃	0.1	1.0	5.6	0.06
CaO	55.3	29.1	33.9	55.5
MgO	0.8	17.6	4.48	1.56
Na ₂ O	0.1	< 0.1	0.29	0.1
SO ₃	-	-	6.83	30.5
LOI	43.0	46.3	2.7	8.3
Reference	[35]	[35]	[100]	[69]

LOI: Loss on ignition

The reuse of fly ashes in the prevention and remediation of AMD has been already reported. Blends of CFA with red mud [105], CFA with bio-sludge [106], pulverized CFA [98][99][107], fluidized bed combustion fly ash [108][109] and lignite fly ash [100], have been used to prevent the release of heavy metals by means of spoils solidification or stabilization, as well as neutralizing agent for leachates from spoils and tailings. In addition, the use of fly ashes in the remediation of AMD by active chemical treatment has been reported [35][104] [110][112].

Pérez-López et al. stated that the addition of fly ashes can improve the quality of pyrite sludge [99]. They observed that pyrite oxidation was stopped, as a consequence of the formation of a ferric hydroxide coat on pyrite surface, avoiding the contact of pyrite minerals with oxygen and water. Metal immobilization and oxidation attenuation were the main mechanisms involved, which allowed a decrease in toxic metals concentrations in the drainage.

Fly ashes can be considered as a cost-effective alternative pre-treatment before lime addition. In this case, the reaction rate of fly ashes as neutralizing agent showed to be dependent on the amount and material surface area, contact time and chemical composition of the AMD [35]. Besides, in the reaction between AMD and CFA an increase in pH caused that CFA were able to precipitate more than 90% of sulfate as ettringite and gypsum. Finally, *Polat et al.* tested the neutralization of an extremely acidic sludge and stabilization of heavy metals in fly ash aggregates [113], obtaining an excellent leaching behaviour. The principal mechanisms involved in the stabilization were electrostatic adsorption and coordinative bonding of the metal cations onto neutral surface sites.

Although there is not enough information about the use of CFBC-PCFA to neutralize and reduce the heavy metals concentration in AMD, the high calcium content of CFBC-PCFA may suggest that CFBC-PCFA could be a potential neutralization material for acid wastewaters reducing heavy metals concentration by precipitation coupled with a pH change. In addition, the use of CFBC-PCFA as reactive material in PRB to remediate groundwater contaminated with AMD seems to be also an interesting future application field.

2.3.2 Filling material in permeable reactive barriers

Permeable reactive barrier (PRB) technology is used in USA and Europe to remove *in-situ* a wide spectrum of pollutants from groundwater [114]. In this technology, a reactive filling material decontaminates water plumes in the subsurface level [115]. Continuous barrier, funnel and gate, drain and gate and passive collector with batch reactor cells (Figure 2.3) are some of the PRB systems, which are employed depending on contaminant type, depth, plume size, groundwater flow characteristics and geotechnical considerations.

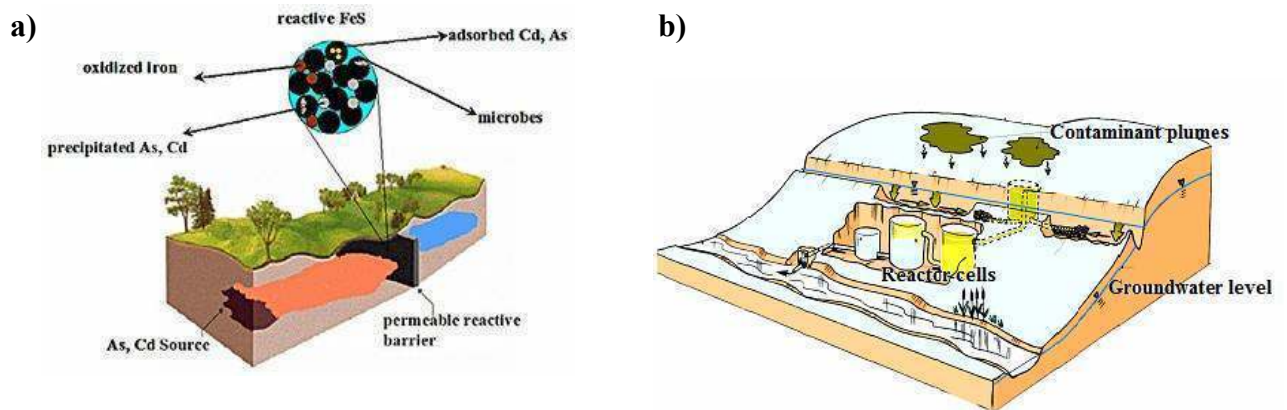


Figure 2.3: Some PRB systems; a) continuous barrier and b) passive collector with batch reactor cells, adapted from [116] and [117], respectively.

The reactive materials can therefore transform the contaminants to less harmful or environmentally immobile species, whereby the involved mechanisms are mainly degradation, precipitation and adsorption. The most employed material in current field application is zero-valent iron [118]. The extensive use of zero-valent-iron is attributed to its capability to degrade a wide spectrum of pollutants and a relative cheap cost: 0.36-0.47 US\$/kg [119][120]. In addition, other materials can also be used in PRB technology, depending on the pollutant to be removed (Table 2.4).

The use of CFA in PRB as reactive filling material to decontaminate groundwater has been studied [95]-[97][121][122]. In general, the varied chemical composition of CFA enables the removal of different pollutants and the versatility as barrier media. It is known that some fly ashes produced from lignite, coal fluidized bed and petroleum coke combustion, have high calcium content, allowing a raise in water pH up to 13, inducing heavy metals precipitation.

Table 2.4: Different reactive materials used in PRB

Contaminants	Reactive materials	References
Trichlorethylene	Surface modified zeolite	[123]
Cr(VI)	Fe(0)	[114]
As	Compost	[124]
Acid mine drainage	Fe(0)	[125]
Acid mine drainage	Compost-lime-Fe(0)	[126]
Pb, Cd, Cu, Ni, Zn	Leaf-compost material	[127]
Zn	Foundry residue	[128]
Pb, Cr(VI)	Modified fly ash	[95]
Cu, Pb, Zn	Fly ash	[129]
Nitrate, Mn	Limestone-dolomite	[130]
Sulphate	Compost and gravel	[131]
Sulphate	Fly ash	[132]

Komnitsas et al. [96] reported that lignite fly ash is effective to decontaminate extreme acidic leachates with high concentrations of heavy metals. For high initial concentrations of Fe (1500 mg/L), Al (100 mg/L), Co (5 mg/L), Ni (5 mg/L), Cu (5 mg/L), Mn (5 mg/L) and Zn (29 mg/L), after treatment, all concentrations were below detection limits. The results indicated that precipitation is not the only mechanism involved in acidic wastewaters decontamination, but also adsorption at the surface and co-precipitation. *Rostami & Silverstrim* [97] utilized alkaline activated CFA, as reactive material in PRB. The results in column tests indicated that the removal efficiencies for cadmium and chromium were near to 100% at a pH less than 4. The removal mechanisms were established to be precipitation and adsorption.

Some studies have reported that CFA use in PRB may lead to cementation problems, as well as to the formation of gelatinous compounds, causing a decrease in the hydraulic conductivity and in the removal efficiency of the reactive material [94]. On the opposite, *Prashanth et al.* [93] reported that CFA hydraulic conductivity could increase in the presence of highly acidic leachates such as acid mine drainage. One of the most studied solutions to the compaction problem of CFA is the use of feasible agglomeration techniques, to increase the hydraulic conductivity in a reactive barrier [133][134]

To select an appropriate reactive material for a PRB system, it is necessary to obtain data about the reactivity, hydraulic and environmental performance of the reactive material [135]. This data is not always available, especially for non-conventional materials like fly ashes. Therefore, batch and fixed bed column tests should be performed to acquire sorption rate constant and sorption capacity, as well as the potential leaching toxic elements through a standard leachability test.

2.4 Evaluation of a potential reactive material

2.4.1 Batch removal tests

Batch tests are a useful tool as an initial screening tool for evaluating different media and also to gain information about removal kinetics mechanisms and maximum removal capacities.

Based on the kinetic experimental data, various models have been suggested which enlighten on the sorption mechanisms and potential rate controlling steps. The models applied to examine the dynamics of the sorption process include several models such as first-order, second-order, Lagergren's pseudo-first order, Ho's pseudo-second order and the intraparticle surface diffusion model by Weber & Morris [136].

According to *Wang & Wu* [49], pseudo-first and -second-order models predict better the behavior of heterogeneous materials such as fly ashes and these can be represented by their linearized equations. The pseudo-first-order model developed by *Lagergren & Svenska* is represented by Equation 4 [137], whereas pseudo-second-order model by *McKay & Ho* [138] is represented by Equation 5.

$$\log(q_e - q_t) = \log(q_e) - \frac{k_f}{2.303} t \quad (4)$$

$$\frac{t}{q_t} = \frac{1}{k_s q_e^2} + \frac{1}{q_e} t \quad (5)$$

Where q_e and q_t (mg/g), are the sorption capacity at equilibrium and any time “t” (min) and k_f and k_s are the pseudo-first-order (min^{-1}) and -second-order (g/mg min) rate constant, respectively.

Sorption capacity can be obtained from modeling of sorption isotherms. The Langmuir (Equation 6) and Freundlich (Equation 7) models are the most frequently used models and these can be represented by the following linearized equations.

$$\frac{1}{q_e} = \frac{1}{K_L b C_e} + \frac{1}{b} \quad (6)$$

$$\log(q_e) = \log(K_F) + \frac{1}{n} \log(C_e) \quad (7)$$

Where q_e is the sorption capacity (mg/g), C_e is the concentration of heavy metal at equilibrium in solution (mg/L), the constants K_L y b represented the equilibrium constant (L/mg) and the maximal

sorption capacity (mg/g), whereas the constants K_F and n are empirical and related with the maximum sorption capacity and an indicator of sorption intensity.

2.4.2 Column removal tests

Data of fixed bed-column operations are essential for parameters determination and scale-up design. The dynamic behavior of a fixed bed column is described through the breakthrough curve (Figure 2.4).

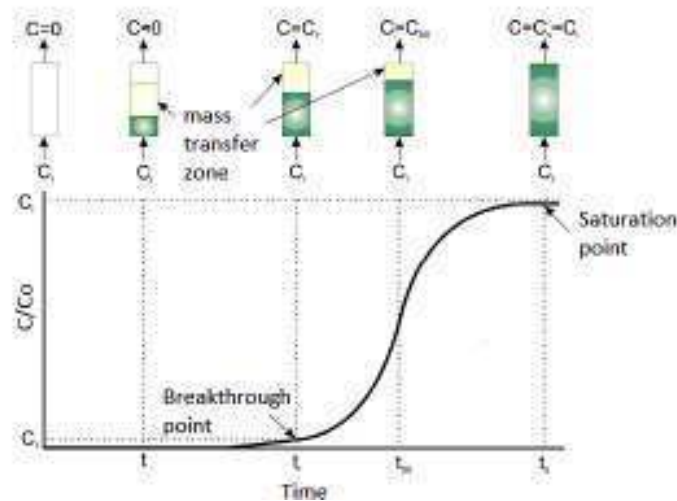


Figure 2.4: General representation of a typical s-shape breakthrough curve extracted from [133]

The breakthrough curve is usually expressed in terms of removed contaminant concentration (C_{re}) or normalized concentration (C/C_0) defined as the ratio of effluent contaminant concentration (C) to inlet contaminant concentration (C_0) as a function of flow time (t) or effluent volume (V_{eff}) for a given bed height. Total removed contaminant quantity (q_{total}) is defined by the area under the breakthrough curve (G is the flow rate), integrating the removed concentration (C_{re}) versus t or

V_{eff} (Equation 8) and column sorption capacity (q_e) is determined by the Equation 9, where m is the sorbent mass [134].

$$q_{\text{total}} = G \int_{t=0}^{t=t_{\text{total}}} C_{re} dt \quad (8)$$

$$q_e = \frac{q_{\text{total}}}{m} \quad (9)$$

Parameters such as breakthrough time and the shape of breakthrough curve are important to design and operate fixed bed columns and these depend on the operation variables [141]. Several models have been developed and applied to describe breakthrough curves and calculate fixed-bed sorption rates. Such models range over from empirical up to models with complicated numerical solutions [142]. Bohart-Adams, Thomas and Yoon-Nelson are empirical models (represented by Equation 10, 11, 12; respectively) and have been widely used due to its simplicity to determine removal rate and sorption bed capacity [143]. Nevertheless, they are not adequate to explain removal process.

$$\frac{C}{C_0} = e^{(K_{AB}C_0t) - \frac{K_{AB}N_0h}{v}} \quad (10)$$

$$\frac{C}{C_0} = \frac{1}{1 + e^{\left(\frac{K_{Th}}{G}(q_e m - C_0 V_{\text{eff}})\right)}} \quad (11)$$

$$\frac{C}{C_0} = \frac{1}{1 + e^{K_{Y-N}(\tau-t)}} \quad (12)$$

Where K_{AB} (L/mg min), K_{Th} (mL/g min), K_{Y-N} (min^{-1}) are the Bohart-Adams, Thomas and Yoon-Nelson rate constants, respectively; h is the bed height (cm); v the linear flow velocity (cm/min); τ time required for 50% sorbate breakthrough (min); N_o the sorption capacity (mg/L) and G is the flow rate (mL/min).

There are also complex models, which include mass transfer coefficients as main indicators for the sorption process. These models intend to describe and understand the process phenomena inside of the reactive material fixed bed [144]-[146].

2.4.3 Environmental performance

The evaluation of the environmental performance of reactive materials is important for predicting the potential risks of toxic elements leaching during removal or disposal process [47][61][147]. Several methods such as sequential extraction and batch and column leaching tests may simulate the leaching conditions when reactive materials such as CFBC-PCFA are exposed to water or acid wastewaters (These procedures will be treated in the *section 3 and 4*).

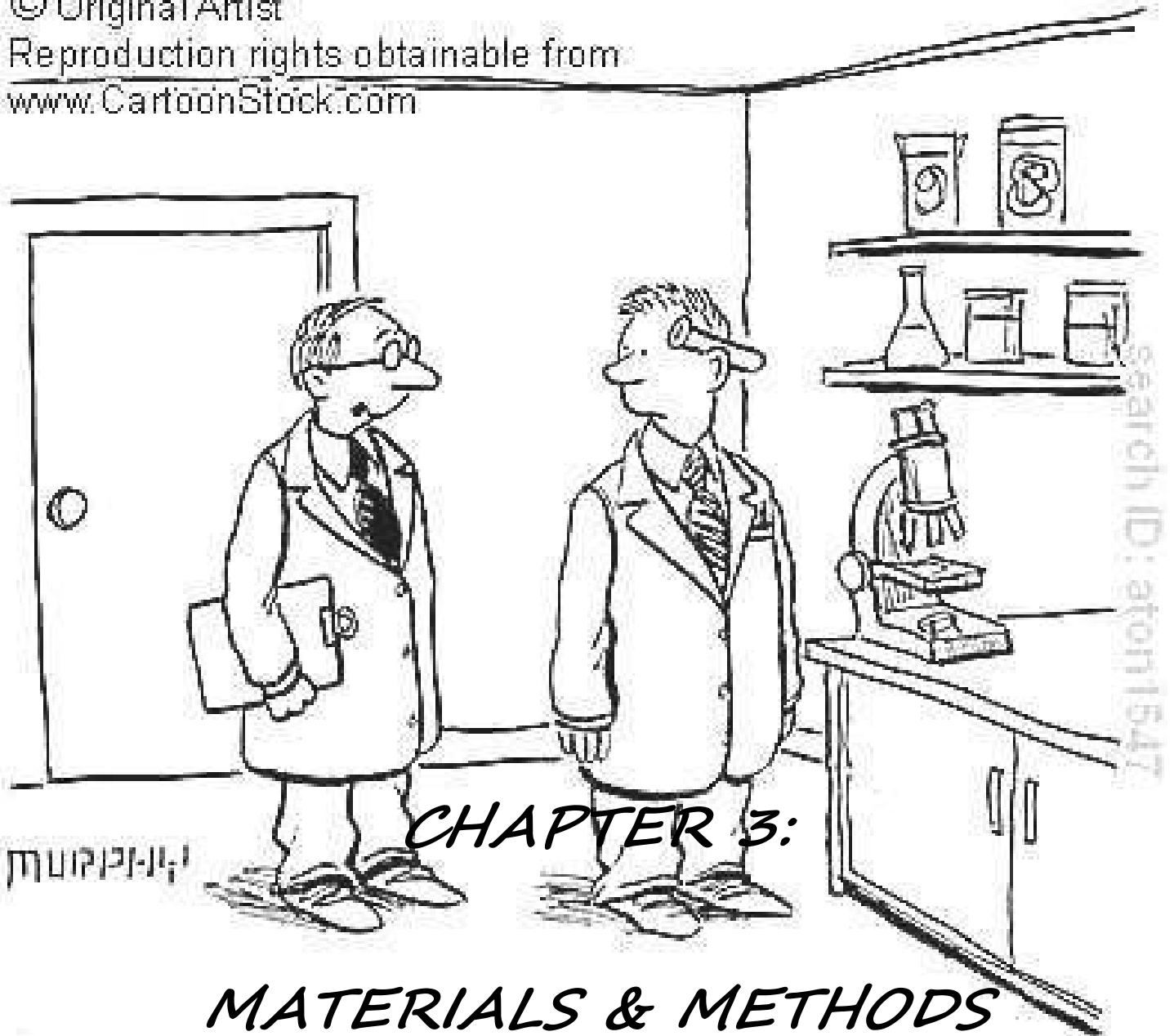
Through a sequential extraction, the mobility grade of the pollutant can be assessed. This procedure consists of a sample treatment with a series of reagents (increasing vigor) in order to partition the trace elements total content [148]. Tessier sequential extraction procedure is usually adopted by researchers [149]. Nevertheless, this approach favors trace elements leaching in acid environments, while Sposito's procedure [150] was developed for leaching under basic conditions.

Disposal or reuse of by-products like as CFBC-PCFA requires in some countries a special permit, which is related to toxic trace elements leaching from CFBC-PCFA. Batch and column tests are employed to check the leaching behavior. In USA, EPA-TCLP-1311 method [151] and

in EU the EN 12457-2 procedure [152][153], are commonly used to determine the hazardous character of wastes and by-products.

In addition, the utilization of geochemical speciation methods by means of computational programs is another available tool to determine possible risks associated to wastes and by-products. They are based on the possible equilibrium reactions and mass balance transfer in solution where it takes place. The most used biogeochemical models are GEOCHEM [154], MINTEQA2 [155] and PHREEQC [156].

© Original Artist
Reproduction rights obtainable from
www.CartoonStock.com



"They hate it when you carry the testtubes that way."

3.1 Materials

Petroleum coke fly ash

A petroleum coke fly ash sample from a circulating fluidized bed combustion power plant (CFBC-PCFA) from the Region of Bío Bío, Chile, was sampled in 2006 and 2008 and used for this study without any further treatment. Fully characterization was performed twice for sample CFBC-PCFA-2006 (2006 and 2007) and once for CFBC-PCFA-2008.

Lignimerin

An organic material recovered from a KCMW in southern Chile, called “*lignimerin*” [37], was used as the carbon precursor of NCS1. Lignimerin is constituted mainly by polyphenols (lignin and condensed tannins), carbohydrates, proteins and metal cations, corresponding to 57.0%, 22.3%, 7.4% and 6.9%, respectively.

NCS1 consisted of a blend of 6 g CFBC-PCFA, 4 g Lignimerin and 10 mL distilled water. All together were manually homogenized and dried at 65°C for 24 h. Subsequently, the dried blend was heated at 500°C for 2 h.

Black liquor

This by-product, which normally is burned in a recovery boiler to recover energy from lignin oxidation and the cooking chemicals from digester house [157], was sampled from a Chilean Kraft cellulose mill facility. According to *Demirbas* [149], black liquor (BL) consist mainly of organic material (61.8%) such as lignin, polysaccharides and resinous compounds and inorganic salts (38.1%), being sodium and potassium salts about 20% and 2%, respectively.

Black liquor (BL) was selected as carbon precursor of NCS2 and NCS3. 1000 mL of BL were evaporated at 85°C until reaching a final volume of 250 mL and a density of 1.16 g/cm³. NCS2 and NCS3 were prepared by manually blending 8.5 and 13.5 mL of BL respectively with 6 g CFBC-PCFA. Both blends were dried at 65°C for 24 h and heated at 500°C for 1h.

Chemicals

Cu²⁺ and Pb²⁺ base solutions of 1000 mg/L were prepared in distilled water for respectively removal tests using CuCl₂ and PbCl₂ salts of analytical grade Merck. A solution of 500 mg/L of Cr(VI) was prepared using K₂Cr₂O₇ of analytical grade. Base solutions were stored at 4°C. All other chemicals used were also of analytical grade.

All experiments were performed in triplicate. Reported values in this work are the average from these measurements.

3.2 Characterization analyses

NCS, CFBC-PCFA samples, spent materials from batch and column removal tests, and international reference materials (NBS 1633b and SARM 19, used as control samples in analytical methods accuracy checking) were acid-digested by using a special two step digestion method proposed by *Querol et al.* [159]. Major, minor and trace elements concentrations were determined by inductively coupled plasma atomic emission spectrometry (ICP-AES) and inductively coupled plasma mass spectrometry (ICP-MS). Hg concentration was directly analyzed on solid samples with a Mercury Analyzer LECO AMA 254. Besides, hydrofluoric acid digestion as described by *Thompson & Walsh* [160] was carried out to determine the silica content.

The mineralogical characterization of NCS, CFBC-PCFA and spent materials from batch and column removal tests was performed using a X-ray diffractometer (Bruker, D8 Advance model) with a primary Göbbel crystal, equipped with a detector based on dispersion of SOL-X energies, with a Cu tube and a wavelength of $\lambda=1.5405 \text{ \AA}$, using the work conditions at kV = 40 and mA = 40.

The physical characterization of NCSs and CFBC-PCFA samples included moisture, loss on ignition (LOI), particle size distribution, scanning electron microscopy (SEM) and BET surface area. Moisture and LOI were determined at 105 and 1050 °C, respectively [161]. NCS particle size distribution was performed through dry mechanical sieving, whereas CFBC-PCFA particle size distribution was measured by means of laser diffraction particle size analysis (Malvern Mastersize/E-model). Specific surface area was measured by BET method means of a nitrogen porosimeter NOVA 1000 (Quantachrome). SEM-EDX analyses were performed by means of a scanning electron microscope (SEM-EDX, JEOL6400) in NCS, CFBC-PCFA samples and residual materials from batch and column removal tests. Finally, the hydraulic conductivity of NCS and CFBC-PCFA samples was determined through the falling head permeability method described by *Espinosa* [162]

In order to find out a vanadium-free CFBC-PCFA fraction, CFBC-PCFA characterization was also performed with the cascade impactor instrument (Figure 3.1), which is used for the classification of particulate matter according to a specified size. This instrument permits the separation of a fraction lower than 65 μm in 7 fractions (0.4, 1, 2, 4, 9, 17 and 30 μm), to determine grain size distribution and subsequently a chemical, morphological and mineralogical characterization of each recovered fine fraction.



Figure 3.1: Cascade impactor equipment

3.3 Leaching test

Leaching tests were utilized as selection criteria among the NCS, in order to use the selected NCS for posterior applications. The NCS with the lowest concentration of elements of environmental concern in the performed leaching tests was selected.

3.3.1 Batch leaching test

The potential mobility of specific trace elements from NCS and CFBC-PCFA samples was determined according to the compliance leaching test EN 12457 Part 2 procedure [152] and comparing with the limit values from Council Decision 2003/33/EC [153]. This test is a single batch leaching test performed at a liquid/solid ratio of 10 L/kg, with an agitation time of 24 h and Milli-Q grade water as eluting agent.

Major, minor and trace elements from the leachates were analyzed by ICP-MS and ICP-AES. Hg concentration was directly analyzed with a LECO AMA 254 Mercury Analyzer and pH and electric conductivities (EC) values were measured with MYRON Ultrameter 6P pH- and conductivity-meter.

3.3.2 Column leaching test

Leaching column tests for CFBC-PCFA and NCS were performed in columns with 10 cm of height and 5 cm of diameter (Figure 3.2) according to *Querol et al.* [164]. Milli-Q grade water was employed as eluting agent with a flow rate of 0.2 mL/min. The leachates were filtered with 0.45 μm filter paper and EC and pH values were determined by means of a MYRON Ultrameter 6P pH- and conductivity-meter. Major, minor and trace elements from the leachates were also analyzed by ICP-MS and ICP-AES. Detected concentrations of elements of environmental concern in all NCS leachates were compared with the maximum permissible concentrations from Chilean regulation DS N° 148 [163].



Figure 3.2: Performance of leaching column test

3.4 Sequential extraction

To evaluate the mobility of elements of environment concern from the produced NCS, CFBC-PCFA and spent materials from batch and column removal tests, the proposed sequential extraction procedure (SEP) by *Sposito et al.* [150] was carried out. This test includes five consecutive extraction processes to extract species associated to different fractions (S1 to S5). S1 is the water soluble fraction; S2 is the weakly adsorbed fraction onto CFBC-PCFA and NCS

surface; S3 is the fraction associated to organic matter; S4 is the fraction associated to a carbonates phase and S5 is associated to a sulphide phase and non silicate matrix. Trace elements from the extractions were analyzed by ICP-MS and ICP-AES.

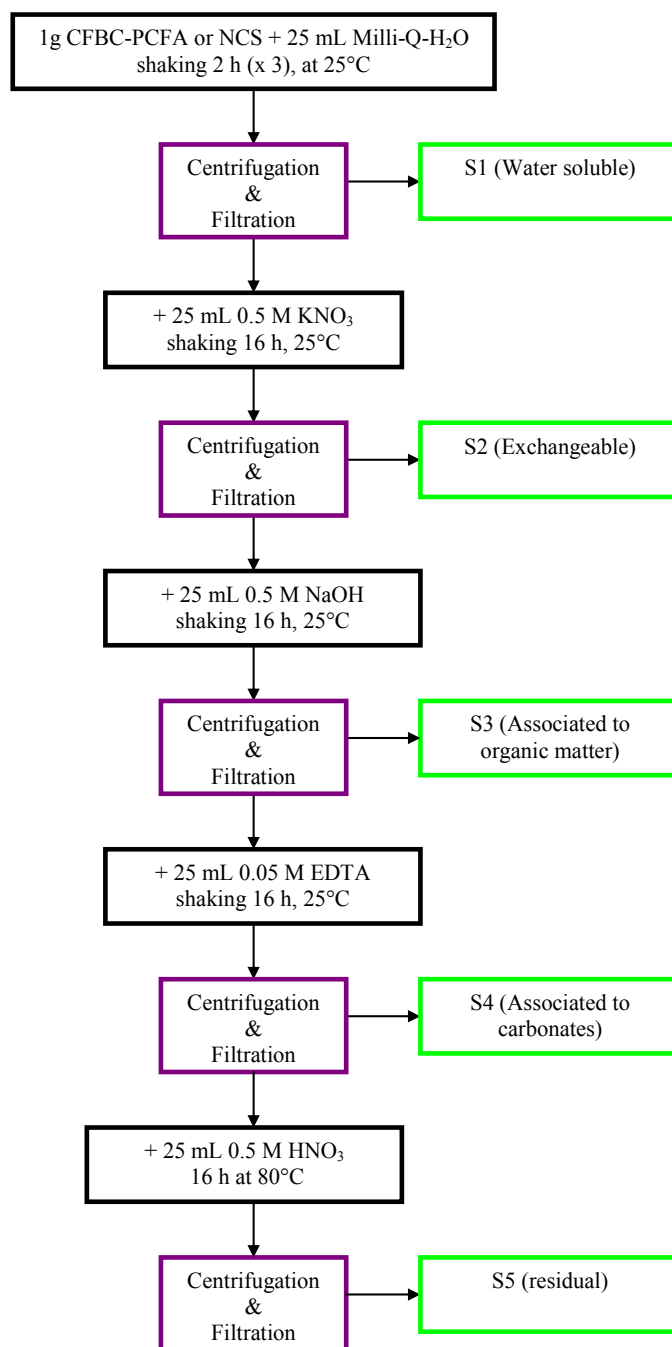


Figure 3.3: Chemical sequential extraction procedure after [150].

3.5 Batch tests

3.5.1 Neutralization trials using CFBC-PCFA

Batch neutralization tests were performed in polyethylene beakers by the addition of 1 L distilled water with different doses of CFBC-PCFA, ranging between 0.2 and 3 g/L. The pH value of distilled water was adjusted at 2, 4 and 6 with HNO₃ or NaOH 1M. After 1 h, the supernatant was collected, filtered through a 0.45µm filter, acidified and analyzed for S, Ca, Ni and V concentration by means of ICP-MS and ICP-AES. Additionally, the final pH value, total alkalinity and EC were determined.

3.5.2 Cu²⁺, Pb²⁺ and Cr(VI) removal kinetics

A predetermined amount of CFBC-PCFA sample was mixed with 45 mL distilled water in polyethylene bottles to obtain slurries of 0.2, 0.6 and 1 g/L, corresponding to 10, 30 and 50 mg of CFBC-PCFA. The dissolved Cu²⁺, Pb²⁺ and Cr(VI) was added to the bottles at pH 4 to reach a concentration of 100 mg/L for Cu²⁺ and Pb²⁺ and of 50 mg/L for Cr(VI). The bottles were stirred for 20 hours and 25°C and in different time intervals, samples were collected, filtered and analyzed residual Cu²⁺ and Pb²⁺ concentrations were determined by means of UNICAM-AAS, whereas Cr(VI) was determined by means of the colorimetric method, using diphenylcarbazide at 540 nm [165]. Moreover, pH and EC values were monitored periodically.

3.5.3 Cu²⁺, Pb²⁺ and Cr(VI) sorption isotherms

Using 0.01 g of CFBC-PCFA in polyethylene bottles containing 50 mL of test solution, sorption isotherms were carried out. Cu²⁺, Pb²⁺ and Cr(VI) concentrations in the bottles varied from 0 to 100 mg/L. The bottles were stirred for 12 h at 25°C. The supernatant was filtered, acidified and

residual Cu^{2+} and Pb^{2+} in solution were measured by means of UNICAM-AAS, while Cr(VI) was determined by a colorimetric method.

Langmuir and Freundlich models were adjusted to the resulting sorption isotherms experimental data.

3.6 Column tests

3.6.1 Neutralization trials using NCS3 and CFBC-PCFA

The effect of pH and bed height on a NCS3 fixed bed was evaluated in 1.3 cm diameter polypropylene (PP) columns. The test consisted of feeding the acid solution at pH 2 and 4 to the PP column at a flowrate of 1.5 mL/min using a peristaltic pump through the two NCS3 bed heights: 3 (h_3) and 6 (h_6) cm. The output solution was collected and filtered for pH measurements. Major, minor and trace elements in output samples from the acid solution passing through NCS3 were analyzed by ICP-MS and ICP-AES.

Similar experiment with CFBC-PCFA was performed at pH 2 at a flowrate of 0.1 mL/min.

3.6.2 Cu^{2+} and Pb^{2+} removal kinetics in fixed bed column

In fixed bed column tests, the influence of flowrate (1.5 and 5 mL/min), pH (2 and 4) and bed height variation (3 cm: h_3 and 6 cm: h_6) on the heavy metals removal capacity of NCS3 was evaluated.

Therefore, fixed bed experiments were performed in 1.3 cm diameter PP columns packed with NCS3 and at a determined bed height. Heavy metal input solution (C_0) was fed at 100 mg/L and a certain flow rate (G) and pH, using a peristaltic pump. The output solution (C) was collected

and filtered for pH measurements. Elements release from NCS3 was analyzed by ICP-MS and ICP-AES. In addition, used NCS3 was also analyzed by means of XRD and SEM-EDX.

Empirical models Bohart-Adams, Thomas and Yoon-Nelson were used to adjust to the resulting experimental breakthrough curves for obtaining the corresponding rate constants and heavy metals removal capacity.

3.7 Geochemical modeling

Mineral saturation index (SI) of selected mineral phases was calculated using PHREEQC software [156] and the MINTEQV4 database. Chemical analysis data of neutralization and removal tests were the input and used to estimate SI. Cation/anion balance ranged from 5% to 10%. When $SI = 0$, there is equilibrium between the mineral and solution; $SI < 0$ reflects under-saturation, whereas $SI > 0$ indicates super-saturation. For a state of under-saturation dissolution of the solid phase is expected, while super-saturation suggests precipitation.

CHAPTER 4:
RESULTS & DISCUSSION

4. 1 Mineralogical, chemical and physical characterization of the studied materials

Before the analysis of environmental performance of circulated fluidized bed combustion petroleum coke fly ash (CFBC-PCFA), information about main minerals, major and main trace elements from CFBC-PCFA should be gained. This information is valuable in order to target potential toxic elements and to link the chemical, mineralogical and physical properties to the behaviour of CFBC-PCFA during neutralization and heavy metals removal.

Generally, the color of fly ash can vary from tan to gray or to black [166], depending on the amount of unburned carbon in the ash. Our study object, CFBC-PCFA is visually characterized by a gray fine powder with lighter shades, suggesting the presence of relative high amounts of unburned carbon as well as Ca-bearing minerals (Figure 4.1). NCS presented a predominant black color, indicating carbonization process and higher grain size than CFBC-PCFA.

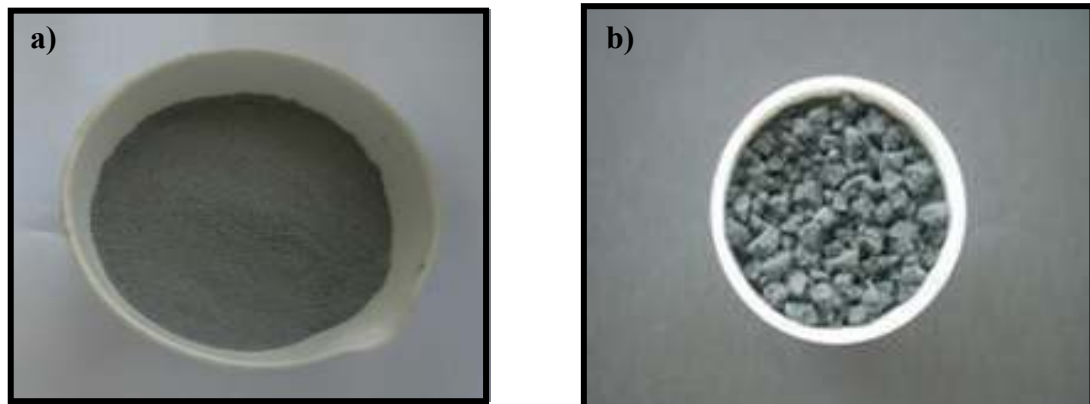


Figure 4.1: Photos of CFBC-PCFA (a) and NCS (b)

Figure 4.2 shows the X-ray diffraction (XRD) patterns of the studied materials. CFBC-PCFA samples are characterized by a predominant contribution of crystalline phases, including anhydrite (CaSO_4), which is the main compound formed in the desulphurization process [67], and portlandite (Ca(OH)_2), lime (CaO) and traces of calcite (CaCO_3) and quartz (SiO_2). These XRD results are in concordance with the major and minor crystalline mineral phases already reported by *Anthony et al.* [69] and *Jia et al.* [70].

However, CFBC-PCFA samples show some differences in their XRD patterns. The CFBC-PCFA sample analyzed in 2007 presented more defined calcite, portlandite and anhydrite peaks, whereas lime peaks disappear. This XRD pattern from CFBC-PCFA-2007 indicates a possible hydration and carbonation process of lime (See *section 2.1.2*), promoting in a long term a decrease of its reactivity. *Rao et al.* [167] has described this process and stated that fluidized bed ashes carbonation reduces the leaching toxic compounds of the ash. The detection of CFBC-PCFA carbonation process (or aging process) implies the application of new storage measurements in case of CFBC-PCFA potential applications. Regarding CFBC-PCFA valorization as reactive material, it is recommended that CFBC-PCFA should be stored in a CO_2 and moisture free environment or reused so soon as possible.

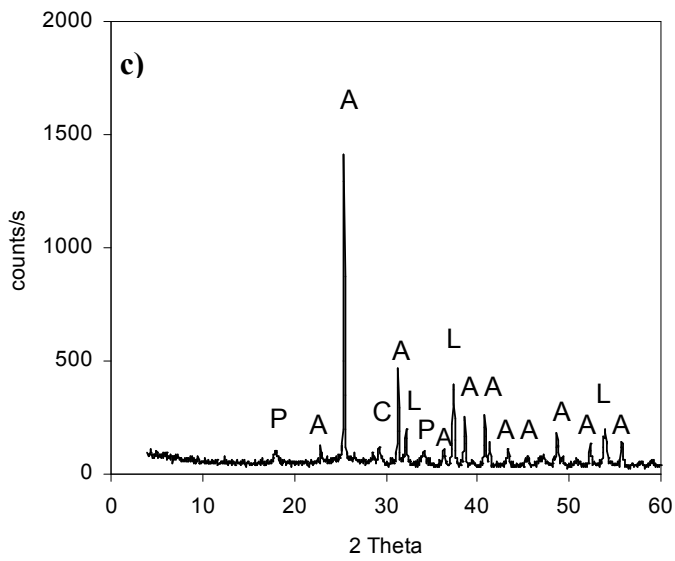
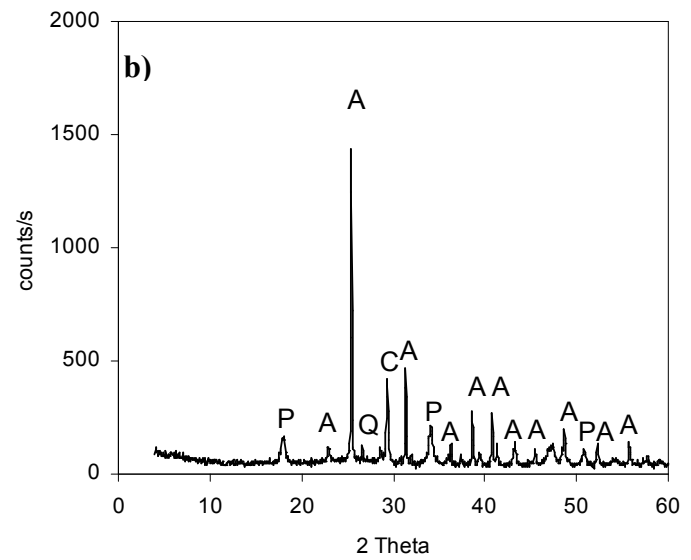
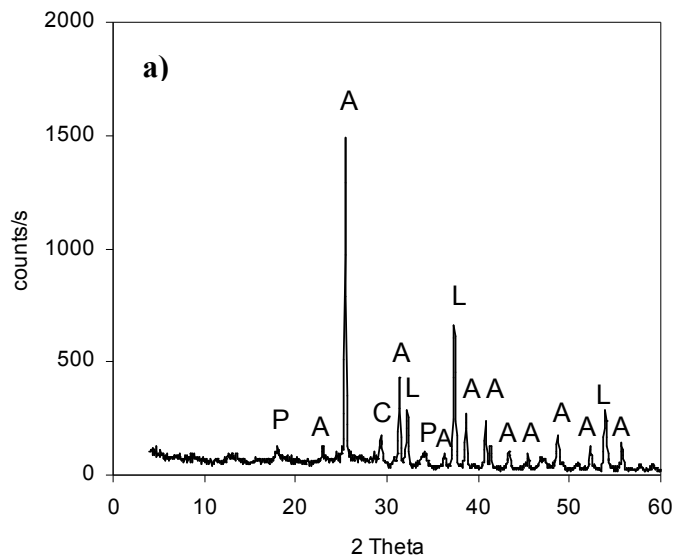


Figure 4.2: XRD results from CFBC-PCFA 2006 (a), 2007 (b) and 2008 (c). C: calcite, CaCO_3 ; A: anhydrite, CaSO_4 , L: lime, CaO and Q: quartz, SiO_2

X-ray diffraction (XRD) analysis showed that mineral phases of CFBC-PCFA, such as calcite and anhydrite were present also in NCS1, NCS2 and NCS3 (Figure 4.3). The blending between CFBC-PCFA and lignimerin or BL accounted for the synthesis of new crystalline species in NCS. Trace mineral phases were also detected: Thenardite (Na_2SO_4) for NCS1, and merwinite ($\text{Ca}_3\text{Mg}(\text{SiO}_4)_2$) for NCS2 and NCS3.

The occurrence of thenardite in NCS1 cannot be attributed to a new binding phase between lignimerin and CFBC-PCFA. A similar crystalline mineral ($\text{Na}_2\text{CO}_3\cdot\text{Na}_2\text{SO}_4$) has been detected by *Fierro et al.* [168] in lignin from Kraft processes, whereas for NCS2 and NCS3 the crystalline phase merwinite may be attributed to a new binding phase between CFBC-PCFA and BL. It is observed that except for the new phases, the three obtained NCS present similar XRD patterns compared to CFBC-PCFA. Nevertheless, the XRD peaks intensities of all crystalline species present in NCS are significantly lower than that of CFBC-PCFA, suggesting a possible coating of CFBC-PCFA by the carbonaceous material produced during the oxidation of lignimerin (NCS1) and BL (NCS2 and NCS3) increasing the amorphous phase.

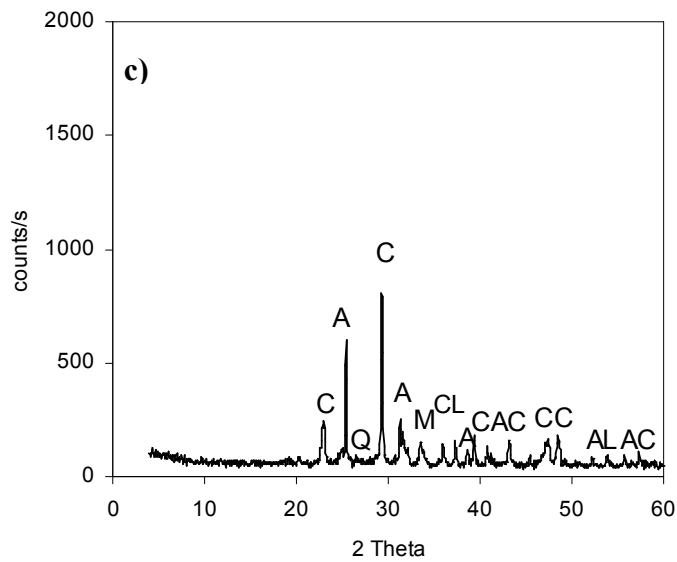
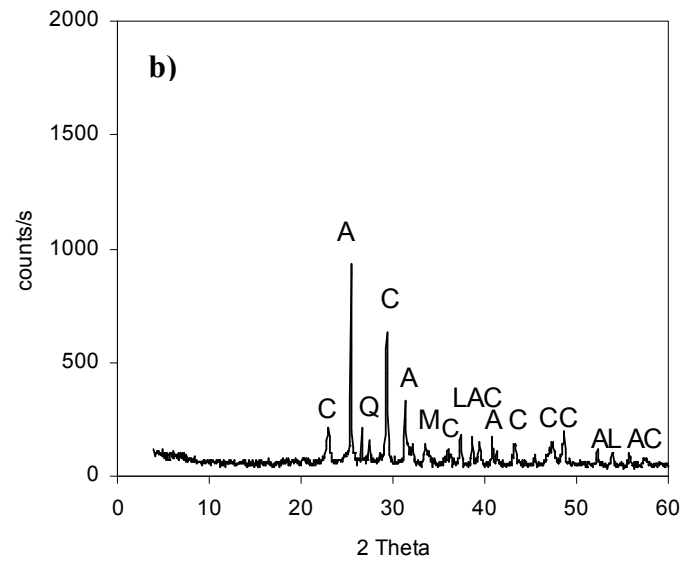
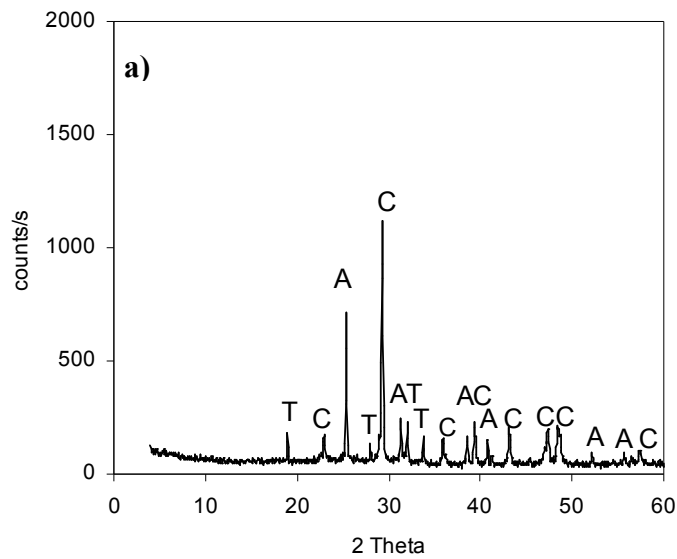


Figure 4.3: XRD pattern from NCS1 (a), NCS2 (b) and NCS3 (c). C: calcite; A: anhydrite; T: thenardite, Na_2SO_4 ; M: merwinite, $\text{Ca}_3\text{Mg}(\text{SiO}_4)_2$ and Q: quartz

Tables 4.1 and 4.2 list CFBC-PCFA major oxides and trace elements contents. Table 4.1 shows that CFBC-PCFA consists of CaO (47.0%) and SO₃ (27.3%) as major compounds. Moreover, a high Ca content (66%) is detected in the finest fractions (0.4 μm) of CFBC-PCFA samples by means of cascade impactor, suggesting high reactivity of CFBC-PCFA in aqueous media (Table A.1.1 in *Appendix I*).

Table 4.1: Major oxides present in CFBC-PCFA and NCS samples

%	CaO	SO ₃	LOI	SiO ₂	Al ₂ O ₃	Fe ₂ O ₃	MgO	Na ₂ O	K ₂ O	P ₂ O ₅	M
CFBC-PCFA ¹	47.7	27.9	22.7	0.5	0.1	0.2	0.5	0.1	<0.05	<0.05	0.42
CFBC-PCFA ²	43.7	24.3	29.7	0.6	0.1	0.1	0.4	0.1	<0.05	<0.05	0.03
CFBC-PCFA ³	44.8	29.7	23.4	1.6	0.2	0.2	0.4	0.3	<0.05	<0.05	0.01
NCS1	32.1	19.7	50.8	1.0	0.0	0.1	0.3	6.0	0.4	0.1	0.06
NCS2	31.5	24.1	52.7	1.3	0.0	0.2	0.2	8.5	0.7	<0.05	0.02
NCS3	27.6	22.2	53.4	1.2	0.0	0.2	0.2	10.5	0.8	<0.05	0.02

¹: CFBC-PCFA sampled in 2006; ²: CFBC-PCFA sampled in 2006 and characterized in 2007; ³: CFBC-PCFA sampled in 2008. M: moisture

The chemical composition of CFBC-PCFA is clearly different from that of CFA [55], but it presents some similarities regarding CaO content compared to CFBC-CFA [169] and lignite FA [170] (Figure 4.4). Regarding previous reported chemical composition of other CFBC-PCFA, it is observed that the analyzed CFBC-PCFA has major elements content in the range of those reported by *Iribarne et al.* [171] and *Anthony et al.* [69].

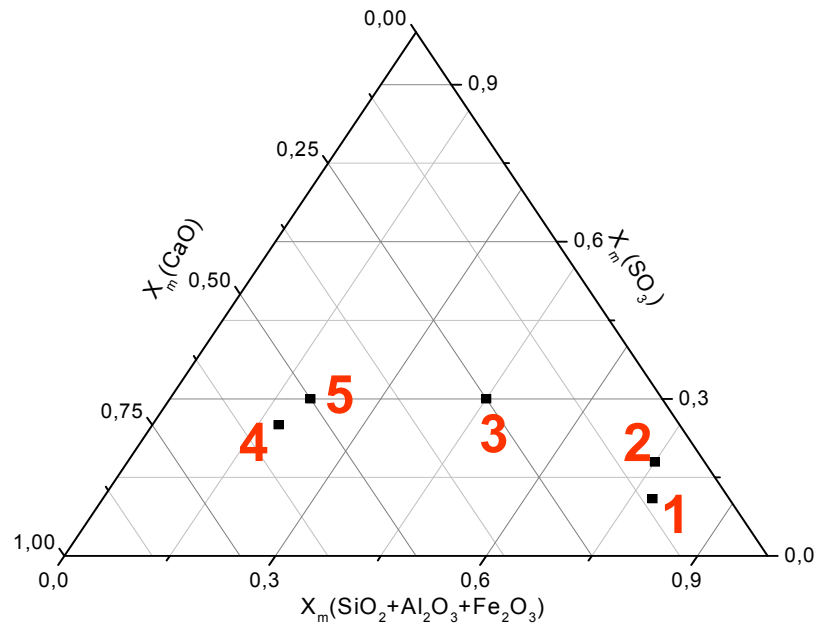


Figure 4.4: Ternary diagram of different fly ashes: (1) circulated fluidized bed combustion fly ash [169], (2) Lignite fly ash [170], (3) coal fly ash [55], (4) petroleum coke fly ash [69] and (5) petroleum coke fly ash from this study. Values reported as mass fraction (X_m).

Chemical composition of NCS is indicated in Table 4.1. It is observed that SO_4^{2-} (19.7-24.1 %), CaO (27.6-32.1 %) and Na_2O (6.0-10.5%) are the predominant oxides in NCS. These oxides were also detected in CFBC-PCFA, excepting Na_2O . Moreover SiO_2 and K_2O contents increased in NCS because lignimerin and BL are contributing to a higher content of Na, K and SiO_2 in the resulting NCS. Black liquor and KCMW (precursor of lignimerin) come from chemical Kraft pulping process, where high amounts of cooking chemicals Na_2S and NaOH are used to dissolve lignin bonded to cellulose. A temperature of 500°C in carbonization process to obtain NCS were not high enough to gasified sodium (boiling point 883°C [172]), therefore, high amounts of Na are detected in the resulting NCS.

The high CaO content detected suggests that CFBC-PCFA and NCS could be used in heavy metal removal by means of precipitation processes, in the neutralization of acid mine wastewaters and as reactive filling material in permeable reactive barriers (PRB)

The obtained LOI values between 23 and 30% of CFBC-PFA are very high compared to previous reported LOI values in other fly ashes of 3.9% [171] and 8.3% [69]. As shown in the SEM microphotography of Figure 4.5a, this may be related to the residual unburned carbon content, which corroborates the total carbon content (elemental analysis) in CFBC-PCFA, reported by *González et al.* [173]. In addition, *Brown & Dykstra* [174] stated that LOI values in fly ashes from fluidized bed combustion may be overestimated due to portlandite dehydration and carbonates calcination.

High contents of Ni (2164 mg/kg) and V (5473 mg/kg) were detected in CFBC-PCFA samples (Table 4.2) in all particle size ranges analyzed (Table A.1.1 in *Appendix I*), discarding the possible reuse of any CFBC-PCFA fraction free of V and Ni.

These results could be related to a limitation in the potential applications of CFBC-PCFA and NCS. These two elements are not considered in the environmental regulations of several countries, however, the possible leachability of these elements may be of environmental concern and leaching tests must be performed to evaluate their potential mobility. Trace elements such as As, B, Ba, Cu, Cr, Mn and Rb could also limit NCS and CFBC-PCFA potential applications. As seen in Table 4.2, Ni and V content in all NCS is lower than those of CFBC-PCFA, whereas Rb, B and Mn were found in high amounts compared to CFBC-PCFA. Copper, Cr, Mn, and Zn were found in high amount only in NCS1.

Table 4.2: Minor and trace elements in CFBC-PCFA and NCS samples

mg/kg	CFBC-PCFA	CFBC-PCFA	CFBC-PCFA	NCS1	NCS2	NCS3
	2006	2007	2008			
As	1.3	1.6	2.0	2.6	2.6	3.6
B	15.7	7.8	4.6	20.1	21.8	24.2
Ba	15.7	13.3	19.5	11.4	12.9	15.5
Co	52.1	46.7	42.4	31.5	26.0	25.3
Cr	8.4	6.8	8.4	26.8	5.5	5.5
Cu	4.8	4.1	4.7	12.5	4.3	5.2
Mn	24.6	20.6	26.0	43.3	23.7	29.6
Mo	13.4	12.6	19.6	9.2	12.9	12.6
Ni	2155.7	2569.3	3946.0	1724.4	2612.6	2536
Pb	5.8	3.2	3.8	2.6	2.6	2.4
Rb	0.0	<0.8	1.1	7.3	16.0	19.7
Sr	648.1	615.6	613.5	410.4	377.1	363.0
V	5451.6	5369.0	7701.6	3640.8	4797.5	4671.0
Zn	31.1	15.2	17.5	17.6	5.7	7.7

Regarding general particle morphology, SEM-EDX analysis (Figure 4.5a) shows that CFBC-PCFA samples are mainly composed by irregular particles including coarser porous coke-like particles of unburned carbon material with angular and sharp edges. Finer particles of Ni-, V- and Ca-bearing particles were also detected. These particles are smaller than 10 μm and are associated to coarse particles made of anhydrite and unburned carbon (Figure 4.5b). Analyses of

CFBC-PCFA samples $< 65 \mu\text{m}$ (Figure A.1.1 and A.1.2 in *Appendix I*) indicated the appearance of anhydrite in particles smaller than $10 \mu\text{m}$ and the presence of spheroid and spherical particles (Figure 4.5c), with the presence of Si and Al, corroborating chemical composition of CFBC-PCFA samples.

NCS particles morphology is shown in Figure 4.6. NCS SEM-EDX analyses show an increase of grain size and more particles with similar morphology compared to CFBC-PCFA. In NCS2 and NCS3, SEM-EDX showed that particles are coated with elements such as Na, Cl and K from BL. Environmental concern elements detected in CFBC-PCFA by SEM-EDX such as Ni and V were not detected in NCS SEM-EDX, indicating a possible covering of the inorganic fraction by the organic fraction.

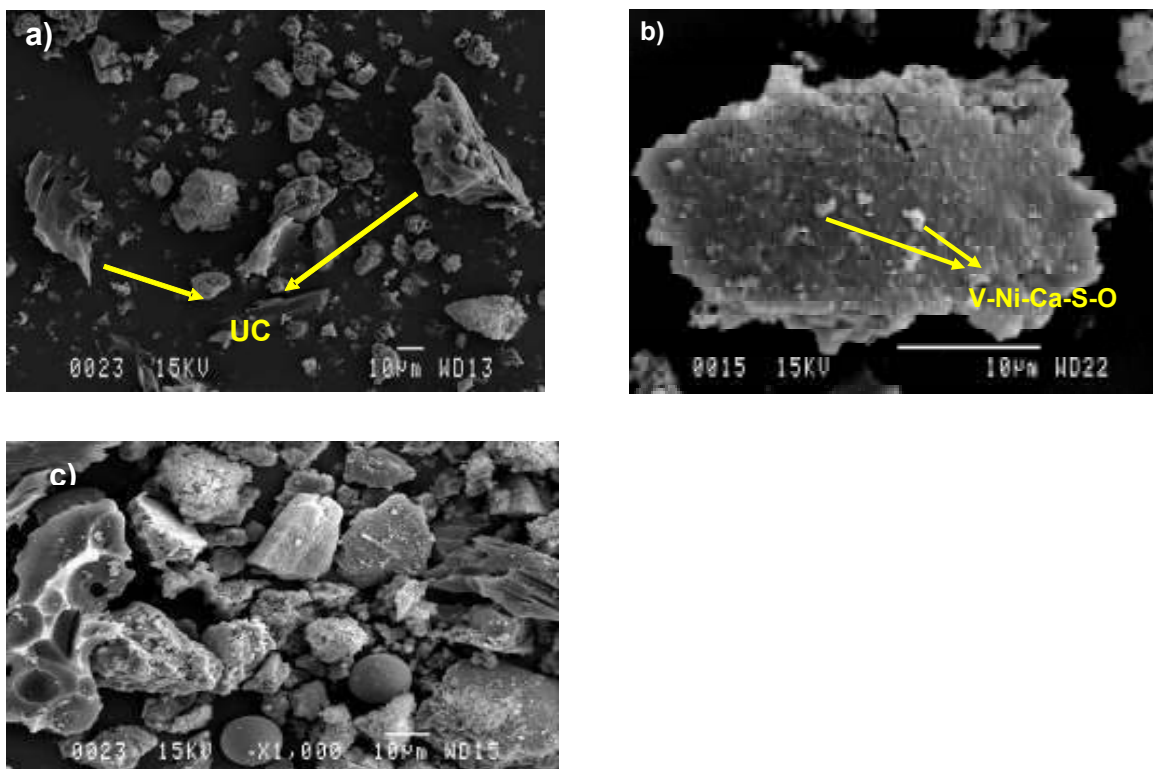


Figure 4.5: SEM coupled with energy-dispersive X-ray spectroscopy (EDX) of CFBC-PCFA samples with the presence of (a) unburned carbon (UC), (b) vanadium crystals associated to calcium and (c) spherical particles in a fraction of $17 \mu\text{m}$.

The specific surface area of CFBC-PCFA samples reached $5 \text{ m}^2/\text{g}$, a very low value compared to activated carbon (about $1000 \text{ m}^2/\text{g}$) [24], volcanic soils (about $176\text{-}223 \text{ m}^2/\text{g}$) [175] and nano zero valent iron particles ($32 \text{ m}^2/\text{g}$) [176]. However, fly ashes with specific surface area ranging between 2 and $8 \text{ m}^2/\text{g}$, have been already evaluated for possible utilization in environmental technology [177].

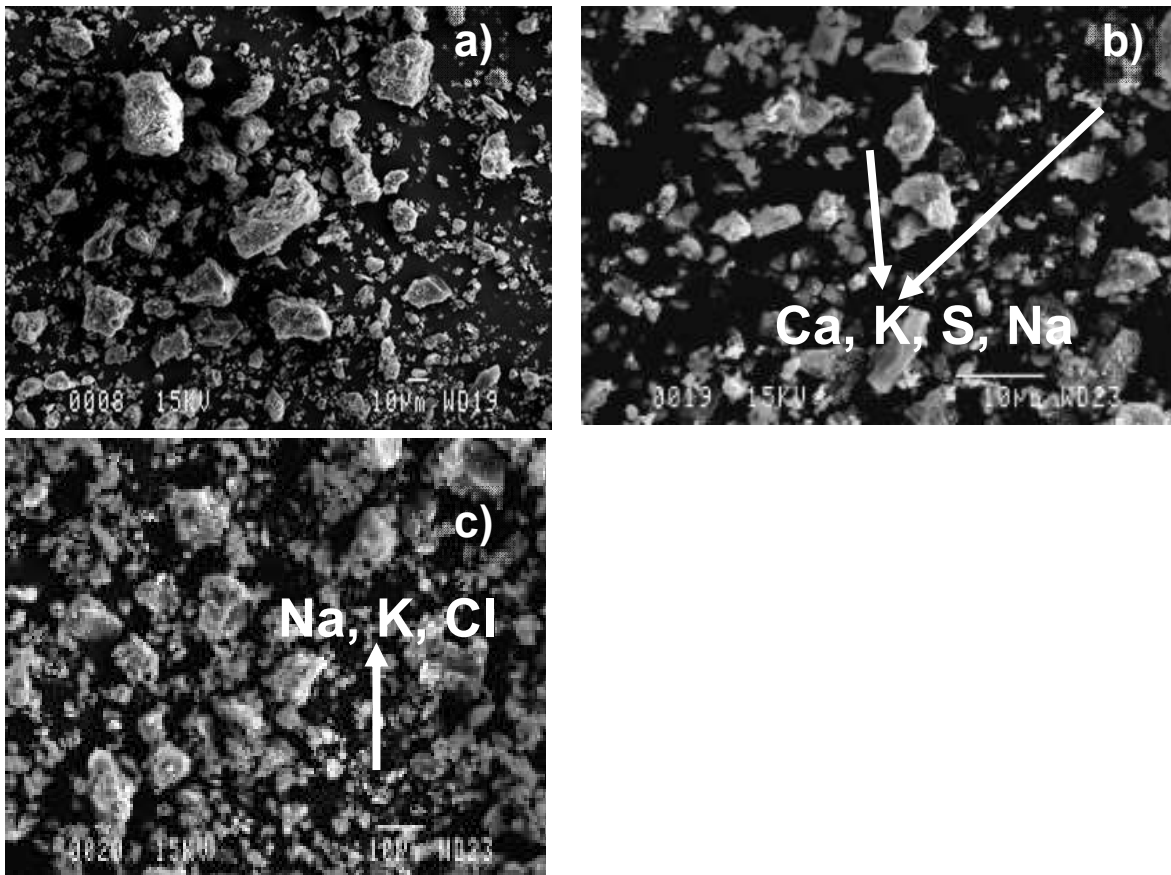


Figure 4.6: SEM-EDX of NCS1 (a), NCS2 (b) and NCS3 (c), using the same magnification

It was expected that the application of the *Zhang & Itoh* procedure to the fly ashes increases the grain size and specific surface area of the resulting NCS for posterior applications in heavy metals removal in column trials. The specific surface area of NCS was determined to be 22

(NCS1), 11 (NCS2) and 18 (NCS3) m^2/g respectively, being all values very low compared to others reported by several authors in the blend of fly ash and polyethylene terephthalate (PET) by Zhang & Itoh procedure (115-485 m^2/g) [38], in activated carbon from lignin (3000 m^2/g) [168] and alternative sorbents developed from discarded tires and sewage sludge (472 m^2/g) [40]. The measured specific surface areas of NCS were superior to the parental materials CFBC-PCFA and lignimerin (1.12 m^2/g) [178], probably as a consequence of the heating treatment (500°C).

As shown in Figure 4.7, the results on the particle size distribution analyses of CFBC-PCFA indicate a gauss-symmetric distribution with a mode value between 20 and 70 μm , being the 10, 50 and 90 percentile of 7, 29 and 85 μm respectively.

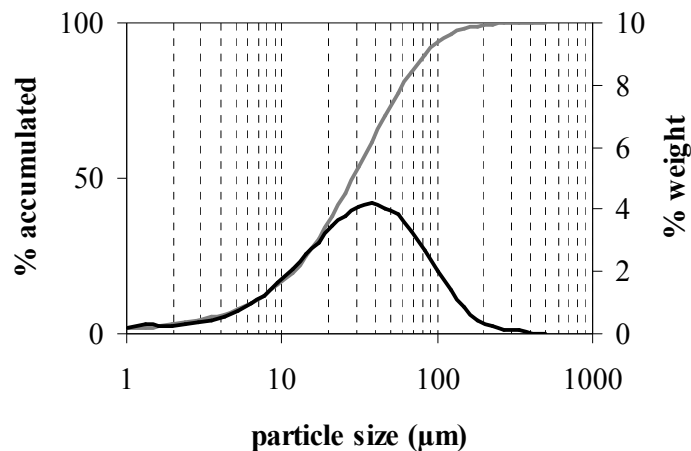


Figure 4.7: Particle size distribution of CFBC-PCFA, gray line corresponds to % accumulated and black line to % weight.

The fine particle size distribution of CFBC-PCFA will suppose an affinity of CFBC-PCFA particles to aggregate in aqueous medium. In addition, the presence of unburned carbon may increase porosity, enhancing the hydraulic conductivity of CFBC-PCFA. In the case of possible CFBC-PCFA use as reactive material in PRB, it would be mandatory to find a way of

agglomerating CFBC-PCFA particles to improve its hydraulic conductivity, simultaneously avoiding compaction problems in the filling material. Some procedures regarding the formation of pellets of such inorganic materials by using organic residues like PET bottles have been already developed [38][179]. In this case, blending process with lignimerin or BL was performed. All developed NCS presented a higher grain size than CFBC-PCFA, being for NCS1 the 10, 50 and 90 percentile, 1200, 2000 and 3350 μm respectively. Related to NCS2 and NCS3, both materials presented similar grain size distribution, being the median and 90 percentile, 1200 and 2000 μm respectively (Table 4.3). In conclusion, a higher surface area and particle size distribution was obtained for all NCS samples compared to the original fly ashes.

Table 4.3: Particle size distribution of the developed NCS

Material	10%	50%	90%
	(μm)		
CFBC-PCFA	6.5	28.3	85
NCS1	1200	2000	3350
NCS2	500	1200	2000
NCS3	250	1200	2000

Anthony et al. [180] measured the hydraulic conductivity of a CFBC-FA ($5.8 \cdot 10^{-7}$ m/s), stating that main reasons for the low value could be attributed to low particle size and chemical composition ashes. CFBC-PCFA evidenced a k value of $4.1 \cdot 10^{-6}$ m/s. This result indicates that the presence of unburned carbon in CFBC-PCFA could play an important role in the hydraulic conductivity. Nevertheless, a compaction problem can not be discarded due to the formation of precipitation products during neutralization and removal in continuous flow systems. NCS

presented higher values of k compared to CFBC-PCFA, being $7.3 \cdot 10^{-3}$, $8.5 \cdot 10^{-3}$ and $8.2 \cdot 10^{-3}$ m/s for NCS1, NCS2 and NCS3, respectively. Hydraulic conductivity values of NCS were similar as those reported for granular activated carbon used as reactive material in PRB (10^{-3} m/s) [181].

4.2 Leaching tests

4.2.1 Leaching batch test

Leaching tests are useful techniques to predict potential risks and mobility behavior of toxic trace elements from heterogeneous reactive materials such as CFBC-PCFA and could be also considered as a criteria selection among several reactive materials. As explained in *Section 2.4.3*, there are various leaching procedures, being one of them the European leaching protocol 12457-Part 2, which was performed in this study.

The results of leaching tests, regarding to the European leaching protocol 12457-2 are listed in Table 4.4. For comparison purposes the values of two CFBC-PCFA samples (from 2006 and 2008) and the limit values from the Council Decision 2003/33/EC [153] are presented.

CFBC-PCFA-2006 and NCS may be characterized as non-hazardous materials as the analyzed elements concentration did not exceed the limit values for non-hazardous wastes. According to the Council Directive 2003/33/EC, CFBC-PCFA-2008 should be considered as a hazardous waste.

In fact, CFBC-PCFA-2008 SO_4^{2-} leachate concentration (23421.4 mg/kg) is higher than the limit value for non-hazardous wastes (20000 mg/kg). Nevertheless, as this value is lower than 50000 mg/kg, CFBC-PCFA-2008 does not require any further stabilization treatment before disposal in a hazardous waste landfill.

Leachates from all materials reached alkaline pH values between 10.3-10.9 and EC between 10800 and 35900 $\mu\text{S}/\text{cm}$. pH and EC values indicate a high dissolution capacity of species, which for the two CFBC-PCFA samples are mostly associated with calcium compounds (lime, portlandite, calcite and anhydrite), whereas for NCS samples the high EC values are related to the dissolution of Ca-, Na- and K-bearing minerals.

Table 4.4: Leaching batch test values of European Norm EN 12457-2 [152]. Limit values from Council Decision 2003/33/EC [153]

	Inert	Non-hazardous	Hazardous	CFBC-PCFA ¹	CFBC-PCFA ²	NCS1	NCS2	NCS3
	Concentration (mg/kg)							
As	0.5	2	25	0.02	0.12	0.12	0.02	0.02
Ba	20	100	300	1.21	0.16	0.3	0.4	0.4
Cd	0.04	1	5	<0.01	<0.01	<0.01	<0.01	<0.01
Cr	0.5	10	70	0.2	0.17	0.06	<0.01	<0.01
Cu	2	50	100	0.03	0.02	0.05	0.05	0.1
Hg	0.01	0.2	2	<0.01	<0.01	<0.01	<0.01	<0.01
Mo	0.5	10	30	2.2	4.6	3.4	6.8	7.1
Ni	0.4	10	40	0.25	0.27	0.05	0.05	0.04
Pb	0.5	10	50	0.02	<0.01	0.02	<0.01	<0.01
Sb	0.06	0.7	5	<0.01	<0.01	0.01	<0.01	<0.01
Se	0.1	0.5	7	0.04	0.06	0.04	0.06	0.07
Zn	4	50	200	0.06	0.04	0.06	0.09	0.1
SO₄²⁻	1000	20000	50000	19335	23421.4	9766	10713	14604

¹CFBC-PCFA-2006, ²CFBC-PCFA-2008

High concentrations of sulphate and calcium were detected for CFBC-PCFA-2006 (19335 and 19508 mg/kg, respectively) and for CFBC-PCFA-2008 (23421 and 23928 mg/kg, respectively) samples. These values, coupled with the measured alkaline leaching pH indicate that anhydrite dissolved partially during the leaching test. In addition, a high Na content in leachates of NCS samples was observed, being 13026, 19987 and 23961 mg/kg for NCS1, NCS2 and NCS3 respectively, indicating that besides anhydrite dissolution, thenardite and other Na-S-compounds dissolution did occur.

In CFBC-PCFA and NCS leachate samples, Ni, Cu, Zn, Ba, Mo and V (77.9 mg/kg) were detected as the main trace elements. Concentrations of Mo and V in NCS leachates were found to be significantly higher than that of CFBC-PCFA samples. An explanation may be the change in the mobile species, attributed to the blending between both alkaline materials and subsequent heating treatment, which may increase the solubility of those elements.

4.2.2 Leaching column tests

Leaching column procedure from *Querol et al.* [159] was performed in this study. Figure 4.8 indicates that the pH values from CFBC-PCFA-2008 and NCS leaching samples range from moderate to high alkaline values. CFBC-PCFA-2008 leachate samples present a continuous pH decrease from 10.7 to 9.1, whereas NCS leaching samples reached a maximum pH value of 9.2, 10.0 and 11.0 for NCS1, NCS2 and NCS3 respectively, decreasing to 6.4, 7.5 and 9.0 during the column assays. Regarding EC in the output leaching samples, CFBC-PCFA-2008 leachate samples undergo a continuous decreasing in EC values from 4995 to 200 $\mu\text{S}/\text{cm}$, whereas NCS leachate samples showed a slight increase between 6 and 10 h, reaching a maximum of 222, 613 and 478 $\mu\text{S}/\text{cm}$ for NCS1, NCS2 and NCS3, respectively. After reaching the maximum values, a

continuous decrease was observed, leading to the conclusion that CFBC-PCFA-2008 and all NCS presented a similar time evolution pattern for pH and EC.

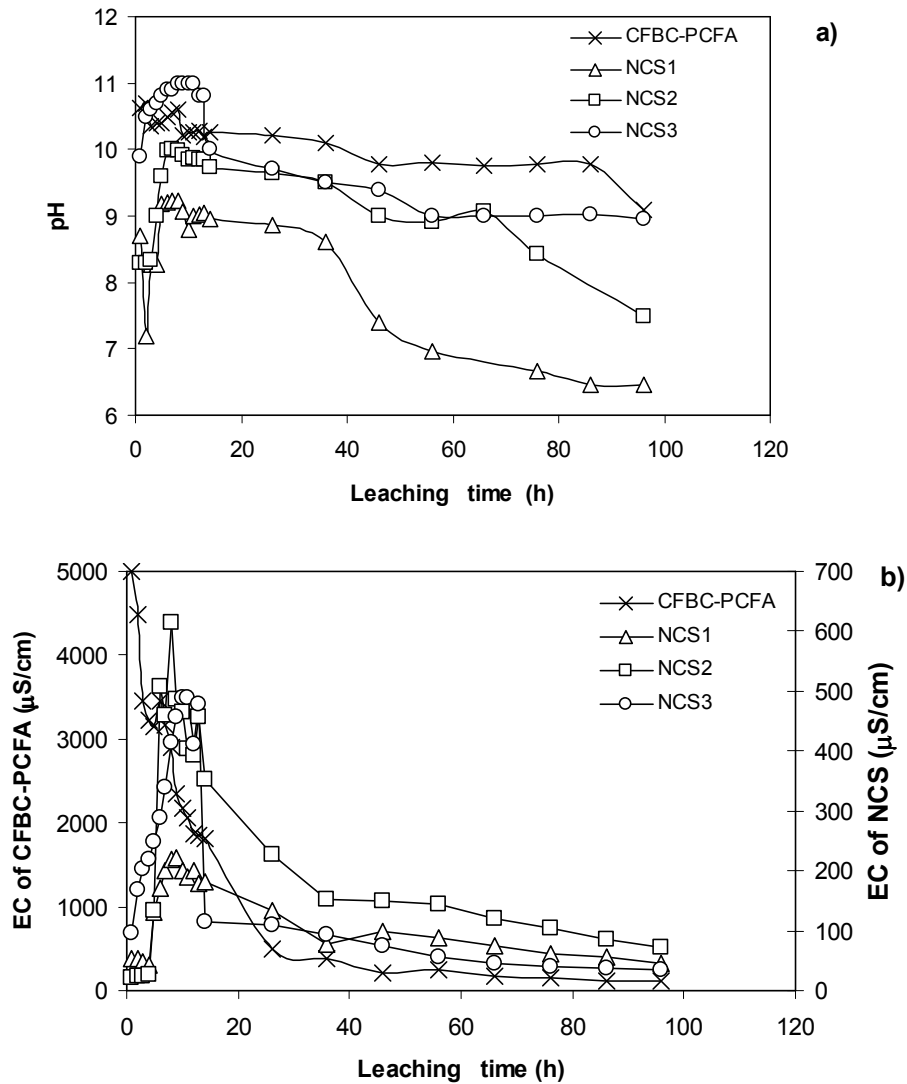


Figure 4.8: pH (a) and EC (b) during column leaching tests of CFBC-PCFA, NCS1, NCS2 and NCS3.

Figure 4.9 shows the main elements detected in the leaching samples of CFBC-PCFA and NCS columns, being Ca, Na, S (as SO_4^{2-}), Ni, Mo, V, Ba, Sr, As and Zn the most important.

CFBC-PCFA-2008 major leaching elements Ca and S (as SO_4^{2-}) initially reached maximum concentrations of 605 and 444 mg/L, respectively. Their leaching trend was similar regardless of

the evolution pattern of pH over time, indicating that Ca and SO_4^{2-} concentrations may be controlled mainly by anhydrite dissolution. This result corroborated statements from batch leaching test. Maximum values of 1.6 and 3.1 mg/L for Sr (from calcium-minerals) and V was reached at 36 h, respectively, while as highest values of Ni, Mo and Ba were lower than 80 $\mu\text{g/L}$. The detection of these trace elements could be attributed to dissolution of their water soluble salts, which commonly are enriched as finer particles attached to the CFBC-PCFA surface [171][183].

Calcium seems to play a secondary role in NCS leaching, being only low Ca concentrations detected in leachates for all NCS columns. Contrary, Na concentration in leachates increased up to 7 times (values ranging between 78 and 105 mg/L). Sulfate concentration diminished considerably (between 80 and 136 mg/L) in NCS leachate samples compared to CFBC-PCFA-2008 (444 mg/L). Apart from Sr and V detection, most trace elements associated to CFBC-PCFA were only sporadically detected. A possible reason may be that CFBC-PCFA is covered with lignimerin or BL, decreasing CFBC-PCFA elements leaching. The occurrence of Na, Zn and As in NCS leachate samples (Figure 4.9) may be also attributed to the presence of lignimerin or BL as coating, which makes those elements easily available in aqueous media. The highest values of Zn in leachates were found in NCS1 column (53.6 $\mu\text{g/L}$), and the lowest in NCS3 column (14.2 $\mu\text{g/L}$). This difference could be attributed to a higher content of inorganic salts in BL than in lignimerin, making a stronger binding between BL and CFBC-PCFA-2008 possible. Arsenic values in NCS2 leachates exceed As maximum permissible concentration from Chilean regulation DS° 148 [163], leading us to discard NCS2. In this sense, NCS3 was selected as the best option (the lowest As concentrations in leachates). As a result of the leaching column tests, NCS3 was selected as a suitable sorbent for column trials applications.

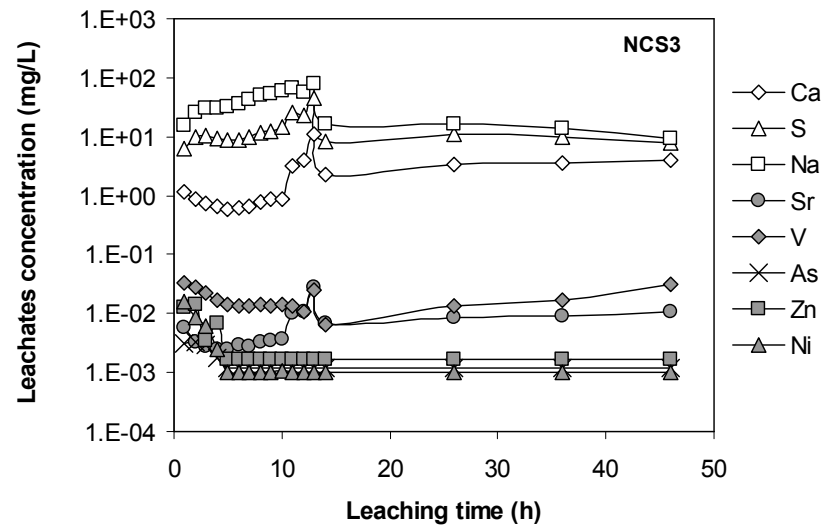
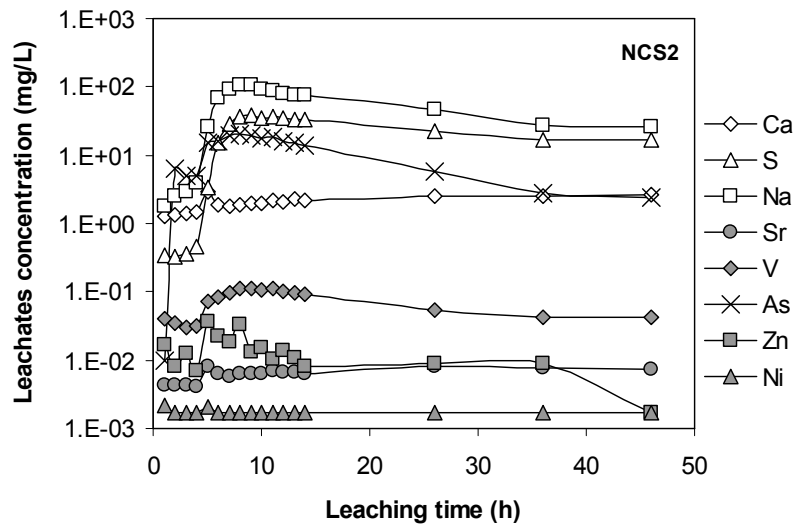
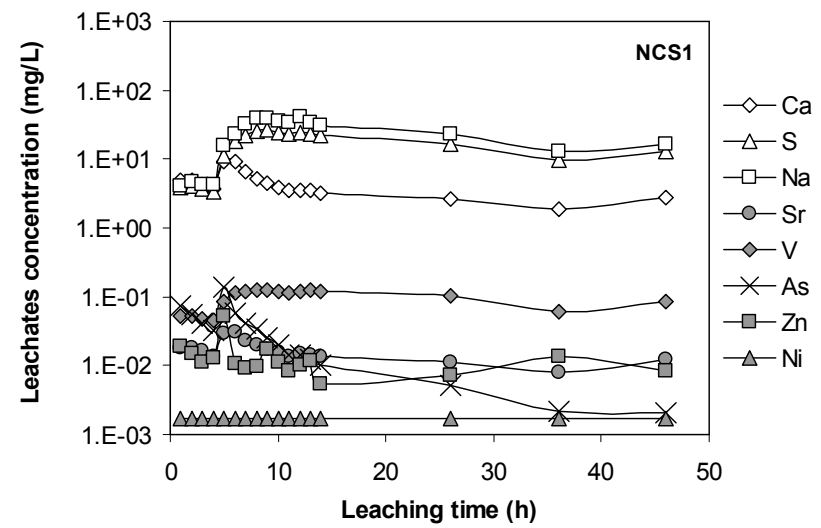
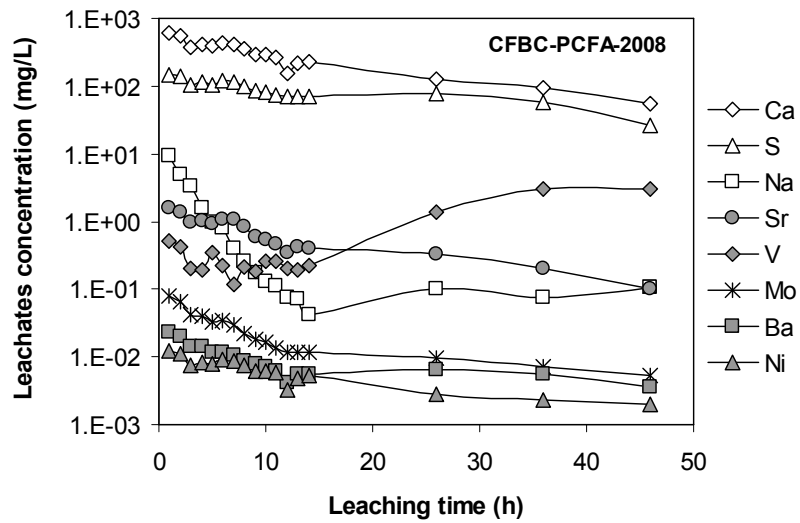


Figure 4.9: Main major and trace elements detected during column leaching test of CFBC-PCFA, NCS1, NCS2 and NCS3.

4.3 Applications in batch tests using CFBC-PCFA

4.3.1 Neutralization batch trials using CFBC-PCFA

As observed in *Section 4.1*, mineralogical characterization indicated that CFBC-PCFA is constituted by several calcium minerals such as lime, portlandite, anhydrite and calcite. In these neutralization batch tests, it is expected that CFBC-PCFA can neutralize different levels of acidity through the dissolution of detected main minerals in CFBC-PCFA. According to *Stumm & Morgan* [102], these dissolution reactions in acid conditions are represented by the equation 12 to 15.

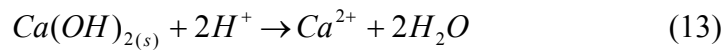
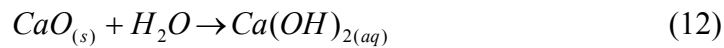


Figure 4.10 shows the values of pH, alkalinity, EC, and Ca, S and V concentrations with increasing CFBC-PCFA doses. The doses between 0.2 and 2.2 g/L at pH 2 yielded a slightly raise of pH (Figure 4.10a) and alkalinity (Figure 4.10b). The dissolution of lime, portlandite and anhydrite was not enough to neutralize the acidity, being a reason the low CFBC-PCFA amounts employed. In addition, EC high values (8602 to 3953 $\mu\text{S}/\text{cm}$: Figure 4.10c) together with Ca (as Ca^{2+}) and S (as SO_4^{2-}) high concentrations (Figure 4.10d and e) corroborated the above mentioned dissolution reactions. It is important to note that the CFBC-PCFA dose of 2.2 g/L yielded a high dissolution degree of anhydrite, which was accompanied with V high contents in

solution. However, in almost all the studied CFBC-PCFA dosage range, Ni and V presented low leachate concentrations, oscillating between 0.02 and 0.2, and 1 and 8 mg/L, respectively.

Moreover, and starting from the 2.6 g/L CFBC-PCFA dose, pH increased sharply from 2.6 to 6.7 (Figure 4.10a), whereas EC values remained stable around 1320 $\mu\text{S}/\text{cm}$ (Figure 4.10c). Levels of V in leachates show a similar behavior as calcium concentrations during this assay (Figure 4.10f), indicating that the V associations may be V-Ca-O and Ca-V-SO₄²⁻, which was observed during characterization of CFBC-PCFA (See *section 4.1*).

In case of experiments at pH 4 and 6, it is also detected Ca and S but in lower concentrations than at pH 2 (Figure 4.10d and e), indicating that portlandite, anhydrite and lime dissolve in lower degree than at pH 2 and gradually with increasing CFBC-PCFA dose. Experiment at pH 4 behaved very similar as pH 6 (Figure 4.10a), indicating that at slight acid pH, CFBC-PCFA is able to neutralize the added H⁺ at low CFBC-PCFA doses of 0.2 g/L, observing no significant differences between experiments at pH 4 and 6 (Figure 4.10a,b,c,d and e).

XRD and SEM-EDX analyses of CFBC-PCFA resulting from neutralization tests at pH 2 (using 1.4 and 2.6 g/L CFBC-PCFA) were performed. XRD patterns show peaks associated to anhydrite and calcite, being anhydrite peaks higher for the CFBC-PCFA after neutralization using 1.4 g/L compared to the 2.6 g/L dose (Figure A.2.1 in *Appendix II*). Furthermore, the disappearance of portlandite and lime peaks was observed in CFBC-PCFA after neutralization, suggesting that the gradually increase of Ca concentration may be attributed to portlandite and lime dissolution. SEM-EDX showed the disappearance of small CFBC-PCFA particles after neutralization tests, which are more reactive. According to cascade impactor results, these particles are mainly constituted by Ca (66%), which corroborates also the Ca concentration increase during neutralization tests (Figure A.1.1 and Table A.1.1 in *Appendix I*).

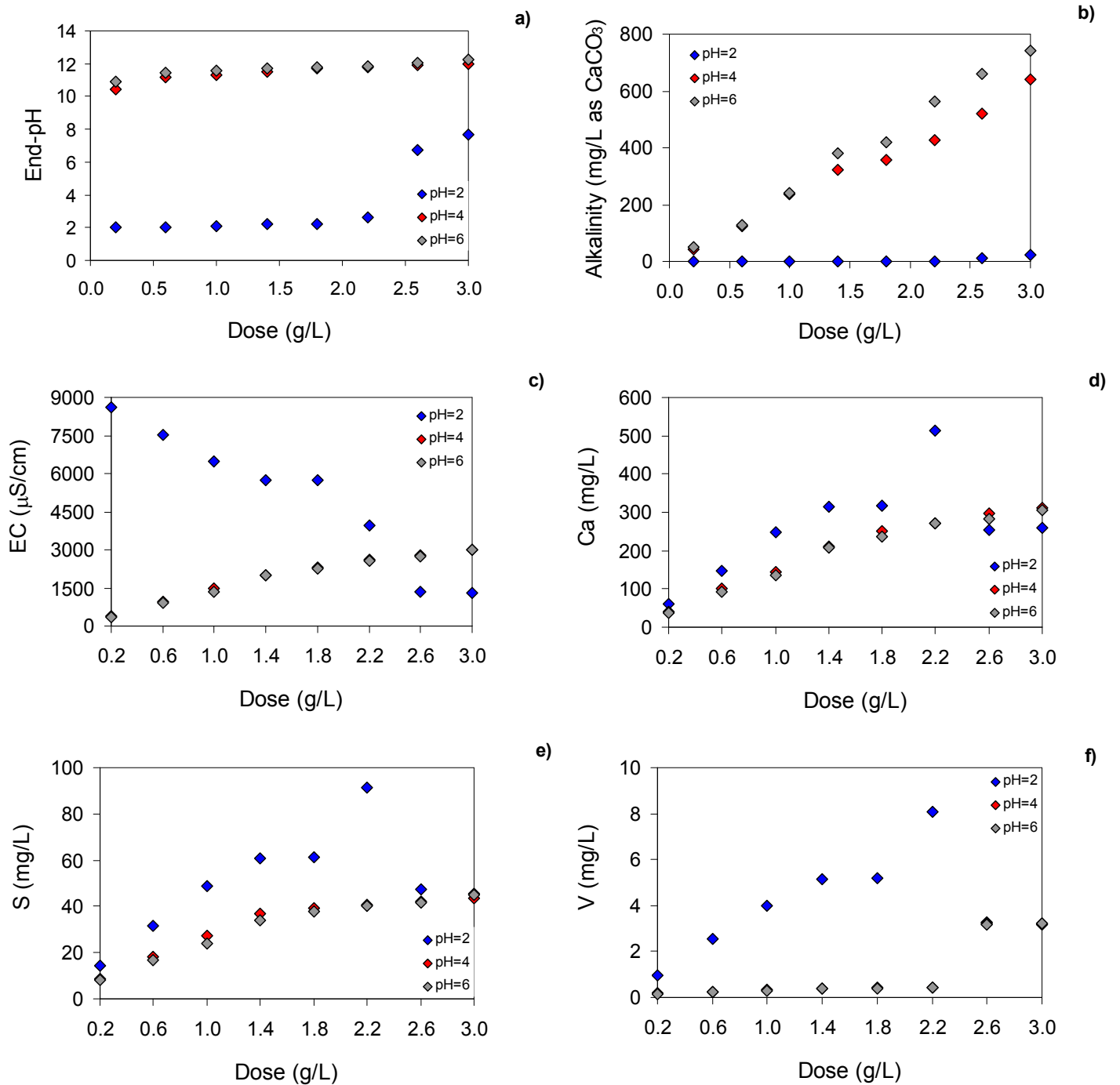


Figure 4.10: pH (a), alkalinity (b), EC (c), and Ca (d), S (e) and V concentration (f) during neutralization batch test with increasing CFBC-PCFA dose from 0.2 to 3 g/L at pH 2, 4 and 6 at 25°C.

4.3.2 Cu^{2+} , Pb^{2+} and Cr(VI) removal kinetics

Among the several mechanisms proposed in heavy metals removal using fly ashes, surface precipitation and chemical adsorption seem to play the dominant role in heavy metal cations removal [184]. Petroleum coke fly ash from circulated fluidized bed combustion presents an isoelectric point (IEP) value of 3.3 (Figure A.3.1 in *Appendix III*). This means that CFBC-PCFA is negatively charged in almost all the pH range, being able to attract metal cations. In addition, the alkaline characteristics of aqueous leachate obtained from CFBC-PCFA in conjunction with CaO , Ca(OH)_2 and CaSO_4 constituents of this material should account for hydrolytic metal precipitation reactions.

4.3.2.1 Cu^{2+} removal kinetics

The removal kinetics for Cu^{2+} at variable pH and at the CFBC-PCFA doses 0.2, 0.6 and 1 g/L is shown in Figure 4.11. All the dosages applied showed high removal efficiencies (between 90 and 99%). The lowest removal efficiency value (90%) corresponded to the dose of 0.2 g/L, reaching equilibrium at 4 h, whereas the highest (99%) corresponded to the 0.6 and 1 g/L dose.

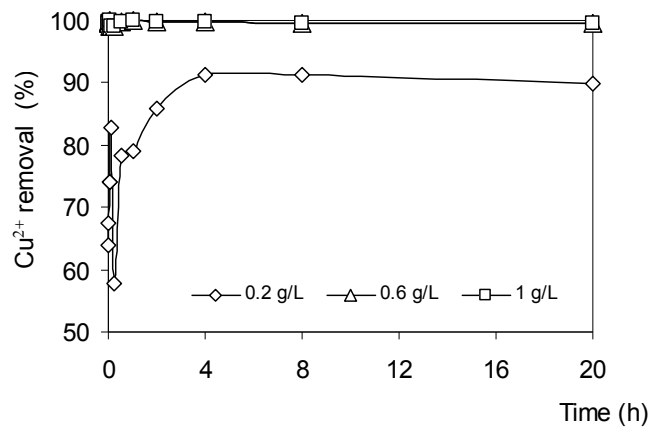


Figure 4.11: Cu^{2+} removal kinetic test at 25°C and 0.1M KCl using CFBC-PCFA doses of 0.2, 0.6 and 1 g/L

Similar results have been reported by *Bayat* [185] and *Alinnor* [186], showing Cu^{2+} removal efficiencies between 80% and 91% using CFA at similar experimental conditions.

The predominant species predicted by PHREEQC at pH values between 5.8 and 6.2 (Figure A.4.1-A.5.1 in *Appendix IV and V*) are Cu^{2+} , CuOH^+ , $\text{Cu}_2(\text{OH})_2^{2+}$ and CuSO_4 , accounting for fast 90% of the species. The positively charged species experience an attraction to CFBC-PCFA surface. Regarding Cu^{2+} removal conditions, geochemical program indicated super-saturation of the minerals antlerite ($\text{Cu}_3(\text{OH})_4\text{SO}_4$), brochantite ($\text{Cu}_4(\text{OH})_6\text{SO}_4$) and malachite ($\text{Cu}_2(\text{OH})_2\text{CO}_3$). From these results, it can be suggested that in high degree copper is removed from bulk solution through precipitation of CuSO_4 . Small percent of copper is removed through adsorption onto CFBC-PCFA.

Cu^{2+} removal kinetics using a 0.2g/L dose showed two different stages (Figure 4.11): (1) between 0 and 8 min, visually detecting flock formation in the solution (between CFBC-PCFA and Cu^{2+}) and (2) starting on 16 min until 20 h, observing flock disappearance. To explain this particular behavior, SEM-EDX and XRD of CFBC-PCFA before 8 min and at 20 h were performed (Figure 4.12). Both materials showed the formation of a crystalline mineral of posnjakite ($\text{Cu}_4\text{SO}_4(\text{OH})_6\text{H}_2\text{O}$), detecting as main differences, the crystallization degree and morphology. The CFBC-PCFA before 8 min shows other crystalline mineral phases from raw CFBC-PCFA (Figure 4.12a), whereas spent CFBC-PCFA obtained at 20 h exhibits a high intensity of XRD patterns of posnjakite (Figure 4.12b). On the one hand, SEM-EDX analysis indicated like-gel embedded particles in the CFBC-PCFA obtained before 8 min, mainly composed by Cu. On the other hand, in CFBC-PCFA at 20 h a different morphology was observed, posnjakite coating of CFBC-PCFA surface. It can be concluded that during Cu^{2+} removal, the main involved

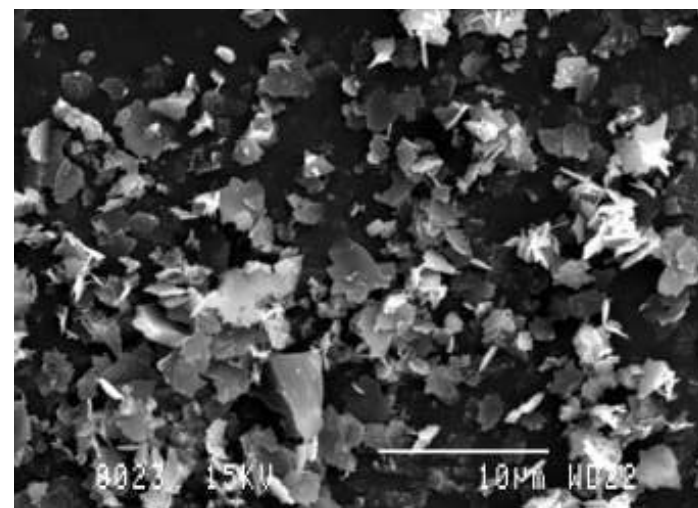
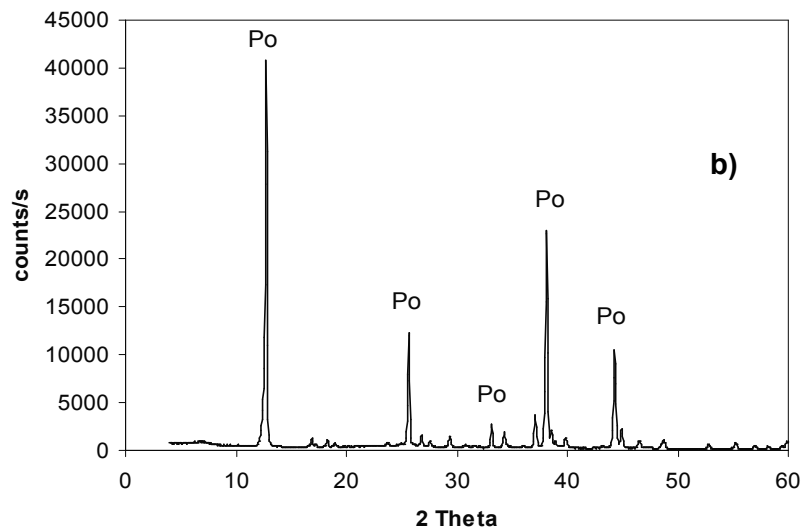
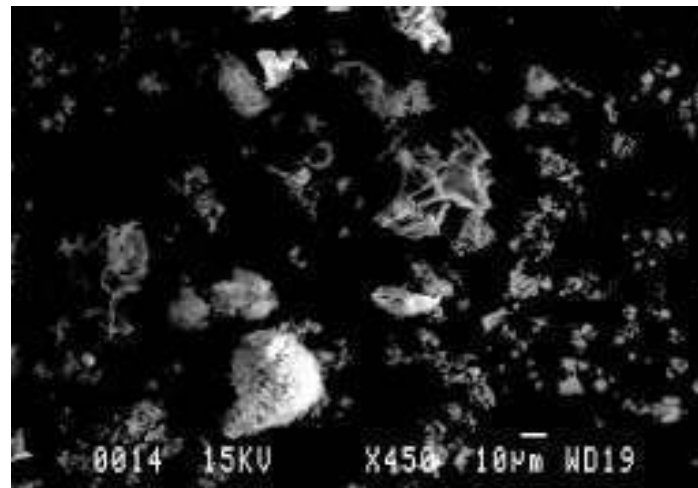
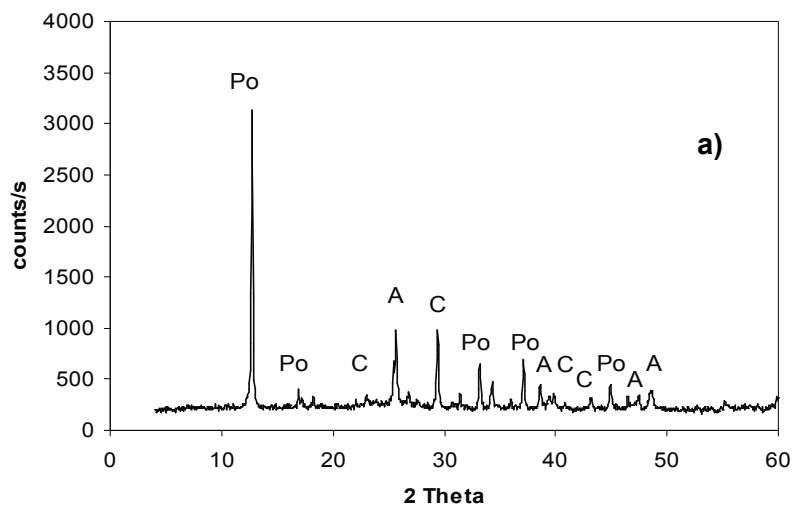


Figure 4.12: SEM-EDX and XRD of CFBC-PCFA from Cu^{2+} removal kinetics test, (a) at 8 min and (b) at 20 h. Po: posnjakite, $\text{Cu}_4\text{SO}_4(\text{OH})_6\text{H}_2\text{O}$; A: anhydrite and C: calcite

mechanism could be precipitation of copper sulfate compounds onto CFBC-PCFA surface, corroborated by the formation of the posnjakite mineral phase.

4.3.2.2 Pb^{2+} removal kinetics

Regarding to the used CFBC-PCFA doses it is observed that all of them reached high values of Pb^{2+} removal efficiency, ranging between 87.0 and 96.6% (Figure 4.13). The lowest removal value (87%) corresponded to the dose of 0.2 g/L CFBC-PCFA, whereas the highest value (96.6%) corresponded to the dose of 1 g/L. Regarding the equilibrium time, it is observed that the three doses reached the equilibrium at about 4 h.

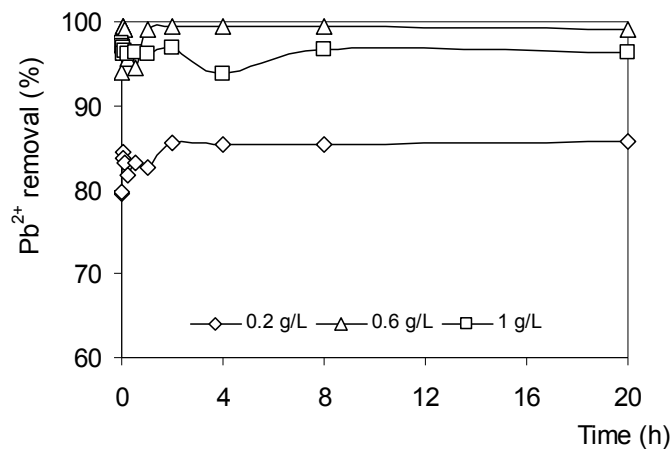


Figure 4.13: Pb^{2+} removal kinetics test at 25°C and 0.1M KCl using CFBC-PCFA doses of 0.2, 0.6 and 1 g/L

A fast Pb^{2+} removal process was observed, being the pH values almost constant and alkaline during the performed experiments. Regarding Pb^{2+} removal at pH between 10.5-10.8, the predominant species predicted by PHREEQC are $Pb(OH)_4^{2-}$, $Pb(OH)_3^-$, $Pb(OH)_2$, $PbOH^+$, $Pb_3(OH)_4^{2+}$ and $Pb_4(OH)_4^{4+}$, accounting for fast 100% of the species (Figure A.4.2-A.5.2 in *Appendix IV and V*). The geochemical program PHREEQC predicted, under the studied Pb^{2+}

removal conditions, the super-saturation of $\text{Pb}(\text{OH})_2$, $\text{Pb}_3(\text{OH})_2(\text{CO}_3)_2$, PbCO_3 and SO_4^{2-} -bearing minerals such as $\text{Pb}_4(\text{OH})_6\text{SO}_4$ and $\text{Pb}_4\text{O}_3\text{SO}_4$, accounting for 30% of lead species (positively charged). Therefore, part of lead removed suffers precipitation onto CFBC-PCFA surface with carbonates and sulfates present in solution. The negatively charged lead species could suffer a specific interaction with the CFBC-PCFA surface (with specific sites of CFBC-PCFA, being possible cation exchange with Ca^{2+}). Pb^{2+} removal kinetics may be attributed to surface precipitation and adsorption, although a precipitated mineral phase (as observed in copper removal) was visually not detected. The resulting CFBC-PCFA after Pb^{2+} was analyzed by SEM-EDX and XRD. SEM-EDX (Figure 4.14) shows a pale powder onto CFBC-PCFA particles, containing Pb, S and O, suggesting the formation of a new solid phase (probably a lead sulfate compound), which was not detected by XRD, but was predicted by PHREEQC.

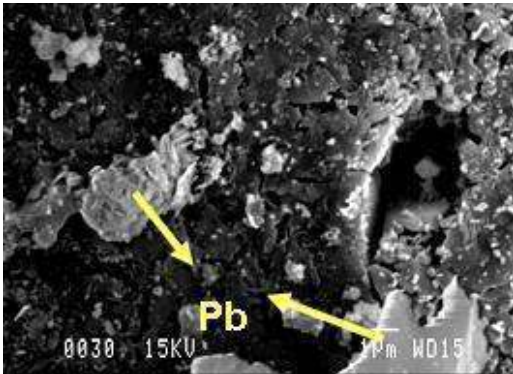


Figure 4.14: SEM-EDX of CFBC-PCFA from Pb^{2+} removal kinetics test

4.3.2.3 *Cr(VI) removal kinetics*

Removal of Cr(VI) by CFBC-PCFA was very fast as shown in Figure 4.15, reaching the equilibrium at 3 h for the CFBC-PCFA doses 0.2 and 0.6 g/L, and obtaining a removal efficiency of 97%.

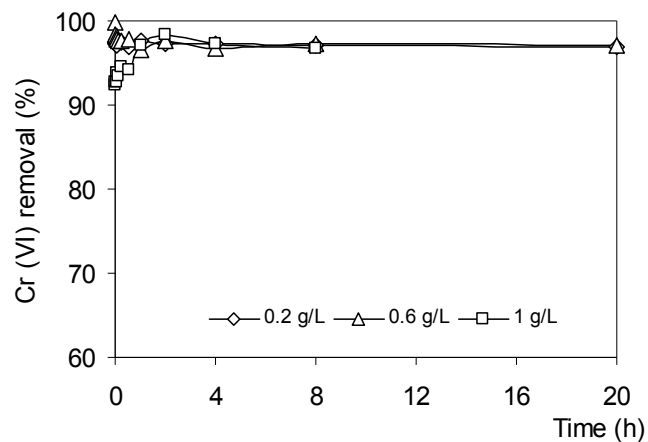


Figure 4.15: Cr(VI) removal kinetics test using CFBC-PCFA doses of 0.2, 0.6 and 1 g/L at 25°C and 0.1M KCl

Rao et al. [187] showed similar results, reaching Cr(VI) removal efficiencies of about 96% at equilibrium time using bagasse fly ash. Furthermore, *Mohan & Pittman* [188] reviewed information about aqueous removal of Cr(VI) using coal fly ashes. They clearly stated that lime content in coal fly ash seems to play a significant role in Cr(VI) removal.

During Cr(VI) removal, pH value ranged between 6.4-7.6. The predominant species (HCrO_4^- with 43% and CrO_4^{2-} with 40%) detected for Cr(VI) by PHREEQC are all negatively charged (Figure A.4.3-A.5.3 in *Appendix IV and V*), indicating that Cr(VI) species experienced repulsion from CFBC-PCFA surface. This leads us to state that Cr(VI) removal mechanism could not be attributed to adsorption. Moreover, in our experiments, an almost instantaneous color change (Figure 4.16) was observed, indicating a possible reduction of Cr(VI) as the species CrO_4^{2-} to Cr(III) from orange to green for all probed doses.

The results obtained from the geochemical model PHREEQC did not evidenced a clear trend regarding Cr(VI) reduction. However, after Cr(VI) reduction, PHREEQC predicted that a precipitation process occurs, being the predominant species amorphous $\text{Cr}(\text{OH})_3$ (stable between pH 4-7) and Cr_2O_3 .



Figure 4.16: Evidence about color change during Cr(VI) removal*.

Analyses by means of SEM-EDX and XRD were performed to the CFBC-PCFA after Cr(VI) removal kinetics test, to find the differences between raw CFBC-PCFA and residual CFBC-PCFA. The appearance of other mineral phases was not observed in this case, but calcite peaks increased in intensity. Additionally, Cr was not detected by SEM-EDX analysis (Figure 4.17). However, a grain size decrease of the calcium crystals was observed, indicating possible dissolution of calcium-containing minerals and subsequent of small Ca-bearing particles formation.

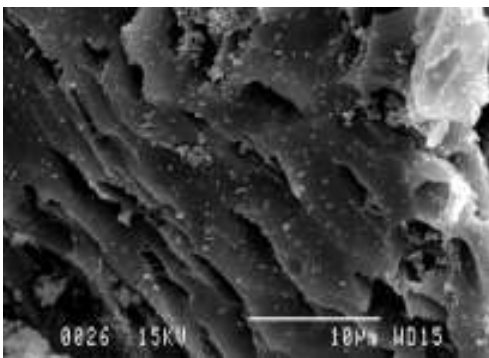


Figure 4.17: SEM-EDX of used CFBC-PCFA after Cr(VI) removal kinetics test

*In the middle original solution ($K_2Cr_2O_7$) and at both sides two different samples from Cr(VI) removal using CFBC-PCFA

4.3.3 Kinetic parameters

In order to investigate the controlling mechanism of the sorption processes such as mass transfer and chemical reaction, the pseudo-first-order and pseudo-second-order equations are applied to model the kinetics of heavy metals sorption onto CFBC-PCFA. Most of the researches about heavy metals removal using fly ashes indicate that the process is controlled by mass transfer or chemical reaction [49]. Therefore, this section attempts to corroborate this last statement.

The results show, by comparing the correlation coefficients (R^2) obtained for both kinetic models (Table 4.5), that pseudo first order is not fully valid for the entire removal time interval, being R^2 values for Cu^{2+} (0.8959), Cr(VI) (0.8305) and for Pb^{2+} (2.10^{-6}). As shown in Table 4.5, pseudo second order R^2 values range between 0.9996 and 0.9998, meaning a better fit to this model.

These results indicate that the removal of Cu^{2+} , Pb^{2+} and Cr(VI) obeys a pseudo-second order kinetic model, corroborating the statements of *Wang & Wu* [49]. The pseudo second order kinetic model assumes that the removal of the studied heavy metals on CFBC-PCFA is due to chemical linkage by sharing or exchanging electrons between CFBC-PCFA and heavy metals [189].

Table 4.5: Kinetic parameters from removal kinetics batch tests at 25°C using a CFBC-PCFA dose of 0.2 g/L

	Pseudo-first order			Pseudo-second order		
	k_f	q_e	R^2	k_s	q_e	R^2
Cu^{2+}	0.006	842	0.8959	0.0011	417	0.9998
Pb^{2+}	1.2 E-05	6.5	2 E-06	0.0009	435	0.9996
Cr(VI)	0.003	2.1	0.8305	0.0015	250	0.9997

q_e : Sorption capacity at equilibrium (mg/g), k_f : Pseudo-first order rate constant (min^{-1}) and k_s : Pseudo-second order rate constant (g/mg min)

4.3.4 Sequential extraction from original and residual CFBC-PCFA after removal kinetics

By means of the chemical sequential extraction procedures, the mobility grade of the retained heavy metals on CFBC-PCFA and certain potential toxic elements such as Ni and V can be assessed (See section 2.4.3).

Generally in the literature is commonly employed the *Tessier* sequential extraction procedure (SEP) (see Figure A.6.1 in *Appendix VI*) [149]. For comparison purposes, *Sposito* and *Tessier* SEP were performed. The detection of a reaction between carbonates from CFBC-PCFA and resulting NCS and acetic acid (HAc) limited the use of *Tessier* SEP in our study. From these results, it is recommended to avoid the use of *Tessier* SEP in fly ashes or materials with a carbonates content higher than 2.4%. Therefore, the *Sposito* procedure [150] was selected as the appropriate sequential extraction in this study.

As shown in Figure 4.18a, the sequential extraction procedure (SEP) of CFBC-PCFA shown different behaviors for the elements B, V, Ni, Zn, Ca, S and As. Only B presented extraction yields of 70% (11 mg/kg) and was found in all extracted fractions. Arsenic release was not detected in raw and spent CFBC-PCFA, which means that As is strongly attached to the CFBC-PCFA matrix. Trace elements such as Ni, Zn and V were found associated to the less mobile fraction (S5), being the extractability levels Zn (52%), V (33%) and Ni (19%). Major elements such as Ca and S were found in high concentrations in the first extractions. These results show that Ca and S from CFBC-PCFA are easy available. Elements of interest from removal kinetics Cu, Pb and Cr(VI) were released in low amounts, being maximum values of 1.3, 1.1 and 0.93 mg/kg, respectively.

Most of the residual CFBC-PCFA after the removal tests presented similar extraction patterns for Ni and V (Figure 4.18b-d) compared to the original CFBC-PCFA (Figure 4.18a), showing a

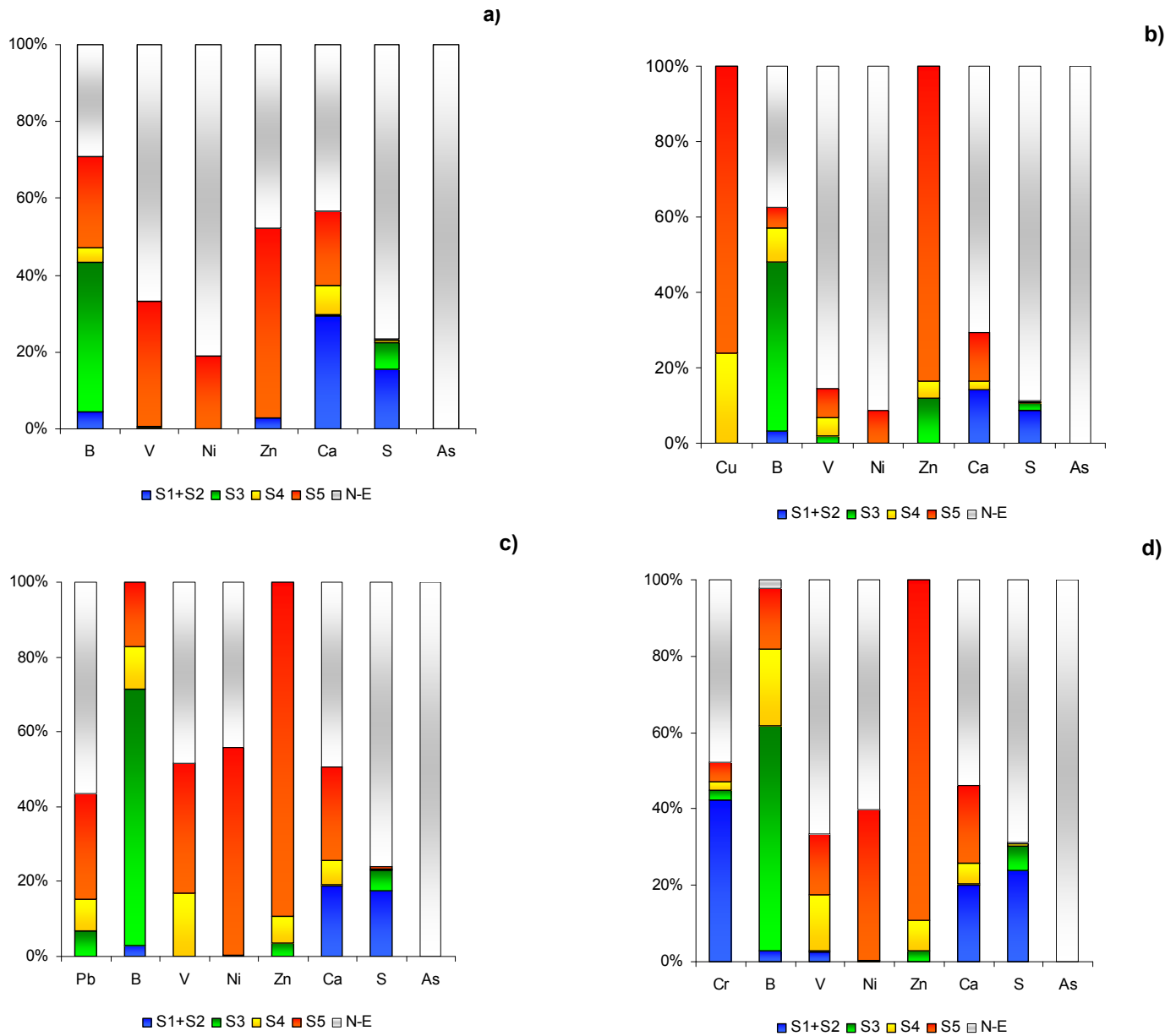


Figure 4.18: Release of different elements during SEP of CFBC-PCFA (a), and after (b) Cu²⁺, (c) Pb²⁺ and (d) Cr(VI) removal kinetics tests*.

* S1+S2 indicates extractions from soluble and exchangeable phases; S3 associated to organic matter; S4 to carbonates and S5 non-silicates matrix. N-E: Not extracted.

lower content in most cases. A reason could be that CFBC-PCFA may initially dissolve during kinetic trials, releasing elements such as Ni and V.

Copper, Pb and Cr showed different extraction patterns for raw and residual CFBC-PCFA after Cu^{2+} , Pb^{2+} and Cr(VI) removal kinetics trials. The extraction pattern for Cu (Figure 4.18b) shows that all of the removed Cu was extracted in the fraction associated to carbonates (S4) and non silicate minerals (S5), meaning that the removed Cu is only present in the less mobile fractions from the residual CFBC-PCFA from removal kinetics, confirming the formation of posnjakite. This characteristic may be of high relevance when managing the residual CFBC-PCFA directly to a safe disposal landfill or to a copper recovery facility.

Similar results were observed for residual CFBC-PCFA after Pb^{2+} removal kinetics trials. Lead was extracted in S3, S4 and S5 fractions, being the presence of Pb in S3 fraction of a possible environmental concern (Figure 4.18c). Moreover, only a 40% of Pb was extracted, which may corroborate that part of lead could be adsorbed in specific sites of CFBC-PCFA.

The extraction pattern for Cr indicates that the important part of the retained Cr was extracted from S1 and S2 fractions, which are the most mobile (Fig. 4.18d). This result shows that Cr has a limited affinity, having a weak linkage with CFBC-PCFA.

4.3.5 Heavy metals sorption isotherms

Sorption isotherms indicate how the sorbed molecules distribute between the liquid phase and the solid phase when the sorption process reaches an equilibrium state. The analysis of the isotherm data by fitting them to different isotherm models is an important step in finding a suitable model that can be used for design purposes. The isotherm models Langmuir and Freundlich were used to determine sorption capacity of the CFBC-PCFA, although precipitation is one of the main

mechanisms. In addition, these models have been widely reported in the heavy metals removal process using fly ashes (See *section 2.4.1*).

Resulting experimental data were fitted to Freundlich and Langmuir models for comparison purposes. The main parameters calculated using both models are presented in Table 4.6. Both models provided an acceptable fit to the experimental data for Cu^{2+} removal with an R^2 of 0.9784 for Langmuir and 0.9629 for Freundlich model, respectively. Furthermore, the “n” value higher than 1 obtained in Freundlich model for Cu^{2+} indicates high removal intensity.

Table 4.6: Heavy metals sorption isotherm parameters at 25°C and 0.1 M KCl using a CFBC-PCFA dose of 0.2 g/L

	Langmuir			Freundlich		
	K_L	b	R^2	K_F	n	R^2
Cu²⁺	8.33	400	0.9784	311.5	8.19	0.9629
Pb²⁺	0.39	277.8	0.5241	247.2	4.70	0.4247
Cr(VI)	0.26	27.8	0.2072	3743.7	0.74	0.5020

K_L : Equilibrium sorption constant (L/mg), b : Maximum sorption capacity (mg/g), K_F : Related to maximum sorption capacity $(\text{L/mg})^{1/n}$ (mg/g) and n : Indicator of sorption intensity (dimensionless).

According to *Limousin et al.* [190], Pb^{2+} sorption isotherm behaves as an “S” isotherm (Figure A.7.1 in Appendix VII). The “S” isotherm curve (sigmoidal) implies that two mechanisms may be involved in Pb^{2+} removal in CFBC-PCFA. The first mechanism involves a low Pb species affinity (at pH 10.5 predominant species negative charged) for CFBC-PCFA surface (observed also in kinetic study, see *Section 4.3.2.2*), while the second one may be related to an affinity increase due to the formation of a new solid phase with higher affinity to CFBC-PCFA surface. Experimental data adjustment to Langmuir and Freundlich models presented relative low R^2 values. In addition,

the obtained “n” value (> 1) from the Freundlich model indicates high intensity sorption behavior for Pb^{2+} .

Isotherm curves of Cu^{2+} and Pb^{2+} obtained in this study (Figure A.7.1 in *Appendix VII*) were similar as the reported by Apak et al. [184], whereas removal capacities (also obtained by Langmuir model) were quite different as the calculated in this study (Table 4.6), being for Cu^{2+} (207 mg/g) and for Pb^{2+} (444 mg/g).

In the case of Cr(VI) no characteristic isotherm type was identified [190], showing the Cr(VI) experimental data adjustment to Langmuir and Freundlich models low R^2 values. This fact indicates a low affinity of Cr(VI) to the CFBC-PCFA surface, corroborating its possible reduction to Cr(III). This is also in agreement with the data observed in the chemical sequential extraction of CFBC-PCFA from Cr(VI) removal kinetics test, where Cr(VI) was present in the most mobile phases. From these results, a deeper research about Cr(VI) reduction mechanisms coupled with Cr(III) removal is recommended. Therefore, Cr(VI) removal was not further evaluated in column removal tests.

4.4 Applications in column tests

4.4.1 Neutralization in fixed bed column tests using CFBC-PCFA

The CFBC-PCFA characterization (See *section 4.1*) evidenced a low hydraulic conductivity (4.1. 10^{-6} m/s), which coupled with a small grain size distribution may imply potential compaction problems in column trials. In addition, developed neutralization products during the counteracting of acidity by CFBC-PCFA could also affect hydraulic and neutralization performance of CFBC-PCFA using fixed bed columns. Nevertheless, a neutralization fixed bed test to analyze CFBC-PCFA as potential neutralizer of acid wastewaters was performed.

When CFBC-PCFA contacts the synthetic acid wastewater, it begins a dissolution process, triggering several processes among them with a pH increase. During the continuous addition of acid solution at pH 2, CFBC-PCFA evidenced a high neutralization capacity (Figure 4.19), observing a pH increase up to 11.6 in the first collected volumes (up to 40 bed volumes (BV)) for both column bed heights. Nevertheless, lowest CFBC-PCFA bed height showed a rapid exhaustion process after 40 BV.

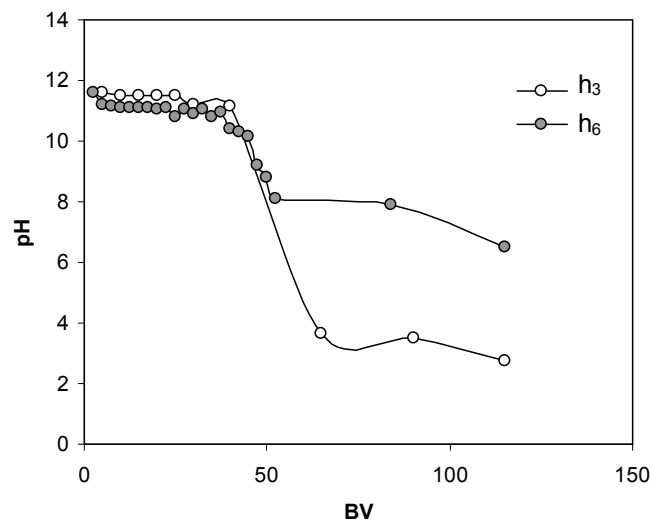


Figure 4.19: pH development in fixed-bed column neutralization test using CFBC-PCFA at pH 2. BV: Bed volume

pH curve at bed height h_6 indicated a stepwise and slow acidification, suggesting a strong neutralization capacity of CFBC-PCFA between 11.6 and 11.0 (Figure 4.19). This behavior may be attributed to portlandite and lime dissolution, as observed by neutralization in batch tests, which is corroborated by geochemical model predictions and the detected concentrations in collected volumes. Furthermore, a high S concentration was detected suggesting also anhydrite dissolution. Similar behavior has been reported for fluidized bed combustion coal fly ashes by *Karapanagioti & Atalay* [191].

The doubling of bed height caused that pH remains stable during a longer time interval and also an increase of almost all elements concentrations (Figure A.8.1 in Appendix VIII), mainly of Ca and S. In our experiment main elements detected may be controlled by dissolution and precipitation of mineral phases like anhydrite, favored at pH 2 as observed by *Doye & Duchesne* [192], and *Reardon et al.* [182].

To detect some neutralization products, an X-ray diffraction analysis of the residual CFBC-PCFA from the neutralization column test was performed (Figure 4.20). XRD evidence shows the disappearance of lime and portlandite peaks, a decrease of anhydrite and calcite peaks and the appearance of gypsum ($\text{CaSO}_4 \cdot 2\text{H}_2\text{O}$), corroborating the mentioned equations 12 to 15 in section 4.3.1.

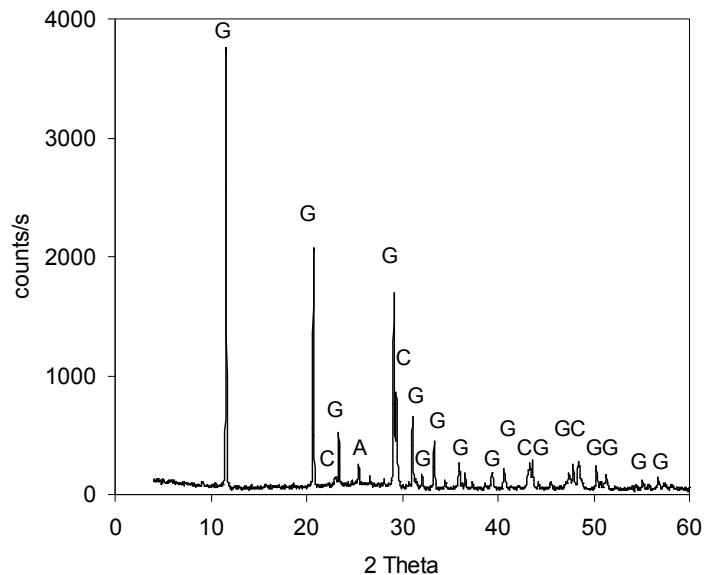


Figure 4.20: XRD pattern of residual CFBC-PCFA from fixed-bed column neutralization test at pH 2. C: calcite; A: anhydrite and G: gypsum ($\text{CaSO}_4 \cdot 2\text{H}_2\text{O}$)

4.4.2 Neutralization in fixed bed column tests using NCS3

Results from *section 4.4.1* showed that raw CFBC-PCFA presented difficulties to neutralize acid wastewaters in fixed bed column tests due to the accumulation of gypsum (neutralization product) in the CFBC-PCFA fixed bed. In this section, it is expected to avoid compaction problems observed in *section 4.4.1* due to NCS3 presented a higher hydraulic conductivity value ($8.2 \cdot 10^{-3}$ m/s).

In order to evaluate the neutralization capacity of NCS3, it were performed the neutralization fixed bed column tests at pH 2 and 4. All experiments showed that NCS3 undergoes a rapid pH decrease at pH 2 (Figure 4.21a), whereas in the experiment at pH 4, the pH values decrease sharply in the first collected volumes, being constant during a long time interval (Figure 4.21b).

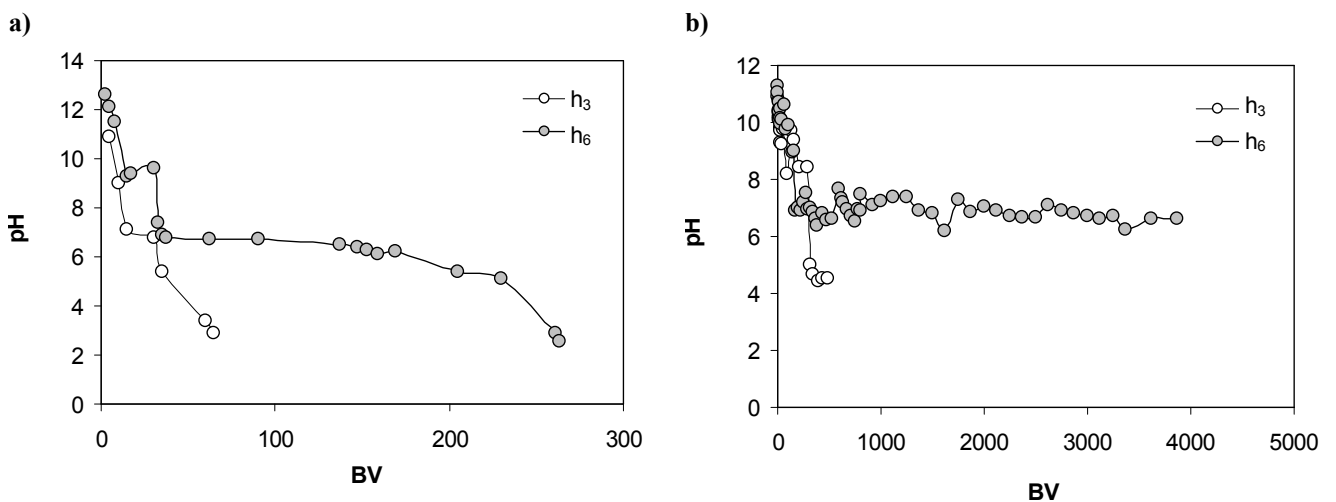


Figure 4.21: pH development in fixed-bed column neutralization tests using NCS3 at pH 2 (a) and 4 (b).
BV: Bed volume

Experiments at pH 4 (Figure 4.21b) developed similar initial pH values and trend. In the first 40-80 bed volume (BV), both column bed heights showed a slowly pH decrease from 10.9 to 9.2 (h_3) and from 11.3 to 9.9 (h_6), suggesting mineral dissolution of NCS3.. After 170 BV, pH was still

constant, indicating a potential neutralization zone for h_6 , ranging pH value between 6 and 7. This final result indicates that NCS3 contributes to an increase in pH by means of neutralization reactions at pH 4. The possible involved neutralization reactions are represented by the equations 12-15 reported in neutralization batch tests using CFBC-PCFA *section 4.3.1*. In addition, calcite and Na-S bearing minerals are also involved in the neutralization reactions, presenting the last minerals similar behavior as anhydrite (CaSO_4) (see Equation 14). Moreover, it is a fact that BL may contribute with other compounds, implying other possible interactions with acid wastewater. The interaction between NCS3 and acid synthetic wastewater leads to the release in all experiments of Na, S, and Ca in high concentrations (Figure 4.22) due to the dissolution of soluble salts on the surface of NCS3 and major crystalline minerals such as lime and anhydrite, also including Na and S bearing minerals. In all experiments, Na and S showed a similar leaching performance, corroborating the data obtained from leaching column tests. High concentrations of Na and S (3776 and 2483 mg/L, respectively) were detected at pH 2 (Figure 4.22b), while lower concentrations of 1661 and 1511 mg/L were detected at pH 4, respectively (Figure 4.22c). The high concentrations of Na and S were measured in the first collected volumes, rapidly decreasing at longer times.

SEM-EDX and XRD analyses of residual material of NCS3 after neutralization column test were performed (Figure A.9.1 in *Appendix IX*). SEM-EDX showed differences between residual NCS3 after neutralization column tests at pH 2 and 4. The previous detected enrichment (Na- and K-salts) in NCS3 disappeared during neutralization tests, corroborating that dissolution of water soluble salts takes place. Nevertheless, products from the neutralization test were not detected through XRD analyses, suggesting that these products may have an amorphous character or are present in quantities lower than 5% w/w.

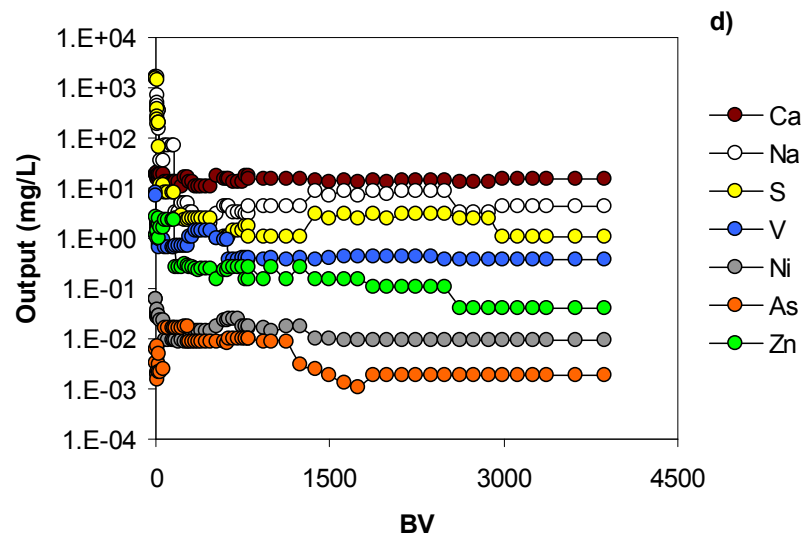
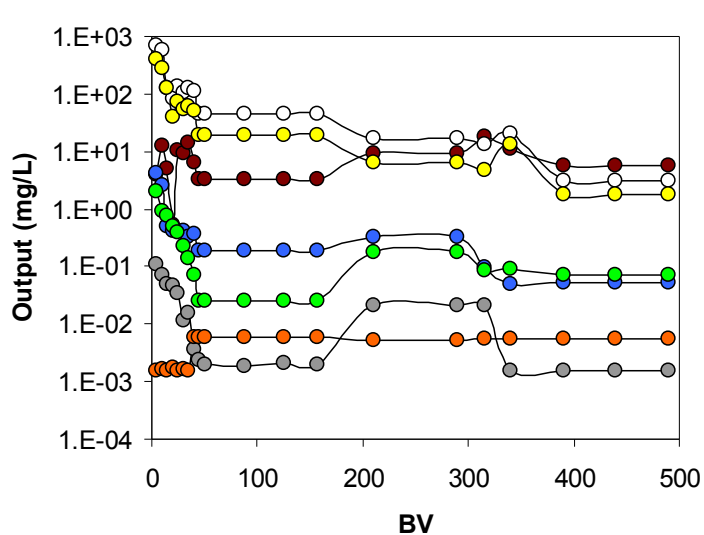
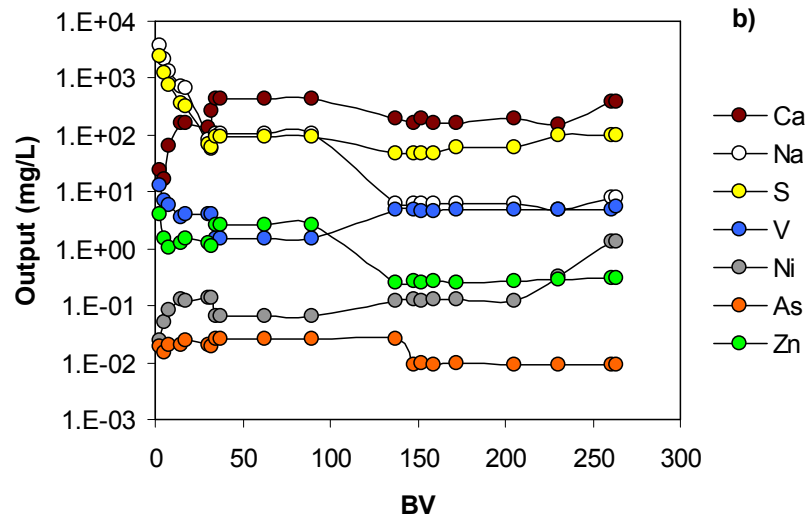
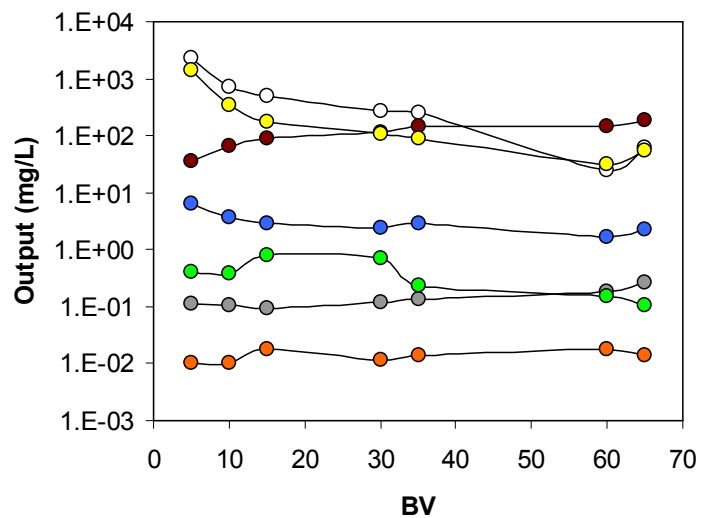


Figure 4.22: Main major and trace elements detected from neutralization column tests using NCS3 at h_3 and pH 2(a) and 4 (b) and h_6 at pH 2 (c) and 4 (d). BV: Bed volumes

Furthermore, trace elements such as As, Zn, Ni and V were detected in low concentrations in the collected volumes, being the maximum values 0.02, 4.1, 0.1 and 13 mg/L, respectively. Most of these trace elements were detected in the experiments performed at pH 2 (Figure 4.22a and c), suggesting that dissolution of small particles enriched with such trace elements is stronger than at pH 4. These results lead to state that NCS3 is able to neutralize acid to moderate acid wastewaters (with pH higher than 4) with an excellent neutralization capacity of 5633 L/kg.

Comparing neutralization performance in column tests between CFBC-PCFA and NCS3 it is observed that both materials presented at pH 4 a strong neutralization capacity. However, NCS3 released lower S, V and Ni amounts during neutralization column tests and did not present compaction problems as observed in the case of CFBC-PCFA.

4.4.3 Cu²⁺ and Pb²⁺ removal in fixed bed column tests using NCS3

The design of any PRB should include the execution of laboratory feasibility tests, whose main objectives are the selection of a suitable filling material for the PRB and the evaluation of its capacity for removing contaminants of interest (Cu²⁺ and Pb²⁺, in our case). Typically, this knowledge is achieved in a first step through batch and column experiments [119].

Breakthrough curves for copper and lead at pH 4 are presented for a bed height of 3 and 6 cm in Figure 4.23. It is observed that NCS3 reached the bed saturation point faster in case of copper than lead, showing saturation times of 600 min (10 h) and 1666 min (28 h) for Pb²⁺ and 150 min (2.5 h) and 453 min (7.6 h) for Cu²⁺ at h₃ and h₆, respectively.

Difference in saturation times were obtained due to a higher bed height (6 cm). As the bed height increases from 3 to 6 cm (Figure 4.23), more effluent passed through the NCS3 bed, implying an increase of saturation time and total removed heavy metals quantity, as a higher amount of NCS3

is available to remove heavy metal cations from the solution by a determined sorption mechanism (Table 4.7). It is also observed that a decrease in bed height has a more significant effect in Cu^{2+} than Pb^{2+} removal.

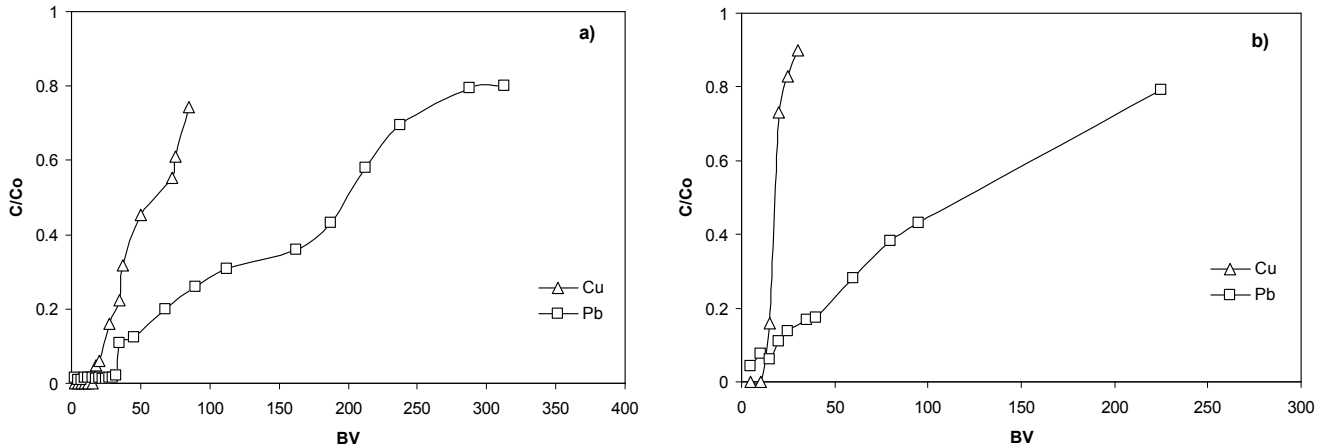


Figure 4.23: Cu^{2+} and Pb^{2+} removal test in fixed bed columns at pH 4 and at bed height of 6 cm (a) and 3 cm (b).

Heavy metals removal column tests were also performed at pH 2 (Figure A.10.1 in *Appendix X*). Cu^{2+} and Pb^{2+} removal was also influenced by pH changes, observing that at pH 2 NCS3 was saturated faster. This result indicates that Pb^{2+} and Cu^{2+} removal is not favored at pH 2 which may be attributed to a competition with H^+ ions in the solution for NCS3. Furthermore, during column removal tests, NCS3 released high concentrations of V and Zn, being the maximum concentrations of 21 mg/L for V (Pb^{2+} at pH 2) and of 1 mg/L for Zn (Cu^{2+} at pH 2). These results indicate that NCS3 is not recommended for acid wastewaters at pH lower than 2.

The best results were achieved at pH 4, reaching a maximum sorption capacity of 28.3 mg/g for Pb^{2+} , and a maximum sorption capacity was for Cu^{2+} of 4.6 mg/g at pH 4 (Table 4.7). NCS3 Cu^{2+}

and Pb^{2+} maximum sorption capacities are lower compared with other materials reported in the literature such as tea waste 13 and 46 mg/g [43] and granulated biomass 40 and 192 mg/g for Cu^{2+} and Pb^{2+} , respectively [44]. However, NCS3 presents a higher Cu^{2+} removal capacity compared to a mixture of sawdust and brine sediments 0.31 mg/g [42].

The sorption capacities of both heavy metals indicate that NCS3 presents a higher affinity for Pb^{2+} than for Cu^{2+} . This difference could be explained by the hydration enthalpies of both heavy metals. Hydration enthalpy is the energy required to the detachment of a water molecule from a cation. According to several authors [41][193], high hydration enthalpy of heavy metal cations (Me^{2+}) means that interaction between Me^{2+} and sorbent (NCS3) is weak. Pb and Cu hydration enthalpies are -1481 and -2100 kJ/kg which reflects that Pb may have a higher affinity for NCS3 than Cu and hence a higher removal capacity compared to Cu.

Experiments at flow rate of 1.5 and 5 mL/min indicated that heavy metals removal capacity is also affected by flow rate variation (Figure A.10.2 in Appendix X). As seen in Table 4.7, an increase of flow rate causes that breakthrough curves for both heavy metals are sharper, decreasing saturation time and total removed heavy metals quantity. This behavior may be explained by insufficient residence time of heavy metals solutions in the column (Table 4.7). Furthermore, flowrate increase influenced Cu^{2+} than Pb^{2+} removal capacities, observing that removal capacities decreased from 8.1 to 0.9 mg/g for Cu^{2+} , whereas for Pb^{2+} from 28.3 to 18 mg/g.

Considering Cu^{2+} and Pb^{2+} removal column tests results, it can be predicted that for small-scale PRB (NCS3 volume = 1 m³) and experimental conditions at pH 4, NCS3 PRB could function for about 3 and 4 years for Cu^{2+} and Pb^{2+} , respectively; maintaining Cu^{2+} and Pb^{2+} concentrations in the effluents lower than 1.0 mg/L. Nevertheless, careful design and control of NCS3 PRB is

required to optimize its performance and avoid operational difficulties (seasonal variation of flowrate) under field conditions. Therefore, detailed experiments at pilot-scale are recommended for the obtaining of real data for predicting long-term scale NCS3 PRB performance.

Table 4.7: Sorption column parameters of Cu^{2+} and Pb^{2+} in NCS3 fixed-bed column tests at bed heights of 3 and 6 cm and at pH 2 and 4.

	<i>G</i>	Bed mass	t_s	m_{total}	q_{total}	Bed removal capacity
pH 2	(mL/min)	(g)	(min)	(mg)	(mg)	(mg/g)
Cu^{2+} -h ₆	1.5	5.4	200	30	22.2	3.8
Pb^{2+} -h ₆	1.5	4.9	80	11	9	1.8
pH 4						
Cu^{2+} - h ₃	1.5	2.4	150	22	6.8	2.7
Cu^{2+} - h ₆	1.5	5.8	453	88	43.3	8.1
Cu^{2+} - h ₆	5	5.9	26	13	5.5	0.9
Pb^{2+} -h ₃	1.5	2.6	600	90	40.7	15.5
Pb^{2+} - h ₆	1.5	4.8	1666	250	138.2	28.3
Pb^{2+} - h ₆	5	5.8	209	104	103	18

m_{total} : total amount of heavy metal cross the NCS3 bed, q_{total} : total removed amount of heavy metal, t_s : time at NCS3 bed is saturated and G : flowrate

4.4.3.1 Prediction of breakthrough curves

Prediction of breakthrough curves and sorption capacity were performed using the Bohart-Adams, Thomas and Yoon-Nelson models. These models are widely used due to mathematical simplicity and were derived for sorption processes. Sorption process covers all process that contribute to the appearance or transformation of a surface by the presence of a solute as well as to the phase-transfer of the solid. These mechanisms are precipitation/dissolution, ion exchange, surface complexation, surface precipitation and hydrophobic interactions. This leads to consider

rate constants obtained from the above mentioned models as a global rate constant, especially when complex removal process take place.

In Table 4.8 the obtained parameters for each breakthrough curves model are shown, for different flowrates, bed heights and pH values. High linear regressions coefficients are observed for Bohart-Adams model, especially for Cu (0.9728 and 0.9856) at both pH and h_6 . Nevertheless, this result is only valid for the initial region of the breakthrough curve. Above the level $C/Co = 0.5$ large discrepancies between experimental and predicted values were detected (Figure A.11.1 in Appendix XI). This result corroborates statements from several authors, which reported that Bohart-Adams model is used only for the description of the initial part of the breakthrough curve, being C/Co between 0.1 and 0.5 [141][194][195].

Table 4.8: Parameters from the used linearized models to predict Cu^{2+} and Pb^{2+} column removal tests.

pH	G	Bohart-Adams			Thomas			Yoon-Nelson			
		K_{AB}	N_o	R^2	K_{Th}	q_o	R^2	K_{Y-N}	τ_{YN}	τ_{exp}	R^2
Cu^{2+} - h_6	1.5	4.4 E-04	4735	0.9856	0.303	4.2	0.9463	0.030	167	162	0.9463
Pb^{2+} - h_6	1.5	5.4 E-04	1748	0.8559	0.318	4.3	0.9403	0.032	136	147	0.9403
pH 4	G										
Cu^{2+} - h_3	1.5	4 E-04	3341	0.6993	0.912	3.1	0.8545	0.091	51	48	0.8545
Cu^{2+} - h_6	1.5	1.1 E-04	5336	0.9728	0.134	8.5	0.8945	0.013	304	327	0.8945
Cu^{2+} - h_6	5	4 E-03	328	0.8478	0.549	0.6	0.8836	0.3955	14	12	0.9055
Pb^{2+} - h_3	1.5	4.6 E-05	15344	0.7699	0.072	20.3	0.9009	0.007	360	325	0.9009
Pb^{2+} - h_6	1.5	3 E-05	19316	0.7980	0.039	33.1	0.8839	0.004	1078	1033	0.8837
Pb^{2+} - h_6	5	2 E-04	17497	0.8554	0.250	15.1	0.9095	0.03	146	147	0.9095

K_{AB} (L/mg min), K_{Th} (mL/g min), and K_{Y-N} (min^{-1}): Bohart-Adams, Thomas and Yoon-Nelson sorption rate constants, q_o : sorption capacity (mg/g), h: Bed height (cm), v: linear flow velocity (cm/min), τ : Time required for 50% sorbate breakthrough (min), N_o : volumetric sorption capacity (mg/L) and G: flowrate (mL/min)

In general for all tested models, the values of the kinetic constant were influenced by flowrate, increasing with flowrate. According to *Aksu & Gönen* [141], this result suggests that the overall system kinetics may be dominated by external mass transfer in the initial part of NCS3 column.

An increase in bed height corresponds to higher removal capacity and a slow increase in heavy metals removal rate. As the bed height increases from 3 to 6 cm, all models predicted a rate constant decrease, corroborating this last statement.

Except for Cu^{2+} removal, fine linear regression coefficients were obtained for Thomas and Yoon-Nelson models (Figure A.11.2 and A.11.3 in *Appendix XI*). Predicted sorption capacities by Thomas model and τ (time required for 50% sorbate breakthrough) by Yoon-Nelson models were near to the reached experimental values and described better the breakthrough curve. According to *Tenorio* [139], Thomas and Yoon-Nelson models could better describe with a high degree of accuracy a certain part of the heavy metals removal breakthrough curves, being C/C_0 between 0.25 and 0.8.

Bohart-Adams, Thomas and Yoon-Nelson models were useful to predict heavy metals removal capacity in fixed-bed columns for comparing purposes. In addition, the kinetics constant rates obtained from the tested models gave information about a global rate constant.

4.4.3.2 Sorption mechanism

According to the wide effluent pH range measured during Cu^{2+} (10.7-6.4) and Pb^{2+} (10.9-6.9) column removal tests (Figure A.12.1 in *Appendix XII*), the possible removal mechanism may be attributed to precipitation as occurred using CFBC-PCFA. Both materials are negatively charged in the studied pH range, where Cu^{2+} and Pb^{2+} removal takes place. Moreover, at the first bed volumes (with pH values between 11 and 9.5), precipitation of $\text{Cu}(\text{OH})_2$ and $\text{Pb}(\text{OH})_2$ (Figure

A.4.1-A.5.1 and A.4.2-A.5.2 in *Appendix IV and V*) occurred. Then, with the drop of pH between 6 and 7, predominant Cu and Pb species are positively charged ($\text{Cu}_2(\text{OH})_2^+$, Cu^{2+} , CuOH^+ , $\text{Pb}_3(\text{OH})_4^{2+}$, PbOH^+ and Pb^{2+}), consequently these species are attracted by NCS3 surface. When these species are exposed to the high amounts of sulfate, carbonate and hydroxyl, a precipitation process of copper or lead hydroxo-sulfate or carbonates takes place. It was also observed that higher Cu^{2+} and Pb^{2+} removal capacities corresponded to pH values higher than 7. For pH values lower than 7, Cu^{2+} and Pb^{2+} removal capacities decreased rapidly.

The modeling of experimental data by PHREEQC showed that in the case of Cu^{2+} removal, possible predominant precipitation products ($\text{SI} > 0$) are malachite ($\text{Cu}_2(\text{OH})_2\text{CO}_3$), azurite ($\text{Cu}_3(\text{OH})_2(\text{CO}_3)_2$), copper carbonate (CuCO_3) and $\text{Cu}(\text{OH})_2$. In the case of Pb^{2+} removal, precipitation products are $\text{Pb}(\text{OH})_2$, cerrusite (PbCO_3) and hydrocerrusite ($\text{Pb}_3(\text{OH})_2(\text{CO}_3)_2$).

XRD and SEM-EDX of residual NCS3 after reaching Cu^{2+} and Pb^{2+} maximum sorption capacities were also performed. In both cases the presence of Cu and Pb coating NCS3 surface was detected (Figure 4.24). Copper and Pb were found to be associated to Ca-, C- and O- bearing minerals, suggesting that the main precipitation products onto NCS3 surface are carbonate minerals of Cu and Pb, which support the proposed reactions.

Copper and Pb were detected in SEM-EDX analyses, as particles with a possible crystalline structure onto residual NCS3 surface. In addition, XRD results showed no new crystalline minerals with the presence of these elements. This result may be related to their amorphous nature, low concentration or dilution effect by the main mineral phases [196].

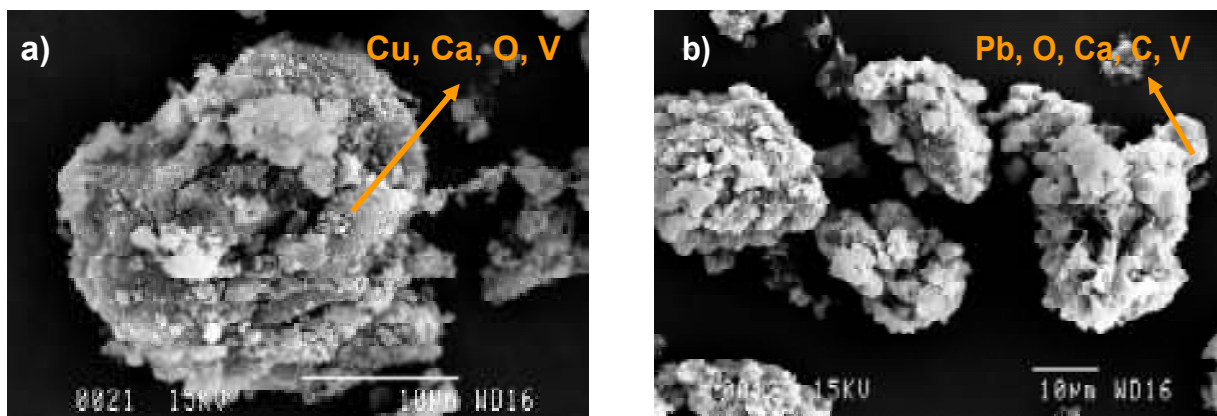


Figure 4.24: SEM-EDX of residual NCS3 from Cu^{2+} (a) and Pb^{2+} (b) removal column tests at maximum saturation capacity, pH 4 and bed height of 6 cm.

4.4.4 Sequential extraction from raw and residual NCS3 residual after heavy metals removal column tests

The information about retention of removed Cu^{2+} and Pb^{2+} (See section 4.4.3) on the surface of NCS3 and how easy could be the release of Cu^{2+} and Pb^{2+} and other elements such as Ni, V and Zn from NCS3 surface is important to estimate the leaching behavior of these heavy metals under certain environmental conditions, especially in case of disposal in landfills. Therefore, this section deals with the chemical sequential extraction of the used materials. As shown in Figure 4.25, the elements V, Ni, Zn, Ca, S, Na and As (raw NCS3) show different behaviors. Ni and V extraction yields from NCS3 increased (42%, 51% and 31% and 56%, 76% and 43%, respectively) in comparison to CFBC-PCFA (Figure 4.18a). These results indicate that the blending and thermal processes of two alkaline materials caused an increment in the availability of Ni and especially V. Nevertheless, most of Ni and V were extracted from the S5 fraction (30.5% and 33.8%), indicating that both trace elements still have a low mobility. This fact corroborates the results from batch and column leaching tests, where low concentrations of Ni and V were found in the leachate samples. Zinc and As were mainly found in S4 and S5 fractions

with extraction yields 84% and 42%, whereas Cu and Pb extraction patterns showed low mobility, being total bulk concentrations of 1.94 and 0.96 mg/kg.

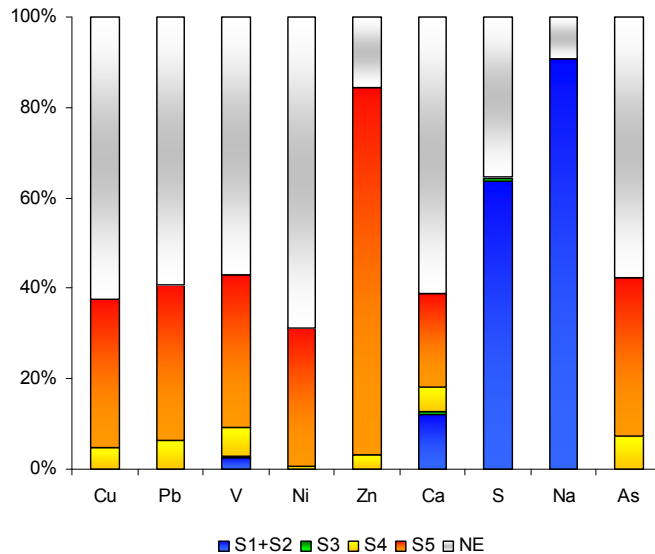


Figure 4.25: Chemical sequential extraction of NCS3*.

Major elements Ca, Na and S were found in high concentrations in S1 plus S2 fraction (bulk contents of 70994 and 53162 mg/kg). Sodium showed the highest extraction yield (91%), being almost all extracted in S1 and S2 fractions. Calcium extraction yield decreased compared to CFBC-PCFA (see Figure 4.18), reaching 38%. This result may be attributed to BL coating calcium minerals. Sulphur presented also high extraction yields in S1 plus S2 fractions (64%). These results indicate that Na and S are especially mobile in aqueous medium.

* S1: exchangeable extraction; S2: soluble extraction, S3: associated to organic matter; S4: associated to carbonates minerals and S5: associated to sulfides and non silicate minerals. NE: Not extracted.

Figure 4.26 shows the sequential extraction procedure (SEP) of residual NCS3 after Cu^{2+} and Pb^{2+} removal column tests at pH 2 (Figure 4.26a and c) and at pH 4 (Figure 4.26b and d), respectively. In these figures the extraction pattern of V, Ni, Cu, Pb, Zn, Ca, S and As is shown.

The Cu extraction pattern (Figure 4.26a and b) shows that the retained Cu on NCS3 surface presented a 100% extraction yield (from removal column test) at both pHs. Around 90% of the extracted Cu was extracted in the fractions associated to carbonates (S4) and non silicate matrix (S5), indicating that a higher amount of Cu is present in the less mobile fractions from NCS3 (Figure 4.26a and b).

The removed Pb presented a similar extraction pattern and yield as Cu (Figure 4.26c and d), and in this case, the results revealed a small fraction of Pb associated to organic matter (S3), which may imply Pb mobility increase. The SEP for Cu and Pb corroborates SEM-EDX results of residual NCS3 after removal column tests (Figure 4.26) and precipitation as main removal mechanism.

The extraction patterns for major elements (Ca, Na and S) suggest that after Pb and Cu removal, NCS3 matrix is damaged, being easier the release of these elements. Changes in the mobility of As, Zn and V have been also observed. Arsenic and Zn extraction patterns indicate a low mobility of these elements, whereas V experienced a mobility increase, being detected V in almost all fractions.

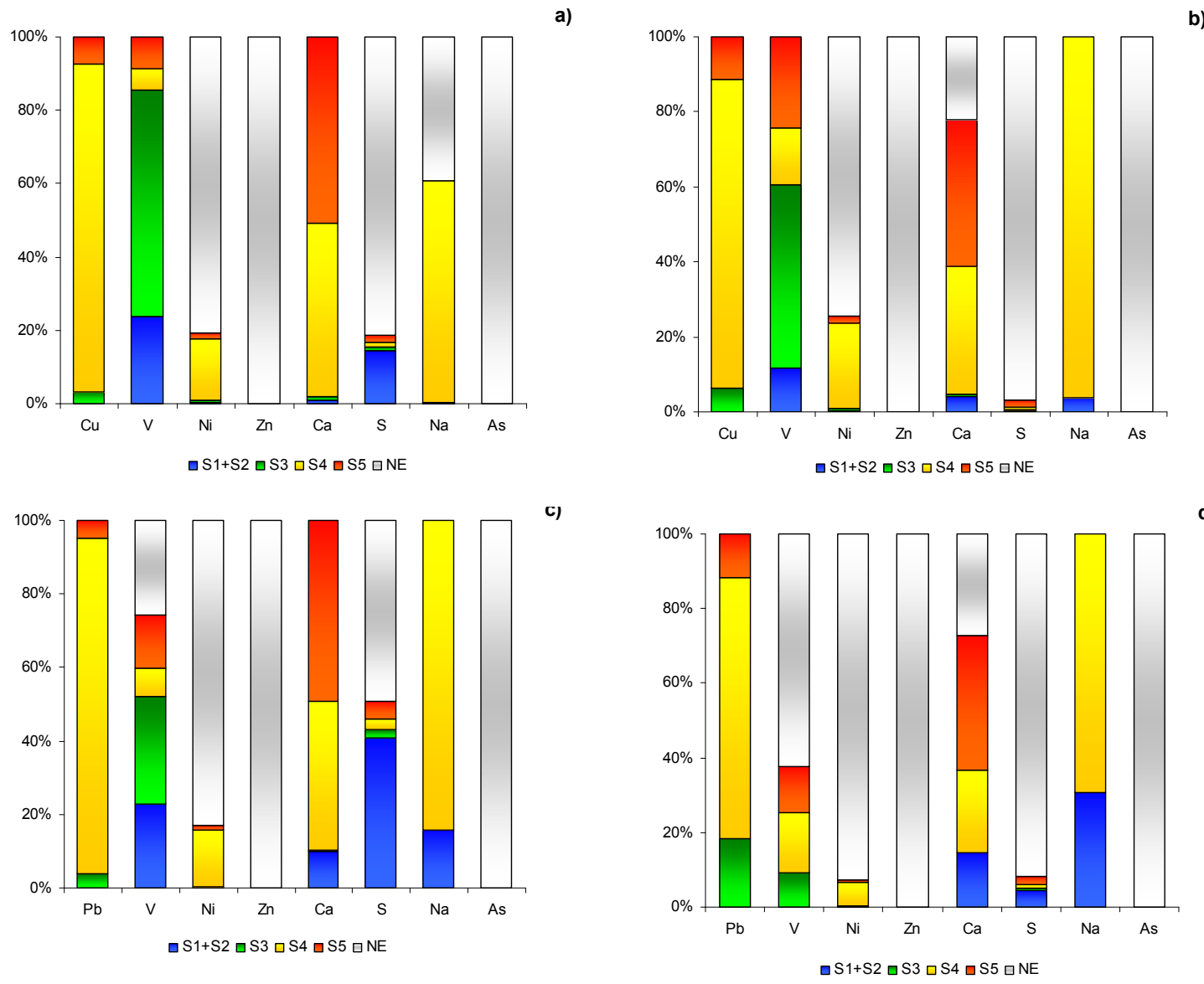


Figure 4.26: Release of different elements during SEP of NCS3 after a) Cu²⁺ at pH 2, b) Cu²⁺ at pH 4, c) Pb²⁺ at pH 2 and d) Pb²⁺ at pH 4 removal column tests*.

* S1: exchangeable extraction; S2: soluble extraction; S3: associated to organic matter; S4: associated to carbonates minerals and S5: associated to sulfides and non silicate minerals. NE: Not extracted.

CHAPTER 5:
GENERAL CONCLUSIONS

Taking into account the main results, it can be concluded that:

- Raw CFBC-PCFA and NCS3 could be considered as potential reactive materials to neutralize acid wastewaters simultaneously removing high heavy metals content. NCS3 could be considered an appropriate potential filling material in conventional permeable reactive barriers due to the satisfactory results in the leaching tests, neutralization and heavy metals removal column tests.

The following more specific conclusions may be drawn from this study.

- NCS3, the blending between 13.5 mL of black liquor and CFBC-PCFA resulted in the best option from all tested NCS (selection process from batch and column leaching tests). NCS3 performance shows a high neutralization capacity after 17 days and Cu^{2+} and Pb^{2+} removal capacity at pH 4 compared to pH 2, as well as a higher affinity to Pb^{2+} than Cu^{2+} .
- The proposed agglomeration technique indeed improves the physical properties of raw CFBC-PCFA, increasing grain size, hydraulic conductivity and specific surface area in all resulting NCS. Moreover, chemical composition remains similar compared to the raw CFBC-PCFA, implying a similar removal performance and mechanism for NCS and CFBC-PCFA.
- Results achieved from neutralization and heavy metals removal in batch tests using CFBC-PCFA lead us to propose the reuse of CFBC-PCFA in the neutralization of acidic wastewaters at pH 4 (with a consequent heavy metals removal), simultaneously replacing natural raw materials. In spite of the slow flowrates and compaction problems (low

hydraulic conductivity value) in column tests, CFBC-PCFA could be reused as reactive material in non-conventional PRB systems such as batch reactor cells.

- The low SO_4^{2-} detected values of the resulting NCS from leaching tests suggest that agglomeration of CFBC-PCFA with black liquor could be proposed as a procedure to decrease SO_4^{2-} leaching from CFBC-PCFA.
- Chemical sequential extraction shows that most of the Pb^{2+} and Cu^{2+} precipitation products from batch and column tests are retained on the carbonates mineral phases and sulfides and non-silicate matrix (least available phases), being the disposal in landfills of the residual NCS3 after neutralization and heavy metals removal, a possible safe option.
- At least, according to the levels of Ni and V detected in the chemical composition and the release of them during all experiments, it is recommended carefully monitoring of Ni and V levels to discard any potential hazardous risk.

Future proposals

Regarding to the results obtained from CFBC-PCFA characterization in this study, two new application fields are open.

- First, CFBC-PCFA is an alkaline material with potential application as calcareous amendment to acid soils and as possible catalyzer in the transesterification process to produce biodiesel.
- Second, CFBC-PCFA presents a certain affinity for CO₂, suggesting their use for CO₂ sequestration from flue gases in power plants and after carbonation process, CFBC-PCFA could be used as SO₂ sorbent, saving raw natural resources (dolomite and limestone), and decreasing operational costs.

REFERENCES

- [1] Adriano DC. Trace elements in terrestrial environments: Biogeochemistry, Bioavailability and risks of metals. 2nd Edition, 2001. In Springer Verlag, New York, USA
- [2] He Z L, Yang XE, Stoffella P. Trace elements in agroecosystems and impacts on the environment. *J. Trace Elem. Med. Biol.* 2005, 19: 125-140
- [3] U.S. Congress, Office of Technology Assessment. Managing industrial solid wastes from manufacturing, mining, oil and gas production, and utility coal combustion-background. Paper OTA-BP-O-82, Washington, D.C.: U.S Government Printing office, February, 1992.
- [4] Mulligan CN, Yong RN, Gibbs BF. Remediation technologies for metal-contaminated soils and groundwater: an evaluation. *Eng. Geol.* 2001; 60: 193-207
- [5] Johnson DB, Hallberg KB. Acid mine drainage remediation options: a review. *Sci. Total Environ.* 2005; 338: 3-14
- [6] Gray NF. Environmental impact and remediation of acid mine drainage: a management problem. *Environ. Geol.* 1997; 30
- [7] Banco Central de Chile. Producto interno bruto por clase de actividad económica, serie anual. http://www.bcentral.cl/estadisticas-economicas/series-indicadores/index_aeg.htm. Santiago de Chile, Chile. Visited on 30.03.09
- [8] Organization for Economic Cooperation and Development (OECD). OECD Global Forum on International Investment Conference on Foreign Direct Investment and the Environment. Lessons to be learned from the Mining sector. 7-8 February 2002. <http://www.oecd.org/dataoecd/45/21/1819617.pdf>
- [9] Oyarzún R, Guevara S, Oyarzún J, Lillo J, Maturana H, Higuera P. The As-contaminated Elqui river basin: a long lasting perspectiva (1975-1995) covering the initiation and development of Au-Cu-As mining in the high Andes of northern Chile. *Environ. Geochem. Health* 2006; 28: 431-443.
- [10] Oyarzún R, Lillo J, Oyarzún J, Higuera P, Maturana H. Strong metal anomalies in stream sediments from semiarid watersheds in Northern Chile: when geological and structural analyses contribute to understanding environmental disturbances. *Int. Geol. Rev.* 2006; 48:1133-1144

- [11] Oyarzún R, Oyarzún J, Lillo J, Maturana H, Higuera P. Mineral deposits and Cu-Zn-As dispersión-contamination in stream sediments from the semiarid and Coquimbo Region. *Environ. Geol.* 2007; 52: 283-294.
- [12] Pizarro J, Vergara PM, Rodríguez JA, Valenzuela AM. Heavy metals in northern Chilean rivers: Spatial variation and temporal trends. *J. Hazard Mater.* 2010; 181: 747-754.
- [13] Organization for Economic Cooperation and Development (OECD). OECD Environmental performance reviews-Chile-2005.
- [14] Bezama A, Sánchez M. State-of-the-art management technologies for contaminated soils and groundwaters with focus on the copper industry. I International Workshop on Process Hydrometallurgy-Hydroprocess 2006. GECAMIN, Iquique, Chile, October 11-13.
- [15] Solomons W, Förstner U. Metals in the hydrocycle. Springer, Verlag, New York, 1984.
- [16] Elbaz-Poulichet F, Seidel J-L, Casiot C, Tusseau-Vuillemin M-H. Short-term variability of dissolved trace element concentrations in the Marne and Seine Rivers near Paris. *Sci. Total Environ.* 2006; 367: 278-287
- [17] Vicente-Martorell JJ, Galindo-Riaño MD, García-Vargas M, Granado-Castro MD. Bioavailability of heavy metals monitoring water, sediments and fish species from polluted estuary. *J. Hazard. Mater.* 2009; 162: 823-836.
- [18] Krishna AK, Satyanarayanan M, Govil PK. Assesment of heavy metal pollution in water using multivariate statistical techniques in an industrial area: a case study from Patancheru, Medak District, Andhra Pradesh, India. *J. Hazard. Mater.* 2009; 167: 363-373
- [19] Neal HP, Jarvie BA, Whitton BA, Gemell J. The water quality of the river Wear, north-east England. *Sci. Total Environ.* 2000; 251/252: 153-172.
- [20] Qu CH, Chen CZ, Yang YR, Wang LZ, Lu YL. Geochemistry of dissolved and particulate elements in the major rivers of China (The Huanghe, Changjiang, and Zhunjiang Rivers), *Estuaries* 1993; 16: 475-487.
- [21] Guo X, Zhang S, Shan X. Adsorption of metal ions on lignin. *J. Hazard. Mater.* 2008; 151:134-142.
- [22] Wu Y, Zhang S, Guo X, Huang H. Adsorption of chromium (III) on lignin. *Bioresour. Technol.* 2008; 99:7709-7715.
- [23] Wate BJ, Sibrell PL, Schwartz MF. Acid neutralization within limestone sand reactors receiving coal mine drainage. *Environ. Pollut.* 2005; 137: 295-304

- [24] Babel S, Kurniawan. Low-cost adsorbents for heavy metals uptake from contaminated water: a review. *J. Hazard. Mater.* 2003; B97:219–243.
- [25] Virta R. USGS. Mineral information US geological survey mineral commodity summary2000-2001.
<http://www.minerals.usgs.gov/minerals/pubs/commodity/zeolite/zeomyboo.pdf>
- [26] Cost estimation of limestone, lime and soda ash in treatment plants.
http://www.unh.edu/erg/wttac/WTTAC_Water_Tech_Guide_Vol2/limestone_pdf_files/lc_costs.pdf.
- [27] Miller MM. Mineral industry survey. Lime in the United States.
<http://minerals.usgs.gov/minerals>. (visited 27.04.2007)
- [28] BV Sorbex, Inc. Markets for ion exchange resins and biosorbents.
<http://www.bvsorbex.net/sxMarkets.pdf> (visited 3.10.09)
- [29] Kurniawan TS, Gilbert Y, Chan S, Wai-hung L, Babel S. Comparisons of low-cost adsorbents for treating wastewaters Laden with heavy metals. *Sci. Total Environ.* 2006; 366: 409-426
- [30] Bailey S, Olin TJ, Bricka M, Adrian DD. A review of potentially low cost sorbents for heavy metals. *Water Resour.* 1999; 11:2469-2479
- [31] Gupta VK. Equilibrium uptake, sorption dynamics, process development, and column operations for the removal of copper and nickel from aqueous solution and wastewater using slag, as low cost adsorbent. *Ind. Eng. Chem. Res.* 1998; 37: 192-202
- [32] Brown P, Jefcoat IA, Parrish D, Gill S, Graham S. Evaluation of the adsorptive capacity of peanut hull pellets for the heavy metals in solution. *Adv. Environ. Res.* 2000; 4: 19-29
- [33] Babel S, Kurniawan TA. Cr (VI) removal from synthetic wastewater using coconuts shell charcoal and commercial activated carbon modified with oxidizing agent and/ or chitosan. *Chemosphere* 2004; 54: 951-967
- [34] Gupta GS, Prasad G, Singh VN. Removal of chrome from aqueous solutions by mixed adsorbents: Fly ash and coal. *Water Res.* 1990; 24: 45-50
- [35] Potgieter-Vermaak SS, Potgieter JH, Monama P, Van Grieken R. Comparison of limestone, dolomite and fly ash as pretreatment agents for acid mine drainage. *Miner. Eng.* 2006; 19: 454-462

- [36] Celik A, Demirbas A. Removal of heavy metal ions from aqueous solutions via adsorption onto modified lignin from pulping wastes. *Energy Source* 2005; 27: 1167-77.
- [37] Diez MC, Rubilar O, Cea M, Navia R, De Martino A, Carpasso A. Recovery and characterization of the humate-like salified polymeric organic fraction (lignimerin) from Kraft cellulose mill wastewater. *Chemosphere* 2007; 68: 1798-1805.
- [38] Zhang FS, Itoh H. Adsorbents made from waste ashes and post-consumer PET and their potential utilization in wastewater treatment. *J. Hazard. Mater.* 2003; B101: 323-337.
- [39] Li CJ, Chang JE. Effect of fly ash characteristics on the removal of Cu(II) from aqueous solution. *Chemosphere* 2001; 44:1185-1192.
- [40] F. Rozada, M. Otero, J.B. Parra, A. Morán, A.I. García, Producing adsorbents from sewage sludge and discarded tyres. Characterization and utilization for the removal of pollutants from water. *Chem. Eng. J.* 2005; 114:161-169.
- [41] Pehlivan E, Cetin S, Yanik BH. Equilibrium studies for the sorption of zinc and copper from aqueous solutions using sugar beet pulp and fly ash. *J. Hazard. Mater.* 2006; B135: 193-199.
- [42] Agouborde L, Navia R. Heavy metals retention capacity of a non-conventional sorbent developed from a mixture of industrial and agricultural wastes. *J. Hazard. Mater.* 2009; 167:536-544.
- [43] Amarasinghe BMWPK, Williams RA. Tea waste as a low cost adsorbent for the removal of Cu and Pb from wastewater. *Chem. Eng. J.* 2007; 132: 299-309.
- [44] Hawari AH, Mulligan CN. Heavy metals uptake mechanisms in a fixed-bed column by calcium-treated anaerobic biomass. *Process Biochem.* 2006; 41:187-198.
- [45] Lehmann J, Joseph S. Biochar for environmental management: Science and Technology. Published by Earthscan in the UK and USA, 2009.
- [46] Vidal G. Revisión bibliográfica sobre los compuestos orgánicos producidos en la industria de la pasta y papel: incidencia en la toxicidad y biodegradabilidad anaerobia de sus efluentes. *Afinidad* 481: 152-160.
- [47] Jankowski J, Ward CR, French D, Groves S. Mobility of trace elements from selected Australian fly ashes and its potential impact on aquatic ecosystems. *Fuel* 2006; 85: 243-256.
- [48] Chen J, L X. Progress of petroleum coke combusting in circulating fluidized bed boilers- A review and future perspectives. *Resour. Conserv. Recy.* 2007; 49:203-216.

- [49] Wang S, Wu H. Environmental-benign utilization of fly ash as low-cost adsorbents. *J. Hazard. Mater.* 2006; B136: 482-501.
- [50] Kimoto M, Matsuda H, Shirai H. Influence of coal properties and combustion conditions on specific surface area of fly ash. International Ash Utilization Symposium 2005, Center for Applied Energy Research, University of Kentucky. www.flyash.info. Visited on 19.01.07. Lexington, Kentucky, USA.
- [51] Kikuchi R. Application of coal ash to environmental improvement transformation into zeolite, potassium fertilizer and FGD absorbent. *Resour. Conserv. Recy.* 1999; 27: 336-346.
- [52] Ahmaruzzaman M. A review on the utilization of the fly ash. *Prog. Energ. Combust. Sci.* 2010; 36: 327-363
- [53] Cox M, Nugteren H, Jannssen- Jurkovičová M. Combustion residues: current, novel and renewable applications, 2008. John Wiley & Sons, England.
- [54] Pan JR, Huang C, Kuo JJ, Lin SH. Recycling MSWI bottom and fly ash as raw materials for Portland cement. *Waste Manage.* 2008; 28: 1113-1118.
- [55] Moreno N, Querol X, Andres JM, Stanton K, Towler M, Nugteren H. Physico-chemical characteristics of European pulverized coal combustion fly ashes. *Fuel* 2005; 84: 1351-1363.
- [56] Font O, Querol X, Juan R, Casado, Ruiz CR, López-Soler A, Coaca P, Peña FG. Recovery of gallium and vanadium from gasification fly ash. *J. Hazard. Mater.* 2007; A139: 413-423.
- [57] Mudavaki JR, Narayuna BV, Kiran R. Characterization and utilization of iron-rich dry ash from an electric arc furnace. *Current Sci.* 1999; 76: 473-475.
- [58] Chang FY, Wey MY. Comparison of the characteristics of bottom and fly ashes generated from various incineration process. *J. Hazard. Mater.* 2006; B138: 594-603.
- [59] Sinton CW. Raw Materials for Glass and Ceramics: Sources, Processes and Quality Control, 2006. John Wiley & Sons Inc., New Jersey, USA.
- [60] Querol X, Umaña JC, Alastuey A, Ayora C, López-Soler A, Plana F. Extraction of soluble major and trace elements from fly ash in open and closed leaching systems. *Fuel* 2001; 80: 801-813.
- [61] Jegadeesan G, Al-Abed SR, Pinto P. Influence of metal distribution on its leachability from coal fly ash. *Fuel* 2008; 87: 1887-1893.
- [62] Swain EJ. US petroleum coke production expected to increase. *Oil Gas J* 1997; 95:79-82.

- [63] Wang JS, Anthony EJ, Abanades JC. Clean and efficient use of petroleum coke for combustion and power generation. *Fuel* 2004; 83:1341-1348.
- [64] Anthony EJ. Fluidized bed combustion of alternative solid fuels; status, successes and problems of the technology. *Prog. Energ. Combust.* 1995; 21:239-268.
- [65] Benetto E, Rousseaux P, Blondin J. Life cycle assessment of coal by-products based electric power production scenarios. *Fuel* 2004; 83: 957-970.
- [66] Hower JC, Thomas GA, Mardon SM, Trimble AS. Impact of co-combustion of petroleum coke and coal on fly ash quality: Case study of a Western Kentucky power plant. *Appl. Geochem.* 2005; 20:1309-1319.
- [67] Anthony EJ, Granatstein DL. Sulfation phenomena in fluidized bed combustion systems. *Prog. Energ. Combust.* 2001; 27:215–236.
- [68] Laursen K, Duo W, Grace JR, Lim J. Sulfation and reactivation characteristics of nine limestones. *Fuel* 2000; 79:153-163.
- [69] Anthony EJ, Iribarne AP, Iribarne JV. Fouling in a utility-scale CFBC boiler firing 100% petroleum coke. *Fuel Process Technol.* 2007; 88:535-547.
- [70] Jia L, Anthony EJ, Charland JP. Investigation of vanadium compounds in ashes from a CFBC firing 100% pet-coke. *Energ. Fuel* 2002; 16:397-403.
- [71] Izquierdo M, Font O, Moreno , Querol X, Huggins FE, Alvarez E, Diez S, Otero P, Ballesteros JC, Gimenez A. Influence of a modification of the pet-coke/coal ratio on the leachability of fly ash and slag produced from a large PCC power plant. *Environ. Sci. Technol.* 2007; 41: 5330-35.
- [72] Izquierdo M, Moreno N, Font O, Querol X, Alvarez E, Antenuci D, Nugteren H, Luna Y, Fernandez-Pereira C. Influence of co-firing on the leaching of trace pollutants from coal fly ash. *Fuel* 2008; 87: 1958-1966.
- [73] ECOBA (European Coal Combustion Products Association) (ed.). Production of CCPs in 2006. <http://www.ecoba.com>: Visited 09.10.06. Essen, Germany.
- [74] ACCA (American Coal Ash Association) (ed.). Production and use survey-2007. www.aaa-usa.org/PDF/2007. Colorado. USA.
- [75] Henke K. Trace element chemistry of fly ashes from combusted petroleum coke and coal. Int Ash Utilization Symposium, 2005. Center for Applied Energy Research, University of Kentucky, Lexington, Kentucky, USA. Paper # 45. www.flyash.info. Visited 20.09.06.

- [76] Scott AN, Thomas MDA. Evaluation of fly ash from co-combustion of coal and petroleum coke for use in concrete. *Aci. Mater. J.* 2007; 104:62-69.
- [77] Sheng GH, Zhai JP, Li Q, Li F. Utilization of fly ash coming from a CFBC boiler co-firing coal and petroleum coke in Portland cement. *Fuel* 2007; 86: 2625-2631.
- [78] Chen LM, Kost D, Dick WA. Petroleum coke circulating bed combustion product as a sulfur source for alfalfa. Communications in *Soil Sci. Plant Anal.* 2008; 39: 1993-2008.
- [79] Thenoux G, Halles F, Vargas A, Bellolio JP, Carrillo H. Laboratory and field evaluation of fluid bed combustion fly ash as granular road stabilizer. *Transp. Res. Record* 2007; 2: 36-41.
- [80] Conn RE, Sellakumar K, Bland AE. Utilization of CFB fly ash for construction applications. Proceedings of the 15th International Conference on Fluidized Bed Combustion; 1999 May 16-19, Savannah, Georgia, USA.
- [81] Querol X, Moreno N, Alastuey A, Andres JM, López-Soler A, Ayora C, Medinaceli A, Valero A. Synthesis of high ion exchange zeolites from coal fly ash. *Geologica Acta* 2007; 5: 47-55.
- [82] Inada M, Euchii Y, Enomoto N, Hojo J. Synthesis of zeolite from coal fly ashes with different silica-alumina composition. *Fuel* 2005; 84: 299-304.
- [83] Moreno N. Valorisation of fly ashes for zeolite synthesis by silica extraction and direct conversion. Environmental applications 2002. (Valorización de cenizas volantes para la síntesis de zeolitas mediante extracción de sílice y conversión directa. Aplicaciones ambientales). PhD Thesis Univesitat Politècnica de Catalunya (UPC), Barcelona, Spain.
- [84] Querol X, Moreno N, Umaña JC, Alastuey A, Hernández E, López-Soler A, Plana F. Synthesis of zeolites from coal fly ash: an overview. *Int. J. Coal Geol.* 2002; 50: 413-423
- [85] Mondragon F, Rincon F, Serra L, Escobar J, Ramírez J, Fernández J. New perspectives for coal ash utilization: synthesis of zeolitic material. *Fuel* 1990; 69: 263-266.
- [86] Miyake M. Resource recovery of inorganic solid waste for reduction of enironmental load. *J. Ceramic Soc. Japan* 2007; 115: 1-8.
- [87] Okada T, Tojo Y, Tanaka N, Masuto T. Recovery of zinc and lead from fly ash from ash-melting and gasification-melting process of MSW-Comparison and applicability of chemical leaching methods. *Waste Manage.* 2007; 27: 69-80.
- [88] Zhang FS, Itoh H. Extraction of metals from muncipal solid waste incinerator fly ash by hydrotheral process. *J. Hazard. Mater.* 2006; B136: 663-670.

- [89] Font O, Querol X, López-Soler A, Chimenos JM, Fernández AI, Burgos S, Peña FG. Ge extraction from gasification fly ash. *Fuel* 2005; 84: 1384-1392.
- [90] Crini G. Non- conventional low-cost adsorbents for dye removal: A review. *Bioresour. Technol.* 2006; 97: 1061-1085
- [91] Kalinski ME, Yerra P. Hydraulic conductivity of compacted cement-stabilized fly ash. Int Ash Utilization Symposium 2005, Center for Applied Energy Research, University of Kentucky, USA. www.flyash.info. Visited on 19.01.07, Lexington, Kentucky, USA.
- [92] Cocka E, Yilmaz Z. Use of rubber and bentonite added fly ash as a liner material. *Waste Manage.* 2004; 24: 153-164.
- [93] Prashanth JP, Sivapullaiah PV, Sridharan A. Pozzolanic fly ash as a hydraulic barrier in landfills. *Eng. Geol.* 2001; 60: 245-252.
- [94] Palmer BG, Edil TB, Benson CH. Liners for waste containment constructed with class F and C fly ashes. *J. Hazard. Mater.* 2000; 76: 193-216.
- [95] Doherty R, Phillips DH, McGreough L, Walsh KP, Kalin RM. Development of modified fly ash as a permeable reactive barrier medium for a former gas plant site, Northern Ireland. *Environ. Geol.* 2006; 50: 37-46
- [96] Komnitsas K, Bartzas G, Paspaliaris I. Clean up of acidic leachates using fly ash barriers: Laboratory column studies. *Global Nest: Int. J.* 2004; 6: 81-89.
- [97] Rostami H, Silverstrim T. In situ removal of cadmium and chromium from groundwater using zeotech reactive barriers. U.S. Department of Energy. N° DE-FG02-99ER82921, 2000. www.energy.gov. Washington, DC, USA.
- [98] Gitari WM, Petrik LF, Etchebers O, Key DL, Iwuoha E, Okuyeni C. Passive neutralization of acid mine drainage by fly ash and its derivatives: A column leaching study. *Fuel* 2008; 87: 1637-1650.
- [99] Pérez-López R, Nieto JM, Almodóvar GR. Utilization of fly ash to improve the quality of the acid mine drainage generated by oxidation of a sulphide-rich mining waste: Column experiments. *Chemosphere* 2007; 67: 1637-1646.
- [100] Xenidis A, Mylona E, Paspaliaris I. Potential use of lignite fly ash for the control of acid generation from sulphidic wastes. *Waste Manage.* 2002; 22: 631-641.
- [101] Johnson DB. Chemical and microbiological characteristics of mineral spoils and drainage waters at abandoned coal and metal mines. *Water Air Soil Pollut.* 2003; 3: 47-66.

- [102] Stumm W, Morgan JJ. Chemical equilibria and Rates in Natural Waters. 3rd Ed, 1996. John Wiley & Sons. Inc., New York, USA.
- [103] Coulton R, Bullen C, Dolan J, Hallet C, Wright J, Marsden C. Wheal Jane mine water active treatment plant-design, construction and operation. *Land Contam. Reclam.* 2003; 11: 245-252.
- [104] Kuhn EMR. Microbiology fly ash-acid mine drainage co-disposal processes. M.Sc. Thesis, 2005. Department of Biotechnology, University of the Western Cape, South Africa.
- [105] Bertocchi AF, Ghiani M, Peretti R, Zucca A. Redmud and fly ash for remediation of mine sites contaminated with As, Cd, Cu, Pb and Zn. *J. Hazard. Mater.* 2006; B134: 112-119.
- [106] Hallbeg RO, Granhagen JR, Liljemark A. A fly ash/biosludge dry cover for the mitigation of AMD at the falun mine. *Chemie der Erde* 2005; 65: 43-63.
- [107] Wang L, Shang JQ, Kovac V, Ho KS. Utilization of Atikokan coal fly ash in acid rock drainage control from Muselwhite Mine tailings. *Can. Geotech. J.* 2006; 43: 229-243.
- [108] Hellier WW. Abatement of acid mine drainage by capping a reclaimed surface mine with fluidized bed combustion ash. *Mine Water Environ.* 1998; 17: 28-40.
- [109] Siriwardane HJ, Kannan RSS, Ziemkiewicz PF. Use of waste materials for control of acid mine drainage and subsidence. *J. Environ. Eng.* 2003; 129: 910-915.
- [110] Gitari WM, Petrik LF, Etchebers O, Key DL, Okuyeni C. Utilization of fly ash for the treatment of coal mines wastewater: Solubility controls on major inorganic contaminants. *Fuel* 2008; 87: 2450-2462.
- [111] Ríos CA, Williams CD, Roberts CL. Removal of heavy metals from acid mine drainage (AMD) using coal fly ash, natural clinker and synthetic zeolites. *J. Hazard. Mater.* 2008; 156: 23-35.
- [112] Madzivire G, Petrik LF, Gitari WM, Ojumu TV, Balfour G. Application of coal fly ash to circumneutral mine waters for the removal of sulphates as gypsum and ettringite. *Miner. Eng.* 2010; 23: 252-257.
- [113] Polat M, Guler E, Lederman E, Cohen H. Neutralization of an extremely acidic sludge and stabilization of heavy metals in fly ash aggregates. *Waste Manage.* 2007; 27: 482-489.
- [114] Blowes DW, Ptacek CJ, Benner SG, McRae WT, Bennett TA, Puls RW. Treatment of inorganic contaminants using permeable reactive barriers. *J. Contam. Hydrol.* 2000; 45: 123-137.

- [115] Powell RM, Puls RW, Blowes DW, Vogan JL. Permeable reactive barriers technologies for contaminant remediation, U.S. Office of Research and Development, U.S. Environmental Office of Solid Waste and Emergency Response, US EPA/600/R-98/125.
- [116] Continuous permeable reactive barrier (Figure). <http://www.serdp.org/Program-Areas/Environmental-Restoration/Contaminated-Groundwater/ER-1375>. Visited on 20.10.2010
- [117] Interstate Technology & Regulatory Council (ITRC). Technical/Regulatory Guidelines Permeable Reactive Barriers. Lessons learned/New directions. 2005. <http://www.itrcweb.org/guidancedocument.asp?TID=5>. Visited on 7.08.08
- [118] NATO/CCMS (ed). Evaluation of demonstrated and emerging technologies for the treatment of contaminant land and ground water (Phase III), 2003. EPA 542-R-02-012, Nr.259. www.nato.int/science/publications. Brussels, Belgium.
- [119] Gavaskar A, Gupta N, Sass B, Janosy R, Hicks J. Design Guidance for Application of Permeable Reactive Barriers for Groundwater Remediation. U.S. Air Force; Air Force Research Laboratory (AFRL). F08637-95-D-6004 DO 5503
- [120] Gavaskar AR, Tatar L, Condit W. Cost and performance report nano-scale zero-valent iron technologies for source remediation. NAVFAC Contract Report CR 05-007-ENV; 2005. Engineering Service Center, Port Hueneme, California, USA.
- [121] Komnitsas K, Bartzas G, Paspaliaris I. Modeling of reaction front progress in fly ash permeable reactive barriers. *Environ. For.* 2006; 7: 219-231
- [122] Hong J-K, Jo HY, Yun S-T. Coal fly ash and synthetic coal fly ash aggregates as reactive media to remove zinc from aqueous solutions. *J. Hazard. Mater.* 2009; 164: 235-246.
- [123] Burt TA, Li Z, Bowman RS. Evaluation of granular surfactant-modified/zeolite zero valent iron pellets as a reactive material for perchloroethylene reduction. *J. Environ. Eng.* 2005; 131: 934-942.
- [124] Köber R, Daus B, Ebert M, Mattusch J, Welter E, Dahmke A. Compost-based permeable reactive barriers for the source treatment of arsenic contaminations in aquifers: Column studies and solid-phase investigations. *Environ. Sci. Technol.* 2005; 39: 7650-7655.
- [125] Wilkin RT, McNeil MS. Laboratory evaluation of zero-valent iron to treat water impacted by acid mine drainage. *Chemosphere* 2007; 53: 715-725.

- [126] Gibert O, Pablo J, Cortina JL, Ayora C. Evaluation of municipal compost/limestone/iron mixtures as filling material for permeable reactive barriers for in-situ acid mine drainage treatment. *J. Chem. Technol. Biotechnol.* 2003; 78: 489-496.
- [127] McGregor RG, Benner S, Ludwig R, Blowes DW, Ptacek C. Sulfate reduction permeable reactive barrier to treat acidity, cadmium, copper, nickel and zinc: two cases studies. In: Naftz DL, Morrison SJ, Fuller CC, Davies JA (Eds). *Handbook of Groundwater Remediation Using Permeable Reactive Barriers-Applications to radionuclides, trace metals and nutrients*. Academic Press, San Diego, California, USA, p. 539.
- [128] Lee T, Park JW, Lee JH. Waste green sands as reactive media for the removal of zinc from water. *Chemosphere* 2004; 56: 571-581.
- [129] Wantanaphong J, Mooney SJ, Bailey EH. Suitability of natural materials and wastes as permeable reactive barriers (PRBs). *Environ. Chem. Lett.* 2005; 3: 19-23.
- [130] Skinner SJW, Schutte CF. The feasibility of a permeable reactive barrier to treat acidic sulphate- and nitrate-contaminated groundwater. *Water SA* 2006; 32: 129-135.
- [131] Benner SG, Blowes DW, Ptacek CJ, Mayer KU. Rates sulfate reduction and metal sulfide precipitation in a permeable reactive barrier. *App. Geochem* 2002; 17: 301-320.
- [132] Golab AN, Peterson MA, Indraratna B. Selection of a potential reactive materials for a permeable reactive barriers for remediating acidic groundwater in acid sulphate soils terrains. *Quarter. J. Eng. Geol. Hydrogeol.* 2006; 39: 209-223.
- [133] Arslan H, Baykal G. Utilization of fly ash as engineering pellet aggregates. *Environ. Geol.* 200; 50: 761-770.
- [134] Harikrishman KI, Ramamurthy K. Influence of pelletization process on the properties of fly ash aggregates. *Waste Manage.* 2006; 26: 846-852.
- [135] Gavaskar AR. Design and Construction techniques for permeable reactive barriers. *J. Hazard. Mater.* 1999; 68: 41-71.
- [136] Khambhaty Y, Mody K, Basha S, Jha B. Pseudo-second-order kinetic models for the sorption of Hg(II) onto dead biomass of marine *Aspergillus niger*: Comparison of linear and non-linear methods. *Colloids Surf. A* 2008; 328: 40-43.
- [137] Lagergren S, Svenska BK. Zur Theorie der sogenannten Adsorption gelöster Stoffe. *Vetenskapakad Handl* 1898; 24:1-39.

- [138] McKay G, Ho YS. Pseudo-second order model for sorption processes. *Process Biochem.* 1999; 34: 451-465.
- [139] Tenorio G. Caracterización de la biosorción de cromo con hueso de aceituna. Tesis Doctoral de la Universidad de Granada. España. 2006.
- [140] Treybal RE. Mass Transfer Operations, 3rd Edition. McGraw-Hill, Tokyo, 1980
- [141] Aksu Z, Gönen F. Biosorption of phenol by immobilized activated sludge in a continuous packed bed: prediction of breakthrough curves. *Process Biochem.* 2004; 39: 599-613.
- [142] Chu KH. Prediction of two-metal biosorption equilibria using a neural network. *Eur. J. Miner. Process Environ. Protect.* 2003; 3: 119-127.
- [143] Ayoob S, Gupta AK, Bhakat PB. Analysis of breakthrough developments and modeling of fixed bed adsorption system for As(V) removal from water by modified calcined bauxite (MCB). *Sep. Purif. Technol.* 2007; 52: 430-438.
- [144] Badruzzaman M, Westerhoff P, Knappe DRU. Intraparticle diffusion and adsorption of arsenate onto granulate ferric hydroxide (GFH). *Water Res.* 2004; 38: 4002-4012.
- [145] Navia R, Inostroza X, Diez MC, Lorber KE. Irrigation model of bleached kraft mill wastewater through volcanic soil as pollutants attenuation process. *Chemosphere* 2006; 63: 1241-1251.
- [146] Sperlich A, Werner A, Gez A, Amy G, Worch E, Jekel M. Breakthrough behavior of granular ferric hydroxide (GFH) fixed-bed adsorption filters: modeling and experimental approaches. *Water Res.* 2005; 39: 1190-1198.
- [147] Dutta BK, Khanra S, Mallick D. Leaching of elements from coal fly ash: Assessment of its potential for use in filling abandoned coal mines. *Fuel* 2009; 88:1314-1323.
- [148] Rao CRM, Sahuquillo A, Lopez-Sanchez JF. A review of the different methods applied in environmental geochemistry for single and sequential extraction of trace elements in soils and related materials. *Water Air Soil Pollut.* 2008; 189:291-333.
- [149] Tessier A, Campbell PGC, Bisson M. Sequential extraction procedure for the speciation of particulate trace metals. *Anal. Chem.* 1979; 51: 844-851.
- [150] Sposito G, Lund IJ, Chang AC. Trace metal chemistry in arid-zone field soils amended with sewage sludge: 1. Fractionation of Ni, Cu, Zn, Cd and Pb in solid phases. *Soil Sci. Soc. Am. J.* 1982; 46:260-264.

- [151] EPA Test Method 1311-TCLP, Toxicity Characteristic Leaching Procedure. www.ehso.com/cssepa/TCLP_fromEHSOcom_Method_1311.pdf.
- [152] European Committee for Standardisation EN 12457-2:2002 Characterisation of waste-leaching-compliance test for leaching of granular waste materials and sludges-Part 2: One stage batch test a liquid to solid ratio of 10 L/kg for materials with particle size below 4 mm.
- [153] Council Decision 2003/33/EC. Stablising criteria and procedures for the acceptance of waste at landfills pursuant to Article 16 of and Annex II to Directive 1999/31/EC.
- [154] Mattigod SV, Sposito G. GEOCHEM: A computer program for the calculation of chemical equilibria in soils and environmental sciences. University of California, Riverside, CA, USA. 1979.
- [155] Allison JD, Brown DS, Novo-Gradac KJ. MINTEQA2/PRODEFA2. A geochemical assessment model for environmental systems: Version 3.0 User's manual 1991. US Environmental Protection Agency, Athens, Georgia. EPA/600/3-91/021.
- [156] Parkhurst DL, Thorstenson DC, Plummer LN. PHREEQC- A computer program for geochemical calculations. US Geological Survey: Investigation resources report 1990: 80-96.
- [157] Gebart R. Black liquor gasification-Large scale production of green transportation fuels. www.etcpitea.se. Extracted on 25. 10.2009 (ETC, Box 726, SE-941 28 Piteå, Sweden).
- [158] Demirbas A. Pyrolysis and steam gasification processes of black liquor. *Energy Convers. Manage.* 2002; 43: 877-884.
- [159] Querol X, Whateley MK, Fernández-Turiel JL; Tuncali E. Geological controls on the mineralogy and geochemistry of the Beypazari lignite, Central Anatolia, Turkey. *Int. J. Coal Geol.* 1995; 33:255-271.
- [160] Thompson M & Walsh N. Handbook of Inductively Coupled Plasma Spectrometry; Chapman and Hall, Inc. New York, 1989.
- [161] ASTM C618-92a. Standard specification for fly ash and raw or calcinated natural pozzolan for use as mineral admixture in Portland cement concrete. *Am. Soc. Testing Mater.* 1994; 04.02. Pennsylvania.
- [162] Espinosa C. Construcción y caracterización de columnas rellenas con suelo para ensayos de eliminación de contaminantes. Tesis de pre-grado. Ingeniería Ambiental. Universidad de La Frontera. 2008.

- [163] Chilean Regulation N° 148. Reglamento Sanitario Sobre Manejo De Residuos Peligrosos 2003.
- [164] Querol X, Umaña JC, Alastuey A, Ayora C, Lopez-Soler A, Plana F. Extraction of soluble major and trace elements from fly ash in open and closed leaching systems. *Fuel* 2001; 80: 801-813.
- [165] US EPA, Method 7196A. Chromium hexavalent (colorimetric). <http://www.epa.gov/osw/hazard/testmethods/sw846/pdfs/7196a.pdf>. (Visited on 10.10.2007).
- [166] Lee SH, Sakai E, Daimon M, Bang WK. Characterization of fly ash directly collected from electrostatic precipitator. *Cement Concrete Res.* 1999; 29: 1791-1797.
- [167] Rao A, Anthony EJ, Jia L, Macchi A. Carbonation of FBC ash by sonochemical treatment. *Fuel* 2007; 86:2603-2615.
- [168] Fierro V, Torné-Fernández V, Celzard A, Montané D. Influence of the demineralization on the chemical activation of Kraft lignin with orthophosphoric acid. *J. Hazard. Mater.* 2007; 149:126-133.
- [169] Wu Y, Anthony EJ, Jia L. Steam hydration of CFBC ash and the effect of hydration condition on reactivation. *Fuel* 2004; 83: 1357-1370.
- [170] Skodras G, Grammelis P, Kakaras E, Karangelos D, Anagnostakis M, Hiniš E. Quality of greek fly ashes and potential uses. *Fuel Process Technol.* 2007; 88: 77-85.
- [171] Iribarne JV, Anthony EJ, Iribarne A. A scanning electron microscopy study on agglomeration in petroleum coke-fired FBC boilers. *Fuel Process Technol.* 2003; 82:27-50.
- [172] Periodic Table. Sodium. <http://www.chemicalelements.com/elements/na.html>. Visited on 2.03.2010
- [173] González A, Moreno N, Navia R. Fly ashes from coal and petroleum coke combustion: Current and innovative potential applications. *Waste Manage Res.* 2009; 27: 976-987.
- [174] Brown RC, Dykstra J. Systematic errors in the use of loss on ignition to measure unburned carbon in fly ash. *Fuel* 1995, 74: 570-574.
- [175] Navia R, Hafner G, Raber G, Lorber KE, Schöffmann E, Vortisch W. The use of volcanic soil as mineral landfill liner-I. Physicochemical characterization and comparison with zeolites. *Waste Manage. Res.* 2005; 23: 249-259.
- [176] Joo SH, Cheng FI. Nanotechnology for environmental remediation. *Modern Inorganic Chemistry*. Series Editor: John P Fackler, Jr. 1st Edition, 2006, page 26.

- [177] Doherty R, Phillips DH, McGeough KL, Walsh KP, Kalin RM. Development of modified fly ash as a permeable reactive barrier medium for a former gas plant site, Northern Ireland. *Environ. Geol.* 2006; 50:37-46.
- [178] Sáez JA. Desarrollo de un material adsorbente no convencional a partir de cenizas volantes. Trabajo para optar al título de Ingeniero Ambiental, 2007, Universidad de La Frontera.
- [179] Navia R, Schmidt KH, Behrend G, Lorber KE, Rubilar O, Diez MC. Improving the adsorption capacity and solid structure of natural volcanic soil using a foaming-sintering process based on recycled polyethylene terephthalate (PET). *Waste Manage. Res.* 2007; 25:119-129.
- [180] Anthony EJ, Berry EE, Blondin J, Bulewicz EM, Burwell S. Advanced ash management technologies for CFBC ash. *Waste Manage.* 2003; 23: 503-516.
- [181] Natale FD, Natale MD, Greco R, Lancia A, Laudante C, Musmarra D. Groundwater protection from cadmium contamination by permeable reactive barriers. *J. Hazard. Mater.* 2008; 160: 428-434.
- [182] Reardon EJ, Czank CA, Warren CJ, Dayal R, Johnston HM. Determining controls on element concentrations in Fly ash leachate. *Waste Manage. Res.* 1995; 13: 435-450.
- [183] Smith IM. Trace elements from coal combustion: emissions, IEA Coal Research, London, 1987.
- [184] Apak R, Tütem E, Hügül M, Hizal J. Heavy metal cation retention by unconventional sorbents (Red Muds and Fly Ashes). *Wat. Res.* 1998; 32: 430-440
- [185] Bayat B. Comparative study of adsorption properties of Turkish fly ashes I. The case of nickel (II), copper (II) and zinc (II). *J. Hazard. Mater.* 2002; B95: 251-273.
- [186] Alinnor IJ. Adsorption of heavy metals ions from aqueous solution by fly ash. *Fuel* 2007; 86: 853-858.
- [187] Rao M, Parwate AV, Bhole HG. Removal of Cr^{6+} and Ni^{2+} from aqueous solution using bagasse and fly ash. *Waste Manage.* 2002; 22: 821-830.
- [188] Mohan D, Pittman CU. Activated carbon and low cost adsorbents for remediation of trihexavalent chromium from water. *J. Hazard. Mater.* 2006; 137: 762-811.
- [189] Ho YS. Review of second-order models for adsorption systems. *J. Hazard. Mater.* 2006; B136: 681-689.

- [190] Limousin G, Gaudet J-P, Chalet L, Szenknect S, Barthés V, Krimissa M. Sorption isotherms: A review on physical bases, modeling and measurement. *Appl. Geochem.* 2007; 22: 249-275.
- [191] Karapanagioti HK, Atalay AS. Laboratory evaluation of ash materials as acid-disturbed land amendments. *Global Nest: Int. J.* 2001; 3: 11-21.
- [192] Doye I, Duchesne J. Neutralization of acid mine drainage with alkaline industrial residues: laboratory investigation using batch-leaching tests. *App. Geochem.* 2003; 18: 1197-1213.
- [193] Martin-Dupont F, Gloagven Y, Garnet R, Guilloton M, Morvan H, Krausz P. Heavy metal adsorption by crude coniferous barks: a modeling study. *J. Environ Sci. Health* 2002; A37: 1063-1073.
- [194] Sag Y, Aktay Y. Application of equilibrium and mass transfer models to dynamic removal of Cr(VI) ions by chitin in packed column reactor. *Process Biochem.* 2001; 36: 1187-1197.
- [195] Liao X, Zhang M, Shi B. Collage fiber immobilized tannins and their adsorption of Au(III). *Ind. Ing. Chem. Res.* 2004; 43:2222-2227.
- [196] D.G. Schulze, Differential X-ray diffraction analysis of soil mineralogy. Madison (WI): Soil Science Society of America Miscellaneous Publication (1994), Chapter 13, pp. 412-429.

APPENDIXES

*Appendix I: Cascade impactor results***Table A.1.1:** Chemical characterization and particle size distribution of CFBC-PCFA <65 μm

Fraction (μm)	CaO (%)	SO₃ (%)	Al₂O₃ (%)	Fe₂O₃ (%)	MgO (%)	Na₂O (%)	Ni (%)	V (%)	Particle size distribution (%)
<0.4	66	20	nd	0.4	0.7	0.1	0.25	0.5	0.2
0.4-1	57	23	0.7	0.4	0.7	0.1	0.22	0.5	0.8
1-2	42	22	0.5	0.3	0.5	0.2	0.21	0.4	3.1
2-4-	58	32	0.9	0.4	0.6	0.3	0.32	0.7	7.5
4-9	40	26	0.4	0.3	0.4	0.2	0.26	0.6	11.7
9-17	36	26	0.4	0.1	0.4	0.04	0.29	0.6	5.8
17-65	44	19	0.1	0.1	0.4	0.01	0.2	0.4	70.9

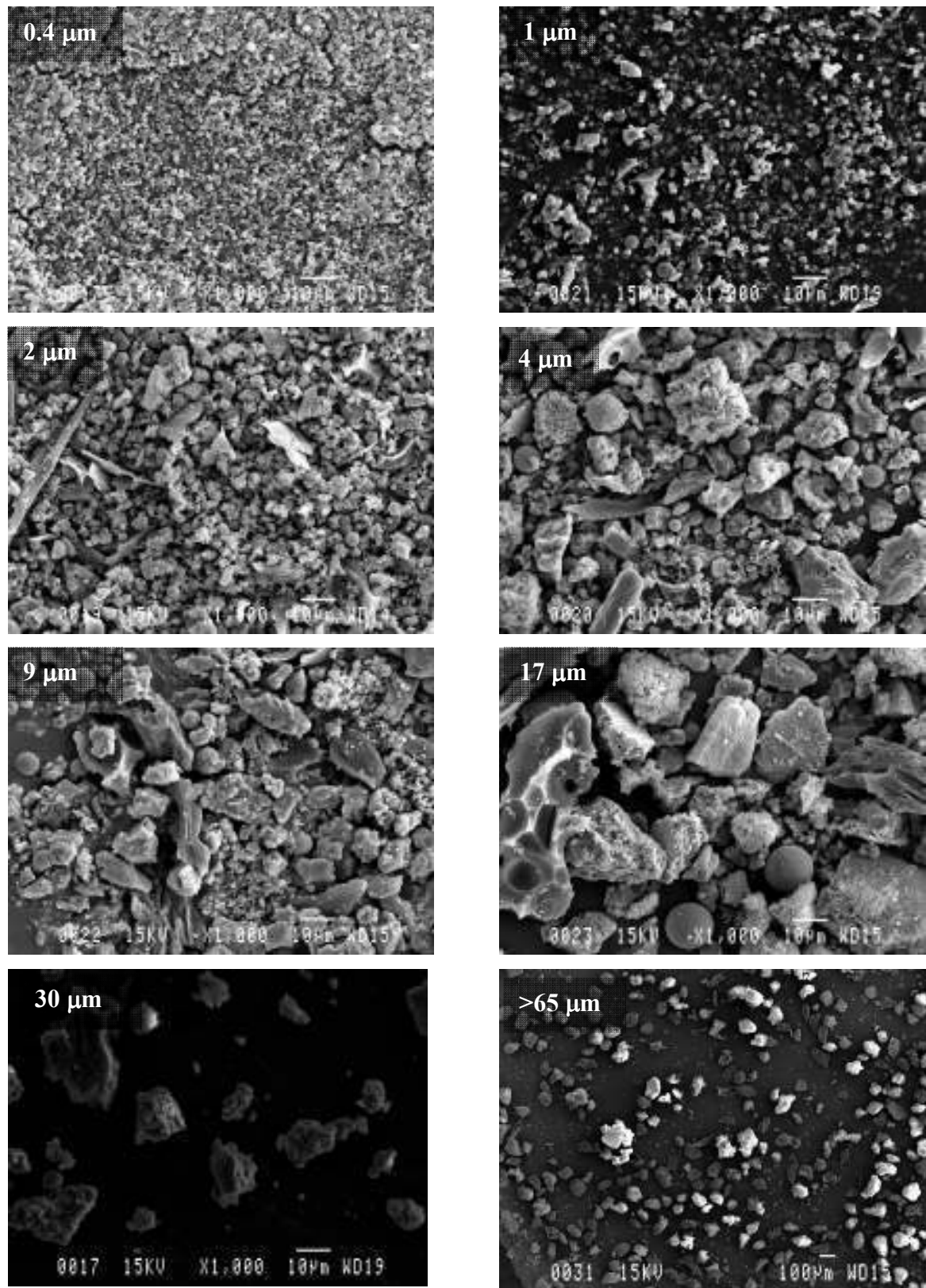


Figure A.1.1: SEM-EDX analyses of CFBC-PCFA fractions with the same magnification, except fraction >65 μm.

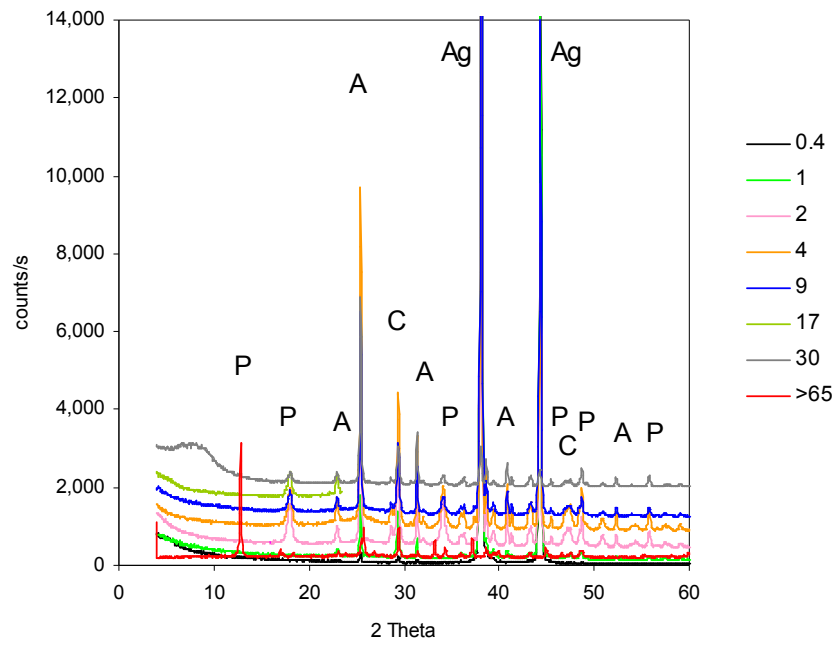


Figure A.1.2: XRD of different grain size of CFBC-PCFA < 65 and > 65 μm samples. P: portlandite, C: calcite and A: anhydrite

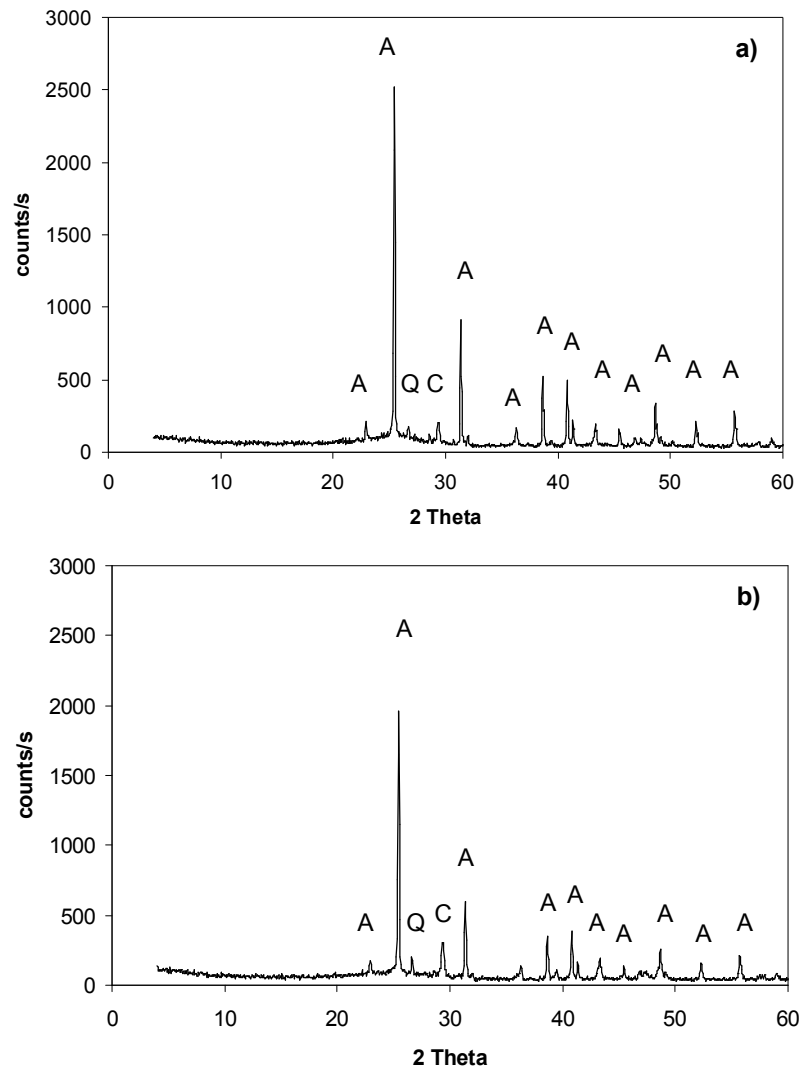
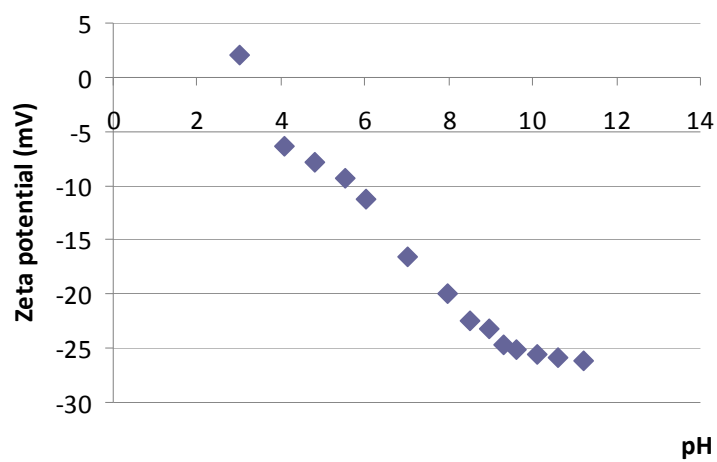
Appendix II: Neutralization batch trials using CFBC-PCFA

Figure A.2.1: XRD spectra from CFBC-PCFA dose of 1.4 (a) and 2.6 g/L (b) from neutralization test at pH 2. A: anhydrite; C: calcite and Q: quartz

Appendix III: Isoelectric point (IEP) of CFBC-PCFA**Figure A.3.1:** Electrophoretic mobility measurement of CFBC-PCFA at 0.1 M KCl

Appendix IV: Speciation diagram of Cu^{2+} , Pb^{2+} and Cr(VI) without to consider initial conditions of the solution.

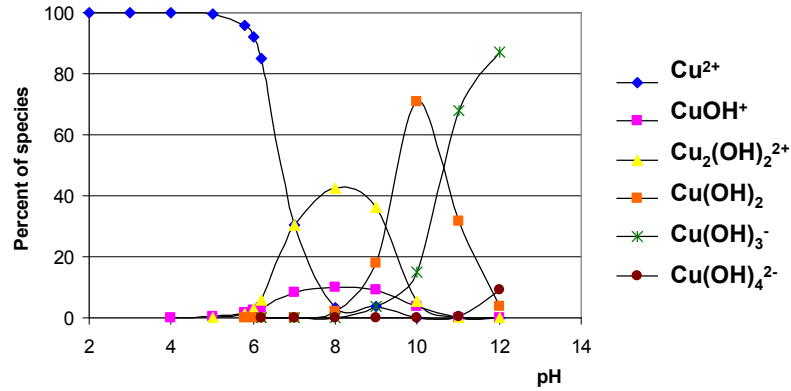


Figure A.4.1: Speciation diagram for Cu (100 mg/L of Cu^{2+} at 25°C)

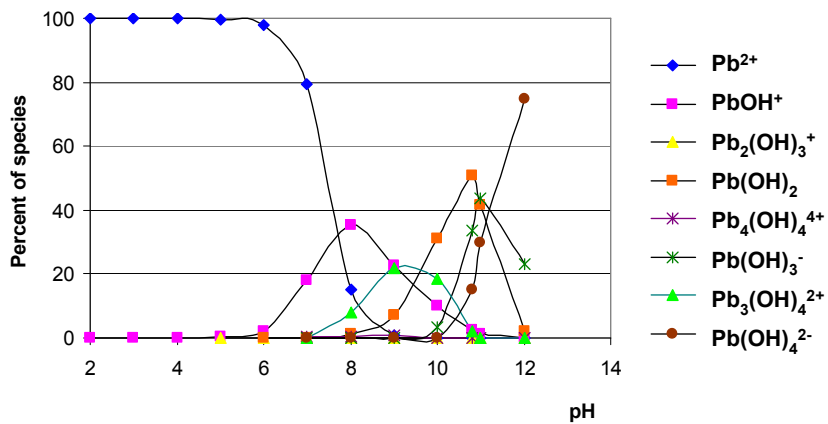


Figure A.4.2: Speciation diagram for Pb (100 mg/L of Pb^{2+} at 25°C)

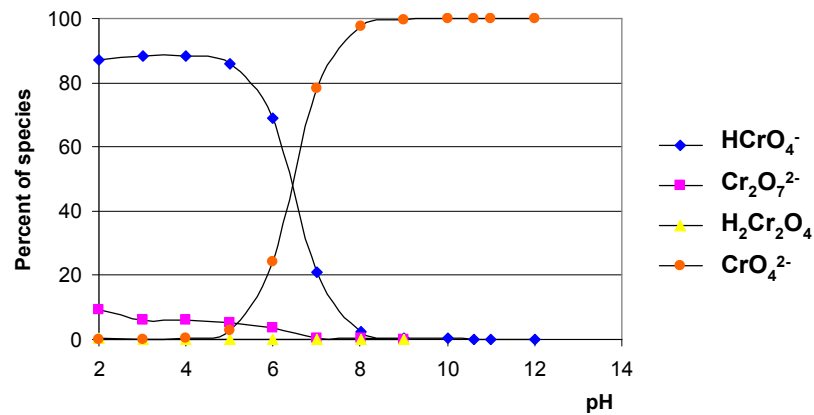


Figure A.4.3: Speciation diagram for Cr(VI) (100 mg/L of Cr(VI) at 25°C)

Appendix V: Speciation diagram of Cu^{2+} , Pb^{2+} and Cr(VI) , considering sulfur and carbon content

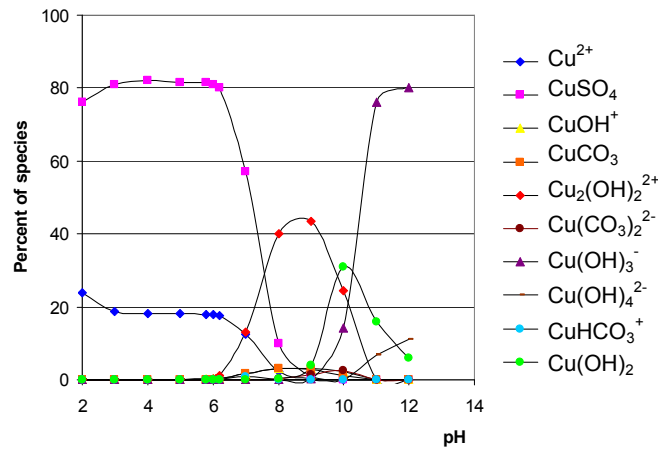


Figure A.5.1: Speciation diagram for Cu^{2+} (100 mg/L at 25°C, including solution initial conditions)

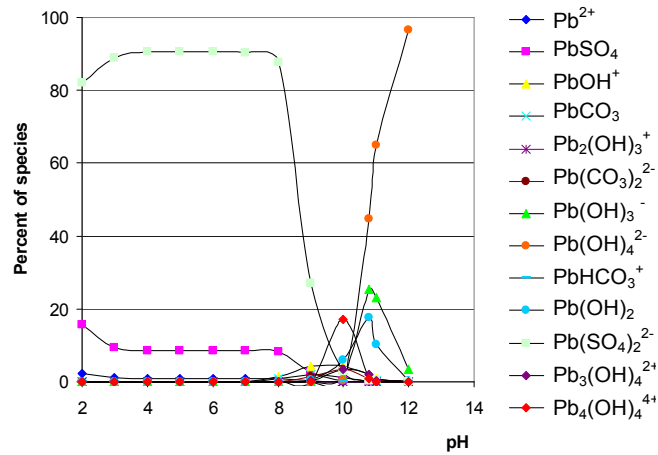


Figure A.5.2: Speciation diagram for Pb^{2+} (100 mg/L at 25°C, including solution initial conditions)

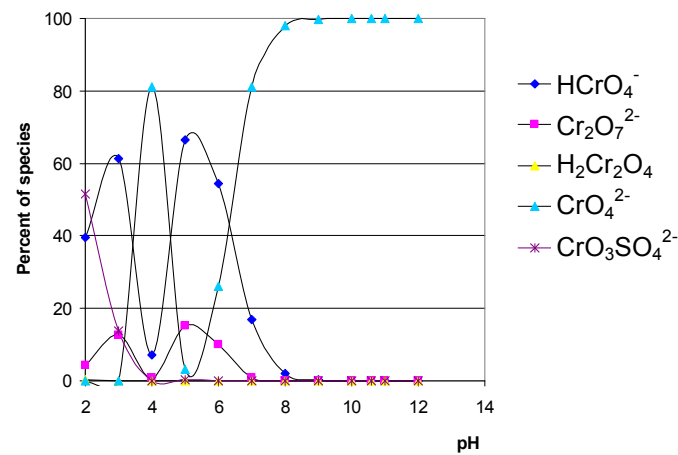


Figure A.5.3: Speciation diagram for Cr(VI) (100 mg/L at 25°C, including solution initial conditions)

Appendix VI: Tessier chemical sequential extraction

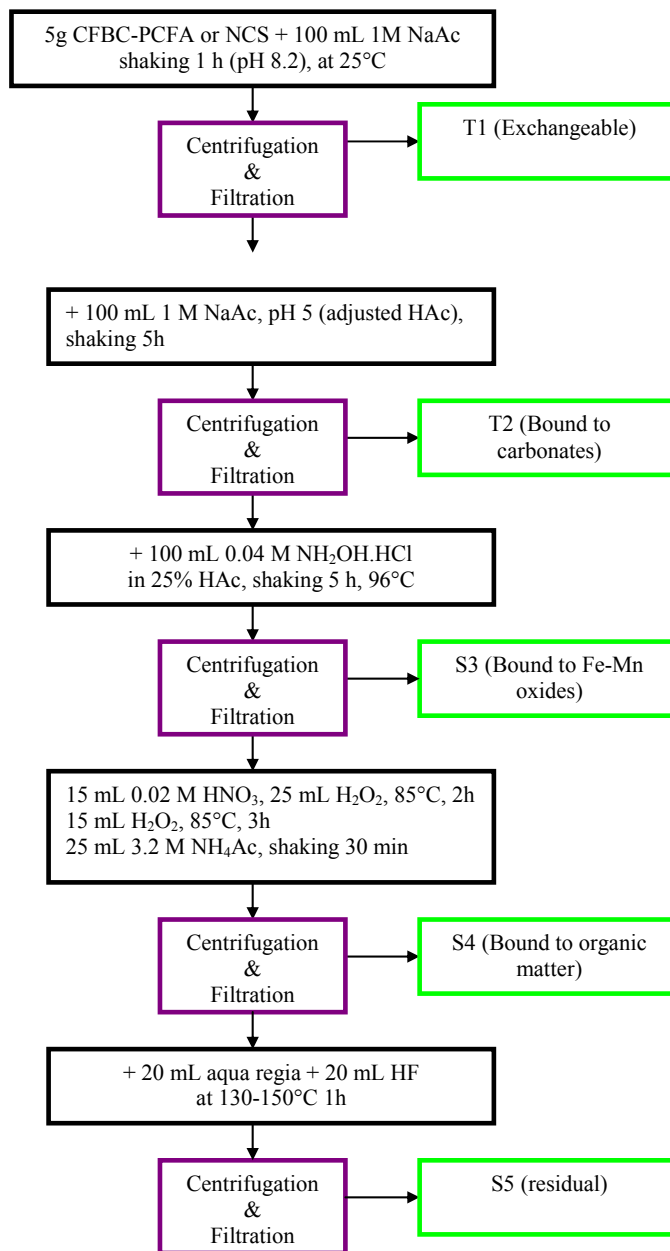
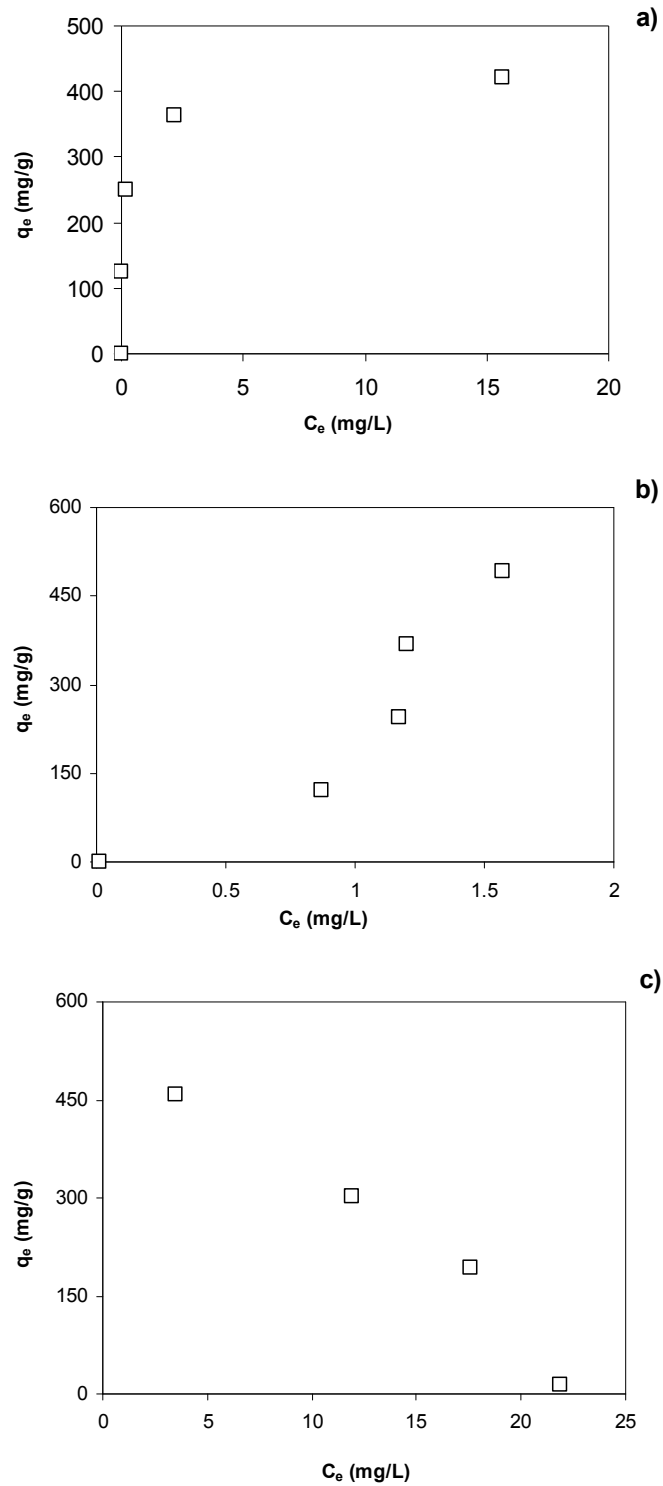


Figure A.6.1: Chemical sequential extraction procedure after [149]

Appendix VII: Cu^{2+} , Pb^{2+} and Cr(VI) removal isotherms**Figure A.7.1:** Cu^{2+} (a), Pb^{2+} (b) and Cr(VI) (c) removal isotherms at 25°C and 0.1 M KCl

Appendix VIII: Neutralization column tests using CFBC-PCFA

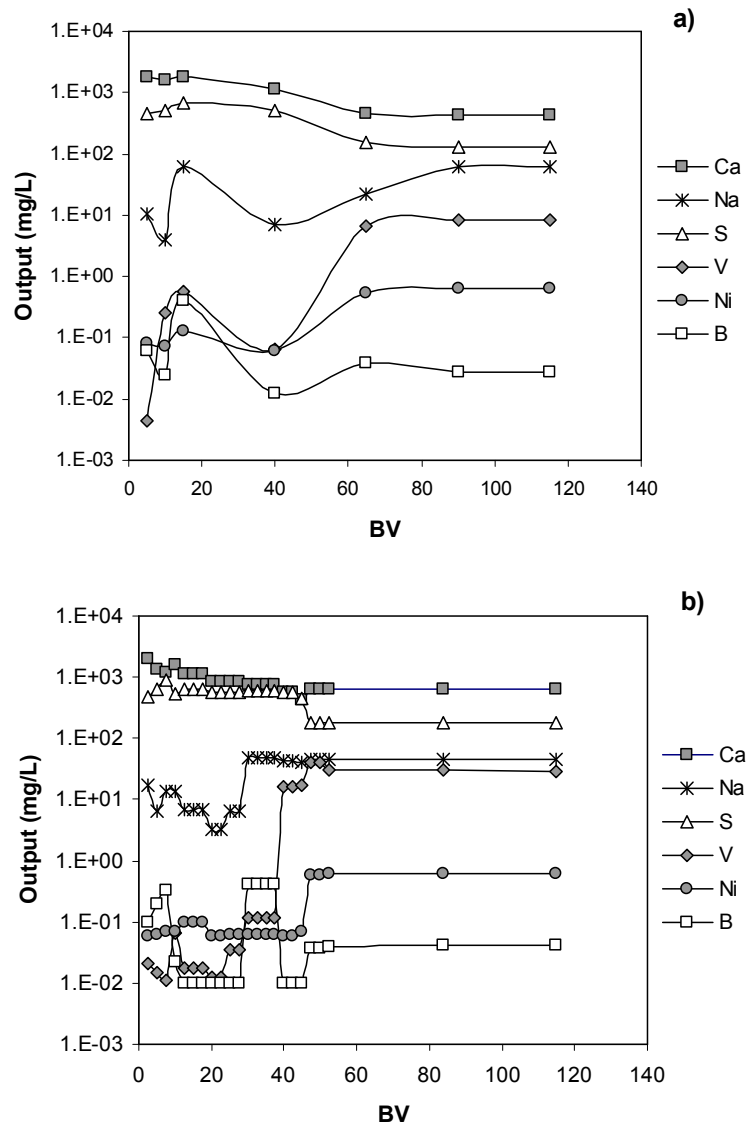


Figure A.8.1: Main major and trace elements detected in neutralization test by CFBC-PCFA at pH 2 for h₃ (a) and h₆ (b).
BV: Bed volume

Appendix IX: Neutralization fixed bed column test using NCS3

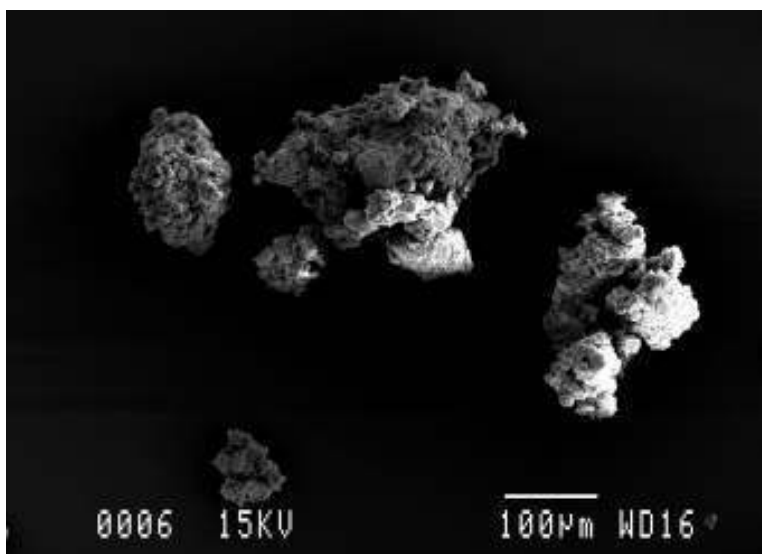


Figure A.9.1: SEM-EDX of NCS3 after neutralization fixed-bed column test at pH 2 and h_6

Appendix X: Cu^{2+} and Pb^{2+} removal column tests using NCS3

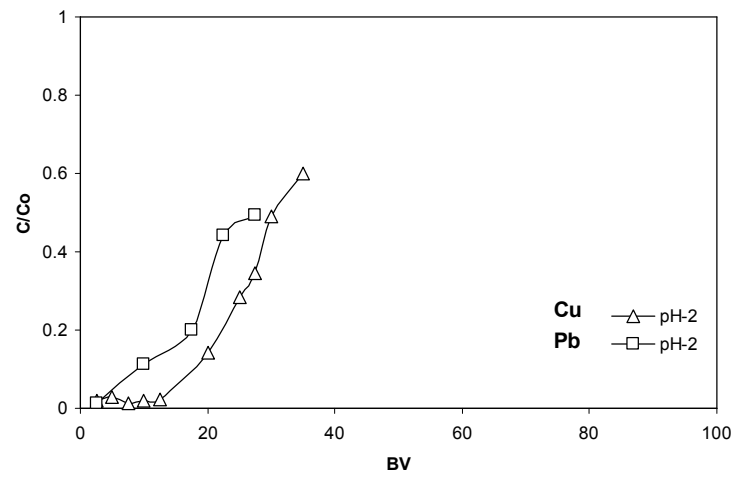


Figure A.10.1: Cu^{2+} and Pb^{2+} removal column tests at pH 2 and at bed height of 6 cm.

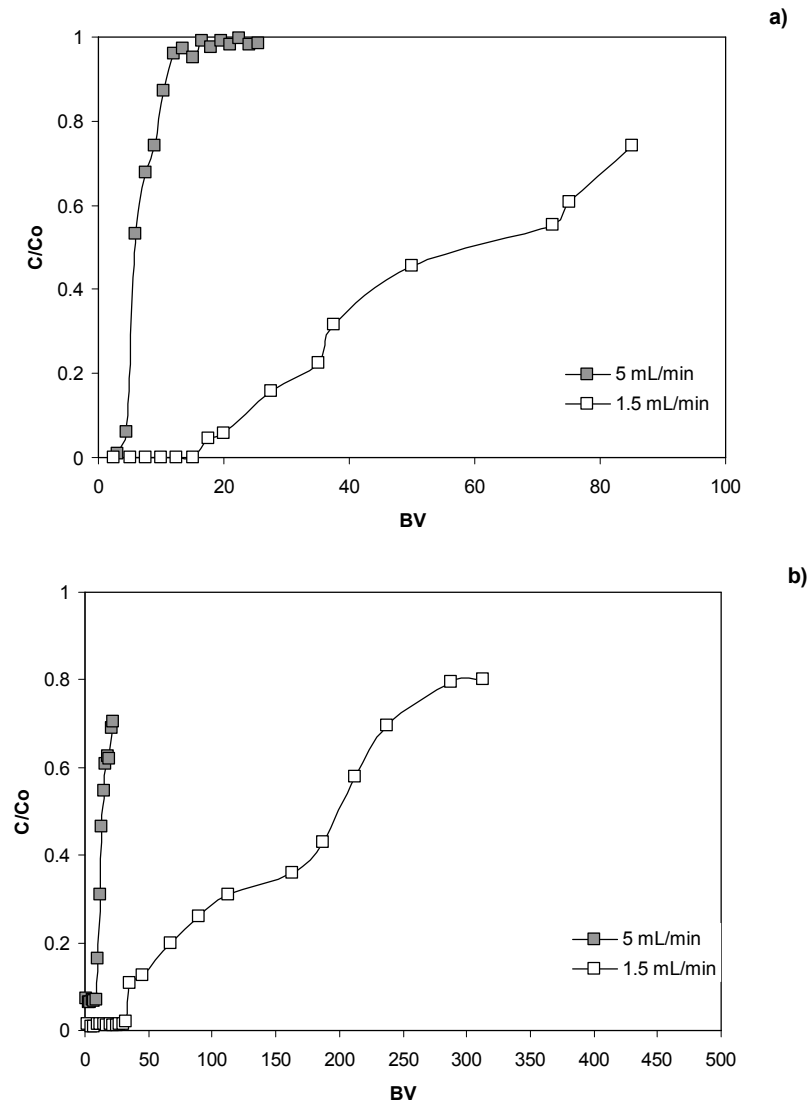


Figure A.10.2: Cu^{2+} (a) and Pb^{2+} (b) removal column tests at flow rate of 1.5 and 5 mL/min.

Appendix XI: Prediction of breakthrough curves

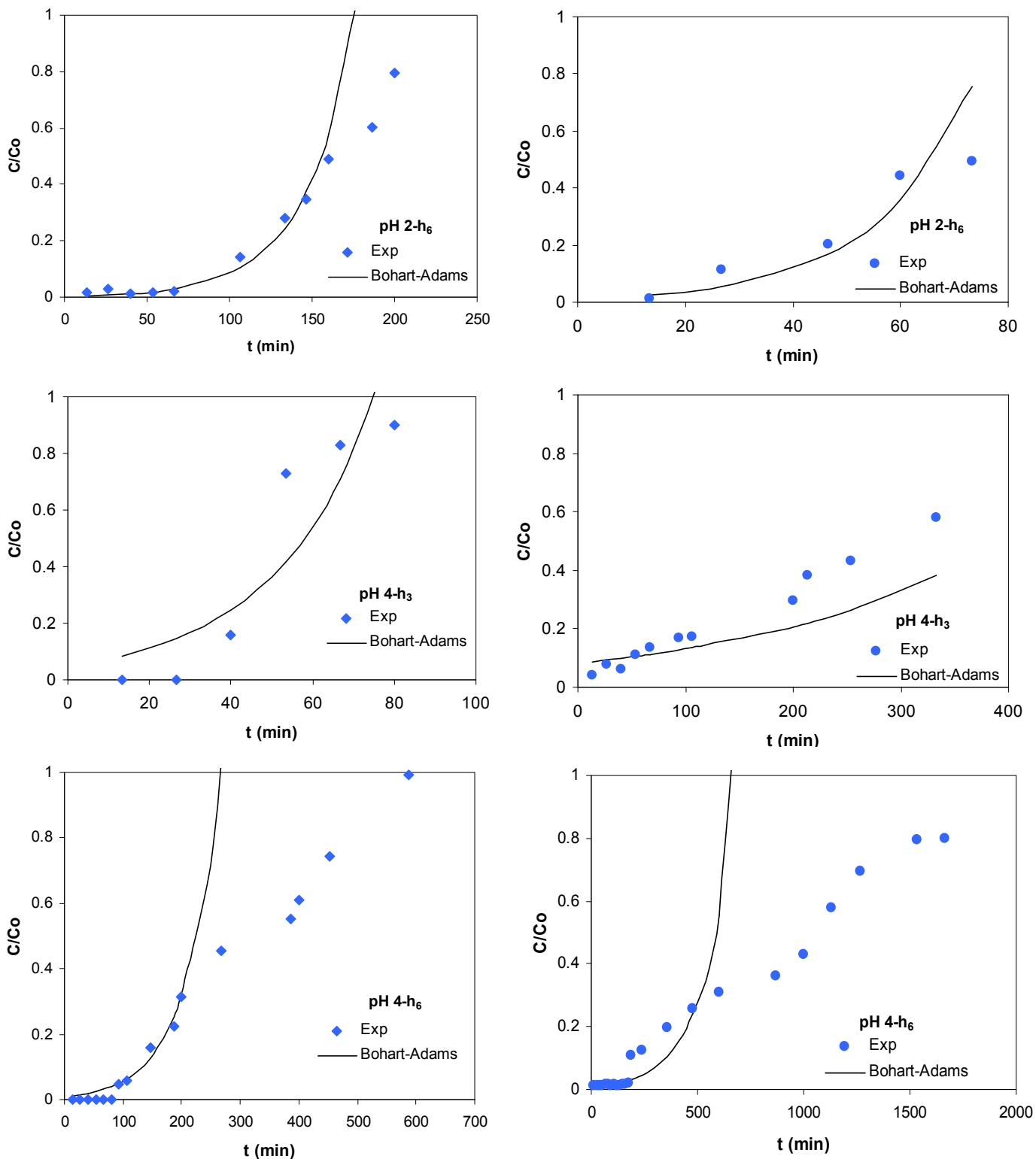


Figure A.11.1: Bohart-Adams model fitting for Cu^{2+} (left) and Pb^{2+} (right) removal column tests using NCS3

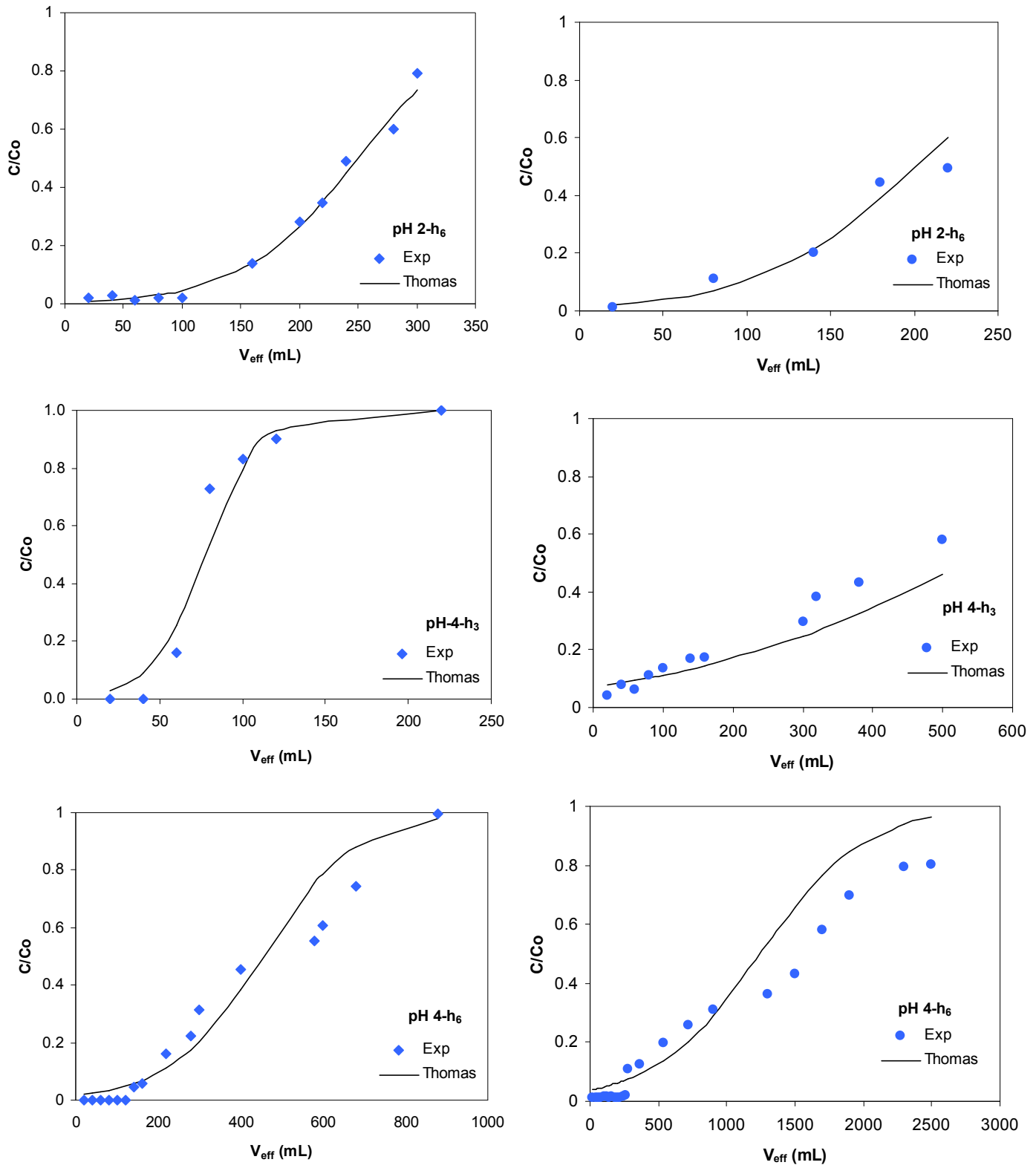


Figure A.11.2: Thomas model fitting for Cu^{2+} (left) and Pb^{2+} (right) removal column tests using NCS3

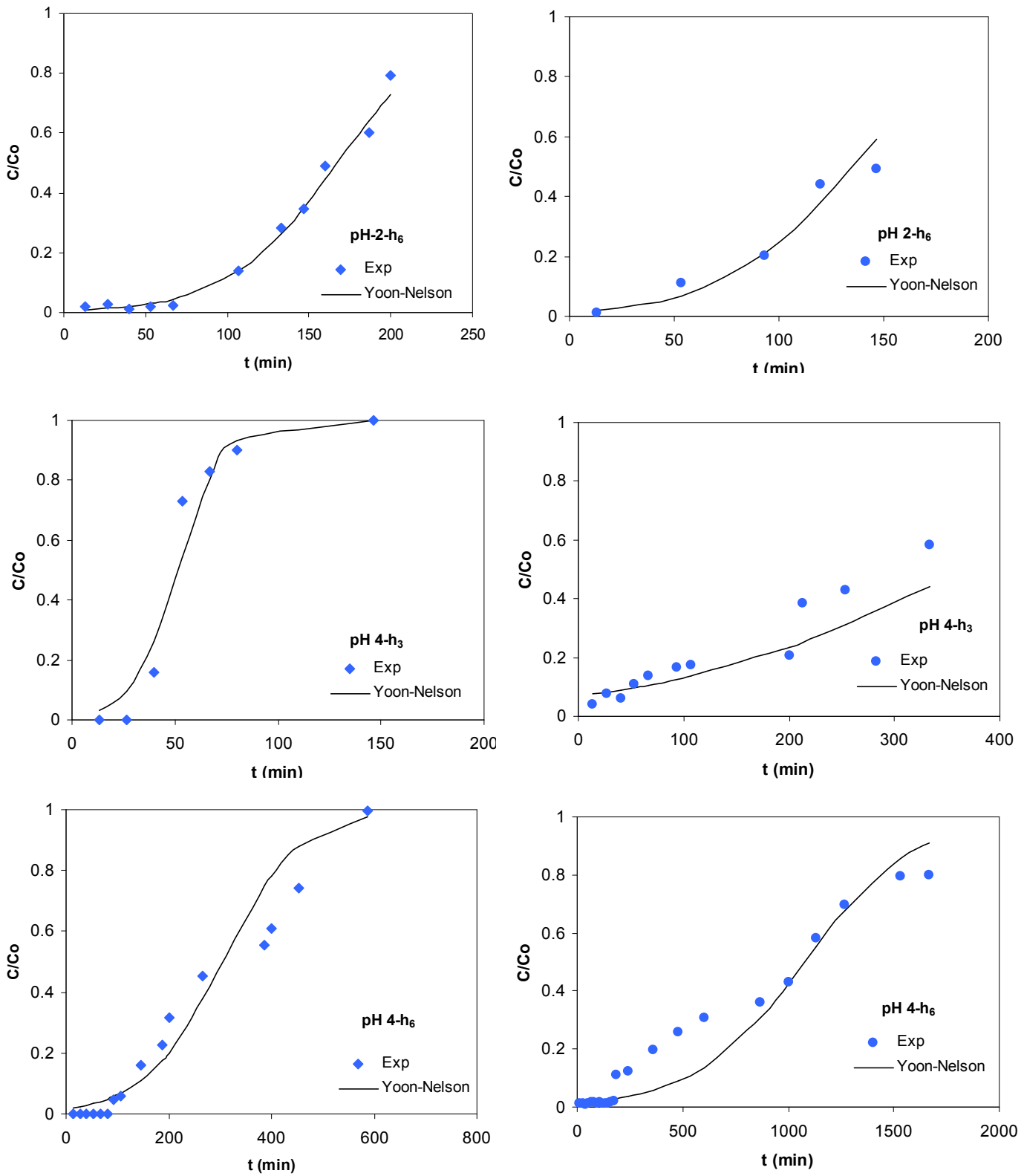


Figure A.11.3: Yoon-Nelson model fitting for Cu^{2+} (left) and Pb^{2+} (right) removal column tests using NCS3

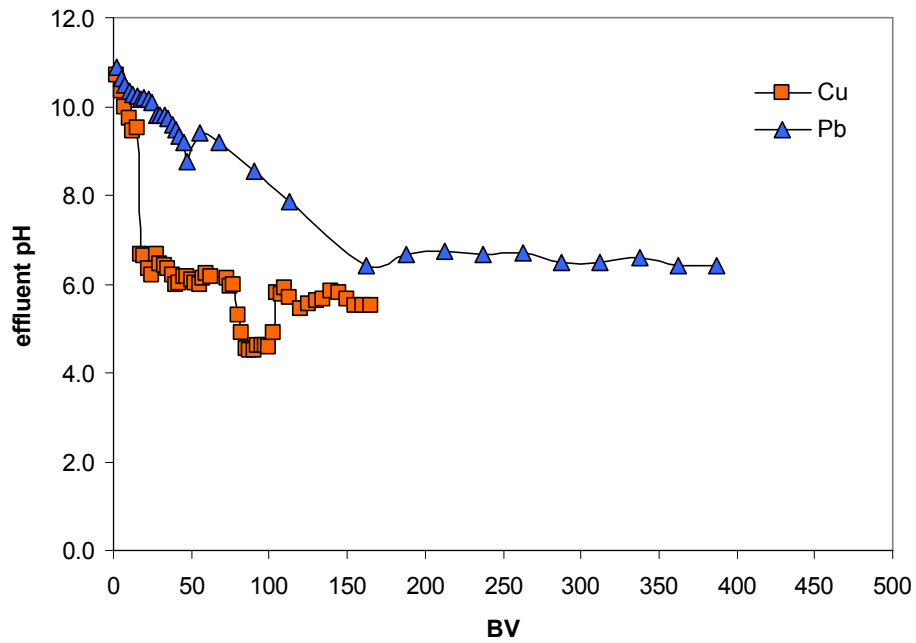
Appendix XII: Effluent pH during Cu^{2+} and Pb^{2+} removal column tests

Figure A.12.1: Effluent pH during Cu^{2+} and Pb^{2+} removal column tests; pH 4 and bed height of 6 cm.

Appendix XIII: Papers



Los Angeles, London, New Delhi
and Singapore
<http://www.sagepub.com>



© The Author(s), 2009. Reprints and permissions:
<http://www.sagepub.co.uk/journalsPermissions.nav>

ISSN 0734-242X

Waste Management & Research

2009: 00: 1-12

DOI: 10.1177/0734242X09103190

Fly ashes from coal and petroleum coke combustion: current and innovative potential applications

Aixa González, Rodrigo Navia

Department of Chemical Engineering, University of La Frontera, Temuco, Chile

Natalia Moreno

Department of Geosciences, IDAEA-CSIC, Barcelona, Spain

Coal fly ashes (CFA) are generated in large amounts worldwide. Current combustion technologies allow the burning of fuels with high sulfur content such as petroleum coke, generating non-CFA, such as petroleum coke fly ash (PCFA), mainly from fluidized bed combustion processes. The disposal of CFA and PCFA fly ashes can have severe impacts in the environment such as a potential groundwater contamination by the leaching of heavy metals and/or particulate matter emissions; making it necessary to treat or reuse them. At present CFA are utilized in several applications fields such as cement and concrete production, agriculture and soil stabilization. However, their reuse is restricted by the quality parameters of the end-product or requirements defined by the production process. Therefore, secondary material markets can use a limited amount of CFA, which implies the necessity of new markets for the unused CFA. Some potential future utilization options reviewed herein are zeolite synthesis and valuable metals extraction. In comparison to CFA, PCFA are characterized by a high Ca content, suggesting a possible use as neutralizers of acid wastewaters from mining operations, opening a new potential application area for PCFA that could solve contamination problems in emergent and mining countries such as Chile. However, this potential application may be limited by PCFA heavy metals leaching, mainly V and Ni, which are present in PCFA in high concentrations.

Keywords: Coal fly ash, petroleum coke fly ash, reuse, utilization, secondary materials, wmr 08-0090

Introduction

According to the World Energy Council the energy demand has astronomically increased in recent years, and the energy demand is forecast to continue growing at an annual average rate of 1.6% between 2004 and 2030 (World Energy Council 2007). This fact, which is based on the current energy mix, implies an increase in the consumption of fossil fuels, of which coal is expected to show the largest demand growth, from about 2772 Mt in 2004 to 4441 Mt in 2030. The two main reasons for this increase are the supply situation for crude oil and natural gas (rising prices, depletion of resources). Therefore, an increase in coal combustion by-products is also expected.

The generation of combustion by-products is a global problem with severe implications for human health, environment and industry. On the one hand, high storage, transport and

disposal costs must be faced by plant operators and waste management companies and, on the other hand, leaching of elements that are of environmental concern through the soil to the groundwater may impact negatively the terrestrial and aquatic ecosystems (Canty & Everett 2006, Jankowski *et al.* 2006). Nowadays industry is very interested in the reuse of such by-products as coal (CFA) and petroleum coke fly ashes (PCFA) whenever the reuse allows costs to be saved and to maintain the product quality as well as process stability at the same time. Many investigations aim to find new applications for these by-products as raw materials, simultaneously avoiding possible potential risks for the environment and human health, when they are disposed of. Therefore, the main objective of this article is to review current and future applications of CFA and PCFA.

Corresponding author: Prof. Dr. Rodrigo Navia, Department of Chemical Engineering, University of La Frontera, P.O. Box 54-D, Temuco, Chile.

Tel: +56 45 325477; fax: +56 45 325053; e-mail: rnavia@ufro.cl

Received 7 August 2008; accepted in revised form 22 January 2009

Table 1: Chemical composition of fly ashes from different sources. Mean values in %w/w. LOI (%): Loss on ignition; MSW: Municipal solid waste.

Fly ash source	SiO ₂	Al ₂ O ₃	Fe ₂ O ₃	CaO	MgO	LOI
MSW incineration ^a	13.6	0.9	3.8	45.4	3.2	nd
Coal combustion ^b	50	27	8	5	2	4
Coal gasification ^c	57	19	3.8	6.4	0.8	4
Steel smelting ^d	8.3	6.4	49.9	24.3	8.2	2.3

^aPan *et al.* (2008).^bMoreno *et al.* (2005).^cFont *et al.* (2007).^dMudavaki *et al.* (1999).*Other compounds present in MSW incineration fly ash are SO₃, Na₂O, K₂O, TiO₂ and Cl with values of 6.3, 4.2, 3.9, 3.1 and 9.7 %, respectively.

nd: not determined.

Table 2: Mineralogical compounds of fly ashes from different sources.

Fly ash source	Main minerals
MSW incineration ^a	calcite, quartz, zincite, halite, silvite
Coal combustion ^b	quartz, mullite, hematite, magnetite, anhydrite, lime, glass
Coal gasification ^c	galena, sphalerite, wurtzite, pyrrhotite, nickeline
Steel smelting ^d	magnetite, zincite, quartz, magnesium aluminium silicate

^aChang & Wey (2006).^bMoreno *et al.* (2005).^cFont *et al.* (2007).^dGonzalez *et al.* (2007).

Fly ashes

Coal fly ashes are generated in large amounts and represent between 60 and 88% of the by-products from pulverized coal combustion. Around 500 Mt fly ashes per year are generated worldwide (Kikuchi 1999) of which the amount generated in the USA is about 72 Mt per year (ACAA 2007) and in Europe 43 Mt per year (ECOBA 2006).

The demand of petroleum coke is also expected to increase. Its current use is mainly as primary and co-firing fuel for power generation (Swain 1997) and it is expected that the demand for this by-product of the petroleum refining process could reach 100 Mt in 2010 (Chen & Lu 2007).

Fly ashes are mainly produced from combustion processes, as well as smelting, gasification and incineration processes of solid residues (Wang & Wu 2006). An understanding of the physical and chemical as well as mineralogical properties of fly ashes is important because these properties influence the opportunities for their reuse. According to several reports, depending on original fuel and process, fly ashes may present differences in their chemical reactivity that depends on the chemical and mineralogical composition (see Tables 1 and 2, respectively) and their physical parameters (Kimoto *et al.* 2005).

Coal fly ashes

Handling CFA is considered to be a very complex issue due to their variable composition and fine particle size. Chemically, CFA mainly consist of silica (SiO₂), alumina (Al₂O₃), calcium oxide (CaO), iron oxide (Fe₂O₃), magnesium oxide

(MgO), sodium oxide (Na₂O) and potassium oxide (K₂O), residual carbon and sulfate (SO₄²⁻) (see Table 1) (Kikuchi 1999, Wang & Wu 2006). In addition, Table 2 summarises the main mineralogical phases of CFA from different sources. It has been reported that CFA may contain some elements of environmental concern, such as arsenic, barium, chromium, cadmium, lead, selenium and mercury, which can limit the potential applications of CFA (Querol *et al.* 2001b, Izquierdo *et al.* 2007, 2008). The study of Jegadeesan *et al.* (2008) based on chemical sequential extraction and leaching tests conclude that the highest mobility of heavy metals in CFA was observed at pH < 4 and pH > 9, depending on the distribution (affinity) of these elements.

Most of the CFA show a similar morphology. They consist of irregularly shaped, oval and spherical particles, such as plerospheres (larger particles filled with smaller ones) and cenospheres (hollow particles).

Another common characteristic of CFA is the particle size distribution, which normally ranges between 0.5 and 400 µm, with an average size between 12 and 80 µm (Moreno *et al.* 2005). Low grain sizes together with the presence of pozzolanic compounds in CFA could lead to a low hydraulic conductivity (k_f), which suggests that CFA could potentially be used as a compacted mineral layer in landfills.

Moreno *et al.* (2005) reported that the real density for European fly ashes can vary between 1.3 and 2.7 kg L⁻¹, whereas the specific surface area ranges between 1.3 and 12.4 m² g⁻¹.

Table 3: Composition of PCFA from fluidized bed combustion and CFA/PCFA from integrated gasification in combined cycle.

Fly ashes	Chemical composition (w/w %)					Trace elements (mg kg ⁻¹)			Process
	SiO ₂	Al ₂ O ₃	Fe ₂ O ₃	CaO	SO ₃	C	Ni	V	
PCFA ^a	0.5	0.1	0.1	47	27	15	2164	5473	Petroleum coke fluidized bed combustion
CFA/PCFA ^b	57	19	4	6.4	3.1	5.5	1147	3302	Coal/petroleum coke gasification

^aGonzález *et al.* (2007).

^bFont *et al.* (2007).

Petroleum coke fly ashes

Petroleum coke, a by-product of the petroleum refining process, is considered to be an attractive primary or supplementary fuel for power generation (Swain 1997). At present, there are three main technologies that allow the efficient combustion of petroleum coke: circulating fluidized bed combustion (CFBC), pressurized fluidized bed combustion (PFBC) and integrated gasification combined cycle (IGCC). One of the most used technologies in the world is CFBC, which has gained widespread acceptance in recent years and has provided important experience in petroleum coke burning performance (Hower *et al.* 2005). In CFBC technology calcium sorbents such as calcite (CaCO₃) are used to remove the high sulfur dioxide (SO₂) content of petroleum coke combustion off-gases. These reactions are summarized in Anthony & Granatstein (2001).

Chemical and mineralogical composition of petroleum coke fly ashes (PCFA) and their possible applications have been investigated in a few studies. However, due to the increasing production of petroleum coke as fuel, it is important to characterize them and investigate the potential applications (Swain 1997).

According to Table 3, PCFA from CFBC have high amounts of calcium and sulfur as well as considerable amounts of unburned carbon and traces of heavy metals such as Ni and V.

Recently, some reports have been published identifying changes in the quality of co-fired fly ashes from coal and petroleum coke (Hower *et al.* 2005, Izquierdo *et al.* 2007, 2008). These studies have demonstrated that the utilization of petroleum coke as fuel contributes to an increase in elements of environmental concern such as Ni, V, Mo and As, in comparison with CFA fly ashes. In fact, Mo and As were identified as the most potentially harmful species in coal/petroleum coke combustion fly ashes. Regarding the mobility of such trace elements Henke (2005) reported that Ni and V were found in very low concentrations in the leachate of coal/petroleum coke combustion fly ashes, with values of 7.2 mg Ni L⁻¹ and 16.8 mg V L⁻¹.

Current applications

According to data from 2005 (Figure 1(a)), fly ash utilization in Europe is about 48% (ECOPA 2006), whereas the cement and concrete industry are the principal application areas (raw material 27% and additive 39.6%). Large amounts are

also used in geotechnical applications (such as grouting, asphalt filler, sub-grade stabilization, pavement base course, general engineering fill, structural fill, soil amendment and infill), which represent 26.7%, and in concrete block manufacturing (5.3%).

The American Coal Ash Association (ACAA) states that fly ash utilization in USA was about 44% in 2007 (Figure 1(b)) (ACAA 2007). Fifty-five percent of the reused fly ashes are delivered to the cement and concrete industry, whereas the contribution of reused CFA in geotechnical applications was about 26%.

Cement and concrete industry

It is well known that the Portland cement industry requires large amounts of energy and raw materials (Gartner 2004). In this sense, this industry has taken important measures to improve energy efficiency, energy costs and raw materials costs, replacing fossil fuels with alternatives and substituting raw material with CFA.

CFA marketing began in 1946 in USA. Their use and acceptance created the need for technical specifications, summarized in the American Society for Testing Materials C 618 (Manz 1999). A distinction between pulverized CFA with pozzolanic (Class F) and cementitious (Class C) fly ash properties was implemented, in order to classify them as different products (see Table 4).

The pozzolanic and cementitious characteristics of CFA may allow their use as a binding agent or as raw material to produce clinker and to replace cement in concrete production (Goumans *et al.* 1994). Additionally, depending on the coal source and combustion technology used these by-products can contain high amounts of CaO that con-

Table 4: Classification of coal fly ashes according to ASTM C.

Properties	Fly ash class	
	Class F	Class C
SiO ₂ + Al ₂ O ₃ + Fe ₂ O ₃ (% min)	70	50
SO ₃ (% max)	5	5
Moisture content (% max)	3	3
LOI ^a (% max)	6 ^b	6

^aLoss on ignition.

^bThe use of Class F containing up to 12% LOI may be approved if acceptable performance results are available (Manz 1999)

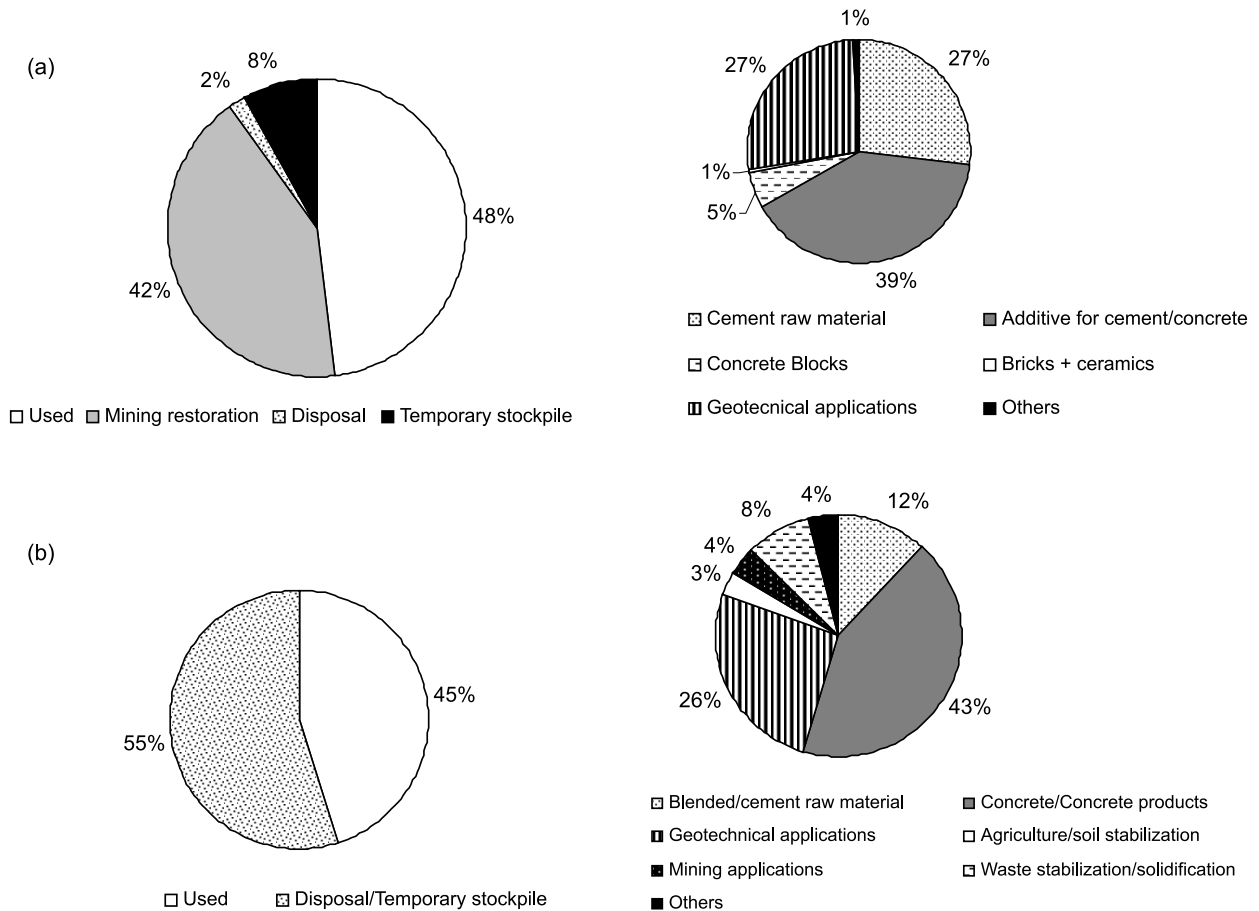


Fig. 1: Current trends in fly ash utilization in (a) Europe (ECOBA 2006) and (b) USA (ACAA 2007).

tribute to enhancement of concrete quality (Sugama *et al.* 2002).

In relation to PCFA from fluidized bed combustion, Conn *et al.* (1999) stated that this by-product develops no pozzolanic reactions, which means that it can not replace cement. However, due to high amounts of calcium sulfate it can be reused as gypsum substitute in the cement industry.

The literature reports several types of blended Portland with CFA, alkali-activated cements with resistance to corrosive environments (Shi & Fernández-Jiménez 2006, Kovalchuk *et al.* 2007) and controlled low-strength material to stabilize and solidify contaminated soils or spoils (Gabr & Bowders 2000, Nataraja & Nalanda 2008). Most of them have similar or even better properties than Portland cement and the main advantages of the use of CFA to replace cement partially are lower water demand and lower evolution of hydration heat (Siddique 2004).

Different types of concrete with CFA have been developed, such as high volume fly ash concrete, high performance concrete (Ravina 1998, Sata *et al.* 2007) and autoclaved aerated concrete (Sutton 1999). They all contain more than 30% (w/w) of CFA class F and exhibit excellent mechanical properties, durability in connection with repeated freezing and thawing, very low permeability to chloride ions,

no adverse expansion when reactive aggregates are incorporated into concrete, and a reduction of cracking at early ages.

However, CFA reuse in concrete production may present some disadvantages due to the variability of their chemical properties, high carbonaceous material content (Pedersen *et al.* 2008) and the contribution to delayed ettringite formation in cement paste in presence of sulfates (Chrysochoou & Dermatas 2006). These are all adverse effects for cement and concrete quality.

Agriculture and soil stabilization

The application of CFA in soil is useful as a resource saver. CFA contains macronutrients for plants such as S, Ca, K and P (Adriano *et al.* 2002, Ram *et al.* 2007). Moreover, CFA contain carbonates, which act as calcareous amendment, enhancing pH levels in soil, improving the availability of nutrients and increasing the water-holding capacity of soils (Stevens & Dun 2004, Mittra *et al.* 2005). Some CFA can act as a buffer, observing that their application in soil permits a significant increase the pH, depending on the dose used and consequently avoids the leaching of relevant cations for plant growth (Mittra *et al.* 2005). Stevens & Dunn (2004) evaluated the neutralization capacity of fly ashes in soil by investi-

gating fly ash doses of 3, 4, 6.7 and 10.1 Mg ha⁻¹, respectively, and they observed a pH value increase from 4.8 to 6.0. The incorporation in soil of macro- (Ca, S, Mg and K) and micro- (Se, B, Mn and Mo) nutrients through fly ashes facilitates plant uptake of these elements, the development of superficial roots and, as a result, improving plant growth and simultaneously saving raw materials (Jala & Goyal 2006). The application of fly ashes in soil has been reported to be successful for alfalfa, wheat, rice, cotton, maize and for forestry plantations, but for other crops such as sea beet the application was connected with toxic effects. In addition, CFA application in soil, mixed with organic waste and chemical fertilizers increased grain yield and nutrient uptake of plants (Ram *et al.* 2007). Application of about 505 Mg ha⁻¹ CFA to soil immediately increased soil pH and the concentration of most extractable elements. Furthermore, no detrimental effects to soil microbial community were found, thereby keeping the heavy metals content below the permissible levels (Shutter & Fuhrman 2001, Mittra *et al.* 2005, Jala & Goyal, 2006). Kikuchi (1999) developed a potassium silicate fertilizer from CFA, which was found to be soluble in acid media, suggesting that this fertilizer may remain in soil until plant necessity, since its consumption is coupled with the release of organic acids from the plant.

Moreover, CFA addition in soil can provoke an improvement in soil texture, increase water-holding capacity, and reduce swelling capacity (Nalbantoglu 2004, Lin *et al.* 2007). These characteristics may be favourable for applications such as the construction of roads, parking places and buildings on stabilized soils, on which it is difficult to build. In Chile, PCFA have been researched as a soil stabilizer increasing soil compressive strength (Thenoux *et al.* 2007).

CFA addition to agricultural land may increase the release of heavy metals and salinity in soil, causing damage to plant species and depleting microbial activity. In addition, heavy metals may leach into water bodies and enter the food chain. Therefore, several studies recommend the use of fly ashes only in non-agricultural soils, such as forestry soils, landfill and coal mining restoration (Cox *et al.* 2008, Singh *et al.* 2008).

Ceramic, glass-like and glass–ceramic materials

The ceramic, glass and glass–ceramic industry are high consumers of silicate-based natural raw materials (clays), but at present, there is a worldwide shortage of clay to produce ceramic materials (Haiying *et al.* 2007). Therefore, it is necessary to find other materials to replace clay. It is well known that fly ashes contain silica in large amounts as well as aluminium and calcium oxides, and so they are able to replace raw materials to produce ceramic products. CFA have already been used to produce ceramic materials (Queral *et al.* 1997, Zimmer & Bergmann 2007, Erol *et al.* 2008). Production processes of glass-like products made from fly ashes allow heavy metal encapsulation and, in addition, may destroy formed dioxins.

In addition, the transformation of fly ashes into glass–ceramic products induces the crystallization of a certain kind

of glass by means of heat controlling treatment. Glass–ceramic products from waste glasses and fly ashes have been reported by several authors (Barbieri *et al.* 2000, Karamberi *et al.* 2007, Károly *et al.* 2007). These kinds of product may present better chemical stability, better mechanical strength and wear resistance than original glasses, implying savings of natural resources and lower production costs.

Future applications

The aforementioned applications may demand smaller quantities of fly ashes in comparison with the increase in their generation. Therefore, it is necessary to establish other applications and markets. Current research has been focused on fly ash zeolitization, valuable elements extraction and low cost adsorbents, filling material in permeable reactive barriers, geological barriers and acid mine drainage and mining residue neutralization.

Extraction of valuable metals

Fly ashes could be a potential source of valuable metals, especially the ashes from coal combustion and gasification, as well as those from municipal waste incinerators. Several studies have shown the feasibility of recovering valuable elements from fly ashes such as titanium (Shabtai *et al.* 1993), gallium (Gutiérrez *et al.* 1997, Font *et al.* 2007), germanium (Font *et al.* 2005), aluminium (Matje *et al.* 2005), iron (Dwivedi *et al.* 2006), vanadium (Font *et al.* 2007), zinc (Okada *et al.* 2007), chromium (Zhang & Itoh 2006), lead (Zhang & Itoh 2006, Okada *et al.* 2007), cadmium (Zhang & Itoh 2006) and others. Their recovery may increase the economic value of fly ashes and, at the same time, it may represent a way to decrease mining activities and the amount of fly ash disposed (Zhang & Itoh 2006, Miyake 2007). In addition, recovering a refined metal from CFA may lead to a less harmful fly ash by-product that can be used for construction purposes (Seggiani *et al.* 2006, Cox, *et al.* 2008).

Low-cost adsorbents

Adsorption is a very important decontamination treatment for wastewater which is widely used, because of its simplicity and effectiveness. Activated carbon is a widely used adsorbent for heavy metals removal in aqueous systems, at the same time it has become an expensive adsorbent (about US\$ 1.0 kg⁻¹). Therefore, there is a growing interest regarding low-cost materials (sub-products or wastes, see Table 5) with relevant adsorption capacity and local availability, which

Table 5: Cost of activated carbon (commercial degree) and some low cost adsorbents (Babel & Kurniawan 2003).

Adsorbent	Cost (US\$ kg ⁻¹)
Activated carbon	1–3
Zeolites	0.03–0.12
Coal fly ash + coal	0.03
Clays	0.04–0.12

could compete with activated carbon (Babel & Kurniawan 2003).

Fly ashes are a promising adsorbent for the removal of several contaminants (Babel & Kurniawan 2003, Wang & Wu 2006). Research studies have shown that the presence of residual carbonaceous material, amorphous iron and aluminum oxides and silicate minerals are responsible for the adsorption properties of fly ashes, which have an amphoteric character in aqueous medium, and therefore, depending on solution pH, metallic ions, oxy-anions or polar molecules can be adsorbed (Bayat 2002a, b). Another important parameter is the CaO content in fly ashes, which raises the pH of an aqueous medium, inducing the precipitation of several metallic ions in the form of hydroxides, oxides and oxy-hydroxides. This property could be useful for treating acid wastewaters from mining activities and in desulfurization processes (Ricou *et al.* 1999). Fly ashes have a great potential to remove heavy metals (Bayat 2002a, b, Babel & Kurniawan 2003, Cetin & Pehlivan 2007) and NO_x by adsorption (Rubel *et al.* 2005) as well as SO_x by means of catalytic oxidation (Lee *et al.* 2006) from flue gases. Additionally, among others, organic compounds such as chlorophenols, phenols, polychlorinated biphenyls and dyes are being removed by adsorption (Nollet *et al.* 2003, Sarkar & Archarya 2006, Crini 2006, Estevihno *et al.* 2007).

Geological barriers

Coal combustion by-products have been used as low permeability geological barriers in a similar way to compacted clay (Gangloff *et al.* 2000, Awe *et al.* 2001, Kalinski & Yerra 2005). Several authors affirm that CFA is a residue with high potential as a construction liner, because of its low grain size and chemical composition (Palmer *et al.* 2000, Mollamahmutoglu & Yilmaz 2001, Cokca & Yilmaz 2004). In fact, fly ash hydraulic conductivity may decrease until reaching a value near to 10⁻⁹ m s⁻¹ in large-scale field applications, blended with water and residues such as rubber, flue gas desulfurization material and blast furnace slag, which may increase the liner strength.

Pandian *et al.* (1998) showed that compacted CFA were less sensitive to moisture changes than soils. Kalinski & Yerra (2005) demonstrated the inversely proportional dependency of hydraulic conductivity of siliceous CFA with water and hydrated lime content. Moreover they observed a lower permeability when 1% (w/w) of gypsum was added. Palmer *et al.* (2000) also showed that field applications of siliceous CFA were not satisfactory; due to the necessity to blend them with cementitious CFA to reach a hydraulic conductivity less than 10⁻⁹ m s⁻¹. Prashanth *et al.* (2001) studied the reuse of pozzolanic CFA as a substitute for clay liners. They found that CFA hydraulic conductivity increased in the presence of diluted acid, making it not useful as a liner. However, the addition of bentonite improved the geotechnical properties of pozzolanic CFA such that this blend can be recommended as a clay liner substitute.

Zeolites synthesis

Coal fly ashes show similarity with some volcanic ashes, which are precursors from natural zeolites. For this reason, Höller & Wirsching (1985) proposed the use of alkaline hydrothermal conversion of CFA to obtain different types of zeolites. Since then, several technical papers and patents have been published in the field of zeolites production from fly ashes (Mondragon *et al.* 1990, Moreno, 2002, Querol *et al.* 2002a, 2007, Inada *et al.* 2005). Almost all publications deal with the hydrothermal alkaline conversion of CFA into zeolite. In fact, the classic alkaline conversion is based on the combination of CFA with an alkaline solution under different conditions, such as solution/CFA ratio, molarity of the alkaline solution, temperature, pressure and reaction time, to obtain diverse zeolite types (see Table 6). Another important process was introduced by the use of microwave treatment that allows a reduction of the reaction time to obtain zeolitic products from hours to minutes (Querol *et al.* 1997).

Querol *et al.* (2002a) reported that from the same CFA more than 10 different zeolite types can be obtained and, depending on the variation of process parameters such as reaction time and activation agent/CFA ratio, zeolite production yield can vary between 20 and 50%. A pilot plant experiment in a single-batch reactor allowed the synthesis of zeolitic material with 55% NaP1 zeolite, by direct conversion from CFA in only 8 h (Querol *et al.* 2001a).

For about 15 years, new processes to improve the conventional alkaline conversion method have appeared. One of them is the introduction of an alkaline fusion step before alkaline hydrothermal conversion. This process increased the conversion performance and the possibility to synthesize different zeolites (Shigemoto *et al.* 1993).

To avoid a synthesis process with the generation of wastewater, Park *et al.* (2000) developed a synthesis strategy called molten-salt or dry conversion, which was based on the use of salt mixtures (NaOH/NaNO₃) instead of aqueous solutions as reaction medium. The limitations of this strategy were that only low cationic exchange capacity zeolites were obtained and high temperature was needed.

The conventional and modified conversion processes present limitations such as low conversion yield (20–65%) and significant amounts of impurities such as heavy metals in the zeolite matrix. These limitations were the starting point to modify the classical hydrothermal alkaline conversion

Table 6. Synthesis of NaP1 with variation of reactions parameters with different CFA (NaOH as activation agent) (Moreno, 2002).

Concentration (mol L ⁻¹)	NaOH/CFA (mLg ⁻¹)	Temperature (°C)	Time (h)	NaP1 content (%)
2	3	90	9	25–30
2	3	90	24	30
2	3	150	4	35–41
3	3	120	9	49
1	18	150	24	28–48

Table 7: Examples of applications of PRB's technology in Europe and USA (NATO/CCMS 2003).

Treated pollutants	Field Applications	Decontamination time
Organic substances TCE, DCE, VC, Benzene	Industrial site, Belfast, Northern Ireland Industrial site, Coffeyville, Kansas, USA. Former dry cleaning site, Rheine Westphalia, Germany	1995–2000 1996–nf 1998–nf
Heavy metals Cr, Ni, Pb, Cu, Co Cd, Zn	Borden Aquifer, Ontario, Canada Cape Canaveral Air Station, Florida, USA Massachusetts Military reservation CS-1 Plume, Falmouth, USA	1991–2001 1998–nf 1998–nf
Nf, not finished.		

Table 8: Different reactive materials used in PRB.

Contaminants	Reactive materials	References
Trichlorethylene	Surface modified zeolite	Burt <i>et al.</i> (2005)
Cr(VI)	Fe(0)	Blowes <i>et al.</i> (2000)
As	Compost	Köber <i>et al.</i> (2005)
Acid mine drainage	Fe(0)	Wilkin & McNeil (2007)
Acid mine drainage	Compost–lime–Fe(0)	Gibert <i>et al.</i> (2003)
Pb, Cd, Cu, Ni, Zn	Leaf-compost material	McGregor <i>et al.</i> (2002)
Zn	Foundry residue	Lee <i>et al.</i> (2004)
Pb, Cr(VI)	Modified fly ash	Doherty <i>et al.</i> (2006)
Cu, Pb, Zn	Fly ash	Wantanaphong <i>et al.</i> (2005)
Nitrate, Mn	Limestone–dolomite	Skinner & Schutte (2006)
Sulfate	Compost and gravel	Benner <i>et al.</i> (2002)
Sulfate	Fly ash	Golab <i>et al.</i> (2006)

process. In fact, Hollman *et al.* (1999) developed a two-stage synthesis procedure that enabled a conversion yield of more than 90% into zeolite. The first step was a silica extraction. Then the silica-solution product was mixed with an aluminium-rich solution, followed by an alkaline hydrothermal conversion. The residual by-products of the process were used to synthesize zeolitic material of lower cationic exchange capacity. Authors such as Moreno *et al.* (2004) optimized the results from Hollman *et al.* (1999) and obtained high purity zeolites (> 98% X and A zeolites) coupled with a zeolitic material (45% NaP1) in a solid residue in the same procedure. These zeolites showed a cationic exchange capacity (CEC) close to that of commercial zeolites. For instance, the synthesized zeolite A-PU4 (II) had a CEC of 5.3 meq g⁻¹, whereas commercial zeolite A-IQE has a CEC of about 5.4 meq g⁻¹.

Zeolites have an interesting potential application in decontamination processes. Due to their high cationic exchange capacity, they can be utilized in the removal of heavy metals and ammonium from wastewater and polluted soils. Several reports suggest that zeolites from fly ashes have a strong affinity for Cu, Cd and Pb from wastewater (Lee *et al.* 2000, Moreno *et al.* 2001, Querol *et al.* 2002b, 2006). For instance, Moreno *et al.* (2001) obtained a considerable contamination reduction when using a synthesized 4 A/X zeolite to remediate a wastewater that was contaminated with acid mine drainage. The observed heavy metals (Zn, Fe and Mn) concentration drop was found to be 174 to < 0.1 mg L⁻¹ for Zn, 444 to 0.8 mg L⁻¹ for Fe and 74 to < 0.1 mg L⁻¹ for Mn.

Flue gas purification technology is another environmental application field of zeolitized fly ashes. Some authors have

reported their use as molecular sieves for selective sorption of specific compounds from flue gas, such as CO₂, SO₂ and NH₃ (Kikuchi 1999, Srinivasan & Grutzek 1999).

Filling material in permeable reactive barriers

Permeable reactive barrier (PRB) technology is used in USA and Europe to remove *in-situ* a wide spectrum of pollutants from groundwater (see Table 7) (Blowes *et al.* 2000). This technology has a reactive filling material, which decontaminates plumes in the subsurface (Powell *et al.* 1998).

The reactive material can transform the contaminants to less harmful or environmentally immobile species (NATO/CCMS 2003), whereby the involved mechanisms are mainly degradation, precipitation and adsorption. The most frequently employed material in current field application is zero-valent iron (NATO/CCMS 2003). The extensive use of iron is attributed to its capability to degrade a wide spectrum of pollutants and its relative cheap cost: US\$ 0.35–0.53 kg⁻¹ (Gavaskar *et al.* 2005). In addition, other materials can also be used in PRB technology, depending on the pollutant to be removed (Table 8).

The use of CFA in PRB as reactive filling material to decontaminate groundwater has been widely studied (Rostami & Silverstrim 2000, Wantanaphong *et al.* 2005, Doherty *et al.* 2006). In general, the varied chemical composition of CFA enables the removal of different pollutants and the versatility as barrier media. It is known that some fly ashes such as lignite, coal fluidized bed and petroleum coke fly ashes, have high calcium content, allowing an increase in water pH up to 13, inducing heavy metal precipitation. Komnitsas *et al.*

(2004) reported that lignite fly ash is effective in the decontamination of extreme acidic leachates with high concentrations of heavy metals. For high initial concentrations of Fe (1500 mg L^{-1}), Al (100 mg L^{-1}), Co (5 mg L^{-1}), Ni (5 mg L^{-1}), Cu (5 mg L^{-1}), Mn (5 mg L^{-1}) and Zn (29 mg L^{-1}) it was found that all concentrations were below detection limits after treatment. The results indicated that precipitation is not the only mechanism involved in acidic wastewater decontamination, but also adsorption at the surface and co-precipitation. Rostami & Silverstrim (2000) utilized alkaline-activated CFA (Class F), as reactive material in PRB. The results of column tests indicated that the removal efficiencies for cadmium and chromium were near to 100% at a pH less than 4. The removal mechanisms were established to be precipitation and adsorption.

Some studies have reported that CFA use in PRB may lead to cementation problems, as well as the formation of gelatinous compounds, causing a decrease in the hydraulic conductivity and in the removal efficiency of the reactive material (Palmer *et al.* 2000). In contrast, Prashanth *et al.* (2001) reported that CFA hydraulic conductivity could increase in the presence of highly acidic leachates such as acid mine drainage. One of the most studied solutions to the compaction problem of CFA is the use of feasible pelletization techniques, to increase the hydraulic conductivity in a reactive barrier (Arslan & Baykal 2006, Harikrishnan & Ramamurthy 2006).

To design a PRB system, data about the reactivity, hydraulic performance and environmental compatibility of the reactive material is necessary (Gavaskar 1999). This data is not always available for the use of fly ashes as reactive material in PRB; therefore, data about pollutants removal kinetics and capacity of fly ashes, as well as hydraulic conductivity studies and leachability tests in fly ashes would be necessary for a proper PRB design.

Acid mine drainage remediation

Acid mine drainage (AMD) is generated by the oxidative dissolution of pyrite and other metallic sulfides, resulting from their long-term exposure to oxygen and water (Johnson 2003). The oxidation leads to an extremely acidic drainage,

enriched with high concentrations of sulfate, iron, aluminium, manganese and other metals (Stumm & Morgan 1996). AMD generates severe environmental and economic impacts (Gray 1997), such as the reduction of biodiversity, contamination of water and corrosion of infrastructures. Several options have been reported to prevent, minimize and remediate AMD and other acid wastewaters (Johnson & Hallberg 2005), namely passive (e.g. anoxic lime drains, permeable reactive barriers and *in-situ* control measures) and active techniques (e.g. neutralizing agent addition and bioreactors). Despite the high number of techniques to remediate or prevent AMD, the most widespread process used is the addition of neutralizing agents (Coulton *et al.* 2003). However, it implies a high economic and environmental cost, because of the use of natural resources as raw materials (Kuhn 2005). Lignite combustion and fluidized bed combustion fly ashes could substitute alkaline materials such as hydrated limestone and dolomite, because of their similar chemical composition (Table 9).

The reuse of fly ashes in the prevention and remediation of AMD has already been reported. Blends of CFA with red mud (Bertocci *et al.* 2006), CFA with bio-sludge (Hallberg *et al.* 2005), pulverized CFA (Wang *et al.* 2006, Pérez-López *et al.* 2007, Gitari *et al.* 2008a), fluidized bed combustion fly ash (Hellier 1998, Siriwardane *et al.* 2003) and lignite fly ash (Xenidis *et al.* 2002), have been used to prevent the release of heavy metals by means of spoils solidification or stabilization, as well as dry cover or neutralizing agent for leachates from spoils and tailings. In addition, the use of fly ashes in the remediation of AMD by active chemical treatment has been reported (Kuhn 2005, Potgieter-Vermaak *et al.* 2006, Gitari *et al.* 2008b). Furthermore, the treatment of AMD-contaminated groundwater in abandoned mines by means of injection of alkaline materials such as fluidized bed coal combustion fly ashes has also been successful (Canty & Everett 2006).

One of the first applications of CFA to treat AMD was performed in an abandoned coal mine in eastern Oklahoma in 1994. (Canty & Everett 2006) employed an *in-situ* technique called 'alkaline injection technology (AIT)', which consisted in the injection of fluidized bed combustion fly ash

Table 9: Composition of some alkaline materials and fly ashes (w/w %).

Compound	Limestone ^a	Dolomite ^a	Lignite fly ash ^b	PCFA ^c
SiO ₂	0.5	3.3	31.2	0.5
Al ₂ O ₃	0.3	0.9	13.0	0.1
Fe ₂ O ₃	0.1	1.0	5.6	0.1
CaO	55.3	29.1	33.9	47.0
MgO	0.8	17.6	4.48	0.4
Na ₂ O	0.1	< 0.1	0.29	0.1
SO ₃	–	–	6.83	27.3
LOI	43.0	46.3	2.7	23.0

^aPotgieter-Vermaak *et al.* (2006).

^bXenidis *et al.* (2002)

^cGonzález *et al.* (2007)

directly into the abandoned mine. The experiment began in 1997 and the initial concentrations of iron (179 mg L^{-1}), manganese (6.7 mg L^{-1}) and aluminium (3 mg L^{-1}) were reduced to 30, 1.5 and 0.1 mg L^{-1} , respectively. The biotic parameters indicated a positive change. For instance, fish were collected after the treatment for the first time in 10 years. However, the AIT has some limitations, such as elevated costs associated with the acquisition and transportation of fly ashes and the injection is only appropriate for small mines.

Pérez-López *et al.* (2007) stated that the addition of fly ashes can improve the quality of pyrite sludge. They observed that pyrite oxidation was stopped, as a consequence of the formation of a ferric hydroxide coat on pyrite surface, avoiding the contact of pyrite minerals with oxygen and water. Metal immobilization and oxidation attenuation were the main mechanisms involved, which allowed a decrease in toxic metals concentrations in the drainage.

Fly ashes can be considered as a cost-effective alternative pretreatment before lime addition. In this case, the reaction rate of fly ashes as neutralizing agent was shown to be dependent on the amount and material surface area, contact time and chemical composition of the AMD (Potgieter-Vermaak *et al.* 2006). Furthermore, in the reaction between AMD and CFA, an increase in pH showed that CFA were able to precipitate more than 90% of the sulfate as ettringite and gypsum. Finally, Polat *et al.* (2007) tested the neutralization of an extremely acidic sludge and stabilization of heavy metals in fly ash aggregates. Class F CFA was used, obtaining an excellent leaching behaviour. The principal mechanisms involved in the stabilization were electrostatic adsorption and coordinative bonding of the metal cations onto neutral surface sites.

Although there is insufficient information about the use of PCFA to neutralize and reduce heavy metal concentration in AMD, the high calcium content of PCFA may suggest that PCFA could be a potential neutralization material for acid wastewater, reducing heavy metals concentration by precipi-

tation coupled with the pH change. In addition, the use of PCFA as a reactive material in PRB to remediate groundwater contaminated with AMD, also seems to be an interesting future application field.

Conclusions

At present, CFA are mainly used in cement and concrete production but this industry is not capable of using all of the CFA produced worldwide and so large amounts of CFA are disposed of in landfills, provoking several environmental impacts. In addition, PCFA generation must be monitored carefully; as petroleum coke consumption in power plants is increasing worldwide. The generation of PCFA is increasing as well, especially from fluidized bed combustion. For this reason, other valorization areas may add more value to CFA and PCFA, such as zeolites synthesis, valuable metals extraction and acid mine drainage remediation.

Currently the market for PCFA from fluidized bed combustion is focused on soil stabilization and gypsum replacement. Due to the high calcium content, the following possible future application fields are suggested.

1. Geological barriers to avoid the leaching of toxic compounds into groundwater.
2. Calcareous amendment to improve pH and calcium content in soil.
3. Reactive media to neutralize and remediate acid wastewaters with high heavy metals content.

The reuse of CFA and PCFA may offer some cost savings for several industrial sectors due to a reduction in disposal and transport costs and saving of natural resources.

Acknowledgements

The authors would like to thank the Soil Laboratory of the Universidad de La Frontera, FONDECYT projects 1060309, 7060298 and 7070022 and CONICYT-CSIC project 2007-136 for financial support.

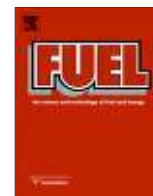
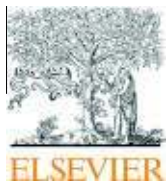
References

- ACAA (American Coal Ash Association) (ed.) (2007) Production and use survey. ACAA, Colorado, USA (www.aaa-usa.org/PDF/2007 (accessed 21 November 2008)).
- Adriano, D.C., Weber, J., Bolan, N.S., Paramasivan, S., Koo, B.-J. & Sajwan, K.S. (2002) Effects of high rates of coal fly ash on soil, turf-grass, and groundwater quality. *Water, Air and Soil Pollution*, **139**, 365–385.
- Anthony, E.J. & Granatstein, D.L. (2001) Sulfation phenomena in fluidized bed combustion systems. *Progress in Energy and Combustion Science*, **27**, 215–236.
- Arslan, H. & Baykal, G. (2006) Utilization of fly ash as engineering pellet aggregates. *Environmental Geology*, **50**, 761–770.
- Awe, Y., Cheeseman, C. & Sollars, C. (2001) Permeability of lime-activated pulverised fuel ash to metal containing permeants. *Waste Management and Research*, **19**, 35–44.
- Babel, S. & Kurniawan, T. (2003) Low-cost adsorbents for heavy metals uptake from contaminated water: a review. *Journal of Hazardous Materials*, **B97**, 219–243.
- Barbieri, L., Bonamartini, A.C. & Lancellotti, I. (2000) Alkaline and alkaline-earth silicate glasses and glass-ceramics from municipal and industrial wastes. *Journal of the European Ceramic Society*, **20**, 2477–2483.
- Bayat, B. (2002a) Comparative study of adsorption properties of Turkish fly ashes: I. The case of nickel(II), copper(II) and zinc(II). *Journal of Hazardous Materials*, **95**, 251–273.
- Bayat, B. (2002b) Comparative study of adsorption properties of Turkish fly ashes: II. The case of chromium(VI) and cadmium(II). *Journal of Hazardous Materials*, **95**, 275–290.
- Benner, S.G., Blowes, D.W., Ptacek, C.J. & Mayer, K.U. (2002) Rates sulfate reduction and metal sulfide precipitation in a permeable reactive barrier. *Applied Geochemistry*, **17**, 301–320.
- Bertocchi, A.F., Ghiani, M., Peretti, R. & Zucca, A. (2006) Red mud and fly ash for remediation of mine sites contaminated with As, Cd, Cu, Pb and Zn. *Journal of Hazardous Materials*, **B134**, 112–119.
- Blowes, D.W., Ptacek, C.J., Benner, S.G., McRae, W.T., Bennett, T.A. & Puls, R.W. (2000) Treatment of inorganic contaminants using permeable reactive barriers. *Journal of Contaminant Hydrology*, **45**, 123–137.
- Burt, T.A., Li, Z. & Bowman, R.S. (2005) Evaluation of granular surfactant-modified/zeolite zero valent iron pellets as a reactive mate-

- rial for perchloroethylene reduction. *Journal of Environmental Engineering*, **131**, 934–942
- Canty, G. & Everett, J. (2006) Alkaline injection technology: Field demonstration. *Fuel*, **85**, 2545–2554.
- Cetin, S. & Pehlivan, E. (2007) The use of fly ash as a low cost, environmentally friendly alternative to activated carbon for removal of heavy metals from aqueous solutions. *Colloids and Surfaces A-Physicochemical and Engineering Aspects*, **298**, 83–87.
- Chang, F.Y. & Wey, M.Y. (2006) Comparison of the characteristics of bottom and fly ashes generated from various incineration processes. *Journal of Hazardous Materials*, **B138**, 594–603.
- Chen, J. & Lu, X. (2007) Progress of petroleum coke combusting in circulating fluidized bed boilers-A review and future perspectives. *Resources, Conservation and Recycling*, **49**, 203–216.
- Chrysochoou, M. & Dermatas, D. (2006) Evaluation of ettringite and hydrocalumite formation for heavy metal immobilization: Literature review and experimental study. *Journal of Hazardous Materials*, **136**, 20–33.
- Cokca, E. & Yilmaz, Z. (2004) Use of rubber and bentonite added fly ash as a liner material. *Waste Management*, **24**, 153–164.
- Conn, R.E., Sellakumar, K. & Bland, A.E. (1999) Utilization of CFB fly ash for construction applications. *Proceedings of the 15th International Conference on Fluidized Bed Combustion*, May 16–19, Savannah, Georgia, USA.
- Coulton, R., Bullen, C., Dolan, J., Hallet, C., Wright, J. & Marsden, C. (2003) Wheal Jane mine water active treatment plant-design, construction and operation. *Land Contamination and Reclamation*, **11**, 245–252.
- Cox, M., Nugteren, H. & Jannssen-Jurkovičová, M.. (2008) *Combustion Residues: Current, Novel and Renewable Applications*. John Wiley & Sons, Chichester, England.
- Crini, G. (2006) Non-conventional low-cost adsorbents for dye removal: A review. *Bioresource Technology*, **97**, 1061–1085.
- Doherty, R., Phillips, D.H., McGeough, K.L., Walsh, K.P. & Kalin, R.M. (2006) Development of modified fly ash as a permeable reactive barrier medium for a former gas plant site, Northern Ireland. *Environmental Geology*, **50**, 37–46.
- Dwivedi, S., Tripathi, R.D., Rai, U.N., Srivastava, S., Mishra, S., Shukla, M.K., Gupta, A.K., Sinha, S., Baghel, V.S. & Gupta, D.K. (2006) Dominance of algae in ganga water polluted through fly ash leaching: Metal bioaccumulation potential of selected algae species. *Bulletin of Environmental Contamination and Toxicology*, **77**, 427–436.
- ECOBA (European Coal Combustion Products Association) (ed.) (2006) *Production of CCPs in 2006*. ECOBA, Essen, Germany. <http://www.ecoba.com> (accessed 09.10.06).
- Erol, M., Küçükbayrak, S., & Ersoy-Meriçboyu, A. (2008) Characterization of sintered coal fly ashes. *Fuel*, **87**, 1334–1340.
- Estevinho, B.N., Martins, I., Ratola, W., Alves, A. & Santos, L. (2007) Removal of 2,4 dDichlorophenol and pentachlorophenol from waters by sorption using coal fly ash from Portuguese thermal power plant. *Journal of Hazardous Materials*, **143**(1–2), 535–540.
- Font, O., Querol, X., López-Soler, A., Chimenos, J.M., Fernández, A.I., Burgos, S. & Peña, F.G. (2005) Ge extraction from gasification fly ash. *Fuel*, **84**, 1384–1392.
- Font, O., Querol, X., Juan, R., Casado, R., Ruiz, C.R., López-Soler, A., Coca, P. & Peña, F.G. (2007) Recovery of gallium and vanadium from gasification fly ash. *Journal of Hazardous Materials*, **A139**, 413–423.
- Gabr, M.A. & Bowders, J.J. (2000) Controlled low-strength material using fly ash and AMD sludge. *Journal of Hazardous Materials*, **76**, 251–263.
- Gangloff, W.J., Ghodrati, M., Sims, J.T. & Vasilas, B.L. (2000) Impact of fly ash amendment and incorporation method on hydraulic properties of a sandy soil. *Water, Air and Soil Pollution*, **119**, 231–245.
- Gartner, E. (2004) Industrially interesting approaches to low-CO₂ cements. *Cement and Concrete Research*, **34**, 1489–1498.
- Gavaskar, A.R. (1999) Design and construction techniques for permeable reactive barriers. *Journal of Hazardous Materials*, **68**, 41–71.
- Gavaskar, A.R., Tatar, L. & Condit, W. (2005) *Cost and Performance Report Nanoscale Zero-Valent Iron Technologies For Source Remediation*. NAVFAC Contract Report CR 05-007-ENV, Engineering Service Center, Port Hueneme, California, USA, 93043-4370.
- Gibert, O., De Pablo, J., Cortina, J.L. & Ayora, C. (2003) Evaluation of municipal compost/limestone/iron mixtures as filling material for permeable reactive barriers for *in-situ* acid mine drainage treatment. *Journal of Chemical Technology and Biotechnology*, **78**, 489–496.
- Gitari, W.M., Petrik, L.F., Etchebers, O., Key, D.L., Iwuoha, E. & Okuyeni, C. (2008a) Passive neutralization of acid mine drainage by fly ash and its derivatives: A column leaching study. *Fuel*, **87**, 1637–1650.
- Gitari, W.M., Petrik, L.F., Etchebers, O., Key, D.L. & Okuyeni, C. (2008b) Utilization of fly ash for treatment of coal mines wastewater: Solubility controls on major inorganic contaminants. *Fuel*, **87**, 2450–2462.
- Golab, A.N., Peterson, M.A. & Indraratna, B. (2006). Selection of potential reactive materials for a permeable reactive barrier for remediating acidic groundwater in acid sulphate soils terrains. *Quarterly Journal of Engineering Geology and Hydrogeology*, **39**, 209–223.
- González, A., Arancibia, N., Jara, A., Mora, M.L. & Navia, R. (2007) Fly ashes as filling material in permeable reactive barriers. ISWA / NVRD World Congress, September 24–27, Amsterdam, The Netherlands.
- Goumans, J.M., Van der Sloot, H.A. & Albers, G. (1994) *Environmental Aspects of Construction with Waste Materials*. Elsevier, Amsterdam.
- Gray, N.F. (1997) Environmental impact and remediation of acid mine drainage: A management. *Environmental Geology*, **30**, 62–71.
- Gutiérrez, B., Pazos, C. & Coca, P. (1997) Recovery of Gallium from coal fly ash by a dual reactive extraction process. *Waste Management and Research*, **15**, 371–382.
- Haiying, Z., Youcai, Z. & Jingyu, Q. (2007) Study on use of MSWI fly ash in ceramic tile. *Journal of Hazardous Materials*, **141**, 106–114.
- Hallberg, R.O., Granhagen, J.R. & Liljemark, A. (2005) A fly ash/biosludge dry cover for the mitigation of AMD at the falun mine. *Chemie der Erde*, **65**, 43–63.
- Harikrishnan, K.I. & Ramamurthy, K. (2006) Influence of pelletization process on the properties of fly ash aggregates. *Waste Management*, **26**, 846–852.
- Hellier, W.W. (1998) Abatement of acid mine drainage by capping a reclaimed surface mine with fluidized bed combustion ash. *Mine Water and the Environment*, **17**, 28–40.
- Henke, K. (2005) Trace element chemistry of fly ashes from combusted petroleum coke and coal. *International Ash Utilization Symposium*, Center for Applied Energy Research, University of Kentucky; Lexington, Kentucky, USA, Paper # 45. www.flyash.info. (accessed 20.09.06).
- Höller, H. & Wirsching, U. (1985) Zeolites formation from fly ash. *Fortschreitende Mineralogy*, **63**, 21–43.
- Hollman, G.G., Steenbruggen, G. & Janssen-Jurkovičová, M. (1999) A two step process for the synthesis of zeolites from coal fly ash. *Fuel*, **78**, 1225–1230.
- Hower, J.C., Thomas, G.A., Mardon, S.M. & Trimble A.S. (2005) Impact of co-combustion of petroleum coke and coal on fly ash quality: Case study of a Western Kentucky power plant. *Applied Geochemistry*, **20**, 1309–1319.
- Inada, M., Eguchi, Y., Enomoto, N. & Hojo, J. (2005) Synthesis of zeolite from coal fly ashes with different silica-alumina composition. *Fuel*, **84**, 299–304.
- Izquierdo, M., Font, O., Moreno, N., Querol, X., Huggins, F.E., Alvarez, E., Diez, S., Otero, P., Ballesteros, J.C. & Gimenez, A. (2007) Influence of a modification of the pet-coke/coal ratio on the leachability of fly ash and slag produced from a large PCC power plant. *Environmental Science and Technology*, **41**, 5330–5335.
- Izquierdo, M., Moreno, N., Font, O., Querol, X., Alvarez, E., Antenucci, D., Nugteren, H., Luna, Y. & Fernandez-Pereira, C. (2008) Influence of co-firing on the leaching of trace pollutants from coal fly ash. *Fuel*, **87**, 1958–1966.
- Jala, S. & Goyal, D. (2006) Fly ash a soil ameliorant for improving crop production-a review. *Bioresource Technology*, **97**, 1136–1147.
- Jankowski, J., Ward, C.R., French, D. & Groves, S. (2006) Mobility of trace elements from selected Australian fly ashes and its potential impact on aquatic ecosystems. *Fuel*, **85**, 243–256
- Jegadeesan, G., Al-Abed, S.R. & Pinto, P. (2008) Influence of metal distribution on its leachability from coal fly ash. *Fuel*, **87**, 1887–1893.

- Johnson, D.B. (2003) Chemical and microbiological characteristics of mineral spoils and drainage waters at abandoned coal and metal mines. *Water, Air and Soil Pollution* 3, 47-66.
- Johnson, D.B. & Hallberg, K.B. (2005) Acid mine drainage remediation options: a review. *Science of the Total Environment*, **338**, 3-14.
- Kalinski, M.E. & Yerra, P. (2005) Hydraulic conductivity of compacted cement-stabilized fly ash. *International Ash Utilization Symposium*, Center for Applied Energy Research, University of Kentucky, Lexington, Kentucky, USA. www.flyash.info. (accessed 19.01.07).
- Karamberli, A., Orkopoulou, K. & Moutsatsou, A. (2007) Synthesis of glass-ceramics using glass cullet and vitrified industrial by-products. *Journal of the European Ceramic Society*, **27**, 629-636.
- Károly, Z., Mohai, I., Tóth, M., Wéber, F. & Szépvölgyi, J. (2007) Production of glass-ceramics from fly ash using arc plasma. *Journal of the European Ceramic Society*, **27**, 1721-1725.
- Kikuchi, R. (1999) Application of coal ash to environmental improvement transformation into zeolite, potassium fertilizer and FGD absorbent. *Resources, Conservation and Recycling*, **27**, 336-346.
- Kimoto, M., Matsuda, H. & Shirai, H. (2005) Influence of coal properties and combustion conditions on specific surface area of fly ash. *International Ash Utilization Symposium*, Center for Applied Energy Research, University of Kentucky, Lexington, Kentucky, USA. www.flyash.info. (accessed 19.01.07).
- Köber, R., Daus, B., Ebert, M., Mattusch, J., Welter, E. & Dahmke, A. (2005) Compost-based permeable reactive barriers for the source treatment of arsenic contaminations in aquifers: Column studies and solid-phase investigations. *Environmental Science and Technology*, **39**, 7650-7655.
- Komnitsas, K., Bartzas, G. & Paspaliaris, I. (2004) Clean up of acidic leachates using fly ash barriers: Laboratory column studies. *Global Nest: The International Journal*, **6**, 81-89.
- Kovalchuk, G., Fernández-Jiménez, A. & Palomo, A. (2007) Alkali-activated fly ash: Effect of thermal curing conditions on mechanical and microstructural development-Part II. *Fuel*, **86**, 315-322.
- Kuhn, E.M.R. (2005) *Microbiology of Fly Ash-acid Mine Drainage Co-disposal Processes*. MSc Thesis, Department of Biotechnology, University of the Western Cape, South Africa.
- Lee, K.T., Bhatia, S., Mohamed, A.R. & Chu, K.H. (2006) Optimizing the specific surface area of fly ash-based sorbents for flue gas desulfurization. *Chemosphere*, **62**, 89-96.
- Lee, M.-G., Yi, G., Ahn, B.-J. & Roddick, F. (2000) Conversion of coal fly ash into zeolite and heavy metal removal characteristics of the products. *Korean Journal of Chemical Engineering*, **17**, 325-331.
- Lee, T., Park, J.W. & Lee, J.H. (2004) Waste green sands as reactive media for the removal of zinc from water. *Chemosphere*, **56**, 571-581.
- Lin, D.F., Lin, K.L. & Lou, H.L. (2007) A comparison between sludge ash and fly ash on the improvement in soft soil. *Journal of the Air and Waste Management Association*, **57**, 59-64.
- Manz, O.E. (1999) Coal fly ash: A retrospective and future look. *Fuel*, **78**, 133-136.
- Matje, R.H., Bunt, J.R. & Van Herden, J.H.P. (2005) Extraction of alumina from coal fly ash generated from selected low rank bituminous South African coal. *Minerals Engineering*, **18**, 299-310.
- McGregor, R.G., Benner, S., Ludwig, R., Blowes, D.W. & Ptacek, C. (2002) Sulfate reduction permeable reactive barrier to treat acidity, cadmium, copper, nickel and zinc: two case studies. In: Naftz, D.L., Morrison, S.J., Fuller, C.C. & Davis, J.A. (eds): *Handbook of Groundwater Remediation Using Permeable Reactive Barriers-Applications to Radionuclides, Trace Metals, and Nutrients*. Academic Press, San Diego, California, USA, pp. 539.
- Mittra, B.N., Karmakar, S., Swain, D.K. & Ghosh, B.C. (2005) Fly ash- a potential source of soil amendment and a component of integrated plant nutrient supply system. *Fuel*, **84**, 1447-1451.
- Miyake, M. (2007) Resource recovery of inorganic solid waste for reduction of environmental load. *Journal of the Ceramic Society of Japan*, **115**, 1-8.
- Mollamahmutoglu, M. & Yilmaz, Y. (2001) Potential coal fly ash and bentonite mixture as liner or cover at waste disposal areas. *Environmental Geology*, **40**, 1316-1324.
- Mondragon, F., Rincon, F., Serra, L., Escobar, J., Ramirez, J. & Fernandez, J. (1990) New perspectives for coal ash utilization: synthesis of zeolitic material. *Fuel*, **69**, 263-266.
- Moreno, N., Querol, X., Ayora, C., Alastuey, A. & Fernández-Pereira, C. & Janssen-Jurkovicová, M. (2001) Potential environmental applications of pure zeolitic material synthesized from fly ash. *Journal of Environmental Engineering*, **127**, 994-1002.
- Moreno, N. (2002) *Valorisation of Fly Ashes for Zeolite Synthesis by Silica Extraction and Direct Conversion*. *Environmental Applications*. (Valorización de cenizas volantes para la síntesis de zeolitas mediante extracción de sílice y conversión directa. Aplicaciones ambientales.) PhD Thesis Universitat Politècnica de Catalunya (UPC), Barcelona, Spain.
- Moreno, N., Querol, X., Andrés, J.M., López-Soler, A., Janssen, M., Nugteren, H., Towler, M. & Staton, K. (2004) Determining suitability of a fly ash for silica extraction and zeolite synthesis. *Journal of Chemical Technology and Biotechnology*, **79**, 1009-1018.
- Moreno, N., Querol, X., Andrés, J.M., Stanton, K., Towler, M. & Nugteren, H. (2005) Physico-chemical characteristics of European pulverized coal combustion fly ashes. *Fuel*, **84**, 1351-1363.
- Mudakavi, J.R., Narayana B.V. & Kiran R. (1999) Characterization and utilization of iron-rich dry ash from an electric arc furnace. *Current Science*, **76**, 473-475.
- Nalbantoglu, Z. (2004) Effectiveness of class C fly ash as an expansive soil stabilizer. *Construction and Building Materials*, **18**, 377-381.
- Nataraja, M.C. & Nalanda, Y. (2008) Performance of industrial by-products in controlled low-strength material (CLSM). *Waste Management*, **28**, 1168-1181.
- NATO/CCMS (ed.) (2003) Evaluation of demonstrated and emerging technologies for the treatment of contaminated land and ground water (Phase III), EPA 542-R-02-012, Nr. 259. NATO/CCMS, Brussels, Belgium. www.nato.int/science/publications (accessed 5 December 2006).
- Nollet, H., Roels, M., Lutgen, P., Van der Meeren, P. & Verstraete, W. (2003) Removal of PCBs from wastewater using fly ash. *Chemosphere*, **53**, 655-665.
- Okada, T., Tojo, Y., Tanaka, N. & Matsuto, T. (2007) Recovery of zinc and lead from fly ash from ash-melting and gasification-melting processes of MSW-Comparison and applicability of chemical leaching methods. *Waste Management*, **27**, 69-80.
- Palmer, B.G., Edil, T.B. & Benson, C.H. (2000) Liners for waste containment constructed with class F and C fly ashes. *Journal of Hazardous Materials*, **76**, 193-216.
- Pan, J.R., Huang C., Kuo J.J. & Lin S.H. (2008) Recycling MSWI bottom and fly ash as raw materials for Portland cement. *Waste Management*, **28**, 1113-1118.
- Pandian, N.S., Rajasekhar, C. & Sridharan, A. (1998) Studies on the specific gravity of some Indian coal ashes. *Journal of Testing and Evaluation ASTM*, **26**, 177-186.
- Park, M., Choi, C.L., Lim, W.T., Kim, M.C., Choi, J. & Heo, N.H. (2000) Molten-salt method for the synthesis of zeolitic materials. I. Zeolite formation in alkaline molten-salt system. *Microporous and Mesoporous Materials*, **37**, 81-89.
- Pedersen, K.H., Jensen, A.D., Skjøth-Rasmussen, M.S. & Dam-Johansen, K. (2008) A review of the interference of carbon containing fly ash with air entrainment in concrete. *Progress in Energy and Combustion Science*, **34**, 135-154.
- Pérez-López, R., Nieto, J.M. & Almodóvar, G.R. (2007) Utilization of fly ash to improve the quality of the acid mine drainage generated by oxidation of a sulphide-rich mining waste: Column experiments. *Chemosphere*, **67**, 1637-1646.
- Polat, M., Guler, E., Lederman, E. & Cohen, H. (2007) Neutralization of an extremely acidic sludge and stabilization of heavy metals in fly ash aggregates. *Waste Management*, **27**, 482-489.
- Potgieter-Vermaak, S.S., Potgieter, J.H., Monama, P. & Van Grieken, R. (2006) Comparison of limestone, dolomite and fly ash as pre-treatment agents for acid mine drainage. *Minerals Engineering*, **19**, 454-462.
- Powell, R.M., Puls, R.W., Blowes, D.W. & Vogan, J.L. (1998) Permeable Reactive Barriers Technologies for Contaminant Remediation. US Office of Research and Development, US Environmental Office of Solid Waste and Emergency Response, US EPA/600/R-98/125: Washington, DC, USA.
- Prashanth, J.P., Sivapullaiah, P.V. & Sridharan, A. (2001) Pozzolanic fly ash as a hydraulic barrier in landfills. *Engineering Geology*, **60**, 245-252.

- Queralt, I., Querol, X., López-Soler, A. & Plana, F. (1997) Use of coal fly ash for ceramics: a case study for a large Spanish power station. *Fuel*, **76**, 787–791.
- Querol, X., Alastuey, A., López-Soler, A., Plana, F., Andrés, J.M., Juan, R., Ferrer, P. & Ruiz, C.R. (1997) A fast method for recycling fly ash: Microwave-assisted zeolite synthesis. *Environmental Science and Technology*, **31**, 2527–2533.
- Querol, X., Umaña, J.C., Plana, F., Alastuey, A., López-Soler, A., Medinaceli, A., Valero, A., Domingo, M.J. & García-Rojo, E. (2001a) Synthesis of zeolites from fly ash at pilot plant scale. Examples of potential applications. *Fuel*, **80**, 857–865.
- Querol, X., Umaña, J.C., Alastuey, A., Ayora, C., Lopez-Soler, A. & Plana, F. (2001b) Extraction of soluble major and trace elements from fly ash in open and closed leaching systems. *Fuel*, **80**, 801–813.
- Querol, X., Moreno, N., Umaña, J.C., Alastuey, A., Hernández, E., López-Soler, A. & Plana, F. (2002a) Synthesis of zeolites from coal fly ash: an overview. *International Journal of Coal Geology*, **50**, 413–423.
- Querol, X., Moreno, N., Umaña, J., Juan, R., Hernández, S., Fernández-Pereira, C., Ayora, C., Janssen, M., García-Martínez, J., Linares-Solano, A. & Cazorla-Amoros, D. (2002b) Application of zeolitic material synthesized from fly ash to the decontamination of waste water and flue gas. *Journal of Chemical Technology and Biotechnology*, **77**, 292–298.
- Querol, X., Moreno, N., Alastuey, A., Alvarez-Ayuso, E., García-Sánchez, A., Cama, J., Ayora, C. & Simón, M. (2006) Immobilization of heavy metals in polluted soils by the addition of zeolitic material synthesized from coal fly ash. *Chemosphere*, **62**, 171–180.
- Querol, X., Moreno, N., Alastuey, A., Andrés, J.M., López-Soler, A., Ayora, C., Medinaceli, A. & Valero, A. (2007) Synthesis of high ion exchange zeolites from coal fly ash. *Geologica Acta*, **5**, 47–55.
- Ram, L.C., Srivastava, N.K., Jha, S.K., Sinha, A.K., Masto, R.E. & Selvi, V.A. (2007) Management of lignite fly ash for improving soil fertility and crop productivity. *Environmental Management*, **40**, 438–452.
- Ravina, D. (1998) Mechanical properties of structural concrete incorporating a high volume of class F fly ash as partial fine sand replacement. *Materials and Structures*, **31**, 84–90.
- Ricou, P., Lécuycer, I. & Le Cloirec, P. (1999) Removal of Cu^{2+} , Zn^{2+} and Pb^{2+} by adsorption onto fly ash and fly ash/lime mixing. *Water Science and Technology*, **39**, 239–247.
- Rostami, H. & Silverstrim, T. (2000) *In-situ Removal of Cadmium and Chromium from Groundwater Using Zeotech Reactive Barriers*. U.S. Department of Energy, Washington, DC, USA. N° DE-FG02-99ER82921. www.energy.gov (accessed 27 January 2007).
- Rubel, A., Andrews, R., Gonzalez, R., Groppo, J. & Robl, T. (2005) Adsorption of Hg and NO_x on coal by-products. *Fuel*, **84**, 911–916.
- Sarkar, M. & Acharya, P.K. (2006) Use of fly ash for the removal of phenol and its analogues from contaminated water. *Waste Management*, **26**, 559–570.
- Sata, V., Jaturapitakkul, C. & Kiattikomol, K. (2007) Influence of pozzolan from various by-product materials on mechanical properties of high-strength concrete. *Construction and Building Materials*, **21**, 1589–1598.
- Seggiani, M., Vitolo, S., Pastorelli, M. & Ghetti, P. (2006) Combustion reactivity of different oil-fired fly ashes as received and leached. *Fuel*, **86**, 1885–1891.
- Shabtai, J., Fleming, G. & Fleming, J. (1993) Extraction of Metal Oxides from Coal Fly Ash by Microorganisms and a New Microorganism Useful. US-Patent 5231018. July/1993.435/168.
- Shi, C. & Fernández-Jiménez, A. (2006) Stabilization/solidification of hazardous and radioactive wastes with alkali-activated-cements. *Journal of Hazardous Materials*, **B137**, 1656–1663.
- Shigemoto, N., Hayashi, H. & Miyaura, K. (1993) Selective formation of Na-X zeolite from coal fly ash by fusion with sodium hydroxide prior to hydrothermal reaction. *Journal of Materials Science*, **28**, 4781–4786.
- Shutter, M.E. & Fuhrman, J.J. (2001) Soil microbial community responses to fly ash amendment as revealed by analyses of whole soils and bacterial isolates. *Soil Biology and Biochemistry*, **33**, 1947–1958.
- Siddique, R. (2004) Performance characteristics of high-volume Class F fly ash concrete. *Cement and Concrete Research*, **34**, 487–493.
- Singh, A., Sharma, R.K. & Agrawal, S.B. (2008) Effects of fly ash incorporation on heavy metal accumulation, growth and yield responses of *Beta vulgaris* plants. *Bioresource Technology*, **99**, 7200–7207.
- Siriwardane, H.J., Kannan, R.S.S. & Ziemkiewicz, P.F. (2003) Use of waste materials for control of acid mine drainage and subsidence. *Journal of Environmental Engineering*, **129**, 910–915.
- Skinner, S.J.W. & Schutte, C.F. (2006) The feasibility of a permeable reactive barrier to treat acidic sulphate- and nitrate-contaminated groundwater. *Water SA*, **32**, 129–135.
- Srinivasan, A. & Grutzeck, M.W. (1999) The adsorption of SO_2 by zeolites synthesized from fly ash. *Environmental Science and Technology*, **33**, 1464–1469.
- Stevens, G. & Dunn, D. (2004) Fly ash as a liming material for cotton. *Journal of Environmental Quality*, **33**, 343–348.
- Stumm, W. & Morgan, J.J. (1996) *Chemical Equilibria and Rates in Natural Waters*. 3rd edition. John Wiley & Sons, Inc., New York, USA.
- Sugama, T., Brothers, L.E. & Weber, L. (2002) Calcium aluminate cements in fly ash/calcium aluminate blend phosphate cement systems: Their role in inhibiting carbonation and acid corrosion at a low hydrothermal temperature of 90 degrees C. *Journal of Materials Science*, **37**, 3163–3173.
- Sutton, M.E. (1999) Autoclaved cellular concrete, the future of fly ash. *International Ash Utilization Symposium*, Center for Applied Energy Research, University of Kentucky, Lexington, Kentucky, USA, Paper # 73. www.flyash.info. (accessed 27.03.07).
- Swain, E.J. (1997) US petroleum coke production expected to increase. *Oil and Gas Journal*, **95**, 79–82.
- Thenoux, G., Halles, F., Vargas, A., Bellolio, J.P. & Carrillo, H. (2007) Laboratory and field evaluation of fluid bed combustion fly ash as granular road stabilizer. *Transportation Research Record*, **2**, 36–41.
- Wang, H.L., Shang, J.Q., Kovac, V. & Ho, K.S. (2006) Utilization of Atikokan coal fly ash in acid rock drainage control from Musselwhite Mine tailings. *Canadian Geotechnical Journal*, **43**, 229–243.
- Wang, S. & Wu, H. (2006) Environmental-benign utilization of fly ash as low-cost adsorbents. *Journal of Hazardous Materials*, **B136**, 482–501.
- Wantanaphong, J., Mooney, S.J. & Bailey, E.H. (2005) Suitability of natural materials and wastes as permeable reactive barriers (PRBs). *Environmental Chemistry Letters*, **3**, 19–23.
- Wilkin, R.T. & McNeil, M.S. (2007) Laboratory evaluation of zero-valent iron to treat water impacted by acid mine drainage. *Chemosphere*, **53**, 715–725.
- World Energy Council (2007) *Survey of Energy Resources 2007*, World Energy Council: London, UK, www.worldenergy.gov (accessed 4 April 2008).
- Xenidis, A., Mylona, E. & Paspaliaris, I. (2002) Potential use of lignite fly ash for the control of acid generation from sulphidic wastes. *Waste Management*, **22**, 631–641.
- Zhang, F.S. & Itoh, H. (2006) Extraction of metals from municipal solid waste incinerator fly ash by hydrothermal process. *Journal of Hazardous Materials*, **B136**, 663–670.
- Zimmer, A. & Bergmann, C.P. (2007) Fly ash of mineral coal as ceramic tiles raw material. *Waste Management*, **27**, 59–68.



Study of a Chilean petroleum coke fluidized bed combustion fly ash and its potential application in copper, lead and hexavalent chromium removal

A. González^{a,b}, N. Moreno^c, R. Navia^{b,d,*}, X. Querol^c

^a Ph.D. Program in Sciences of Natural Resources, University of La Frontera, P.O. Box 54-D, Temuco, Chile

^b Scientific and Technological Bioresource Nucleus, University of La Frontera, P.O. Box 54-D, Temuco, Chile

^c Department of Geosciences, IDAEA-CSIC, C/Jordi Girona, 18-26, E-08034 Barcelona, Spain

^d Department of Chemical Engineering, University of La Frontera, P.O. Box 54-D, Temuco, Chile

ARTICLE INFO

Article history:

Received 4 August 2009

Received in revised form 28 April 2010

Accepted 29 April 2010

Available online 14 May 2010

Keywords:

Petroleum coke

Fly ashes

Heavy metals

Precipitation

Circulating fluidized bed combustion

ABSTRACT

This work deals with the characterization of a circulated fluidized bed combustion (CFBC) Chilean petroleum coke fly ash (FA) from a petroleum coke power plant, and its potential use in neutralization and heavy metals removal from acid wastewaters. FA presents a high Ca and SO_4^{2-} content, being anhydrite the major crystalline mineral phase, with minor proportions of calcite, portlandite and lime. Regarding to environmental characterization of this fly ash, leaching tests allowed concluding that FA is a non-hazardous residue. Heavy metals removal tests indicate that FA is able to remove Cu^{2+} and Pb^{2+} mainly due to a precipitation process, while Cr(VI) is being removed probably due to a reduction process to Cr(III), at high liquid to solid ratios. Cu^{2+} , Pb^{2+} and Cr(VI) kinetic experimental data present acceptable fit to a pseudo-second order kinetic model. According to these results, FA may be used to remove heavy metals and neutralize acid wastewaters, suggesting a possible replacement of pure and costly alkaline materials.

© 2010 Elsevier Ltd. All rights reserved.

1. Introduction

Petroleum coke is a by-product of the petroleum refining process, which is mainly used as supplementary and primary fuel for power generation [1]. Petroleum coke is nowadays considered an attractive fuel, because of its low price and availability [2] and due to its properties such as low volatility and high heating value [3]. Additionally the increasing use of petroleum coke may provoke a decrease in the expected coal mining activities [4] and an increase in the generation rate of fly ashes from the combustion of petroleum coke.

At present, there are three main technologies that allow an efficient combustion of petroleum coke and the attained of the emission standards [5]: Circulating fluidized bed combustion (CFBC), pressurized fluidized bed combustion (PFBC) and integrated gasification combined cycle (IGCC). One of the most currently used technologies to burn petroleum coke is the CFBC, which has provided important experience in petroleum coke burning performance [6]. In CFBC technology calcium compounds such as calcite (CaCO_3) are used to remove the high sulphur dioxide (SO_2) generated during the combustion of petroleum coke. These reactions are summarized in Anthony and Granatstein [7].

Petroleum coke fly ashes from CFBC (FA) have been characterized by Anthony et al. [8]. High contents of trace elements such as molybdenum (20 mg/kg), strontium (472 mg/kg), nickel (743 mg/kg) and vanadium (4940 mg/kg) in FA were detected. It has been shown that vanadium occurs mainly in large particles without any specifically morphology and associated mostly with Ca [9]. Using routine X-ray diffraction analysis (XRD) it is difficult to determine the form of occurrence of vanadium phases in FA due to the presence of major and minor mineral phases such as anhydrite, lime and calcite. However, Jia et al. [9] by means of wet extraction and high resolution XRD analysis deduced the occurrence of a mineral phase described as $(\text{Mg, Ca, Na, K, Fe}) \text{V}_2\text{O}_7 \cdot x\text{H}_2\text{O}$.

Because of the high content of harmful trace elements in FA, research focused on the leachability of trace elements in fly ashes from coal/petroleum coke combustion was carried out [10,11]. These works identified changes in the quality of co-fired fly ashes from coal and petroleum coke and demonstrated that the incorporation of petroleum coke contributes to an increment in elements of environmental concern such as Ni, V, Mo and As compared to coal combustion fly ash (CFA). In fact V, Mo and As were identified as the most potentially harmful species in coal/petroleum coke combustion fly ashes. However, as we know, research about the leachability of 100% FA has not been performed, up to date.

Despite of the occurrence of Ni, V, Sr and unburned carbon, some investigations focused on the reuse of coal/petroleum coke fly ashes or 100% FA. They stated that fly ashes from coal/petroleum

* Corresponding author at: Department of Chemical Engineering, University of La Frontera, P.O. Box 54-D, Temuco, Chile. Tel.: +56 45 325477; fax: +56 45 325053.
E-mail address: rnavia@ufro.cl (R. Navia).

coke combustion could be used as concrete [12] and cement admixture [13], depending on the coal/petroleum coke fly ash ratio used. In case of 100% petroleum coke combustion, some authors have reported that FA may be useful as sulphur-source, improving alfalfa growth and nutrients availability in soil [14]. In addition, Thenoux et al. [15] observed that the addition of FA ameliorates and modifies mechanical properties and water susceptibility of different types of soils. Conn et al. [16] stated that due to the high content of calcium sulphate, FA can replace gypsum in the cement industry. Furthermore, the possibility of employing FA for the neutralization and heavy metals removal in acid wastewaters or to replace clay liners in landfills has been already reviewed [17].

Acid wastewaters such as acid mine drainage (AMD) may cause severe impacts in the environment [18] by acidifying and discharging large amounts of salts and heavy metals into aquifers. Among the various AMD remediation options, the most used and cost-effective is the addition of neutralizing agents such as magnesite, limestone and dolomite [19]. Nevertheless, their use implies a high environmental and economic cost, due to the use of natural resources as raw materials [20]. Several studies have proposed the direct addition of alkaline secondary raw materials such as CFA, replacing natural alkaline materials like limestone and dolomite [21].

Chile is a world leader in copper mining and production [22], being AMD one of the most important industrial environmental problems [23]. Additionally, the Chilean environmental protection commission (CONAMA) has approved several projects concerning petroleum coke combustion in power plants. One of the most important is located in Concepción, Bio-Bio Region, which burns 100% petroleum coke in a CFBC, being the generated fly ashes (FA) disposed, without any further reuse.

Therefore, this work attempts to characterize these FA and evaluate their use for neutralization and heavy metals removal in acid wastewaters.

2. Experimental

2.1. Materials and methods

FA selected for this study was obtained from a power plant located in Concepción, Bio-Bio Region, Chile, which burns 100% petroleum coke, and was used in its original form, without any treatment.

Solutions of 1000 mg/L of Cu^{2+} and Pb^{2+} were prepared in distilled water for Cu^{2+} and Pb^{2+} removal tests, using CuCl_2 and PbCl_2 salts of analytical grade Merck. A solution of 500 mg/L of Cr(VI) was prepared using $\text{K}_2\text{Cr}_2\text{O}_7$ of analytical grade. The solutions were stored at 4 °C. Other chemicals used here have also analytical grade.

2.2. Characterization analyses

Chemical characterization of petroleum coke, FA and RFA arising from removal kinetics and neutralization tests (RFA) was performed after a special two-step digestion method developed for the analysis of trace elements in coal and combustion wastes [24]. Besides, hydrofluoric acid digestion as described by Thompson and Walsh [25] was carried out to determine the silica content in FA and petroleum coke. The analyses were performed in duplicate and in addition, two international reference materials, NBS 1633b (coal fly ash) and SARM 19 (coal), were also digested to check the accuracy of the analytical and digestion methods. The major, minor and trace element concentrations in the solutions were determined by means of inductively coupled plasma mass spectrometry (ICP-MS) and inductively coupled plasma atomic emission spectrometry (ICP-AES). Hg concentration was analyzed with a Mercury

Analyzer LECO AMA 254 (by means of atomic absorption spectrometry with Au amalgam technique), directly on the solid samples.

The mineralogical characterization of petroleum coke, FA and RFA was performed by means of a X-ray diffractometer (Bruker, D8 Advance model) with a primary Göbbl crystal, equipped with a detector based on dispersion of SOL-X energies, with a Cu tube and a wavelength of $\lambda = 1.5405 \text{ \AA}$, using the work conditions at $\text{kV} = 40$ and $\text{mA} = 40$.

Physical characterization of FA and petroleum coke included moisture content, loss on ignition (LOI), specific surface area, particle size distribution and morphology. Moisture yield was determined at 105 °C, while LOI was measured at 1050 °C, according to the ASTM C618-92 Norm [26]. The specific surface area (BET) was determined with a NOVA 1000 porosimeter (QUANTACHROME) by adsorbing and desorbing nitrogen on samples previously dried and out-gassed. The particle size distribution was measured by means of laser diffraction particle size analysis (Malvern Mastersizer/E model). The morphology of petroleum coke, FA and RFA was observed by a scanning electron microscope (SEM-EDX, JEOL6400).

2.3. Leaching test

The potential mobility of specific major and trace elements from the selected FA was determined according to two methodologies: The Chilean hazardous waste management regulation DS No. 148 [27], which employs as leaching test the US toxicity characteristic leaching procedure (TCLP-US EPA Method 1311) [28], and the compliance European leaching test EN 12457 Part 2 procedure [29]. The TCLP test is performed at liquid/solid (L/S) ratio of 20 L/kg, with an agitation time of 18 h and acetic acid as eluting agent, whereas European test is performed at L/S ratio of 10 L/kg, with an agitation time of 24 h and deionized water as eluting agent.

The major, minor and trace elements from the leachates were analyzed by inductively coupled plasma mass spectrometry (ICP-MS) and inductively coupled plasma atomic emission spectrometry (ICP-AES). Hg concentration was directly analyzed with a Mercury Analyzer LECO AMA 254.

2.4. Cu^{2+} , Pb^{2+} and Cr(VI) removal kinetics

A predetermined amount of FA was mixed with 45 mL distilled water in polyethylene bottles to obtain slurries of 0.2, 0.6 and 1 g/L, corresponding to 10, 30 and 50 mg of FA, respectively. The dissolved metal was added to the bottles at pH 4 at a concentration of 100 mg/L for Cu^{2+} and Pb^{2+} , and the bottles were stirred for 20 h at 25 °C. Samples were periodically collected, filtered, acidified and analyzed for Cu^{2+} and Pb^{2+} by means of a UNICAM-AAS and for Cr(VI) by means of colorimetric method. Moreover, the development of pH was also monitored.

After performing the removal kinetics test, the lowest dose was selected. The experimental data was tested in order to examine the controlling mechanisms of heavy metals removal. According to Wang and Wu [30], pseudo-first and -second order kinetic models predicted better the behavior of heterogeneous materials such as fly ashes. Therefore, pseudo-first order kinetic model developed by Lagergren and Svenska [31] and pseudo-second order kinetic model of McKay and Ho [32] were used to determine the kinetic parameters for heavy metals removal by FA.

2.5. Cu^{2+} , Pb^{2+} and Cr(VI) removal isotherms

Batch removal isotherms containing 0.2 g/L FA in contact with 0, 25, 50, 75 and 100 mg/L of heavy metal solutions were

performed. The bottles were stirred until 12 h at 25 °C. The supernatant was filtered and acidified, measuring residual Cu^{2+} and Pb^{2+} in solution by means of UNICAM-AAS and Cr(VI) by means of a colorimetric method. Langmuir and Freundlich models were adjusted to the resulting isotherms experimental data [33].

2.6. Sequential extraction of metals

In order to evaluate the extractability of V, Ni, Mo, B, Cu, Pb and Cr in FA and RFA from removal kinetics tests, chemical sequential extraction was carried out as proposed by Sposito et al. [34]. This test includes five consecutive extractions in order to extract species associated to different fractions (S1–S5). S1 is the water soluble fraction; S2 is the weakly adsorbed fraction onto the FA surface; S3 is fraction associated to organic matter; S4 is the fraction associated to the carbonates phase and S5 is the fraction associated to the sulphide phase and non silicate matrix [35]. Trace elements from the extractions were analyzed by inductively coupled plasma mass spectrometry (ICP-MS) and inductively coupled plasma atomic emission spectrometry (ICP-AES).

2.7. Neutralization trials

Batch tests were performed in polyethylene beakers by the addition of 1 L distilled water with different doses of FA, ranging between 0.2 and 3 g/L. The pH value of distilled water was adjusted at 2 and 6 with HNO_3 or NaOH 1 M respectively. After 1 h (when equilibrium was already reached), the supernatant was collected, filtered, acidified and analyzed for S, Ca, Ni, V and Mo concentrations by means of inductively coupled plasma mass spectrometry (ICP-MS) and inductively coupled plasma atomic emission spectrometry (ICP-AES). Additionally the final pH value and electric conductivity (EC) were also determined.

3. Results

3.1. Mineralogical, chemical and physical characterization of the studied materials

Fig. 1 shows the X-ray diffraction patterns of the studied materials. Fig. 1a shows that the original petroleum coke is made of a main amorphous carbonaceous matter with a high background of

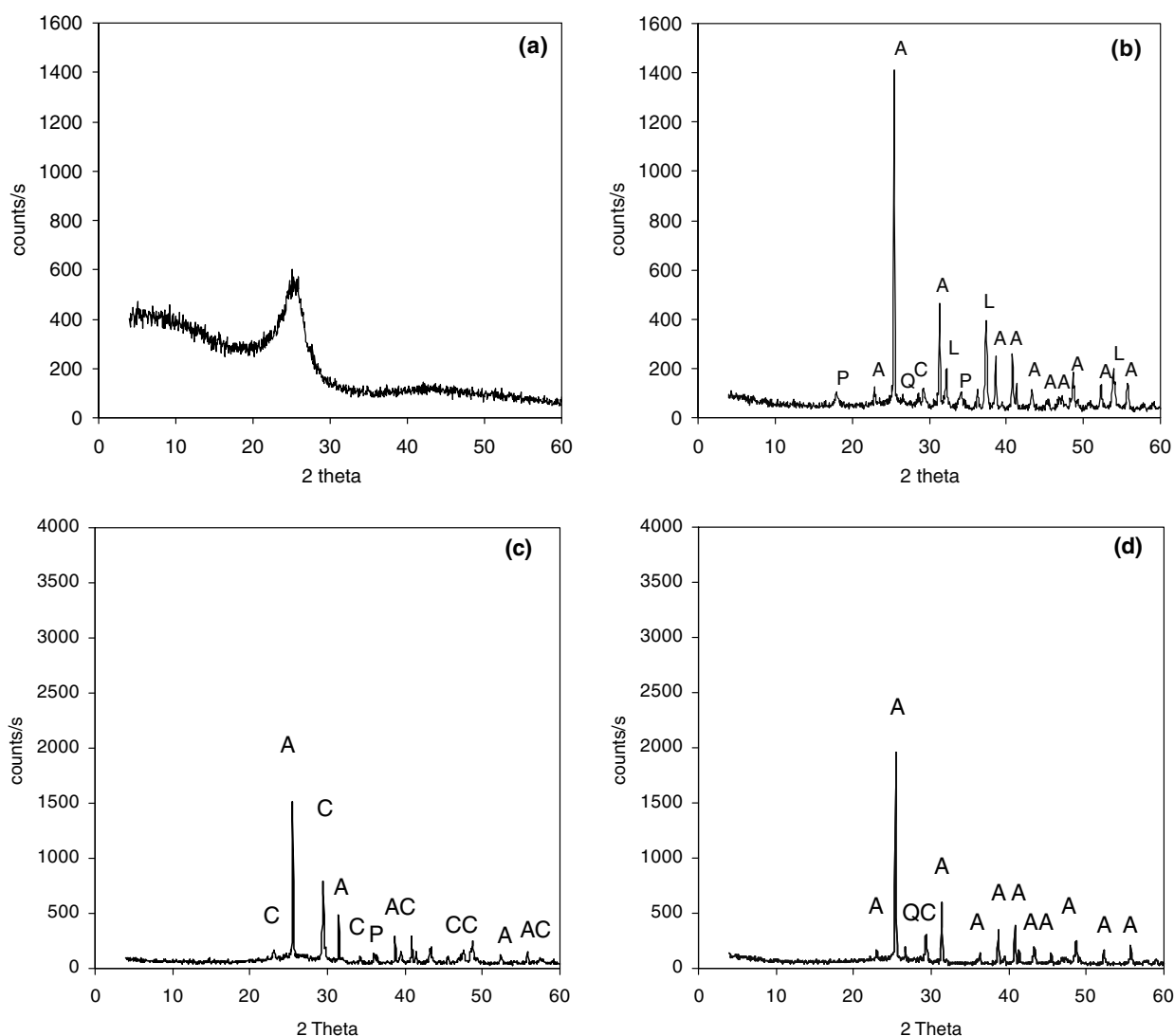


Fig. 1. X-ray diffraction patterns from (a) petroleum coke sampled at harbour of Valencia, (b) FA, (c) RFA arising from Pb^{2+} removal kinetics and (d) RFA arising from neutralization test with dose 2.6 g/L. P: portlandite, $\text{Ca}(\text{OH})_2$; A: anhydrite, CaSO_4 ; C: calcite, CaCO_3 and L: lime, CaO .

XRD between 20° and 30° of 2 θ , without observing the occurrence of XRD detectable crystalline minerals, whereas FA (Fig. 1b) are characterized by a predominant contribution of crystalline phases, including anhydrite (CaSO₄), which is the main compound formed in the desulphurization process [7], and portlandite (Ca(OH)₂), lime (CaO) and traces of calcite (CaCO₃) and quartz (SiO₂). These XRD results are in concordance with the major and minor crystalline mineral phases already reported by Jia et al. [9] and Anthony et al. [8] in FA.

Table 1 lists the petroleum coke and FA major oxides and trace elements contents. Petroleum coke has a 7% of SO₃ and 91.2% of loss on ignition (LOI) [36] being C content responsible for the 81% of LOI [37]. In addition, it is important to highlight the occurrence of trace elements such as Ni and V in relatively high levels (363 and 1876 mg/kg, respectively). All these concentrations are in the range of previously determined concentrations for 22 different petroleum coke samples carried out by Commandré and Salvador [38].

Table 1 shows that FA is constituted by CaO (47.0%) and SO₃ (27.3%) as major compounds. The chemical composition of FA is of course different to that of CFA [39], but presents some similarity regarding the CaO content compared to lignite [40] and CFBC fly ashes [16]. Regarding previous reported chemical composition of other FA, it is observed that the analyzed FA has major and minor elements content in the range of those reported by Iribarne et al. [41] and Anthony et al. [8]. However, the obtained LOI value of 23% is very high compared to the reported LOI values of 3.9% [41] and 8.3% [8]. As seen in the SEM microphotography of Fig. 2a, this may be related to the residual unburned carbon content, which corroborates the total carbon content (elemental analysis) in FA, reported by González et al. [17]. Nevertheless, Brown and Dykstra [42] stated that LOI values in fly ashes from fluidized bed combustion may be overestimated due to portlandite dehydration and carbonates calcination. In addition, its high CaO content suggests that FA could be used in heavy metal removal processes, in the neutralization of acid mine wastewaters, as reactive filling

Table 1
Major oxides and trace elements of petroleum coke fuel (adapted from [37]) and FA studied.

	%		mg/kg		mg/kg			
	Petroleum coke	FA	Petroleum coke	FA	Petroleum coke	FA		
Moisture	0.4	0.01	As	2.2	2.3	Nb	<0.1	<0.1
LOI	91.2	23	B	<0.1	15.7	Nd	<0.1	1.6
SiO ₂	1.5	0.5	Ba	2	15.8	Ni	363	2164
Al ₂ O ₃	<0.01	0.1	Be	<0.1	<0.1	Pb	9.8	5.8
CaO	0.1	47	Bi	<0.1	<0.1	Pr	<0.1	<0.1
Na ₂ O	0.014	0.1	Cd	<0.1	<0.1	Rb	<0.1	<0.1
K ₂ O	<0.01	<0.05	Ce	<0.1	2.1	Sb	<0.1	<0.1
MgO	<0.01	0.4	Co	1.7	52.3	Sc	<0.1	<0.1
SO ₃	7	27.3	Cr	1.8	8.5	Se	2.3	1.7
P ₂ O ₅	<0.01	<0.05	Cs	<0.1	<0.1	Sm	<0.1	<0.1
Fe ₂ O ₃	0.03	0.1	Cu	4	4.8	Sn	<0.1	<0.1
			Dy	<0.1	<0.1	Sr	2.1	650.7
			Er	<0.1	<0.1	Ta	<0.1	<0.1
			Eu	<0.1	<0.1	Tb	<0.1	<0.1
			Ga	0.8	2.8	Th	<0.1	<0.1
			Gd	<0.1	<0.1	Ti	12.5	42.2
			Ge	<0.1	<0.1	Tm	<0.1	<0.1
			Hf	<0.1	<0.1	U	<0.1	0.9
			Hg	0.08	0.02	V	1876	5473
			Ho	<0.1	<0.1	W	<0.1	<0.1
			La	<0.1	1.7	Y	<0.1	2.7
			Li	<0.1	1.3	Yb	<0.1	<0.1
			Lu	<0.1	<0.1	Zn	16.9	31.2
			Mn	1.3	24.7	Zr	0.3	1.6
			Mo	6.9	13.4			

LOI: loss on ignition.

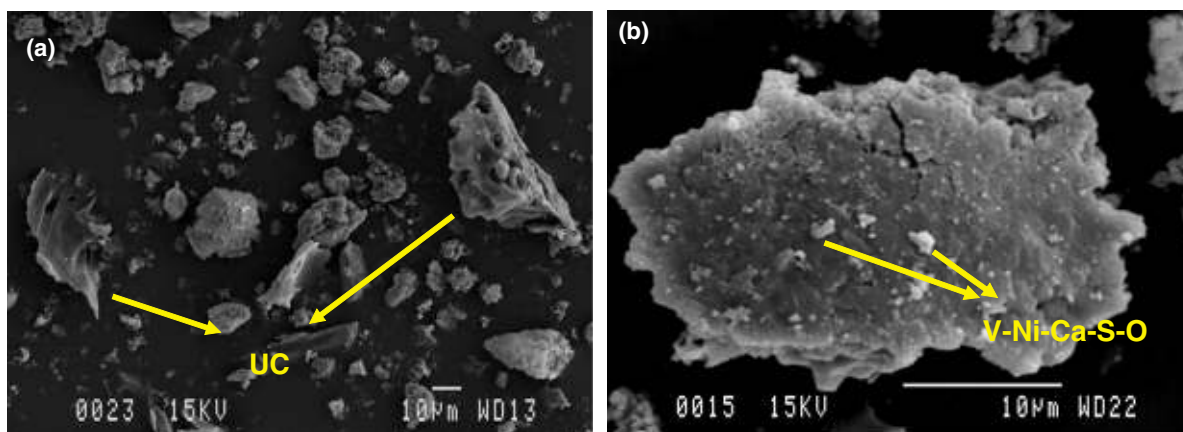


Fig. 2. SEM of (a) FA sample with unburned carbon (UC) and (b) anhydrite particle with presence of crystals of vanadium associated to calcium.

material in permeable reactive barriers (PRB) and as mineral layer in landfills.

The high content of Ni (2164 mg/kg), V (5473 mg/kg) and unburned carbon in FA could limit its potential applications. These two elements are not considered in the environmental regulations of several countries, however the possible leachability of these elements may be of environmental concern and leaching tests must be performed to evaluate their potential mobility. Furthermore, other elements of environmental concern detected in FA are Mo, B, Se and As, which must also be evaluated due to high mobility of their oxyanions in alkaline pH [43].

Regarding particle morphology, SEM analysis (Fig. 2a) shows that FA particles are irregular and that the coarser particles presented porous coke-like particles of unburned carbon material with angular and sharp edges. Finer particles of Ni-, V- and Ca-bearing particles were also detected. These particles were smaller than 10 μm and associated to coarse particles made of anhydrite and unburned carbon (Fig. 2b).

The specific surface area of FA reached 5 m^2/g , a very low value compared to activated carbon (about 1000 m^2/g) [44], volcanic soils [45] and alternative sorbents developed from discarded tires and sewage sludge (472 m^2/g) [46]. However, fly ashes with specific surface area ranging between 2 and 8 m^2/g , have been already evaluated for possible utilization in environmental technology [47].

As seen in Fig. 3 the results on particle size distribution analyses of FA indicate a gauss-symmetric distribution with a mode value between 20 and 70 μm , being the 10, 50 and 90 percentile of 7, 29 and 85 μm , respectively.

This fine particle distribution of FA will suppose an affinity of FA particles to aggregate in aqueous medium. In addition, the presence of unburned carbon may increase porosity, enhancing the hydraulic conductivity of FA. In the case of possible FA use as reactive material in PRB, it would be mandatory to find a way of pelletizing FA particles to improve its hydraulic conductivity, and to avoid the compaction problems of the filling material. Some procedures regarding the formation of pellets of such inorganic materials by using recycled polyethylene terephthalate (PET) have been already developed [33,48].

3.2. Leaching test

Leachability tests were performed to assess the hazardous character of FA, regarding to the European Norm 12457-2. According to the results obtained FA may be characterized as a non-hazardous material (Table 2). In this test, the leachate reached an alkaline pH value of 10.7 and electric conductivity (EC) of 10,330 $\mu\text{S}/\text{cm}$. A higher pH value was expected due to the occurrence of portlandite and lime in FA. The lower alkalinity observed could be due to the occurrence of the carbonation process. pH and EC values indi-

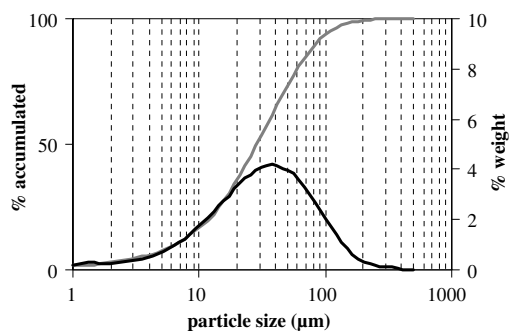


Fig. 3. FA particle size distribution.

Table 2

Leaching test values of European Norm EN 1245-2 (mg/kg).

	Inert	Non-hazardous	Hazardous (mg/kg)	FA sample
As	0.5	2	25	0.02
Ba	20	100	300	1.21
Cd	0.04	1	5	<0.01
Cr	0.5	10	70	0.22
Cu	2	50	100	0.03
Hg	0.01	0.2	2	<0.01
Mo	0.5	10	30	2.18
Ni	0.4	10	40	0.25
Pb	0.5	10	50	0.02
Sb	0.06	0.7	5	<0.01
Se	0.1	0.5	7	0.04
Zn	4	50	200	0.06
SO ₄ ²⁻	1000	20,000	50,000	19,335

Table 3

Leaching test values of Chilean Norm DS 148.

	MPC (mg/L)	FA sample (mg/L)
Ag	5	<0.2
As	5	<0.2
Ba	100	<5
Cd	1	<0.05
Cr	5	<0.1
Hg	0.2	<0.01
Pb	5	<0.2
Se	1	0.26

MPC: maximum permissible concentration.

cate a high dissolution of FA species, most of them associated to calcium compounds. Major elements such as sulphate and calcium were detected in high concentrations of 19,335 and 19,508 mg/kg, respectively. These values indicate that anhydrite dissolved during the leaching test.

Nickel, As, Ba, Sr, Mo and V were detected as the main trace elements in the leachates, being Mo and Sr those with the highest contents. Similar results have been already reported by prior studies in fly ashes from coal and petroleum coke combustion with different ratio [10,11].

Regarding to Chilean Waste Regulation, as seen in Table 3, all measured elements are below the maximal permissible concentration. Therefore, according to both EN and Chilean leaching tests procedures, FA could be classified as a non-hazardous material.

3.3. Heavy metals removal kinetics

3.3.1. Cu²⁺ removal kinetics

Fig. 4a shows the removal kinetics for Cu²⁺ (FA dose 0.2 g/L) at variable pH. All the dosages applied showed high removal efficiencies ranging between 90% and 99% (data not shown). The lowest removal efficiency value (90%) corresponded to the dose of 0.2 g/L, whereas the highest (99%) corresponded to the 0.6 and 1 g/L dose. Using the dose of 0.2 g/L the equilibrium was reached at 4 h (Fig. 4a), whereas at higher doses the equilibrium time were lower, being 0.53 h the lowest one. Similar results have been reported by Bayat [49] and Alinnor [50], showing Cu²⁺ removal efficiencies between 80% and 91% using CFA at similar experimental conditions.

The Cu²⁺ removal kinetics using a 0.2 g/L dose showed two different stages (Fig. 4a): (1) between 0 and 8 min, visually detecting flock formation in the solution (between FA and Cu²⁺) and (2) starting on 16 min until 20 h, observing flock disappearance. To explain this particular behavior, a SEM and XRD of the RFA before 8 min and at 20 h were performed (Fig. 5). Both materials showed the formation of a crystalline mineral phase of posnjakite (Cu₄SO₄(OH)₆H₂O). The

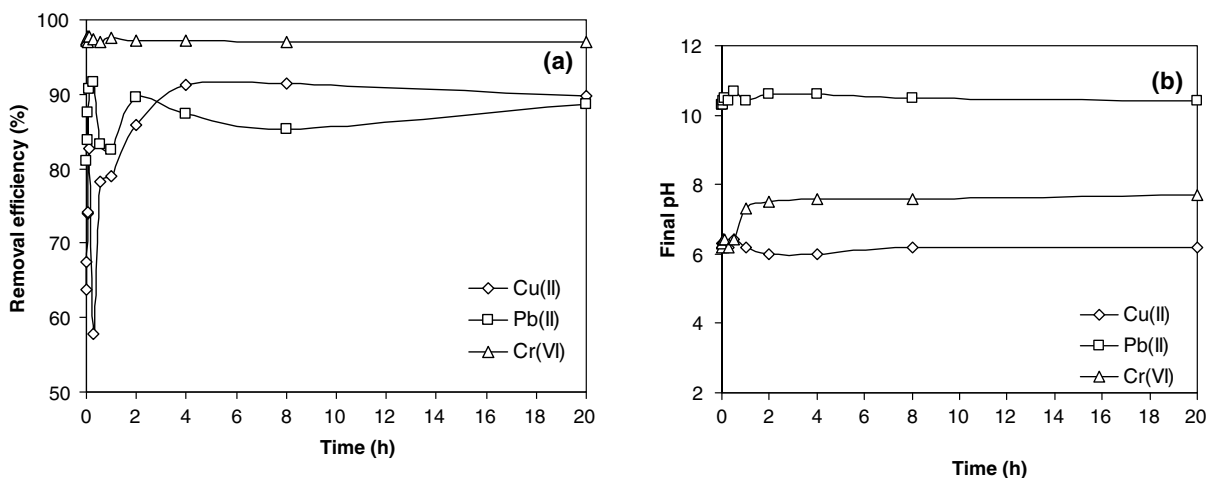


Fig. 4. Cu²⁺, Pb²⁺ and Cr(VI) removal kinetic test using the FA dose of 0.2 g/L (a) removal efficiency and (b) final pH values.

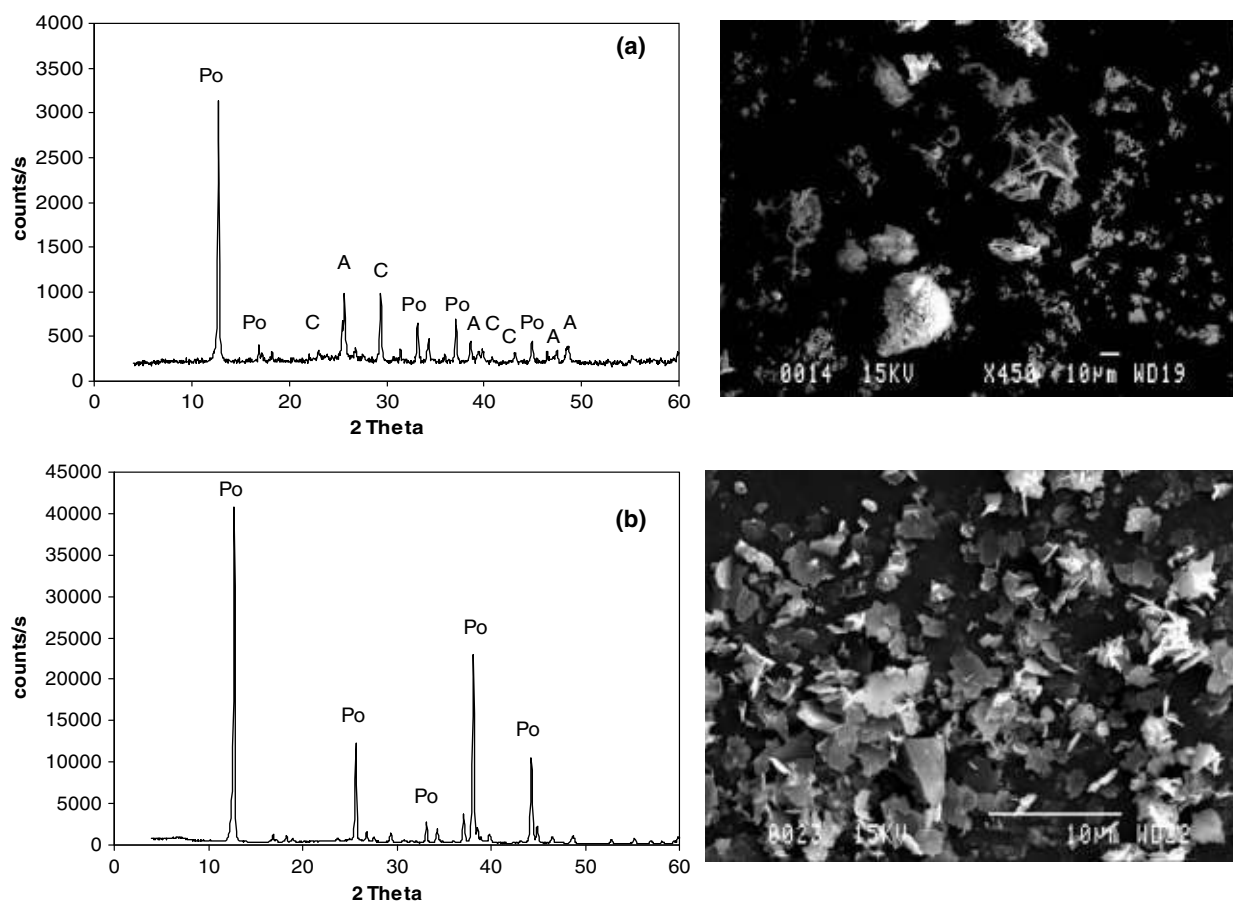


Fig. 5. Microphotographs from Scanning Electron Microscope and X-ray diffraction patterns of fly ashes arising from Cu²⁺ removal kinetic (a) at 8 min and (b) at 20 h. Po: Posnjakite, Cu₄SO₄(OH)₆H₂O; A: Anhydrite and C: Calcite.

differences between both RFA are the crystallization degree and morphology as shown in the SEM. Additionally, the RFA arising before 8 min shows other crystalline mineral phases such as calcite and anhydrite (Fig. 5a), whereas RFA obtained at 20 h exhibits a high intensity of XRD pattern and only posnjakite as crystalline mineral phase (Fig. 5b). Moreover, SEM analysis indicated a change in RFA morphology. On the one hand, in the RFA obtained before 8 min, like-gel embedded particles are visualized, mainly composed by Cu. On the other hand, in RFA at 20 h a totally different morphology

was observed, detecting posnjakite coating of RFA surface. It can be concluded that during Cu²⁺ removal, the main involved mechanism could be precipitation, corroborated by the formation of the posnjakite mineral phase.

3.3.2. Pb²⁺ removal kinetics

Regarding to the used FA doses it is observed that all of them reached high values of Pb²⁺ removal efficiency, ranging between 87.0% and 96.6%. The lowest removal value (87%) corresponded

to the dose of 0.2 g/L FA (Fig. 4a), whereas the highest value (96.6%) corresponded to the dose 1 g/L. Regarding the equilibrium time, it is observed that the three doses reached the equilibrium at about 4 h.

A fast Pb^{2+} removal process was observed, being the pH values almost constant during the performed experiments (Fig. 4b). Due to these high pH values, it is possible to attribute the obtained removal efficiencies to a precipitation process, although a precipitated mineral phase (as occurred in copper removal) was visually not detected. Alinnor [50] reported that Pb^{2+} removal was dependent on bulk pH, observing that also at low pH values, Pb^{2+} removal efficiency may be up to 78%.

The resulting RFA were analyzed by SEM and XRD. The SEM (Fig. 6) shows a pale powder onto RFA particles, containing Pb, S and O, suggesting the formation of a precipitate (Probably $PbSO_4$) that was not detected by XRD.

3.3.3. Cr(VI) removal kinetics

Removal of Cr(VI) by FA was very fast as seen in Fig. 4a, reaching the equilibrium time at 3 h for the FA doses 0.2 and 0.6 g/L, obtaining a removal efficiency of 97%. Rao et al. [51] showed similar results, reaching Cr(VI) removal efficiencies of about 96% at equilibrium time in bagasse fly ash. Furthermore, Mohan and Pittman [52] reviewed information about aqueous removal of Cr(VI) using coal fly ashes. They clearly stated that lime content in coal fly ash seems to play a significant role in Cr(VI) removal. Moreover, in our experiments, an almost instantaneous color change probably indicating a possible reduction of Cr(VI) to Cr(III) from orange to green for all probed doses was observed.

Analyses by means of SEM and XRD were performed to the RFA, in order to find the differences between the original FA and RFA. The appearance of other mineral phases was not observed in this case, but calcite peaks increased in intensity. Additionally, chro-

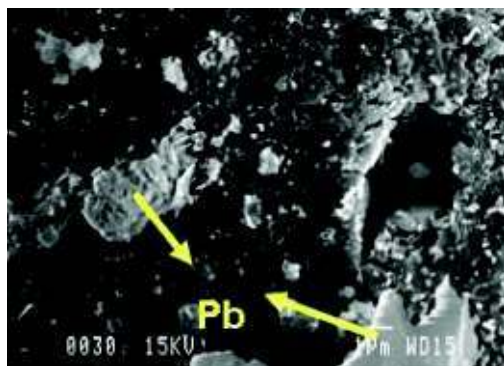


Fig. 6. SEM of RFA from Pb^{2+} removal kinetic test.

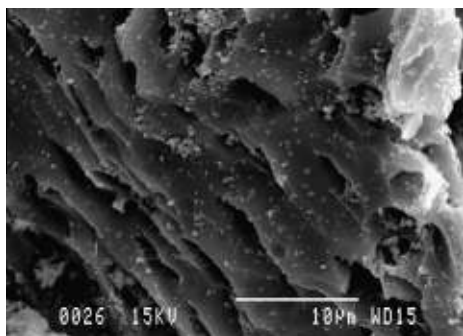


Fig. 7. SEM of RFA from Cr(VI) removal kinetic test.

mium was no detected by SEM analysis (Fig. 7). However, a grain size decrease of the calcium crystals was observed, indicating possible dissolution of calcium-containing minerals and subsequent formation of small Ca-bearing.

3.3.4. Kinetic parameters

The results show, by comparing correlation coefficients (R^2) for both kinetic models (Table 4), that pseudo-first order is not fully valid for the entire removal time interval, being R^2 values for Cu^{2+} (0.8959), Cr(VI) (0.8305) and for Pb^{2+} (2×10^{-6}). As seen in Table 4, pseudo-second order R^2 values range between 0.9996 and 0.9998, meaning a better fit to this model.

These results indicate that the removal of Cu^{2+} , Pb^{2+} and Cr(VI) obeys a pseudo-second order kinetic model, corroborating the statements of Wang and Wu [30]. The pseudo-second order kinetic model assumes that the removal of the studied heavy metals on FA is due to chemical linkage by sharing or exchanging electrons between FA and heavy metals [53].

3.4. Sequential extraction of metals

As seen in Fig. 8a, the elements Mo, Cr, Cu, Pb, Ni and V (FA) show different behaviors. Mo and Cr are mainly extracted in the S1 and S2 fraction, indicating that Mo and Cr are mobile, being available as oxyanions in water at pH around 10.9. A 35% of Mo and a 13% Cr were extracted in S1 and S2. For the other trace elements Ni, Cu, Pb and V higher extractions for the less mobile fraction (S5) were observed. The extractability level was found to be Pb (35%), V (33%), Cu (30%) and Ni (19%). Major elements such as Ca and S were found in high proportions in FA and RFA arising from removal kinetic tests. Calcium was detected in all fractions, whereas S was detected in the soluble (S1) and the exchangeable fractions (S2), as well as the fraction associated to organic matter (S3). These results show that both FA elements are easy available.

Most of the RFA presented similar extraction patterns for Mo, Ni and V compared to the original FA, showing however a lower content in most cases. A reason could be that FA may initially dissolve during kinetic trials, releasing elements such as Mo, Ni and V.

In the case of Cu, Pb and Cr a different pattern was found between FA and RFA. Higher heavy metals extraction content was expected for RFA, as observed in Fig. 8b–d. The extraction pattern for Cu (Fig. 8b) shows that all of removed Cu (from the removal kinetic trial) was extracted in the fraction associated to carbonates (S4) and non silicate minerals (S5), meaning that the removed Cu is only present in the less mobile fractions from RFA, confirming the formation of posnjakite. This characteristic may be of high relevance when managing the RFA directly to a safe disposal landfills or to a copper recovery facility.

In case of Pb, it is observed that the removed Pb was extracted in S3, S4 and S5 fractions, being the presence of Pb in S3 fraction of a possible environmental concern (Fig. 8c).

The extraction pattern for Cr indicates that the important part of the retained Cr was extracted from S1 and S2 fractions, which

Table 4

Kinetic parameters for pseudo-first and -second order model using a FA dose of 0.2 g/L.

FA	Pseudo-first order			Pseudo-second order		
	k_f	q_e	R^2	k_s	q_e	R^2
Cu^{2+}	0.006	841.8	0.8959	0.0001	416.7	0.9998
Pb^{2+}	1.2 E-05	6.5	2 E-06	0.0009	434.8	0.9996
Cr(VI)	0.003	2.1	0.8305	0.0015	250	0.9997

q_e : Removal capacity at equilibrium (mg/g), k_f : pseudo-first order rate constant (min^{-1}) and k_s : pseudo-second order rate constant (g/mg min).

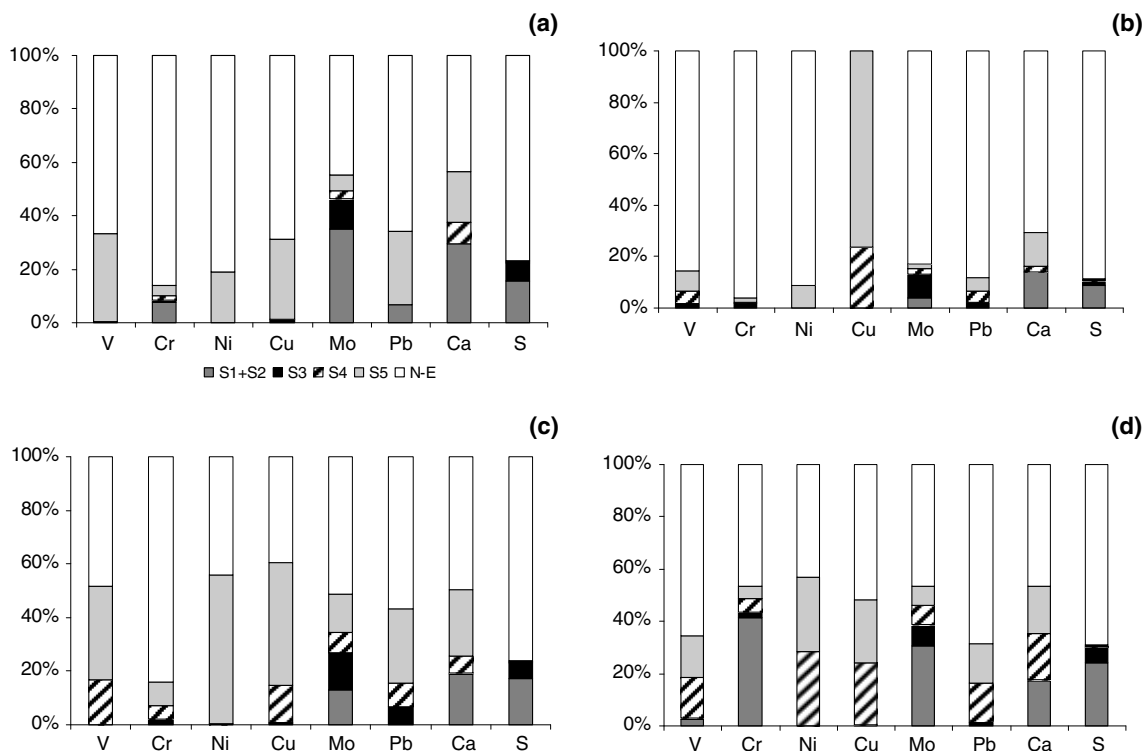


Fig. 8. Release of different elements during chemical sequential extraction of (a) FA and after (b) Cu^{2+} , (c) Pb^{2+} and (d) Cr(VI) removal kinetic tests, respectively. N-E indicates non-extracted.

are the most mobile (Fig. 8d). This result shows that Cr has a limited affinity with FA, having a weak linkage with FA.

3.5. Heavy metals removal isotherms

Resulting experimental data were fitted to Freundlich and Langmuir models for comparison purposes. The main parameters calculated using both models are presented in Table 5. Both models provided an acceptable fit to the experimental data for Cu^{2+} removal with an R^2 of 0.9784 for Langmuir and 0.9629 for Freundlich model, respectively. Furthermore, the “ n ” value higher than 1 obtained in Freundlich model for Cu^{2+} indicates low removal intensity. The higher R^2 value obtained for Langmuir model coupled with a low removal intensity “ n ” coefficient in Freundlich model, lead us to select the Langmuir approach as the most suitable model for Cu^{2+} removal.

According to Limousin et al. [54], Pb^{2+} sorption isotherm behaves as an “S” isotherm (Fig. not shown). The “S” isotherm curve (sigmoidal) implies that two mechanisms may be involved in Pb^{2+} removal in FA. The first mechanism involves a low Pb^{2+} affinity with FA, while the second one may be related to an affinity increase due to the formation of a precipitate with higher affinity

Table 5
Heavy metals removal isotherm parameters using FA dose of 0.2 g/L.

	Langmuir			Freundlich		
	K_L	q_m	R^2	K_F	n	R^2
Cu^{2+}	8.33	400	0.9784	311.5	8.19	0.9629
Pb^{2+}	0.39	277.8	0.5241	247.2	4.70	0.4247
Cr(VI)	0.26	27.8	0.2072	3743.7	0.74	0.5020

K_L : equilibrium constant (L/mg), q_m : maximum removal capacity (mg/g), K_F : related to maximum removal capacity $(\text{L/mg}^n)^{1/n}$ (mg/g) and n : indicator of sorption intensity (dimensionless).

to FA surface. Pb^{2+} experimental data adjustment to Langmuir and Freundlich models presented relative low R^2 values. In addition, the obtained “ n ” value (>1) from the Freundlich model indicates low intensity sorption behavior.

In the case of Cr(VI) no characteristic isotherm type was identified [54], showing the Cr(VI) experimental data adjustment to Langmuir and Freundlich models low R^2 values. This fact indicates a low affinity of Cr(VI) to the FA surface, corroborating its possible reduction to Cr(III) . This is also in agreement with the data observed in the chemical sequential extraction of RFA from Cr(VI) removal kinetics test, where Cr(VI) was present in the most mobile phases.

3.6. Neutralization test

In Fig. 9a, an increase of pH with increasing FA doses is shown. The doses between 0.2 and 2.2 g/L yielded a slightly raise of pH, due to the dissolution of water soluble minerals such as portlandite and anhydrite in acid conditions [55]. These results are in agreement with the detected calcium and sulphate concentrations (Fig. 10a). However their dissolution did not neutralize the added H^+ because of the FA low amounts employed. With increasing FA doses, a decrease in EC values from 8602 to 3953 S/cm was observed, meaning a diminishment in FA dissolution. Moreover, and starting from the 2.6 g/L FA dose, pH increased sharply from 2.6 to 6.7, whereas EC values remained stable around 1320 S/cm. Levels of V in leachates show a similar behavior as calcium concentrations during this assay (Fig. 9b), indicating that the V associations may be V–Ca–O and Ca–V– SO_4^{2-} , which was observed during characterization of FA (Fig. 2b).

It is important to note that the FA dose of 2.2 g/L yielded a high dissolution degree of anhydrite, which was accompanied with V high contents in solution. However, in almost all the studied FA dosage range, Ni and V presented low leachate concentrations

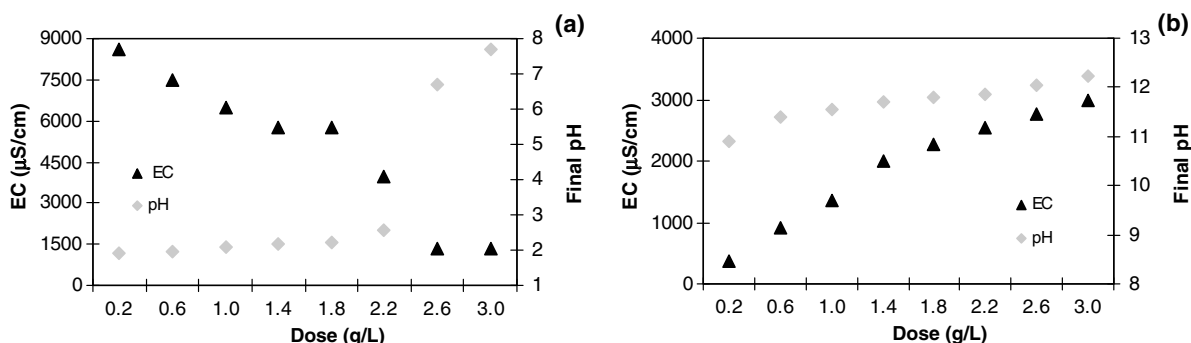


Fig. 9. Final pH and EC values in neutralization test at (a) pH 2 and (b) pH 6.

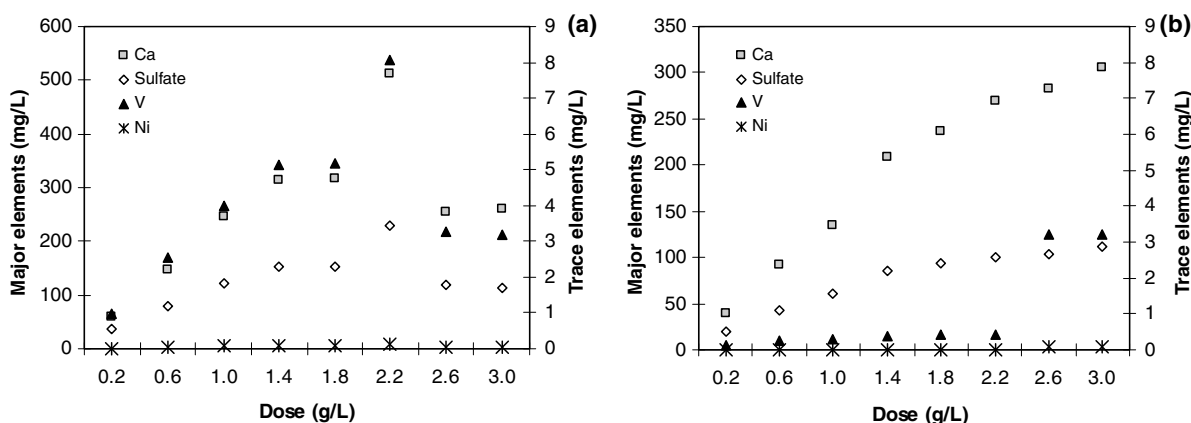


Fig. 10. Neutralization batch test using different FA doses (0.2–3 g/L) at (a) pH 2 and (b) pH 6.

(Fig. 10a). In case of experiments at pH 6, it is observed that minerals portlandite and lime are present in low amounts in the resulting FA, being gradually dissolved with pH increment (Fig. 9b). Anhydrite mineral phase dissolution was also detected (Fig. 10b) with decreasing pH, but in lower degree, observing that calcium, vanadium and sulphate concentrations at pH 6 are lower than at pH 2.

XRD analysis of RFA resulting from neutralization tests at pH 2 (using 1.4 and 2.6 g/L RFA) were performed. XRD patterns show peaks associated to anhydrite and calcite, being anhydrite peaks higher for the RFA using 1.4 g/L compared to 2.6 g/L dose (Fig. 1d). Furthermore, the disappearance of portlandite and lime peaks was observed in RFA after neutralization, suggesting that the gradually increase of calcium concentration may be attributed to portlandite and lime dissolution.

4. Conclusions

The reuse of FA in the neutralization of acidic waste water (for the consequent heavy metals removal) replacing raw alkaline materials is proposed. Removal kinetics and isotherms tests show high removal efficiencies for Cu^{2+} , Pb^{2+} and Cr(VI) , being the possible main mechanisms precipitation (in the case of Cu^{2+} and Pb^{2+}) and a possible reduction (in the case of Cr(VI)). Moreover, according to European and Chilean leaching tests, FA should be considered as a non-hazardous material, despite its high Ni and V contents. Chemical sequential extraction shows that Pb^{2+} precipitate could be of an environment concern, whereas Cu^{2+} precipitate could be safely disposed in landfills or recovered. A possible disadvantage of the proposed FA use may be the spontaneous carbonation process observed in long term FA storage, diminishing FA reactivity.

Acknowledgements

To the FONDECYT Projects 1060309 and 7070022, CONICYT-CSIC Project 2007-136, 2007CL0014 CSIC/CONICYT and CONICYT Interchange scholarship for financial support. To the Soil Laboratory of the University de La Frontera, Carles Ayora from Geosciences Department from IDAEA-CSIC and Josep Elvira from IJA-CSIC for their advices and commentaries.

References

- [1] Swain EJ. US petroleum coke production expected to increase. *Oil Gas J* 1997;95:79–82.
- [2] Wang JS, Anthony EJ, Abanades JC. Clean and efficient use of petroleum coke for combustion and power generation. *Fuel* 2004;83:1341–8.
- [3] Anthony EJ. Fluidized bed combustion of alternative solid fuels; status, successes and problems of the technology. *Prog Energy Combust* 1995;21:239–68.
- [4] Benetto E, Rousseaux P, Blondin J. Life cycle assessment of coal by-products based electric power production scenarios. *Fuel* 2004;83:957–70.
- [5] Chen J, Lu X. Progress of petroleum coke combustions in circulating fluidized bed boilers – a review and future perspectives. *Resour Conserv Recy* 2007;49:203–16.
- [6] Hower JC, Thomas GA, Mardon SM, Trimble AS. Impact of co-combustion of petroleum coke and coal on fly ash quality: case study of a Western Kentucky power plant. *Appl Geochem* 2005;20:1309–19.
- [7] Anthony EJ, Granatstein DL. Sulfation phenomena in fluidized bed combustion systems. *Prog Energy Combust* 2001;27:215–36.
- [8] Anthony EJ, Iribarne AP, Iribarne JV. Fouling in a utility-scale CFBC boiler firing 100% petroleum coke. *Fuel Process Technol* 2007;88:535–47.
- [9] Jia L, Anthony EJ, Charland JP. Investigation of vanadium compounds in ashes from a CFBC firing 100% pet-coke. *Energy Fuel* 2002;16:397–403.
- [10] Izquierdo M, Font O, Moreno N, Querol X, Huggins FE, Alvarez E, et al. Influence of a modification of the pet-coke/coal ratio on the leachability of fly ash and slag produced from a large PCC power plant. *Environ Sci Technol* 2007;41:5330–5.
- [11] Izquierdo M, Moreno N, Font O, Querol X, Alvarez E, Antenucci D, et al. Influence of co-firing on the leaching of trace pollutants from coal fly ash. *Fuel* 2008;87:958–1966.

- [12] Scott AN, Thomas MDA. Evaluation of fly ash from co-combustion of coal and petroleum coke for use in concrete. *Acı Mater J* 2007;104:62–9.
- [13] Sheng GH, Zhai JP, Li Q, Li F. Utilization of fly ash coming from a CFBC boiler co-firing coal and petroleum coke in Portland cement. *Fuel* 2007;86:2625–31.
- [14] Chen LM, Kost D, Dick WA. Petroleum coke circulating bed combustion product as a sulfur source for alfalfa. *Commun Soil Sci Plant Anal* 2008;39:1993.
- [15] Thenoux G, Halles F, Vargas A, Bellolio JP, Carrillo H. Laboratory and field evaluation of fluid bed combustion fly ash as granular road stabilizer. *Transp Res Record* 2007;2:36–41.
- [16] Conn RE, Sellakumar K, Bland AE. Utilization of CFB fly ash for construction applications. In: Proceedings of the 15th international conference on fluidized bed combustion, Savannah, Georgia, USA, May 16–19; 1999.
- [17] González A, Moreno N, Navia R. Fly ashes from coal and petroleum coke combustion: current and innovative potential applications. *Waste Manage Res* 2009;27:976–87.
- [18] Gray NF. Environmental impact and remediation of acid mine drainage: a management. *Environ Geol* 1997;30:62–71.
- [19] Coulton R, Bullen C, Dolan J, Hallet C, Wright J, Marsden C. Wheal Jane mine water active treatment plant-design, construction and operation. *Land Contam Reclam* 2003;11:245–52.
- [20] Pérez-López R, Nieto JM, Ruiz de Almodóvar G. Utilization of fly ash to improve the quality of the acid mine drainage generated by oxidation of a sulphide-rich mining waste: column experiments. *Chemosphere* 2007;67:1637–46.
- [21] Potgieter-Vermaak SS, Potgieter JH, Monama P, Van Grieken R. Comparison of limestone, dolomite and fly ash as pre-treatment agents for acid mine drainage. *Miner Eng* 2006;19:454–62.
- [22] Castro SH, Sánchez M. Environmental viewpoint on small-scale copper, gold and silver mining in Chile. *J Cleaner Prod* 2003;11:207–13.
- [23] Bezama A, Sánchez M. State-of-the-art management technologies for contaminated soils and groundwaters with focus on the copper industry. In: I international workshop on process hydrometallurgy-hydroprocess, GECAMIN, Iquique, Chile, October 11–13; 2006.
- [24] Querol X, Whateley MK, Fernández-Turiel JL, Tuncali E. Geological controls on the mineralogy and geochemistry of the Bepazari lignite, Central Anatolia, Turkey. *Int J Coal Geol* 1995;33:255–71.
- [25] Thompson M, Walsh N. Handbook of inductively coupled plasma spectrometry. New York: Chapman and Hall Inc.; 1989.
- [26] ASTM C618-92a. Standard specification for fly ash and raw or calcinated natural pozzolan for use as mineral admixture in Portland cement concrete. Annual book of ASTM standards 04.02. West Conshohocken, Pennsylvania. Am Soc Test Mater; 1994.
- [27] Chilean Regulation No. 148. Reglamento Sanitario Sobre Manejo De Residuos Peligrosos; 2003.
- [28] EPA Test Method 1311-TCLP. Toxicity characteristic leaching procedure. <www.ehso.com/cssepa/TCLP_fromEHSOcom_Method_1311.pdf>.
- [29] European Committee for Standardisation EN 12457-2:2002. Characterisation of waste-leaching-compliance test for leaching of granular waste materials and sludges-Part 2: One stage batch test a liquid to solid ratio of 10 L/kg for materials with particle size below 4 mm.
- [30] Wang S, Wu H. Environmental-benign utilization of fly ash as low-cost adsorbents. *J Hazard Mater* 2006;B136:482.
- [31] Lagergren S, Svenska BK. Zur Theorie der sogenannten adsorption gelöster Stoffe. *Vetenskapakad Handl* 1898;24:1–39.
- [32] McKay G, Ho YS. Pseudo-second order model for sorption processes. *Process Biochem* 1999;34:451–65.
- [33] Zhang FS, Itoh H. Adsorbents made from waste ashes and post-consumer PET and their potential utilization in wastewater treatment. *J Hazard Mater* 2003;B101:323–37.
- [34] Sposito G, Lund IJ, Chang AC. Trace metal chemistry in arid-zone field soils amended with sewage sludge: 1. Fractionation of Ni, Cu, Zn, Cd and Pb in solid phases. *Soil Sci Soc Am J* 1982;46:260–4.
- [35] El-Demerdashe S, Dahdoh MSA, Hassan FA. Sequential extraction of nine trace elements from sludge-amended soils. *Fertilizer Res* 1995;41:77–85.
- [36] Moreno N, Viana M, Pandolfi M, Alastuey A, Querol X, Chinchón S, et al. Determination of direct and fugitive PM emissions in a Mediterranean harbour by means of classic and novel methods. *J Environ Monitor* 2009;91:133–41.
- [37] Moreno N, Alastuey A, Querol X, Artiñano B, Guerra A, Luaces JA, et al. Characterisation of dust material emitted during harbour operations (HADA Project). *Atmos Environ* 2007;41:6331–43.
- [38] Commandré JM, Salvador S. Lack of correlation between the properties of a petroleum coke and its behaviour during combustion. *Fuel Process Technol* 2005;86:795–808.
- [39] Moreno N, Querol X, Andres JM, Stanton K, Towler M, Nugteren H. Physico-chemical characteristics of European pulverized coal combustion fly ashes. *Fuel* 2005;84:1351–63.
- [40] Komnitsas K, Bartzas G, Paspaliaris I. Clean up of acidic leachates using fly ash barriers: laboratory column studies. *Global Nest J* 2004;6:81–9.
- [41] Iribarne JV, Anthony EJ, Iribarne A. A scanning electron microscopy study on agglomeration in petroleum coke-fired FBC boilers. *Fuel Process Technol* 2003;82:27–50.
- [42] Brown RC, Dykstra J. Systematic errors in the use of loss on ignition to measure unburned carbon in fly ash. *Fuel* 1995;74:570–4.
- [43] Jegadeesan G, Al-Abed SR, Pinto P. Influence of metal distribution on its leachability from coal fly ash. *Fuel* 2008;87:1887–93.
- [44] Babel S, Kurniawan T. Low-cost adsorbents for heavy metals uptake from contaminated water: a review. *J Hazard Mater* 2003;B97:219–43.
- [45] Navia R, Inostroza X, Diez MC, Lorber KE. Irrigation model of bleached Kraft mill wastewater through volcanic soil as a pollutants attenuation process. *Chemosphere* 2006;63:1242–51.
- [46] Rozada F, Otero M, Parra JB, Morán A, García AI. Producing adsorbents from sewage sludge and discarded tyres. Characterization and utilization for the removal of pollutants from water. *Chem Eng J* 2005;114:161–9.
- [47] Doherty R, Phillips DH, McGeough KL, Walsh KP, Kalin RM. Development of modified fly ash as a permeable reactive barrier medium for a former gas plant site, Northern Ireland. *Environ Geol* 2006;50:37–46.
- [48] Navia R, Schmidt KH, Behrend G, Lorber KE, Rubilar O, Diez MC. Improving the adsorption capacity and solid structure of natural volcanic soil using a foaming-sintering process based on recycled polyethylene terephthalate (PET). *Waste Manage Res* 2007;25:119–29.
- [49] Bayat B. Comparative study of adsorption properties of Turkish fly ashes I. The case of nickel(II), copper(II) and zinc(II). *J Hazard Mater* 2002;B95:251–73.
- [50] Alinnor IJ. Adsorption of heavy metals ions from aqueous solution by fly ash. *Fuel* 2007;86:853–8.
- [51] Rao M, Parwate AV, Bhole HG. Removal of Cr⁶⁺ and Ni²⁺ from aqueous solution using bagasse and fly ash. *Waste Manage* 2002;22:821–30.
- [52] Mohan D, Pittman CU. Activated carbons and low cost adsorbents for remediation of tri-hexavalent chromium from water. *J Hazard Mater* 2006;137:762.
- [53] Ho YS. Review of second-order models for adsorption systems. *J Hazard Mater* 2006;B136:681–9.
- [54] Limousin G, Gaudet J-P, Charlet L, Szentknect S, Barthés V, Krimissa M. Sorption isotherms: a review on physical bases, modeling and measurement. *Appl Geochem* 2007;22:249–75.
- [55] Stumm W, Morgan JJ. Chemical equilibria and rates in natural waters. 3rd ed. New York, USA: John Wiley & Sons Inc.; 1996, p. 363.



Contents lists available at ScienceDirect

Chemical Engineering Journal

journal homepage: www.elsevier.com/locate/cejChemical
Engineering
Journal

Development of a non-conventional sorbent from fly ash and its potential use in acid wastewater neutralization and heavy metal removal

A. González^{a,b}, N. Moreno^c, R. Navia^{b,d,*}, X. Querol^c^a Ph.D. Program in Sciences of Natural Resources, University of La Frontera, P.O. Box 54-D, Temuco, Chile^b Scientific & Technological Nucleus in Bioresources, University of La Frontera, P.O. Box 54-D, Temuco, Chile^c Department of Geosciences, IDAEA-CSIC, C/ Jordi Girona, 18-26, E-08034 Barcelona, Spain^d Department of Chemical Engineering, University of La Frontera, P.O. Box 54-D, Temuco, Chile

ARTICLE INFO

Article history:

Received 9 October 2010

Received in revised form

16 November 2010

Accepted 17 November 2010

Keywords:

Petroleum coke

Black liquor

Lignimerin

Heavy metals

ABSTRACT

This work focuses on the development, characterization and use of a non-conventional sorbent (NCS) using a blend of petroleum coke fluidized bed combustion fly ash and the organic waste fraction from a Kraft cellulose wastewater facility. In addition to an increase in specific surface area and particle size distribution, NCS showed a similar chemical composition as petroleum coke fly ashes. Leaching tests revealed the non-hazardous character of all NCSs obtained according to the European standards for landfill disposal of waste materials, being Na, S, Ca, V, Ni, Zn and As detected as mobile major and trace elements. With these results, the sample NCS3 was selected for a further application in experiments of neutralization and heavy metal removal from acid wastewater. Neutralization and heavy metal fixed-bed removal tests showed that NCS3 is a suitable sorbent material (maximum removal capacities of 8.1 and 28.3 mg/g for Cu²⁺ and Pb²⁺, respectively) that can be used at pH 4, showing greater buffering and Cu²⁺ and Pb²⁺ removal capacities.

© 2010 Published by Elsevier B.V.

1. Introduction

High operational costs associated with decontamination process and increasingly stringent environmental regulations have forced industries to find cost-effective effluent treatment and reactive materials with properties similar to conventional reactive materials used in pollutant-removal processes [1]. As a result, in recent years there has been increasing interest in the research on waste materials and by-products, with possible application in adsorption processes [2–6]. These materials are known as non-conventional sorbents (NCSs) or low-cost sorbents due to their high local availability and little or no processing requirements. A wide spectrum of wastes with high carbon content suitable for obtaining NCSs have been already reported in the literature: wastewater from Kraft pulp process [7,8], polyethylene terephthalate [3], fly ash [9], treated sewage sludge [10], sugar beet pulp [11], sawdust [12], tea waste [13] and anaerobic biomass [14]. When treated with heat, these materials generate a carbon precursor, and the resulting NCS is utilized as nutrient source and slow release fertilizer or to replace activated carbon, for subsequent application in wastewater purifi-

cation and heavy metal removal processes [15]. Several reviews have condensed a large literature survey on the excellent performance of different types of NCS in heavy metal removal processes from contaminated waters [2,4,6].

During mineral extraction and processing and subsequent environment exposure, heavy metals are released. Once these elements are emitted into the environment, they can take a number of different pathways, causing several functional disorders and diseases in living organisms [16].

Two important Chilean residues are petroleum coke fluidized bed combustion fly ash (CFBC-PCFA) and Kraft cellulose mill wastewaters (KCMW). Their relevance is related to the severe impact they have on the environment and the large amounts generated. KCMW are characterized mainly by an organic fraction [17], whereas CFBC-PCFA is mainly composed of calcium, sulphate, unburned carbon (UC), vanadium, nickel and molybdenum [18,19].

CFBC-PCFA has been reused as a substitute for alkaline materials in several processes such as soil amelioration [20,21], acid wastewater neutralization and copper and lead removal [18]. According to the results of the particle size distribution [18], CFBC-PCFA has a fine particle size distribution, implying a low hydraulic conductivity coupled with low heavy metal removal efficiencies, in the case of continuous column removal processes.

This problem may be avoided with agglomeration techniques with organic materials and a subsequent heating treatment [3], being interesting in our case, the blending with KCMW. One advan-

* Corresponding author at: Department of Chemical Engineering, University of La Frontera, Av. Francisco Salazar 01145, Temuco, Chile. Tel.: +56 45 325477; fax: +56 45 325053.

E-mail address: rnavia@ufro.cl (R. Navia).

tage of the pellets resulting from this process could be a decrease in toxic trace elements leaching, which would broaden the potential application field of CFBC-PCFA.

One common problem in mining facilities is the generation of acidic wastewaters. Generally, acid wastewaters generate a severe impact in the environment due to their high heavy metal content, suspended solids content and acidity [22]. Chilean copper mining facilities lead the world in copper production. However, at present there are 657 tailing ponds in Chile, of which a 39% have been shown to present deficient conditions [23]. Bezama and Sánchez [24] also found that improper solid waste and wastewater handling may result in copper, molybdates, sulphates, arsenic and high concentration of H^+ reaching soil, rivers and groundwater. Pizarro et al. [25] determined that mainly the mining activities contribute with heavy metal pollution in 12 rivers of central-northern Chile. The authors detected in the rivers, near to mining discharge sites, concentrations of 1705 (As), 6082 (Cu), 147 (Pb) and 446 (SO_4^{2-}) mg/L, requiring urgent treatments for reducing the high levels of heavy metals.

Therefore, this research attempts to develop and characterize NCS from an organic material (recovered from KCMW or black liquor) and CFBC-PCFA, and to evaluate its potential use in neutralization and heavy metal removal from acidic wastewaters.

2. Experimental

2.1. Materials and methods

2.1.1. Lignimerin

An organic material called “lignimerin” recovered from a KCMW in southern Chile [7] was used as the carbon precursor of NCS1. Lignimerin is constituted mainly by polyphenols (lignin and condensed tannins), carbohydrates, proteins and metal cations, corresponding to 57.0%, 22.3%, 7.4% and 6.9%, respectively.

NCS1 consisted of a blend of 6 g CFBC-PCFA, 4 g lignimerin and 10 mL distilled water. These were all manually homogenized and dried at 65 °C for 24 hours (h). Subsequently, the dried blend was heated at 500 °C for 2 h.

2.1.2. Black liquor

This by-product, which normally is burned in a recovery boiler to retrieve energy from lignin oxidation and the cooking chemicals from digester house [26], was sampled from a Kraft cellulose mill facility in southern Chile. According to Demirbas [27], black liquor (BL) consist mainly of organic material (61.8%) such as lignin, polysaccharides and resinous compounds and inorganic salts (38.1%), being sodium and potassium salts about 20% and 2%, respectively.

BL was selected as carbon precursor of NCS2 and NCS3. 1 L of BL was evaporated at 85 °C until reaching a final volume of 0.25 L and a density of 1.16 g/cm³. NCS2 and NCS3 were prepared by manually blending 8.5 and 13.5 mL of BL respectively with 6 g CFBC-PCFA. Both blends were dried at 65 °C for 24 h and heated at 500 °C for 1 h.

2.1.3. Petroleum coke fly ash

A petroleum coke fly ash sample from a circulating fluidized bed combustion power plant (CFBC-PCFA-2008) from the Bío Bío Region in Chile, was sampled in 2008 and used for this study without any further treatment. This CFBC-PCFA is similar as the CFBC-PCFA-2007 fully characterized and reported in 2007 [18].

2.1.4. Chemicals

Cu^{2+} and Pb^{2+} base solutions of 1000 mg/L were prepared in distilled water for removal tests using $CuCl_2$ and $PbCl_2$ salts of ana-

lytical grade Merck. Base solutions were stored at 4 °C. All other chemicals used were also of analytical grade.

Batch and column experiments were performed in duplicates. Reported experimental values are the averages of the replicate measurements. Relative standard deviations were lower than 4.7%.

2.2. Chemical, mineralogical and physical characterization

NCS, CFBC-PCFA-2008, and international reference materials (NBS 1633b and SARM 19, used as control samples in analytical methods accuracy checking) were acid-digested by using a special two step digestion method proposed by Querol et al. [28]. The major, minor and trace elements concentrations were determined by inductively coupled plasma atomic emission spectrometry (ICP-AES) and inductively coupled plasma mass spectrometry (ICP-MS). Hg concentration was directly analyzed on solid samples with a Mercury Analyzer LECO AMA 254. Besides, hydrofluoric acid digestion as described by Thompson and Walsh [29] was carried out to determine the silica content in NCS.

The mineralogical characterization of NCS and CFBC-PCFA-2008 was determined using a X-ray diffractometer (Bruker, D8 Advance model) with a primary Göbbel crystal, equipped with a detector based on dispersion of SOL-X energies, with a Cu tube and a wavelength of $\lambda = 1.5405 \text{ \AA}$, under working conditions at kV=40 and mA=40.

The physical characterization of resulting NCS included moisture, loss on ignition (LOI), particle size distribution, scanning electron microscopy (SEM) and BET surface area. Moisture and LOI were determined at 105 °C and 1050 °C, respectively [30]. NCS particle size distribution was performed through dry mechanical sieving. Specific surface area was measured using the BET method by means of a NOVA 1000 (Quantachrome) nitrogen porosimeter. Finally, SEM-EDX analyses were performed with a scanning electron microscope (SEM-EDX, JEOL6400).

2.3. Leaching tests

Leaching tests were utilized as selection criteria among the NCSs, in order to use the selected NCS for posterior applications. NCS with the lowest concentration of elements of environmental concern in leaching tests was selected.

2.3.1. Batch test

The potential mobility of specific trace elements from NCS and CFBC-PCFA-2008 was determined according to the compliance leaching test EN 12457 Part 2 procedure [31] and comparing it with CFBC-PCFA leaching results [18] and the limit values from Council Decision 2003/33/EC [32]. This test is a single batch leaching test performed at a liquid/solid ratio of 10 L/kg, with an agitation time of 24 h and MQ grade water as eluting agent.

Major, minor and trace elements as well as Hg concentration from the leachates were analyzed as described in Section 2.2. The pH and electric conductivity (EC) values were also measured with MYRON Ultrameter 6P pH- and conductivity-meter.

2.3.2. Column test

Leaching column tests for CFBC-PCFA-2008 and NCS were performed in columns with a height of 10 cm and diameter of 5 cm, according to Querol et al. [33]. MQ grade water was employed as the eluting agent with a flow rate of 0.2 mL/min. The leachates were filtered with 0.45 μm filter paper. The pH and EC values as well as major, minor and trace elements from the leachates were measured as described in Section 2.2. Detected concentrations of elements of environmental concern in all NCSs leachates were compared with the limit values from wastewaters emission Chilean regulation DS N° 90.

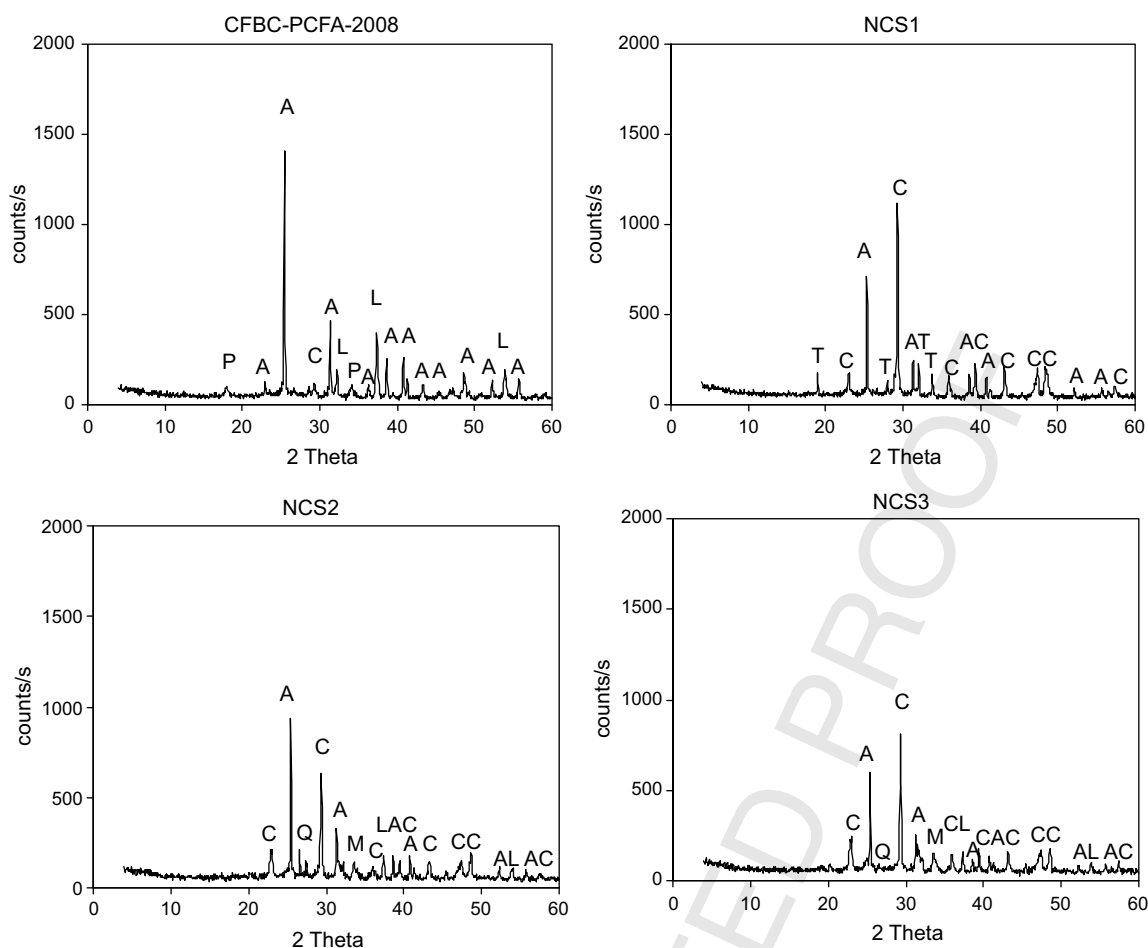


Fig. 1. XRD patterns from CFBC-PCFA-2008 and NCS samples. C: calcite, CaCO_3 ; A: anhydrite, CaSO_4 ; T: thenardite, Na_2SO_4 ; M: merwinite, $\text{Ca}_3\text{Mg}(\text{SiO}_4)_2$; L: lime, CaO and Q: quartz, SiO_2 .

2.4. Acid wastewater neutralization in column tests

The effect of pH in a NCS3 fixed bed (height 6 cm) was performed in 1.3 cm diameter polypropylene (PP) columns. The tests consisted of feeding acid solution at pH 2 and 4 to the PP column at a flow rate of 1.5 mL/min through the NCS3 bed using a peristaltic pump. The output solution was collected and filtered for pH measurements. Major, minor and trace elements in output samples from the acid solution passing through NCS3 were analyzed by ICP-MS and ICP-AES.

2.5. Cu^{2+} and Pb^{2+} removal in column tests

The column fixed bed sorption capacity is a very important design parameter in column performance [34]. Column input (Co) and output (C) heavy metal concentrations (mg/L), G, the solution flow rate (L/min) and t_s , which is the corresponding time at the saturation point, are the parameters known to represent the breakthrough curve and for determining the fixed bed sorption capacity.

Fixed bed column tests were performed in 1.3 cm diameter PP columns packed with NCS3 and a bed height of 6 cm. Heavy metal input solution (Co) was fed at 100 mg/L and a flow rate (G) of 1.5 mL/min, using a peristaltic pump. The output solution (C) was collected and filtered for pH measurements. Then Cu^{2+} and Pb^{2+} residual concentrations and other elements of interest present in NCS3 were determined as described in Section 2.2. In addition, used NCS3 was also analyzed by means of XRD and SEM-EDX.

2.6. Sequential extraction

To elucidate the main Cu^{2+} and Pb^{2+} removal mechanism by NCS3, a sequential chemical extraction was carried out of raw CFBC-PCFA and NCS3, and from Cu^{2+} and Pb^{2+} residual material from removal column test, according to Sposito et al. [35]. Sposito's procedure consists of five consecutive extractions (S1–S5) with solutions of increasing strengths. S1 is the water soluble fraction; S2 is the exchangeable phase (KNO_3); S3 is the fraction associated to organic matter (NaOH); S4 is the fraction associated to the carbonates phase (EDTA) and S5 is the fraction associated to the sulphide phase and non silicate matrix (HNO_3). Elements of interest from the extractions were analyzed as described in Section 2.2.

3. Results and discussion

3.1. NCS characterization

X-ray diffraction (XRD) analyses showed that mineral phases supplied by CFBC-PCFA, such as calcite and anhydrite were present in NCS1, NCS2 and NCS3 (Fig. 1). The blending of CFBC-PCFA and lignimerin and BL accounted for the synthesis of new crystalline species in NCS. Trace mineral phases were also detected: thenardite (Na_2SO_4) for NCS1, and merwinite ($\text{Ca}_3\text{Mg}(\text{SiO}_4)_2$) for NCS2 and NCS3. The occurrence of thenardite in NCS1 cannot be attributed to a new binding phase between lignimerin and CFBC-PCFA. A similar crystalline mineral ($\text{Na}_2\text{CO}_3 \cdot \text{Na}_2\text{SO}_4$) has been detected by Fierro et al. [36] in lignin from Kraft processes, whereas for NCS2 and NCS3

Table 1

Major oxides content for CFBC-PCFA-2008 and NCS samples; (a) in % weight; (b) LOI indicates and (c) M indicates moisture.

%	CaO	SO ₃	LOI	SiO ₂	Al ₂ O ₃	Fe ₂ O ₃	MgO	Na ₂ O	K ₂ O	P ₂ O ₅	M
CFBC-PCFA	44.8	29.7	23.4	1.6	0.2	0.2	0.4	0.3	<0.05	<0.05	0.01
NCS1	32.1	19.7	50.8	1	<0.01	0.1	0.3	6	0.4	0.1	0.06
NCS2	31.5	24.1	52.7	1.3	<0.01	0.2	0.2	8.5	0.7	<0.01	0.02
NCS3	27.6	22.2	53.4	1.2	<0.01	0.2	0.2	10.5	0.8	<0.01	0.02

Table 2

Trace elements concentrations in mg/kg of CFBC-PCFA and NCS samples.

mg/kg	CFBC-PCFA	NCS1	NCS2	NCS3	mg/kg	CFBC-PCFA	NCS1	NCS2	NCS3
As	2.6	1.6	2.5	1.6	Mo	19.6	9.2	12.9	12.6
B	4.6	20.1	21.8	24.2	Nd	1.1	<0.8	<0.8	24.2
Ba	19.5	11.4	12.9	15.5	Ni	3946	1724	2613	2536
Ce	1.8	1.1	1.0	1.2	Pb	3.8	2.6	2.6	2.4
Co	42.4	31.5	26.0	25.3	Rb	1.1	7.3	16.0	19.7
Cr	8.4	26.8	5.5	5.5	Se	1.1	<0.8	1.2	0.8
Cu	4.7	12.5	4.3	5.2	Sr	613	410	377	363
Ga	2.0	1.7	1.3	1.3	Ti	59.9	26.5	41.6	41
Hg	0.03	0.02	0.003	0.002	V	7702	3641	4798	4671
La	2.1	1.1	1.1	1.2	Y	2.1	1.5	1.3	1.2
Li	1.8	1.0	1.3	2.3	Zn	17.5	17.6	5.7	7.7
Mn	26.0	43.3	23.7	29.6	Zr	3.4	1.2	2.3	2.1

the crystalline phase merwinite may be attributed to a new binding phase between CFBC-PCFA and BL. Compared with CFBC-PCFA, it was observed that except for the new phases, the three NCSs obtained present similar XRD patterns compared to CFBC-PCFA-2008. Nevertheless, the XRD peaks intensities of all crystalline species present in NCS are significantly lower than that of CFBC-PCFA-2008, suggesting the possible coating of CFBC-PCFA by the carbonaceous material produced during the oxidation of lignimerin (NCS1) and BL (NCS2-NCS3) or/and increasing of amorphous phase.

Table 1 indicates the major elements content in CFBC-PCFA-2008 and NCS samples. The predominant oxides are CaO (44.8% for CFBC-PCFA, 32.1% for NCS1, 31.5% for NCS2 and 27.6% for NCS3),

SO₃ (29.7 for CFBC-PCFA, 24.1 for NCS2, 22.2 for NCS3 and 19.7% for NCS1) and NaO (10.5 for NCS3, 8.5 for NCS2, 6.0 for NCS1, and 0.3% for CFBC-PCFA). Moreover, K₂O content increased in the developed NCS, implying that lignimerin and BL contribute to the presence of Na and K in the resulting NCS. However, Al was not detected in the produced NCS, suggesting that Al is not involved in the potential binding reactions between CFBC-PCFA and lignimerin and BL. In addition, the high CaO content suggests that NCS could be used in heavy metal removal by means of precipitation processes, in the neutralization of acid mine wastewaters.

Trace elements such as Ni, V, As, B, Cu, Cr, Mn and Rb may limit NCS potential applications. As shown in Table 2, the concentrations

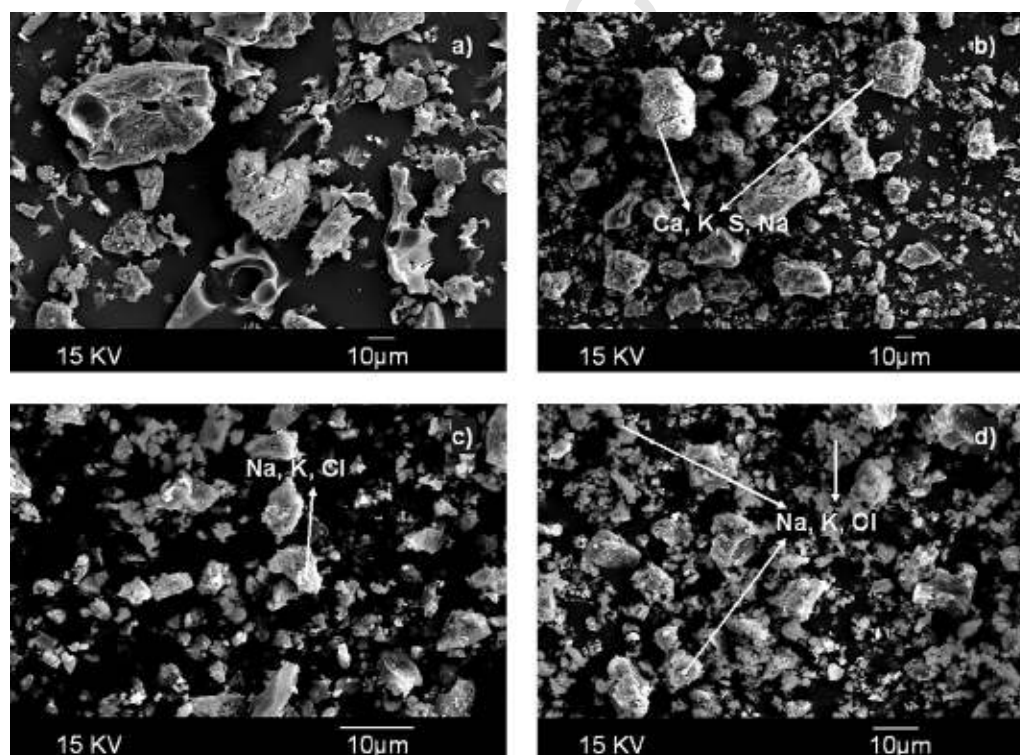


Fig. 2. Microphotographs from SEM-EDX analyses: (a) CFBC-PCFA-2008, (b) NCS1, (c) NCS2 and (d) NCS3. All images have the same magnification.

Table 3Particle size distribution from NCS samples. Values expressed in μm .

Materials	μm		
	10%	50%	90%
CFBC-PCFA ^a	6.5	28.3	85
NCS1	1200	2000	3350
NCS2	500	1200	2000
NCS3	250	1200	2000

^a CFBC-PCFA values obtained through laser diffraction and extracted from [18].

for NCS samples of Ni and V are lower than that of CFBC-PCFA-2008, whereas Rb and B were found in considerable amounts when compared to CFBC-PCFA. Copper, Cr, Mn, and Zn were also found in high amounts but only in NCS1. The possible leaching of these elements may be of environmental concern and therefore leaching tests were performed (Section 3.2).

Regarding particle morphology, the microphotographs of NCS samples and CFBC-PCFA-2008 from SEM-EDX analyses are presented in Fig. 2. The morphology from NCS samples was found to be similar to that of CFBC-PCFA-2008 (Fig. 2a), showing irregular particles with angular and sharp edges. In addition, NCS2 and NCS3 particles (Fig. 2c and d) were detected to be coated with elements such as Na, Cl and K from BL, whereas NCS1, with elements such as Na, K, S and Ca (Fig. 2b). Moreover, Ni and V, elements of environmental concern in CFBC-PCFA, were not detected in NCS SEM-EDX analyses. This result indicates a possible coating of CFBC-PCFA by the organic fraction from lignimerin and BL.

Similar to Zhang and Itoh [3], an increase in grain size and surface area was expected in the NCS samples, these changes may facilitate the application of NCS in heavy metal removal in column processes. The specific surface area of NCS samples was determined to be 22 m²/g (NCS1), 11 m²/g (NCS2) and 18 m²/g (NCS3). All values are lower than those reported by several authors, such as the blend of fly ash and PET described by Zhang and Itoh (115–485 m²/g) [3], the activated carbon from lignin (3000 m²/g) [36] and alternative sorbents developed from discarded tires and sewage sludge (472 m²/g) [10]. However, the measured specific surface area in NCS samples is higher than those of the original materials (CFBC-PCFA 5 m²/g) [18] and lignimerin (1.12 m²/g), probably as a consequence of the heating treatment between at 500 °C.

All NCS samples presented a higher grain size than CFBC-PCFA. For NCS1 the grain size was in the 10th, 50th and 90th percentile, with 1200, 2000 and 3350 μm , respectively (Table 3). In relation to NCS2 and NCS3, both sorbents presented similar grain size distribution, being the median and 90th percentile, 1200 and 2000 μm , respectively. However, for the 10th percentile a difference between

NCS2 (500 μm) and NCS3 (250 μm) was observed. In conclusion, a higher surface area and particle size distribution was obtained for all NCS samples compared to the original materials.

3.2. Leaching tests

3.2.1. Batch tests

The results from leaching tests in relation to the European 12457-2 leaching protocol are listed in Table 4. For comparison purposes the values of two CFBC-PCFA samples (from 2007 and 2008 samplings) are indicated in Table 4. CFBC-PCFA-2007 and NCS may be characterized as non-hazardous materials as the analyzed elements concentration did not exceed the limit values for non-hazardous waste. According to Council Directive 2003/33/EC [32], CFBC-PCFA-2008 should be considered as a hazardous waste. In fact, CFBC-PCFA-2008 SO₄²⁻ leachate concentration (23,421.4 mg/kg) is higher than the limit value for non hazardous waste (20,000 mg/kg). Nevertheless, as this value is lower than 50,000 mg/kg (see Table 4), CFBC-PCFA-2008 does not require any further stabilization treatment before disposal in a hazardous waste landfill.

Leachates from all materials reached alkaline pH values between 10.3–10.9 and EC between 10,800 and 35,900 $\mu\text{S}/\text{cm}$. pH and EC values indicate a high dissolution capacity of species, which for the two CFBC-PCFA samples are mostly associated with calcium compounds (lime, portlandite, calcite and anhydrite), whereas for NCS samples the high EC values are related to the dissolution of Ca-, Na-, K- and S-bearing minerals. Detection of high concentrations of sulphate (Table 4) and calcium (between 19,508 and 23,928 mg/kg) in CFBC-PCFA samples and sodium (between 13,026 and 23,961 mg/kg) and sulphate (Table 4) in NCS samples corroborated dissolution of above mentioned compounds.

Nickel, Cu, Zn, Ba, Mo and V were detected as the main trace elements in CFBC-PCFA and NCS leachate samples. Maxima values detected in the leachates were 0.27 mg/kg (Ni), 0.05 mg/kg (Cu), 0.1 mg/kg (Zn), 0.4 mg/kg (Ba), 7.1 mg/kg (Mo) and 77.9 mg/kg (V). Mo and V concentrations in NCS leachates were found to be significantly higher than that of CFBC-PCFA samples. An explanation may be the change in the mobile species, attributed to the blending between both alkaline materials and subsequent heating treatment, which may increase the solubility of those elements.

3.2.2. Column tests

Fig. 3 indicates that the pH values from CFBC-PCFA-2008 and NCS leaching samples range from moderate and high alkaline values. CFBC-PCFA-2008 leachate samples present a continuous pH decrease from 10.7 to 9.1, whereas NCS leaching samples reached

Table 4

Leaching test values of European Norm EN 1245-2 (mg/kg). Limit values from Council Decision 2003/33/EC [32].

	mg/kg			CFBC-PCFA ^a	CFBC-PCFA ^b	NCS1	NCS2	NCS3
	Inert	Non-hazardous	Hazardous					
As	0.5	2	25	0.02	0.12	0.12	0.02	0.02
Ba	20	100	300	1.21	0.16	0.3	0.4	0.4
Cd	0.04	1	5	<0.01	<0.01	<0.01	<0.01	<0.01
Cr	0.5	10	70	0.2	0.17	0.06	<0.01	<0.01
Cu	2	50	100	0.03	0.02	0.05	0.05	0.1
Hg	0.01	0.2	2	<0.01	<0.01	<0.01	<0.01	<0.01
Mo	0.5	10	30	2.2	4.6	3.4	6.8	7.1
Ni	0.4	10	40	0.25	0.27	0.05	0.05	0.04
Pb	0.5	10	50	0.02	<0.01	0.02	<0.01	<0.01
Sb	0.06	0.7	5	<0.01	<0.01	0.01	<0.01	<0.01
Se	0.1	0.5	7	0.04	0.06	0.04	0.06	0.07
Zn	4	50	200	0.06	0.04	0.06	0.09	0.1
SO ₄ ²⁻	1000	20,000	50,000	19,335	23,421.4	9766	10,713	14,604

^a CFBC-PCFA-2007 [18].^b CFBC-PCFA-2008.

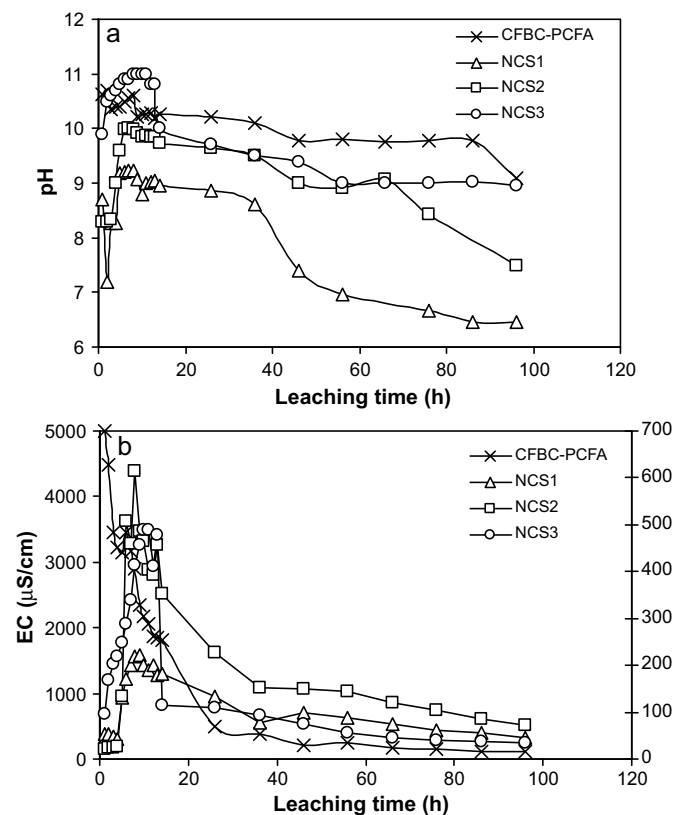


Fig. 3. pH (a) and EC (b) evolution in column leaching test of CFBC-PCFA, NCS1, NCS2 and NCS3.

a maximum pH value of 9.2, 10.0 and 11.0 for NCS1, NCS2 and NCS3 respectively, decreasing to 6.4, 7.5 and 9.0 during the column assays. Regarding EC in the output leaching samples, CFBC-PCFA-2008 leachate samples undergo a continuous decreasing in EC values from 4995 to 200 $\mu\text{S}/\text{cm}$, whereas NCS leachate samples showed a slight increase between 6 and 10 h, reaching a maximum of 222, 613 and 478 $\mu\text{S}/\text{cm}$ for NCS1, NCS2 and NCS3, respectively. After reaching the maximum values, a continuous decrease was observed, leading to the conclusion that CFBC-PCFA-2008 and all NCSs presented a similar time evolution pattern for pH and EC.

Fig. 4 shows the main elements detected in the leaching samples of CFBC-PCFA-2008 and NCS columns; Ca, Na, S (as SO_4^{2-}), Ni, Mo, V, Ba, Sr, As and Zn the most important.

Leaching CFBC-PCFA-2008 major elements Ca and S (as SO_4^{2-}) initially reached maximum values of 605 and 444 mg/L, respectively. After this initial period, both elements progressively decreased in leachate concentrations. This trend is similar regardless of the evolution pattern of pH over time, indicating that Ca and SO_4^{2-} concentrations may be controlled mainly by anhydrite dissolution. This result corroborated statements from batch leaching test. Moreover Mo, Ni and Ba were detected in low concentrations in CFBC-PCFA-2008 leachates (highest values of those elements under 80 $\mu\text{g}/\text{L}$, after 1 h). Strontium (from calcium-minerals) reached a maximum value of 1.6 mg/L, whereas V reached a highest concentration of 3.1 mg/L at 36 h. The detection of these trace elements could be attributed to dissolution of their water soluble salts, which commonly are enriched as finer particles attached to the CFBC-PCFA surface [37,38].

Calcium seems to play a secondary role in NCS leaching, being only low Ca concentrations detected in leachates for all NCS columns (values ranging between 3 and 11 mg/L). On the opposite, Na concentration in leachates increased up to seven times (values ranging between 78 and 105 mg/L). Sulphate concentration diminished considerably (between 80 and 136 mg/L) in NCS leachate samples compared to CFBC-PCFA-2008 (444 mg/L). Besides Sr and V

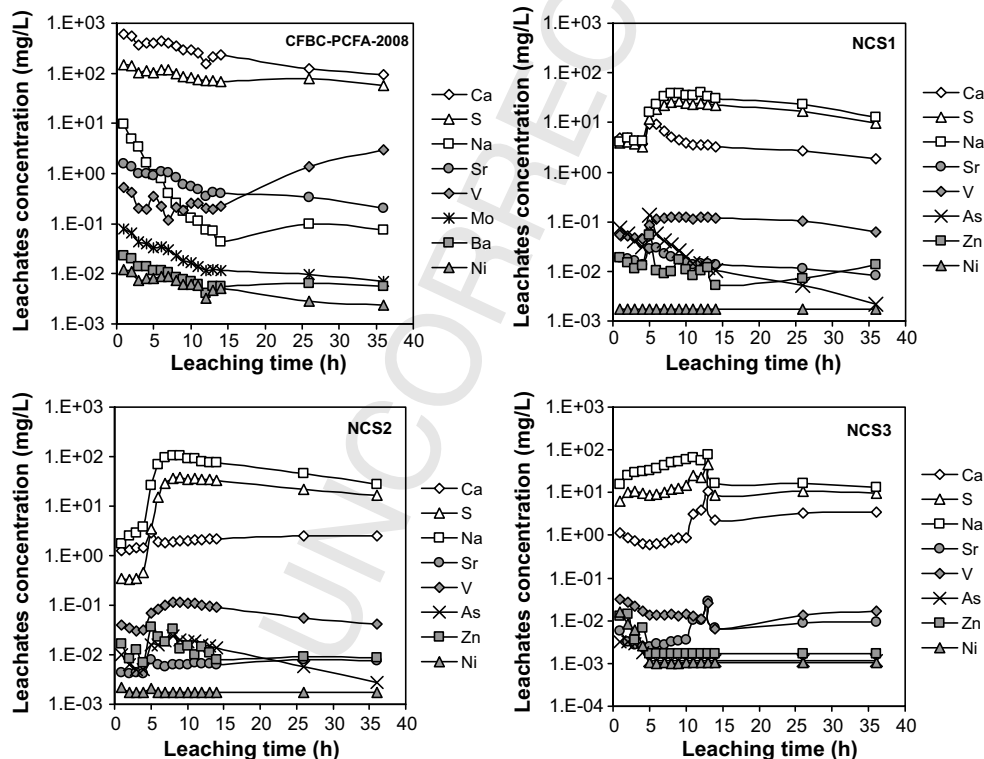


Fig. 4. Main major and trace elements detected during column leaching tests of CFBC-PCFA, NCS1, NCS2 and NCS3. Ordinate axis in logarithm scale.

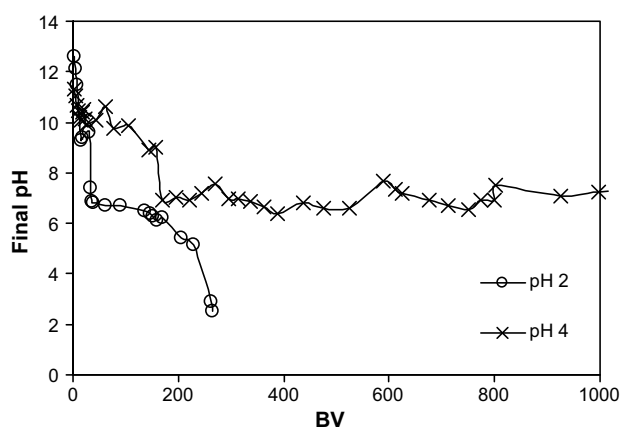


Fig. 5. pH evolution in neutralization test in column at pH 2 and 4. BV: bed volume.

detection, most trace elements associated to CFBC-PCFA were only sporadically detected, being the maximum values for Mo < 11 $\mu\text{g/L}$, Ba < 48 $\mu\text{g/L}$, Ni < 16 $\mu\text{g/L}$ and B < 8 $\mu\text{g/L}$ in all NCS leachate samples. A possible reason may be that CFBC-PCFA is covered with KCMW or BL, decreasing the CFBC-PCFA elements leaching.

The occurrence of Na, Zn and As in NCSs leachate samples (Fig. 4) may be also attributed to the presence of KCMW or BL as coating, which makes those elements easily available in aqueous media. The highest values of Zn and As in leachates were found in NCS1 column (53.6 and 138 $\mu\text{g/L}$ at 5 h, respectively), and the lowest in NCS3 column (14.2 and 3.2 $\mu\text{g/L}$ at 1 h, respectively). This difference could be attributed to a higher content of inorganic salts in BL than in lignimerin, making possible a stronger binding between BL and CFBC-PCFA-2008. Arsenic values in NCS1 leachates exceed As maximum value from Chilean regulation DS° 90 [39], leading us to discard NCS1. Spite As (24.8 $\mu\text{g/L}$) and Zn (36.8 $\mu\text{g/L}$) low concentrations in NCS2 leachates, it was decided as best option between NCS2 and NCS3, NCS3 (lowest As concentrations). As a result of the leaching column tests, NCS3 was selected as a suitable sorbent for column trials applications.

3.3. Neutralization column tests

As expected in neutralization tests at pH 2, NCS3 provoked a rapidly pH decrease from 12.6 to 2.5 in leachate samples, whereas at pH 4, the pH values showed only a sharply decrease between pH 11.3 and 9.0, being then stable around 6.6 and 6.8 (Fig. 5), which suggest a potential buffering zone. This final result indicates that NCS3 contributes to maintain an almost neutral pH by means of buffering reactions, as far as initial pH is higher than 4.

The interaction between NCS3 and acid synthetic wastewater leads to the dissolution of soluble minerals presented from NCS3, which it increases when pH is 2 (Fig. 6a). Main elements released in both experiments were Na, S, Ca, Ni, V, As and Zn (Fig. 6). In both cases, Na, S, Zn and As (elements from BL) presented a similar leaching performance as well as Ca, Ni and V (elements from CFBC-PCFA).

High concentrations of Na and S of 3776 and 2483 mg/L at pH 2 (Fig. 6a), and 1661 and 1511 mg/L at pH 4 (Fig. 6b) were detected in the first collected samples, which decreased rapidly at longer times. A possible reason may be the dissolution of readily soluble Na and S bearing minerals, corroborating the data obtained in the sequential extraction.

In case of Ca and V, the highest concentrations were 426 and 13 mg/L at pH 2, and 20 and 7 mg/L at pH 4, respectively. Ca concentrations remain stable during the observed potential buffering zone at pH 4 (Fig. 5), suggesting that anions associated to calcium

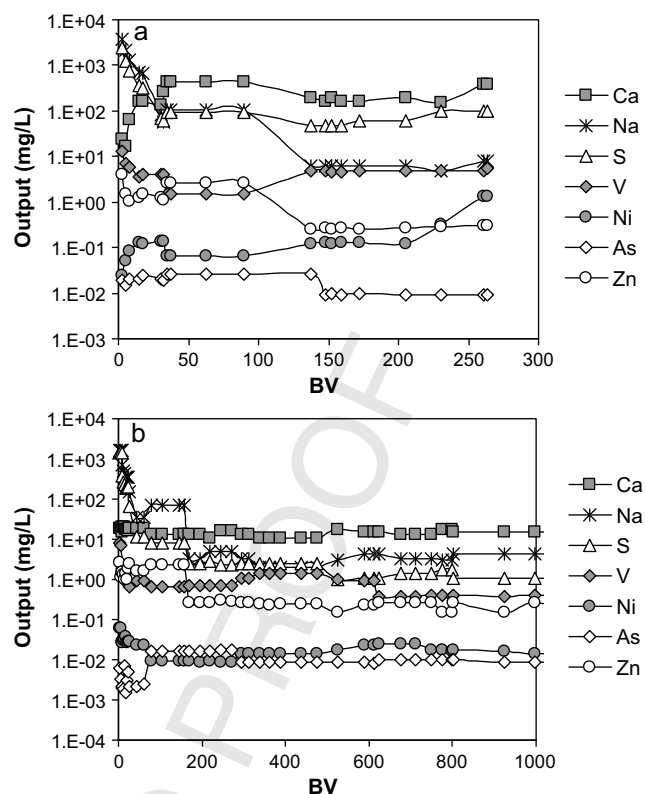


Fig. 6. Main major and trace elements in neutralization test at pH 2 (a) and 4 (b). Ordinate axis in logarithm scale.

play an important role in buffering reactions. NCS3 arising neutralization test (pH 4) was analyzed through XRD (figure not shown), detecting only anhydrite and calcite as mineral phases. The disappearance of portlandite, merwinite and lime peaks and a decreasing of intensity of anhydrite peaks suggest that portlandite, lime and anhydrite dissolution take place in the buffering reactions.

Furthermore, Ni and As were detected in low concentrations, being for both experiments under 2 mg/L, whereas the maximum Zn values were under 4.1 mg/L. These results lead to state that NCS3 is able to neutralize acid to moderate acid wastewaters (of pH higher than 4), for a long period of time.

3.4. Removal column tests

Breakthrough curves for copper and lead are presented for pH 2 and 4 in Fig. 7. It is observed that NCS3 reached bed saturation faster in case of copper than for lead at pH 2 and 4, showing saturation times of 420 min (0.3 day) and 5200 min (3.6 day) for Pb^{2+} and 280 min (0.2 day) and 440 min (0.31 day) for Cu^{2+} at pH 2 and 4, respectively.

As shown in Fig. 7a and b, Cu^{2+} and Pb^{2+} removal was also influenced by pH changes, observing that at pH 2 NCS3 was faster saturated. This result indicates that Pb^{2+} and Cu^{2+} removal is not favored at pH 2 which it may be attributed to a competition with H^+ ions in the solution for NCS3. Furthermore, during column removal tests, NCS3 released high concentrations of V and Zn, being the maxima concentrations of 21 mg/L for V (Pb^{2+} at pH 2) and of 1 mg/L for Zn (Cu^{2+} at pH 2). These results indicate that NCS3 is not recommended for acid wastewaters at pH lower than 2.

Nevertheless, the best results were achieved at pH 4, reaching maximum removal capacity of 28.3 mg/g, for Pb^{2+} (Table 5). In the case of Cu^{2+} the maximum removal capacity was 4.6 mg/g at pH 4 (Table 5). NCS3 Cu^{2+} and Pb^{2+} maximum removal capacities

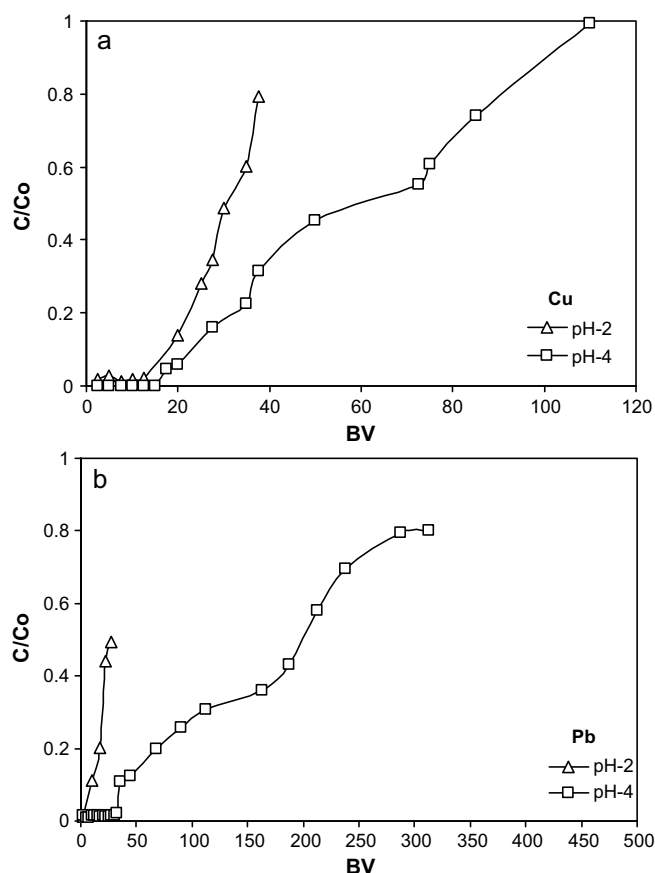


Fig. 7. Cu²⁺ (a) and Pb²⁺ (b) removal test in fixed-bed columns at pH 2 and 4.

are lower compared with other materials reported in the literature such as tea waste 13 and 46 mg/g [13] and granule biomass 40 and 192 mg/g for Cu²⁺ and Pb²⁺, respectively [14]. However, NCS3 presents a higher Cu²⁺ removal capacity compared to a mixture of sawdust and brine sediments 0.31 mg/g [12].

The removal capacities of both heavy metals indicate that NCS3 present a higher affinity for Pb²⁺ than for Cu²⁺. This difference could be explained by the hydration enthalpies of both heavy metals. According to several authors [13,40], high hydration enthalpy of heavy metal cations (Me²⁺) means that interaction between Me²⁺ and sorbent (NCS3) is weak and less. Pb and Cu hydration enthalpies are -1481 and -2100 kJ/kg which reflects that Pb has a higher affinity for NCS3 than Cu and hence a higher removal of Pb compared to Cu.

According to the wide effluent pH range measured during copper and lead column removal, between 10.7-6.4 for Cu²⁺ and 10.9-6.9 for Pb²⁺, it is possible that main removal mechanisms may be attributed to precipitation of their respective hydroxides and

Table 5

Results on removal of Cu²⁺ and Pb²⁺ in NCS3 fixed bed column tests.

pH	Bed mass (g)	t _s (min)	m _{total} (mg)	q _{total} (mg)	Bed removal capacity (mg/g)
Cu²⁺					
2	5.4	200	30	22.2	1.9
4	5.8	586	88	43.3	4.6
Pb²⁺					
2	4.9	80	11	9.0	1.8
4	4.8	1666	250	138.2	28.3

m_{total}: total amount of heavy metal cross the NCS3 bed, q_{total}: total removed amount of heavy metal.

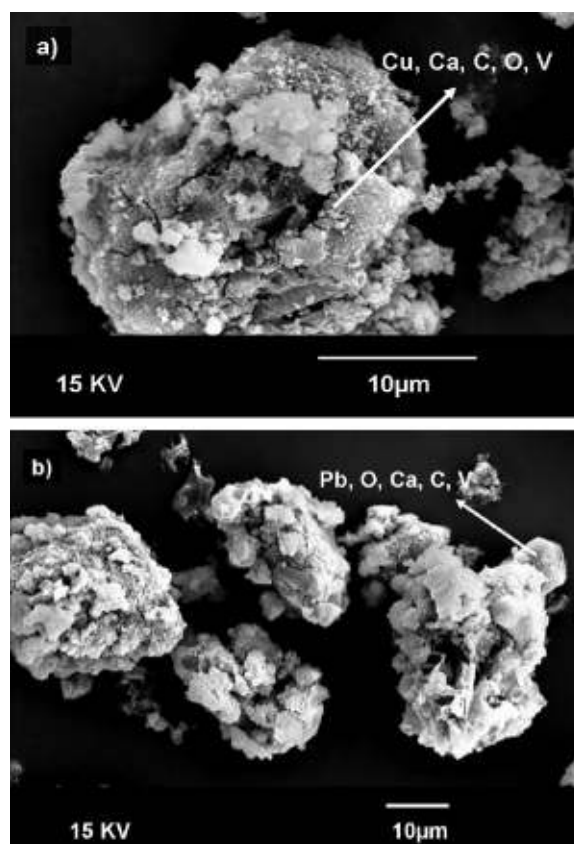


Fig. 8. SEM-EDX of NCS3 arising from Cu²⁺ (a) and Pb²⁺ (b) removal column tests at saturation point and at pH 4.

carbonates. XRD and SEM-EDX of NCS3 after reaching Cu²⁺ and Pb²⁺ maximum removal capacities were performed. In both materials was observed the presence of Cu and Pb coating the NCS3 surface (Fig. 8). In both cases, it was found Cu and Pb associated to Ca-, C- and O-bearing minerals, suggesting that main precipitate forms onto NCS3 are carbonate minerals of Cu and Pb. Despite of detecting Cu and Pb in SEM-EDX analyses, occurring as particles with a possible crystalline structure onto NCS3, XRD results showed no new crystalline minerals with the presence of these elements. Non-detection of other mineral phases in NCS3 by XRD could probably be due to their amorphous nature, low concentration or dilution by the main mineral phases [41].

3.5. Sequential extraction

Fig. 9 shows the sequential extraction procedure (SEP) of raw CFBC-PCFA and NCS3 for comparing purposes with the SEP of Cu²⁺ and Pb²⁺ residual materials obtained from Cu²⁺ and Pb²⁺ removal column tests, at pH 2 and at pH 4. In these figures is only indicated the extraction pattern of Cu and Pb.

The extraction pattern for Cu shows differences between raw NCS3 and Cu²⁺ residual material. It was observed that raw NCS3 presented a low Cu extraction yield of 4.9% (corresponding to a bulk concentration of 0.25 mg/kg) associated to carbonates (S4), whereas Cu²⁺ residual material presented an increase of 82% and 90% of Cu in the carbonate phase for pH 2 and 4 (bulk concentrations of 3600 and 4100 mg/kg, respectively). This result may be mainly attributed to the precipitation of Cu as carbonate species during removal column test. Besides Cu in carbonates phases, it was also Cu detected in sulphide and non-silicate matrix (S5) and a small fraction associated to organic matter, indicating that almost all removed Cu (from removal column tests) is present in the less

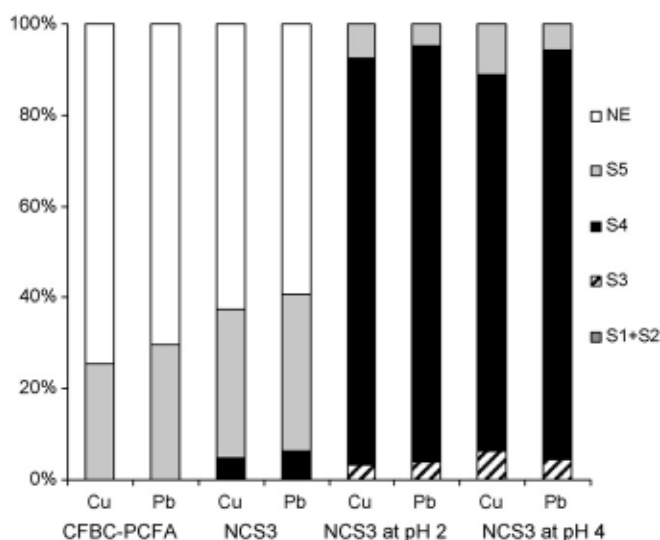


Fig. 9. Sequential extraction results of raw CFBC-PCFA, and Cu^{2+} and Pb^{2+} residual materials obtained from Cu^{2+} and Pb^{2+} removal column tests by NCS3, at pH 2 and at pH 4. S1: exchangeable extraction, S2: soluble extraction; S3: associated to organic matter; S4: associated to carbonates minerals and S5: associated to sulphides and non silicate minerals.

mobile fractions from NCS3. This characteristic may be of high relevance when managing the NCS3 directly to a safe disposal landfill.

In case of Pb extraction pattern, it was observed a similar behavior, detecting Pb in S3, S4 and S5 fractions. Raw NCS3 presented a Pb extraction yield of 6.2% associated to carbonates (S4), whereas Pb^{2+} residual material presented extraction yields values of 89% for both tested pHs, corresponding to bulk concentrations of 1857 and 8959 mg/kg for pH 2 and 4, respectively. This result corroborates that at pH 4, NCS3 reached higher saturation times for Pb^{2+} than for Cu^{2+} removal and then NCS3 could retain more Pb^{2+} than Cu^{2+} . The SEP for Cu and Pb also corroborates the SEM-EDX result of NCS3 after removal column tests (Fig. 8), which it showed that almost all Pb and Cu particles are present as carbonate minerals.

4. Conclusions

It can be concluded that the agglomeration process of CFBC-PCFA increased the grain size in all resulting NCS samples, simultaneously improving their specific surface area. Batch and column leaching tests show that almost all studied materials can be classified as non hazardous wastes (except CFBC-PCFA-2008). Column leaching test showed that it could be useful as selection criteria. The best result was achieved for NCS3, which was used to neutralize acid synthetic wastewater and to remove Cu^{2+} and Pb^{2+} in column tests. NCS3 performance shows a higher buffering and Cu^{2+} and Pb^{2+} maximum removal capacity at pH 4 compared to pH 2, showing NCS3 a higher affinity to Pb^{2+} than for Cu^{2+} . Therefore, the use of NCS3 seems to be an interesting option as non conventional sorbent in the neutralization of acidic wastewater, and the simultaneous removal of Pb^{2+} and Cu^{2+} .

Acknowledgements

To the FONDECYT projects 1060309 and 7070022, CONICYT-CSIC project 2007-136 and 2007CL0014 CSIC/CONICYT.

References

- [1] V.C. Srivastava, D.I. Mall, I.M. Mishra, Treatment of pulp and paper mill wastewaters with poly aluminium chloride and bagasse fly ash, *Colloids Surf. A: Physicochem. Eng. Aspects* 260 (2005) 17–28.

- [2] S. Bailey, T.J. Olin, M. Bricka, D.D. Adrian, A review of potentially low cost sorbents for heavy metals, *Water Resour.* 33 (1999) 2469–2479.
- [3] F.S. Zhang, H. Itoh, Adsorbents made from waste ashes and post-consumer PET and their potential utilization in wastewater treatment, *J. Hazard. Mater. B101* (2003) 323–337.
- [4] S. Babel, T.S. Kurniawan, Low-cost adsorbents for heavy metals uptake from contaminated water: a review, *J. Hazard. Mater. B97* (2003) 219–243.
- [5] T.S. Kurniawan, Y. Gilbert, S. Chan, L. Wai-hung, S. Babel, Comparisons of low-cost adsorbents for treating wastewaters Laden with heavy metals, *Sci. Total Environ.* 366 (2006) 409–426.
- [6] A. Bhatnagar, M. Sillanpää, Utilization of agro-industrial and municipal waste materials as potential adsorbents for water treatment—a review, *Chem. Eng. J.* 157 (2010) 277–296.
- [7] M.C. Diez, O. Rubilar, M. Cea, R. Navia, A. De Martino, R. Carpasso, Recovery and characterization of the humate-like salified polymeric organic fraction (lignimerin) from Kraft cellulose mill wastewater, *Chemosphere* 68 (2007) 1798–1805.
- [8] I. Reyes, M. Villarroel, M.C. Diez, R. Navia, Using lignimerin (a recovered organic material from Kraft cellulose mill wastewater) as sorbent for Cu and Zn retention from aqueous solutions, *Bioresour. Technol.* 100 (2009) 4676–4682.
- [9] C.J. Li, J.E. Chang, Effect of fly ash characteristics on the removal of Cu(II) from aqueous solution, *Chemosphere* 44 (2001) 1185–1192.
- [10] F. Rozada, M. Otero, J.B. Parra, A. Morán, A.I. García, Producing adsorbents from sewage sludge and discarded tyres. Characterization and utilization for the removal of pollutants from water, *Chem. Eng. J.* 114 (2005) 161–169.
- [11] E. Pehlivan, S. Cetin, B.H. Yanik, Equilibrium studies for the sorption of zinc and copper from aqueous solutions using sugar beet pulp and fly ash, *J. Hazard. Mater. B135* (2006) 193–199.
- [12] L. Agouborde, R. Navia, Heavy metals retention capacity of a non-conventional sorbent developed from a mixture of industrial and agricultural wastes, *J. Hazard. Mater.* 167 (2009) 536–544.
- [13] B.M.W.P.K. Amarasinghe, R.A. Williams, Tea waste as a low cost adsorbent for the removal of Cu and Pb from wastewater, *Chem. Eng. J.* 132 (2007) 299–309.
- [14] A.H. Hawari, C.N. Mulligan, Heavy metals uptake mechanisms in a fixed-bed column by calcium-treated anaerobic biomass, *Process Biochem.* 41 (2006) 187–198.
- [15] J. Lehmann, S. Joseph, *Biochar for Environmental Management: Science and Technology*, Published by Earthscan in the UK and USA, 2009.
- [16] C.N. Mulligan, R.N. Yong, B.F. Gibbs, Remediation technologies for metal-contaminated soils and groundwater: an evaluation, *Eng. Geol.* 60 (2001) 193–207.
- [17] G. Vidal, Revisión bibliográfica sobre los compuestos orgánicos producidos en la industria de la pasta y papel: incidencia en la toxicidad y biodegradabilidad anaerobia de sus efluentes. *Afinidad*, 481, 152–160.
- [18] A. González, N. Moreno, R. Navia, X. Querol, Study of a Chilean petroleum coke fluidized bed combustion fly ash and its potential application in copper, lead and hexavalent chromium removal, *Fuel* 89 (2010) 3012–3021.
- [19] A. González, N. Moreno, R. Navia, Fly ashes from coal and petroleum coke combustion: current and innovative potential applications, *Waste Manage. Res.* 27 (2009) 976–987.
- [20] L.M. Chen, D. Kost, W.A. Dick, Petroleum coke circulating bed combustion product as a sulfur source for alfalfa, *Commun. Soil Sci. Plant Anal.* 39 (2008) 1993–1998.
- [21] G. Thenoux, F. Halles, A. Vargas, J.P. Bellolio, H. Carrillo, Laboratory and field evaluation of fluid bed combustion fly ash as a granular road stabilizer, *Transp. Res. Rec.* 2 (2007) 36–41.
- [22] N.F. Gray, Environmental impact and remediation of acid mine drainage: a management, *Environ. Geol.* 30 (1997) 62–71.
- [23] Organization for Economic Cooperation and Development (OECD), OECD Environmental Performance Reviews-Chile-2005.
- [24] A. Bezama, M. Sánchez, State-of-the-art management technologies for contaminated soils and groundwaters with focus on the copper industry, I International Workshop on Process Hydrometallurgy-Hydroprocess; 2006, GECAMIN, Iquique, Chile, October 11–13, 2006.
- [25] J. Pizarro, P.M. Vergara, J.A. Rodríguez, A.M. Valenzuela, Heavy metals in northern Chilean rivers: spatial variation and temporal trends, *J. Hazard. Mater.* 181 (2010) 747–754.
- [26] Gebart, R. Gebart, Black Liquor Gasification-Large Scale Production of Green Transportation Fuels. www.etcpitea.se. Extracted on 25.10.2009 (ETC, Box 726, SE-941 28 Piteå, Sweden).
- [27] A. Demirbas, Pyrolysis and steam gasification processes of black liquor, *Energy Convers. Manage.* 43 (2002) 877–884.
- [28] X. Querol, M.K. Whateley, J.L. Fernández-Turiel, E. Tuncali, Geological controls on the mineralogy and geochemistry of the Beypazari lignite, Central Anatolia, Turkey, *Int. J. Coal Geol.* 33 (1995) 255–271.
- [29] M. Thompson, N. Walsh, *Handbook of Inductively Coupled Plasma Spectrometry*, Chapman and Hall, Inc., New York, 1989.
- [30] ASTM C618-92a, Standard specification for fly ash and raw or calcinated natural pozzolan for use as mineral admixture in Portland cement concrete, *Am. Soc. Test. Mater.*, 1994; 04.02. Pennsylvania.
- [31] European Committee for Standardisation EN 12457-2: 2002, Characterisation of Waste-Leaching-Compliance Test for Leaching of Granular Waste Materials and Sludges—Part 2: One Stage Batch Test A Liquid to Solid Ratio of 10 L/kg for Materials with Particle Size Below 4 mm.

- 619 [32] Council Decision 2003/33/EC, Stabilising Criteria and Procedures for the Acceptance of Waste at Landfills Pursuant to Article 16 of and Annex II to Directive
620 1999/31/EC. 632
621 633
622 [33] X. Querol, J.C. Umaña, A. Alastuey, C. Ayora, A. Lopez-Soler, F. Plana, Extraction
623 of soluble major and trace elements from fly ash in open and closed leaching
624 systems, *Fuel* 80 (2001) 801-813. 634
625 [34] R.E. Treybal, *Mass Transfer Operations*, 3rd edition, Tokyo, McGraw-Hill, 1980. 635
626 [35] G. Sposito, I.J. Lund, A.C. Chang, Trace metal chemistry in arid-zone
627 field soils amended with sewage sludge: 1. Fractionation of Ni, Cu,
628 Zn, Cd and Pb in solid phases, *Soil Sci. Soc. Am. J.* 46 (1982) 260-
629 264. 636
630 [36] V. Fierro, V. Torné-Fernández, A. Celzard, D. Montané, Influence of the dem-
631 ineralization on the chemical activation of Kraft lignin with orthophosphoric
632 acid, *J. Hazard. Mater.* 149 (2007) 126-133. 633
634 [37] I.M. Smith, *Trace Elements From Coal Combustions: Emissions*, IEA Coal
635 Research, London, 1987. 636
637 [38] E.J. Reardon, C.A. Czank, C.J. Warren, R. Dayal, H.M. Johnston, Determining con-
638 trols on element concentrations in fly ash leachate, *Waste Manage. Res.* 13
639 (1995) 435-450. 640
641 [39] Wastewater Emission Chilean Norm, Wastewater Emission Chilean Norm, DS
642 N° 90 (Decreto Supremo N° 90. Norma de emisión de riles). Extracted on
643 20.03.2010, http://www.sinia.cl/1292/articles-29082_Manual90.pdf. 644
645 [40] F. Martin-Dupoint, Y. Gloagven, R. Garnet, M. Guilloton, H. Morvan, P. Krausz,
Heavy metal adsorption by crude coniferous barks: a modeling study, *J. Environ.
Sci. Health A37* (2002) 1063-1073.
[41] D.G. Schulze, *Differential X-ray Diffraction Analysis of Soil Mineralogy*, Soil Science Society of America Miscellaneous Publication, Madison (WI), 1994, pp. 412-429 (Chapter 13).

UNCORRECTED PROOF